ISBN 978-82-326-5486-4 (printed ver.)
ISBN 978-82-326-6137-4 (electronic ver.)
ISSN 1503-8181 (printed ver.)
ISSN 2703-8084 (electronic ver.)

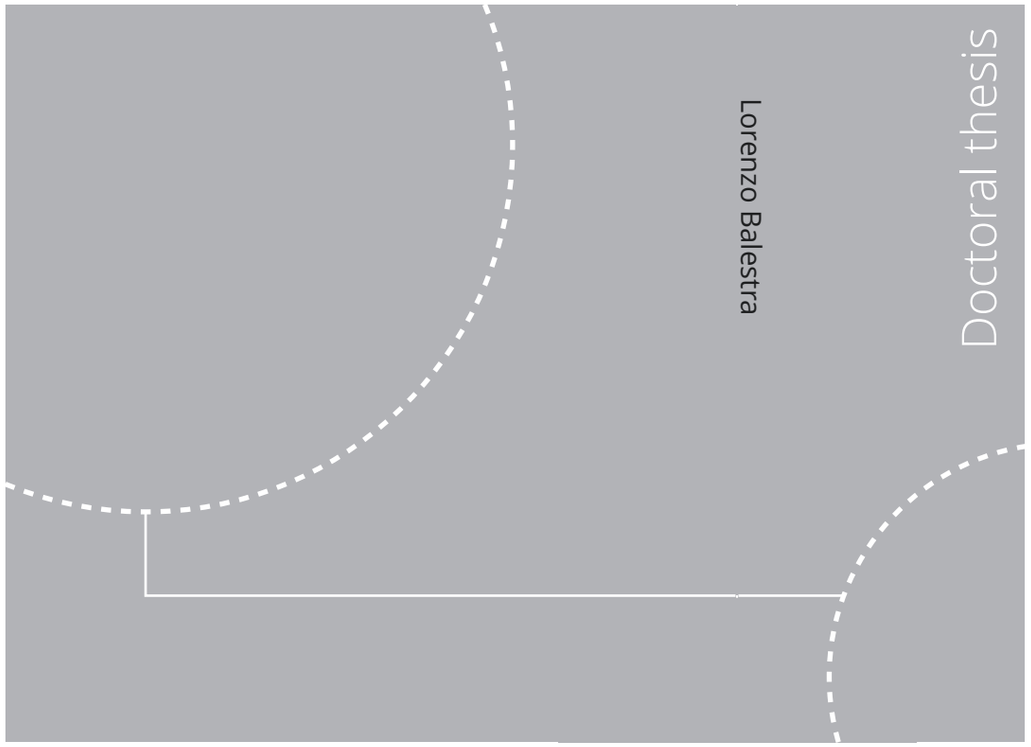

Doctoral theses at NTNU, 2022:281

Lorenzo Balestra

Design of hybrid fuel cell & battery systems for maritime vessels

Doctoral theses at NTNU, 2022:281

NTNU

Norwegian University of Science and Technology

NTNU
Norwegian University of Science and Technology Thesis for the degree of Philosophiae Doctor
Faculty of Engineering
Department of Marine Technology

NTNU

Norwegian University of Science and Technology

Lorenzo Balestra

Design of hybrid fuel cell & battery systems for maritime vessels

Thesis for the degree of Philosophiae Doctor

Trondheim, October 20

Norwegian University of Science and Technology Faculty of Engineering
Department of Marine Technology

NTNU
Norwegian University of Science and Technology

NTNU
Norwegian University of Science and Technology

Thesis for the degree of Philosophiae Doctor

Faculty of Engineering
Department of Marine Technology

ISBN 978-82-326-5486-4 (printed ver.)
ISBN 978-82-326-6137-4 (electronic ver.)
ISSN 1503-8181 (printed ver.)
ISSN 2703-8084 (electronic ver.)

Doctoral theses at NTNU, 2022:281

PRINTED IN NORWAY
NO - 1598

NORDIC SWAN ECOLABEL
Printed matter
2041 0731

Printed by Skipnes Kommunikasjon AS

Preface

This thesis is submitted in partial fulfillment of the requirements for the degree of Philosophiae Doctor (Ph.D.) at the Norwegian University of Science and Technology. The thesis contains work carried out from August 2019 to July 2022. The research was headed by the Institute for Energy Technology (IFE - Institutt for Energiteknikk) based in Kjeller, Norway, and funded by the Norwegian Research Council trough project number 90436501. The research project, named KPN H2Maritime, includes three work packages with different topics and scopes developed both at IFE and at the Norwegian University of Science and Technology NTNU. The research presented in this thesis was carried out at NTNU under the principal supervision of Professor Ingrid Schjølberg, the co-supervision of Professor Ingrid Utne and Dr. Øystein Ulleberg.

The target audience for this thesis encompasses multiple professions across different sectors. In the marine technology sector the target audience includes ship designers, system engineers and also ship owners. The knowledge gained and the software tools developed can be applied both in academia and industry to promote the transition to zero-emission energy generation onboard ships of different class and sizes. The results obtained in this thesis can also be used in other sectors such as heavy duty road transport or rail transport when considering the similarities between vehicle powerplants that include hydrogen fuel cells and energy storage solutions.

At present, the transition to zero-emission vehicles has mainly consisted of a shift towards battery powered electric cars. The automotive sector has managed to take the lead among other transport industries, and produce many different production models that have been successful on the market. Meanwhile, the limited energy density of the battery packs has also highlighted various challenges en-

countered when the energy storage requirements are increased to allow for high power output or long range operations. In applications such as maritime vessels, trains or transport trucks, the weight and volume of the battery pack needed to ensure a satisfactory power delivery may become excessive.
New energy storage techniques are being researched all over the globe, but it is non trivial to find a solution that combines high energy and power density, and that is also portable enough for transport applications. The use of clean hydrogen for onboard energy storage can be the solution to the limitations of batteries for vehicles that have to operate for long periods of time and are not able to rely on grid connection for charging. Vehicles powered by hybrid powertrains utilizing proton exchange membrane fuel cells and batteries are able to use the hydrogen stored onboard to produce electrical power with zero-emission. This type of powertrain can be applied to maritime, rail and road transport to reduce emissions of pollutants and greenhouse gasses.

Acknowledgements

This work is supported by the Norwegian Research Council trough project number 90436501. The project is headed by IFE (Institute for Energy Technology) in Kjeller, Norway, and this work package is developed at the Department of Marine Technology of the Norwegian University of Science and Technology (NTNU) in Trondheim, Norway.

I would like to express my gratitude to my primary supervisor, Ingrid Schjølberg, who guided me throughout this project. I would also like to thank everyone that supported me during these years of research and study.

Abstract

The work described in this thesis encompasses multiple aspects related to the development of hybrid marine power systems utilizing proton exchange membrane fuel cells and batteries. The focus is placed on the definition of methodologies that can help define the composition of the powerplant and its control. The developed methodologies are based upon a series of models that can simulate the powerplant, allowing the observation of the component's behavior during operation. The analysis of the results obtained from simulations is used to evaluate the technical and economic feasibility of a specific powerplant configuration, and allows to set a benchmark for operation optimization.

The first two Chapter of the thesis introduce the KPN H2Maritime project, and important aspects of hydrogen production, storage and distribution. The knowledge of these topics is fundamental in understanding the challenges encountered in relation to the adoption of hydrogen systems for transportation purposes. Such challenges are not limited to the technical limitations of fuel cells, batteries and power electronic components, but include a series of factors that are independent from the powerplant. Some of these factors are hydrogen safety, hydrogen storage and hydrogen production. Chapter three is dedicated to an overview of conventional maritime powerplants, hybrid electric powerplants and possible conversions into fuel cell/battery powerplants. The study of the conventional system, mainly the ones utilizing internal combustion engines, is fundamental as it sets a standard for performances and operational flexibility that has to be met by the newly designed hybrid systems. The definition of design criteria for hybrid powerplants utilizing proton exchange membrane fuel cells and batteries starts in Chapter four with the description of a quasi-static model to study the onboard power generation, storage and distribution during a vessel's operations. The model is developed as a simulation tool and is used to define possible powerplant configurations based

on the energy management strategy selected. The model is used as the base for the development of a software application developed in Matlab. Results obtained using the model can be used to study the technical and economic feasibility of the calculated configurations for the specific use case, or used as an input for validation into a dynamic model of the system. Two types of dynamic models have been developed and are described in Chapter five and six. These models allow to simulate the dynamic behavior of the powerplant's components, and relative power electronics, replicating the operations of the system with a adequate degree of accuracy. Simulations carried out with the dynamic models allow a more in-depth observation of the component's behavior during the vessel's operations compared to the results obtained with the quasi-static model. Different powerplant layouts are tested, configuring the models of the components in different ways, and multiple energy management strategies are tested. The results obtained from these simulations can be used to compare different approaches to the powerplants configuration and control. Such results can also be utilized as a benchmark for further optimization or used as a starting point for laboratory simulations using hardware in the loop.

The software and models developed for the H2Maritime project aim to fill a gap found in relation to the use high power hybrid system using fuel cells in the maritime transport industry. The development of design criteria and models to optimize operations for this type of hybrid system is key to make them an economically viable solution for ship owners. The identification of technical economic viability, even in a limited number of application, can spark the interest of many ship owners willing to innovate and to abandon polluting internal combustion engines. A transition to green hydrogen for a selected number of vessel would still imply a large reduction in the emission of pollutants and greenhouse gasses, reducing the environmental impact of maritime vessels, mitigating the effects of climate change and safeguarding marine and coastal environments.

Contents

List of Tables

List of Figures

Nomenclature

Symbols

α	Penalty coefficient cost function
η_{bc}	Boost converter efficiency
$\eta_{\text{bi-dir}}$	Bi-directional converter efficiency
η_{fc}	Fuel cell efficiency
η_{sys}	Electrical grid efficiency
μ	Tuning factor for penalty coefficient
C_{out}	Capacitance output capacitor [F]
D	Duty ratio
fs	Switching frequency [Hz]
Hpo	High power degradation rate [$\mu V/h$]
I_{b}	Current battery [A]
$I_{\text{demand-b}}$	Current demand at instant t from battery pack [A]
$I_{\text{demand-fc}}$	Current demand at instant t from PEMFC stack [A]
$I_{\text{fc-ideal}}$	Current output fuel cell [A]
I_{fc}	Current output fuel cell considering efficiency [A]
I_{max}	Maximum current value [A]

L	Inductor rating [H]
Lpo	Low power degradation rate [$\mu V/h$]
n_{b}	Number of batteries installed
n_{fc}	Number of fuel cells installed
$P_{\text{b-tot}}$	Total power of all batteries cells considered [W]
P_{b}	Power I/O single battery [W]
$P_{\text{fc-rated}}$	Rated power of the fuel cell stack [W]
$P_{\text{fc-tot}}$	Total power of all fuel cells considered [W]
P_{fc}	Power output single fuel cell stack [W]
P_{f}	Fuel cells output for peak shaving strategy [W]
P_{L}	Fuel cells output for load leveling strategy [W]
P_{op}	Total power demand [W]
R_{t}	Fuel cell response time [s]
t	Time [s]
t_{hp}	Time at high-power operation [s]
t_{lp}	Time at low-power operation [s]
t_{s}	Sample rate operational profile [s]
t_{tot}	Total simulation time [s]
Tl	Transient loading degradation rate [μV/Δkw]
V_{b}	Voltage battery [V]
$V_{\text{DC-Load}}$	Voltage value for the DC-Bus [V]
$V_{\text{fc-ideal}}$	Voltage output fuel cell [V]
V_{fc}	Voltage output fuel cell considering efficiency [V]
V_{in}	Voltage input converter [V]
V_{out}	Voltage output converter [V]

Abbreviations

AFC	Alkaline fuel cell
BOP	Balance of plant
CCS	Controlled current sink
CS	Component sizing
$DMFC$	Direct methanol fuel cell
DP	Dynamic positioning
ECU	Electronic control unit
EMS	Energy management strategy
EPA	U.S. Environmental Protection Agency
$FPSO$	Floating production storage offloading
$GH2$	Compressed hydrogen (Gas state)
GHG	Greenhouse gas
HFO	Heavy fuel oil
ICE	Internal Combustion Engine
$IDHL$	Immediately Dangerous To Life or Health
IFE	Institute for Energy Technology (Norway)
IMO	International Maritime Organization
$LH2$	Hydrogen stored in liquid form at cryogenic temperature
LNG	Liquefied natural gas
$LOHC$	Liquid organic hydrogen carriers
$LT-PEMFC$	Low temperature proton exchange membrane
$MARPOL$	The International Convention for the Prevention of Pollution from Ships
$MCFC$	Metal carbonates fuel cell

MEA	Membrane electrode assembly
MGO	Marine diesel oil
MGO	Marine gas oil
MLI	Multi layer insulation
NMA	Norwegian Maritime Authority
OP	Operational profile (power demand over time)
$PAFC$	Phosphoric acid fuel cell
$PEMFC$	Proton exchange membrane fuel cell
PWM	Pulse width modulation
$SECA$	Sulphur emission control areas
SEI	Solid electrolyte interphase
$SMCR$	Specific maximum continuous rate
SOC	State of charge
$SOFC$	Solid oxide fuel cell
$SOFC$	Solid oxide fuel cells
$SPBC$	Single phase boost converter
TEU	Twenty-foot equivalent unit
TRL	Technology readiness level
WP	Work Package

Chapter 1

Introduction

1.1 Emissions and regulations

Maritime transport today still heavily relies on fossil fuels such as heavy fuel oil (HFO), marine gas oil (MGO), marine diesel oil (MDO), and other types of bunker fuel. These fuels contain high levels of asphalt, carbon residues, sulfur (which may amount to as high as 5 %) and metallic compounds [1]. The combustion of these fuels, in internal combustion engines, produces air pollutants that get released into the atmosphere and also large quantities of carbon dioxide, the most significant long-lived greenhouse gas (GHG) in Earth's atmosphere. The emission of these pollutants and climate-altering agents has a negative impact on climate, globally, and on air quality, locally, with the potential of harming both the human population aswell as animals.

A joint effort of 174 nations to limit the air pollution generated by maritime engines and the preservation of the marine environment has led to the ratification of numerous protocols by the International Maritime Organization (IMO). Annex VI of MARPOL (International Convention for the Prevention of Pollution from Ships) specifically addresses the need to reduce volatile organic compounds, particulate matter and hazardous air pollutants (NO_x and SO_x). This annex is relatively recent and entered into force the 19 of May 2005. The United Nations (UN) with sustainability goal n.14 highlights the importance of conservation and sustainable use the oceans, seas and marine resources. This sustainability goal is mainly directed towards the conservation of marine diversity fighting unreported and unregulated fishing, but also includes the importance of reduction of CO_2 and pollutants emissions to fight the increase of ocean acidity produced by acid rains. It is reported that, if the situation is not changed, a 100 to 150 % increase in acidity will affect

half of marine lifeforms.

These international resolutions are implemented alongside specific national environmental policies. In Norway, studies have been conducted to evaluate the level of emissions along the coast by the Ministry of Climate and Environment and the Norwegian Maritime Authority (NMA) [2]. Particular focus has been placed on world heritage fjords [3], where cruise ships currently moor during tourist season. Based on the scientific assessments and surveys made, it emerges that the level of nitrogen oxides (NO_x) in Geiranger and Flåm, at times, exceed values that could have a negative impact on health. NO_x together with soot/smoke particles and water vapour also contribute to the formation of smoke clouds in the fjords. In periods, the combination of older ship machinery, emissions, the number of ships and meteorological conditions leads to high formation of smoke. The proposed solution is to cap the NO_x from ships to the values set out in MARPOL Annex VI, regulation 13.4 (Tier II) by 2018 and regulation 13.5 (Tier III) by 2020. This is done by only allowing the use of fuel with a low sulphur content, regardless of whether the ship has air pollution control devices (scrubbers) installed. The visible emissions of smoke from ships should also have a density that reduces transparency by not more than 50% during cold start or 10% when underway. The speed in defined zones of the fjords is also limited to reduce fuel consumption and emissions to a minimum.

National and international regulations are a step in the right direction, limiting the effects of global warming and reducing the health risk for populations living in proximity of busy coastal routes. In the automotive industry, regulations on emissions have been in place since 1963 with the goal to reduce tail-pipe emissions and control the amount of smog measured in cities. The Clean Air Act passed by the U.S. Congress in 1970 has lead to the national effort to reduce the emissions of road transport and the creation of increasingly stringent standards with time. Similar emission control regulation are also adopted in Europe and identified with the "Euro" denomination. These emission standards have pushed producers to innovate and research ways to improve the efficiency of the vehicle, reducing fuel consumption and emissions. The effect of such regulation was successful as new passenger vehicles are 98-99% cleaner for most tailpipe pollutants compared to the 1960s. Similarly to road transport, it is important to limit the emissions of vessels through regulations and limitations, but it is also necessary to provide feasible alternatives for propulsion systems that do not use fossil fuels. Proposing technically and economically feasible alternatives using zero or low emission energy carries gives a choice to the ship owners when ordering a new vessel or upgrading an older vessel. The adoption of carbon-free systems can put them at an advantage in the long term with restrictions becoming more and more stringent, while also

cutting their carbon footprint to zero during operations. It is for this reason that this thesis takes into consideration hybrid systems including hydrogen fuel cells.

1.2 H2 Maritime project overview

This thesis, and enclosed publications, describe work carried out for the KPN H2Maritime project. The project is supported by the Norwegian Research Council through project number 90436501, with many major industrial partners such as ABB and Equinor providing the funding. The project is headed by the Institute for Energy Technology (IFE) in Kjeller, Norway. The H2Maritime project is divided into 3 work packages (WP): WP1 researching hydrogen bunkering and storage solutions, WP2 researching hydrogen safety, and WP3 researching the integration of fuel-cells and hydrogen systems in maritime powertrains (see Fig. 1.1). The PhD research focuses objectives defined in WP3, aiming to define design guidelines and energy management strategies for maritime powertrains using fuel cells powered by hydrogen, and batteries.

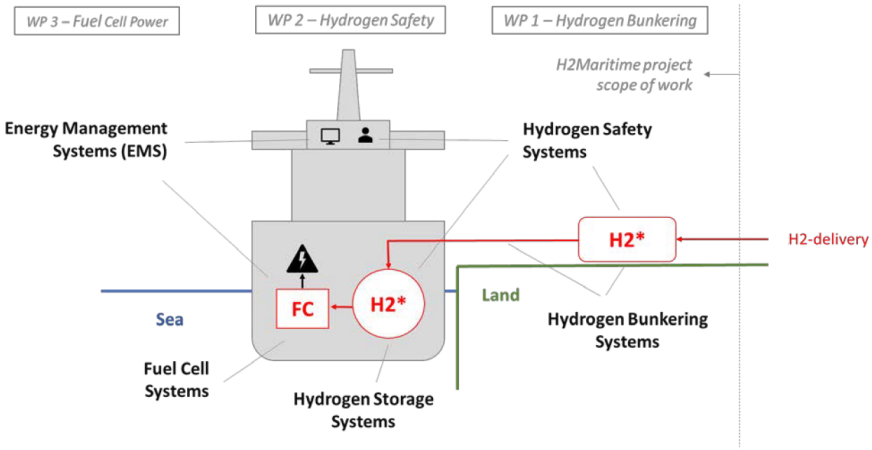

Figure 1.1: Visual representation of the H2Maritime project, showing the focus area for each work package, from hydrogen delivery (right), to onboard hydrogen storage (center), and finally to hydrogen usage (left). Each focus area is labeled with its respective work package at the top of the figure.

The defined objectives are achieved through the creation of software and digital tools based on mathematical models replicating the operational behavior of a hybrid maritime powertrain utilizing hydrogen fuel-cells and battery technologies. The work focuses on vessels in the 1 to 10 MW range. The goal of the developed models is to provide a way to analyze and optimize such powertains, calculate key parameters, and evaluate the technical and economic feasibility of these system in

specific use-cases.

1.3 Research objectives

The main question posed at the beginning of the research was: *"How can the design of the powerplant and energy management system for hybrid fuel cell vessels be optimized with respect to overall efficient operation and lifetime of the batteries and fuel cells?"* This question was investigated by developing a series of tasks, as listed below, defined in the research plan.

1. Introduction to fuel cells and hydrogen systems. Differences between conventional and hybrid powertrains in the maritime industry, positive and negative aspects of each technology. A general introduction to the safety challenges of hydrogen systems, maintanence, and degradation of the components.

2. Development of a software based model (in MATLAB) to investigate and optimize design criteria for the operation of fuel cell and battery hybrid systems for maritime vessels.

3. Review of existing methodologies for the energy management of hybrid systems utilizing fuel cells and batteries. Study of methodologies across different industries, including the automotive and heavy duty industry. Evaluation of existing methods aimed at the optimization of the power generation and distribution within the vessel's electrical grid.

4. Development of a detailed digital model of a hybrid maritime powerplant utilizing hydrogen fuel cells and batteries. This model is developed in Simulink and is the platform for testing different configurations of component sizing and energy management strategies for the optimization of the system's operations. The focus is also on key parameters such as hydrogen consumption, fuel cell degradation and operational life.

5. Test of the powerplant dynamic model including different energy management strategies. Testing is conducted using real-world data relative to maritime vessels in the power range of interest. Publication of the test results for peer-review.

1.4 Scientific background in the literature

The work described in this thesis and enclosed articles is built upon knowledge gained from a literature review which includes scientific publications de-

scribing hybrid powertrains in the transport industry, hydrogen systems for the production of onboard electric power, and energy storage solutions for power delivery optimization. The review is not limited to applications in the maritime sector, but includes the automotive, and heavy duty road transport aswell. A secondary aim of the literature review is to identify gaps in the current research that can be filled with novel solutions. The main focus is both on the composition of the powerplant, defined as component sizing (CS), and its control through an energy management strategy (EMS). As the main research question targets operation optimization, it is only possible to fully optimize the system when CS and EMS are considered in a combined package, as the definition of one impacts the other and vice versa.

The component sizing of hybrid systems is non-trivial, since the operational profile of the vessel is not always known, and because operations are usually affected by the EMS. To perform an accurate component sizing it is necessary to know the powertrain system in details. The review carried out by Jayasinghe et al. [4] provides basic scientific background necessary to familiarize with operations in an isolated electrical grid for both AC and DC systems. The review from Geertsma et al. [5] also provides a comprehensive overview on recent developments in the maritime industry. These articles are used in the development of the models that describe the electrical power generation and distribution in both Article 2 and 5.

The importance of the operational profile when estimating the power requirements of a system are illustrated in the study performed by Baldi et al. [6]. In this article it is observed of how much power is allocated to the different systems on a vessel equipped with a multi-megawatt powerplant with an known operational profile. Several articles present approaches to perform component sizing for hybrid vehicles across different industries. The article from Feroldi et al. [7] describes a sizing method for a fuel cell car used for road transport; the article from Cai et al. [8] considers an unmanned underwater vehicle; and the study from Ravey et al. [9] focuses on a collection truck. These component sizing methodologies provided a base for the development of the model based softwares presented in Article 1 and 5.

The development of an energy management strategy for the optimization of operations has been analysed in multiple articles. A comprehensive review and classification of EMSs for hybrid vehicles is presented by Huang et al. [10]. The article from Carignano et al. [11], Bassam et al. [12, 13] both present possible approaches to the optimization process through the development of smart EMSs. Other articles on this topic considered for this thesis include th work from from Amin et al. [14], Yuan et al. [15], and Kim et al. [16]. The considered work is used for the development of the study presented in Article 4.

As defined at the start of this section, the selection made during CS affects the design of the EMS, and vice-versa. To achieve the best possible optimization in the hybrid fuel cell system is therefore necessary to consider component sizing and energy management concurrently. Some articles describe methodologies that can be used for the concurrent optimization of CS and EMS, but few of these articles consider the maritime sector. The study from Pivetta et al. [17, 18] considers the optimization of both designs and operations for a small size passenger ferry. The study from Murgowski et al. [19] focuses on a generic plug-in hybrid electric powertrain applicable to maritime applications. Also the study from Jiang et al. proposes a methodology to perform the sizing and energy management concurrently [20].

The methodologies presented in this section provide an overview on possible approaches that can be used to solve the optimization problem of CS and EMS. Such methodologies are adapted to consider maritime applications, with large power requirements and long range capabilities, and used to create the models presented in this thesis.

1.5 Hydrogen powered vessels and future applications

In this section, a list of vessels utilizing powertrains powered by hydrogen fuel cells is presented. Using these vessels as reference, two vessels are selected for the studies carried out in this thesis. These vessels are a harbor tugboat and a double-ended ferry. These vessels are both in the 1 to 10 MW power output range defined as a boundary condition in the research plan.

1.5.1 Industrial projects for hydrogen powered hybrid vessels

In the maritime sector, starting in the 2000s, a series of projects have demonstrated the feasibility of operating fuel cell powered vessels. These vessels benefit greatly from a reduction in the size and weight of the battery required to ensure a satisfactory power demand. The first vessels developed were characterized by a relatively small size. The FCS Alsterwasser, operational in Hamburg as a passenger ferry is equipped with two 48 kW (140 V DC) fuel cells and a set of lead-gel battery of 360 Ah (560V). The vessel has a capacity of 100 passengers, with a length of 25.56 m and a width of 5.2 m [21]. A similar project involved the Nemo H2 passenger ship. This ship has a capacity of 88 passengers and operates in Amsterdam. The vessel is equipped with 70 kW PEM fuel cell and an integrated 30-50 kW battery. The dimensions are 21.95 m in length, and 4.25 m width with a depth of 1 meter [22].

Further advances in fuel cell technology have allowed the development of different project both in the European Union and in the United States. The avail-

ability of fuel cell stacks with a power output between 100 kW and 400 kW has opened the possibility for a multi-megawatt application. An example is the development of the MF hydra, a double-ended ferry operating in Norway's national waters. The vessel's powerplant is configured to use two 200 kW proton exchange membrane fuel cells stacks and a 1.36 MWh battery pack [23]. Diesel generators are included for passive redundancy. Another recent maritime application is in the golden gate zero emission marine project. This project has led to the development of the Sea Change high speed ferry. The powerplant of this vessel is comprised of 360 kW of PEM fuel cells and hydrogen storage tanks with a capacity of 246 kg. This system is integrated with 100 kWh of lithium-ion batteries [24].

Numerous other projects are currently in the early stage of development and are set to be finalized by 2024. This shows how the maritime industry is willing to innovate and adopt new cleaner energy carriers when possible [25].

1.5.2 Maritime and road vehicles considered in the study

The thesis focuses on maritime vessels that require the installation of a powerplant with a power output between 1 and 10 MW. In this range, the use of hydrogen as an energy carrier allows increased operational flexibility and ensures longer range when compared to solutions of equal volume and weight using exclusively batteries. Considering the technology that is currently available, battery powered vessels in the multi-megawatt range are only suitable for short range operations, and applicable in cases where it is possible to frequently recharge from the land based electrical grid. Vessels above 10 MW, usually operating over long range, such as oil carriers or container carriers, are excluded from the study. Propelling these vessels with currently available fuel cells requires incredibly large volumes of hydrogen stored onboard to ensure the same operational flexibility over long range. In addition, on this type of vessel are usually installed internal combustion engines operating using a two stroke cycle that can achieved a high thermal efficiency, similar to the one of fuel cells operating at rated values. Within the power range considered, the fuel cells can provide either the base-load, defined as the minimum level of demand on an electrical grid over a span of time, or act as a range extender, allowing in both cases to operate with zero-emission.

While not focusing on the economic aspect of the hybrid powertrain, it is believed that through careful optimization of the powerplant's composition and energy management strategy it is possible to design a system that combines good performances in terms of power delivery, and also is comparable to a traditional diesel electric installation in terms of initial costs. The use of hydrogen fuel cells is, however, not the best solution for all vessels in the considered power range and needs to be carefully evaluated considering the vessels operational profile and

conditions. More cost efficient solutions, both in terms of initial investment and running costs, can be applied in particular cases. The use of hybrid systems using hydrogen is to be taken into consideration if one or more of the conditions listed below is met:

- The maximum range requirements calculated for the vessel when considering the operated route are not compatible with a powertrain using only battery power, but the vessel is limited to zero-emission solutions.
- It is not possible, or economically viable, to create a high voltage recharging infrastructure on the departure or arrival dock of the vessel. Limitations of the land based electrical grid in remote areas have to be considered.
- Renewable energy sources installed at or in proximity of the harbor where the vessel stops can be used to produce green hydrogen. The economic feasibility is increased if the green hydrogen produced is used not only for maritime vessels, but also for road transport vehicles operating in the harbor, such as forklifts or harbor based trucks.

In light of previously listed conditions, data was obtained from a series of vessels within the specified power range. The data obtained from these vessels is used in different case studies using the models and software's developed in the thesis. The scope is to evaluate operations using the zero-emission hybrid powerplant.

Figure 1.2: Langeland double-ended ferry operated by Langelandslinjen in Danemark

The first vessel taken into consideration is a double ended ferry. Data for this vessels were made available by the ship owner for research purposes as they were used for previous studies relative to the optimization of the route [26]. The

ferry is 100 meters of length and 18.2 m of beam (Fig.1.2). The ferry can transport 600 passengers and 122 cars and operates a 45 minute crossing in Danish national waters. The crossing is 7.7 nautical miles and is operated 18 times in a normal day. The vessel is equipped with 5 diesel generators powering 4 Azimuth thrusters and auxiliary loads. This type of vessel is similar to the double ended ferries operating on many routes along the Norwegian coastline, with a powerplant producing 4 MW within the range considered in the project. It was decided that this vessel could be taken as a reference to study possible hybrid configurations and evaluate the feasibility and requirements of a hydrogen solution. The large amount of data released for research purposes has allowed for extensive testing of the model and allowed for a comparison with the diesel electric solution currently installed aboard.

The second vessel taken into consideration is a harbor tug. Data for this ferry was obtained under a non disclosure agreement and therefore the name of the vessel or the company operating it is not reported here. The vessel is a harbor tugboat powered by 2 diesel engines, each rated 1500kW at 750rpm and 1 diesel gen-set rated at 100kW. The vessel has a gross tonnage of 179 tons and an overall length of 33.2 m. A vessel belonging to the same class of the one considered in the study can be observed in Figure 1.3.

Figure 1.3: Harbor tugboat used for towing large vessels during maneuvering operations

The tugboat provides an interesting case study with a highly irregular operational profile characterized by many high frequency transients during service. This condition differs substantially from the operations of the double ended ferry where the high frequency transients are limited and found only during the docking phase. Operations including high frequency transients are non trivial cases for the optimization problem as the fuel cells have relatively long response time determined by the auxiliary components and the electrochemical reactions. A careful optimiz-

ation of the EMS and the powerplant components is required to make a hybrid system utilizing fuel cells and batteries suitable on this type of vessel.

To test the flexibility of the models described in this thesis, the last vehicle considered is not a maritime vessel, but a city bus (see Fig. 1.4). The decision to include a different vehicle, not belonging to the power range considered or to the type of vehicles specified, has been made to prove that the software tools developed can be used outside the boundary condition of the study, with limited reconfiguration. The bus, in its current configuration, is equipped with an inline 6 cylinder diesel engine of 7700 cm^3. The maximum output is equal to 220 kW at 2200 rpm and the maximum torque is 1200 Nm at 1200 rpm. The data used for the driving cycle of the bus are derived from driving cycles obtained using the U.S. Environmental Protection Agency (EPA) public database. All the vehicles presented in this section represents an interesting case study for the evaluation of a hybrid retrofit including hydrogen fuel cells.

Figure 1.4: Mercedes Citaro city bus 4 wheel chassis variant

1.6 Overview of contributions

The main focus of this work has been put on providing theoretical validation of models and software developed using real world data from maritime and road vehicles. This section chronologically summarizes the key academic and industrial contributions made through the articles attached to this thesis. The contributions from all the the co-authors are dually disclosed and satisfy the co-authorship requirements laid down by The Vancouver Group in 1985(The Vancouver Convention, 2016).

The categorization of the enclosed articles, considered as their placement in the presented framework, can be observed in Figure 1.5. In this framework, Articles 2 and 4 contribute to development and testing of Energy Management System, Articles 3 and 6 focus on Hydrogen Safety systems, and Articles 1 and 5 to powerplant design definition. The contributions of each article is described in

detail in the following.

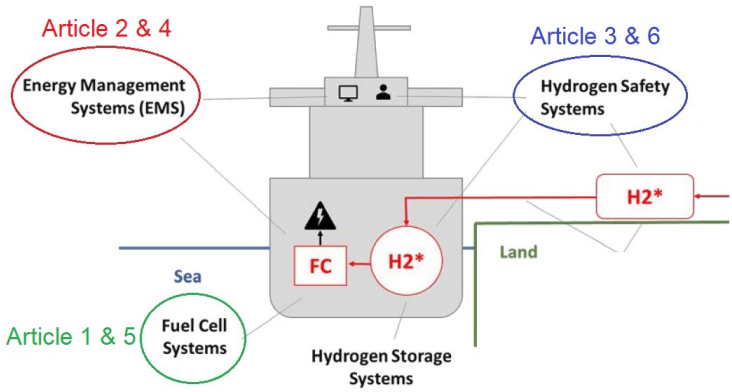

Figure 1.5: Topics targeted in the enclosed articles, and their location within the project visual representation

Article 1 - Conference paper

Balestra, Lorenzo; Schjølberg, Ingrid. (2020) Study on the Architecture of a Zero Emission Hydrogen Fuel Cell Vessel Power Generating Unit. ASME 2020 39th International Conference on Ocean, Offshore and Arctic Engineering - Volume 6A: Ocean Engineering.

- Contribution 1: Presents a software application for the sizing of a hybrid powerplant utilizing proton exchange membrane fuel cells and batteries.
- Contribution 2: Automates the process of powerplant sizing, providing configuration of components and energy management strategies to be validated on a dynamic model.

The article presents a preliminary approach to solve the challenges described in research objective 2 from Section 1.3.

Article 2 - Journal paper

Balestra, Lorenzo; Schjølberg, Ingrid. (2021) Modelling and simulation of a zero-emission hybrid power plant for a domestic ferry. International Journal of Hydrogen Energy. vol. 46 (18).

- Contribution 3: Presents a dynamic model representing the operation of the hybrid powerplant of a maritime vessel utilizing proton exchange membrane fuel cells and batteries.
- Contribution 4: Provides a platform for the validation of results obtained with quasi static models of the powerplant.
- Contribution 5: Test of the dynamic model using real world data collected from a maritime vessel.

The article is used to address research objective 4 from Section 1.3. The case study developed in the article, considering a rule-based EMS, is carried out as a part of objective 5.

Article 3 - Conference paper

Balestra, Lorenzo; Yang, Ruochen; Schjølberg, Ingrid; Utne, Ingrid Bouwer; Ulleberg, Øystein. (2021) Towards Safety Barrier Analysis of Hydrogen Powered Maritime Vessels. ASME 2021 40th International Conference on Ocean, Offshore and Arctic Engineering Volume 6: Ocean Engineering.

- Contribution 6: Adapts the Barrier Operational Risk Analysis method, common for the oil and gas industry, to a scenario involving a hydrogen vessel.
- Contribution 7: Presents the qualitative risk analysis of a vessel equipped with cryogenic hydrogen storage considering the scenario of a leak below deck.

The article analyzes safety challenges related to hydrogen usage onboard a maritime vessel with a qualitative analysis. These challenges were identified during the development of objective 1 in Section 1.3.

Article 4 - Journal paper

Balestra, Lorenzo; Schjølberg, Ingrid. (2021) Energy management strategies for a zero-emission hybrid domestic ferry. International Journal of Hydrogen Energy. vol. 46 (77).

- Contribution 8: Using the dynamic model described in Article 2, performs a comparative analysis of different rule-based energy management strategies.
- Contribution 9: Compares the effectiveness of the presented energy management strategies using real-world data collected from a maritime vessel.

The article is used to expand on the work carried out in article 2, with the main focus directed at testing different EMSs, as specified in objective 5 from Section 1.3.

Article 5 - Journal paper

Balestra, Lorenzo; Schjølberg, Ingrid. (2022) Hybrid powerplant configuration model for marine vessel equipped with hydrogen fuel-cells **Submitted to:** International Journal of Hydrogen Energy.

- Contribution 10: Improves upon work carried out in Article 1, presenting a new quasi-static model for the evaluation of the power generation, storage and distribution in the vessel's electrical grid.
- Contribution 11: Present the new software based application that is built on the model, to automate the hybrid powerplant sizing process.

The article expands on the concept presented in article 1, where the first version of a model based application is introduced. The article's aim is to provide a comprehensive presentation of the new version of the model based application used for component sizing. This work is carried out according to research objective 2 from Section 1.3.

Article 6 - Conference paper

Balestra, Lorenzo; Schjølberg, Ingrid; Lenti, Manuel. (2022) Bayesian networks approach for safety barriers analysis: A case study on cryogenic hydrogen leakage. ASME 2022 41th International Conference on Ocean, Offshore and Arctic Engineering Volume 6: Ocean Engineering.

- Contribution 12: Performs the quantitative risk analysis of a scenario considering a leak onboard a hydrogen vessel with a cryogenic hydrogen storage. The analysis is performed using Bayesian networks and is a continuation of the work carried out in Article 3.

The article analyzes safety challenges relative to hydrogen usage onboard a maritime vessel with a quantitative analysis. This analysis is the continuation of the work carried out in article 3. These challenges were identified during the development of objective 1 in Section 1.3.

Chapter 2

Hydrogen in the transport industry

This thesis aim is to build in-depth knowledge about power generation and distribution onboard maritime vessels using proton exchange membrane fuel cells as energy source. This chapter provides scientific background informations that can be considered an introduction to hydrogen systems. Topics include hydrogen production, consumption, storage, and also related safety challenges. This brief overview is considered necessary to be able to evaluate the results obtained in this thesis and enclosed articles.

2.1 Hydrogen usage

In the transport sector, hydrogen can be used as a form of chemical energy storage onboard the vehicle. The key difference with fossil fuels is that hydrocarbons are harvested and split during their combustion phase (simplified example in Equation 2.1), releasing thermal energy through an irreversible reaction, and cannot be recombined to reform a hydrocarbon molecule unless a disproportionate amount of energy is used. On the contrary, hydrogen can be isolated from different sources, such as water, at the expense of energy, and is infinitely renewable.

$$2C_8H_{18} + 25O_2 \rightarrow 16CO_2 + 18H_2O \tag{2.1}$$

Hydrogen can be burned in internal combustion engines [27, 28] producing heat and mechanical power, or used in a chemical reactor, called fuel cell, where it is combined with oxygen producing electricity and water. The energy released

by the fuel cell is created by a flow of electrons through the reactor between anode and cathode. In this thesis, ICEs are not considered, and only the use of hydrogen inside a fuel cell is studied.

There are various types of fuel cells available on the market with different characteristics: alkaline fuel cells (AFC), proton exchange membrane fuel cells (PEMFC), direct methanol fuel cells (DMFC), phosphoric acid fuel cells (PAFC), molten carbonate fuel cells (MCFC) and solid oxide fuel cells (SOFC) (see Table 2.1). These fuel cells operate using different electrolytes, temperatures, efficiencies, fuel mixtures and can output power within different ranges. The performances of the fuel cell depend on the type of technology used, with most of them having an efficiency equal to around 55%, while AFC can reach up to 70% and DMFC are limited to 30%. The selection of a fuel cell for a specific application depends on performances, electrical efficiency, and operating temperature. Fuel cells requiring high operating temperature, such as SOFCs, are normally preferred in stationary applications where it is possible to take advantage of large sources of heat from industrial production or powerplants. The fuel cells with a low operating temperature are suitable for transport application.

Table 2.1: Different fuel cell types characterization [29]. The power range indicated in column 5 is not relative to the single fuel cell unit but to the total power of the application in which such type of fuel cell is used.

Fuel Cell	**Electrolyte**	**Operating Temperature**	**Fuel Mix**	**Power Range**
AFC	Potassium hydroxide (KOH) solution	20-90 C	H_2-O_2	100W-100kW
PEMFC	Proton exchange membrane	20-80 C	H_2-O_2	10W-10MW
DMFC	Proton exchange membrane	20-130 C	CH_2-OH-O_2	1-100W
PAFC	Phosphoric acid	160-220 C	Nat. Gas, Bio-gas H_2-O_2	100kW-100MW
MCFC	Molten Mixture of alkali metal carbonates	620-660 C	Nat. Gas, Bio-gas H_2-O_2	100kW-100MW
SOFC	Oxide Ion conducting ceramic	800-1000 C	Nat. Gas, Bio-gas H_2-O_2	1kW-100MW

The proton exchange membrane fuel cell (PEMFC), also referred to as polymer electrolyte membrane fuel cell, is the type of fuel cell that has seen the widest adoption in vehicles and transport applications. This type of fuel cells has a low operating temperature and pressure, and a good electrical efficiency with units reaching 60% peak efficiency. PEMFCs are built using a membrane electrode assembly which includes the electrodes, electrolyte, catalyst, and gas diffusion layers. More information on this type of fuel cell are presented in the dedicated section 5.1, where technical characteristics are discussed to lay the base for the PEMFC modelling. The H2maritime project focuses on the use of PEMFC for the transformation of hydrogen in electrical power onboard the considered maritime vessels. This type of fuel cell was considered the most suitable not only because of the performances, bus also due to the numerous commercial units available that have obtained certification to be used in maritime powerplants.

2.2 Hydrogen production

Hydrogen is referred to as energy carrier and not an energy source. This means that hydrogen cannot be harvested in its pure form, but to use its energy potential it is necessary to isolate it from other elements available on our planet. The production techniques are currently classified using colors defining the process used to isolate this energy carrier from other elements available in nature. The commonly used classification consists of:

- **Green**: Hydrogen produced by electrolysis of water, using electricity from renewable sources like hydro-power, wind and solar. Zero carbon emissions are produced.
- **Turquoise**: Hydrogen is produces by thermally splitting methane (methane pyrolysis). Instead of CO_2, solid carbon is produced.
- **Yellow**: Hydrogen is produced by electrolysis using grid electricity.
- **Blue**: Grey or brown hydrogen with CO_2 sequestration.
- **Red**: Hydrogen produced by electrolysis using nuclear power.
- **Grey**: Hydrogen extracted by natural gas using steam methane reforming.
- **White**: Hydrogen produced as a byproduct of industrial processes.
- **Brown**: Hydrogen extracted from fossil fuels using gassification.

In 2015, it was reported that 95% of the hydrogen produced was "grey" hydrogen [30], and in 2019 the situation was basically unchanged with only 4% of

the total hydrogen production being Green [31]. The production of Green hydrogen is expensive with current technology, hard to scale and is encountering the same challenges that other carbon-free technologies, like solar, have encountered and overcame in the past. The success of hydrogen heavily relies on the creation of an infrastructure that produces the majority of its hydrogen cheaply and using carbon-free methods, but currently only a few commercial companies are investing in this type of production. Grey hydrogen is currently obtained from hydrocarbon molecules, such as methane (CH_4), with the energy necessary for this process also obtained from fossil fuels. The process is called steam-methane reforming reaction. The reaction is conducted in a reformer vessel where a high pressure mixture of steam and methane are put into contact with a nickel catalyst. Catalysts with high surface-area-to-volume ratio are preferred because of diffusion limitations due to high operating temperature [32]. The reaction is represented by this equilibrium:

$$\mathrm{CH_4 + H_2O + Heat \longrightarrow CO + 3\,H_2} \tag{2.2}$$

The capital cost of steam reforming plants is considered prohibitive for small to medium size applications and can be considered as one temporary solution to supply hydrogen while new carbon free technologies are developed. Building a hydrogen infrastructure mainly based on steam reforming is not sustainable for the future and is counterproductive in terms of efficiency, when the natural gas can be used directly in solid oxide fuel cells with fewer losses in the energy chain.

Currently the alternative to steam reforming is water electrolysis. The basic process for electrolysis was developed at the beginning of the 17th century, and has become a well matured technology for hydrogen production up to the megawatt range. Water electrolysis for the production of hydrogen constitutes the most extended electrolytic technology at a commercial level worldwide [33]. In this technology, a DC electrical power source is connected to two electrodes, typically made from some inert metal such as platinum or iridium, which are placed in water. Hydrogen will appear at the cathode, where electrons enter the water, and oxygen will appear at the anode. Assuming ideal faradaic efficiency, the amount of hydrogen generated is twice the amount of oxygen, and both are proportional to the total electrical charge conducted by the solution. In pure water at the cathode a reduction reaction takes place, with electrons (e-) from the cathode being given to hydrogen cations to form hydrogen gas. The half reaction, balanced with acid, is:

$$\mathrm{2\,H^+ + 2\,e^- \rightarrow H_2} \tag{2.3}$$

At the anode, an oxidation reaction occurs, generating oxygen gas and giving electrons to the anode to complete the circuit:

$$2\,H_2O\,(l) \rightarrow O_2(g) + 4\,H^+(aq) + 4\,e^- \tag{2.4}$$

The same half-reactions can also be balanced with the base, at the cathode:

$$2\,H_2O\,(l) + 2\,e^- \rightarrow H_2(g) + 2\,OH^-(aq) \tag{2.5}$$

And at the anode:

$$2\,OH^-(aq) \rightarrow \frac{1}{2}\,O_2(g) + H_2O\,(l) + 2\,e^- \tag{2.6}$$

Not all half-reactions must be balanced with acid or base. Many do, like the oxidation or reduction of water listed here. To add half reactions they must both be balanced with either acid or base. The acid-balanced reactions predominate in acidic (low pH) solutions, while the base-balanced reactions predominate in basic (high pH) solutions. Combining either half reaction pair yields the same overall decomposition of water into oxygen and hydrogen:

$$2\,H_2O\,(l) \rightarrow 2\,H_2(g) + O_2(g) \tag{2.7}$$

Conventional alkaline electrolysis has an efficiency of about 70% [34].

Electrolysis can be carried out using proton exchange membrane, also referred to as polymer electrolyte membrane. PEM electrolyzers can operate at much higher current densities, capable of achieving values above 2A cm^{-2}, this reduces the operational costs and potentially the overall cost of electrolysis [35]. Accounting for the accepted use of the higher heat value, because inefficiency via heat can be redirected back into the system to create the steam required by the catalyst, average working efficiencies for PEM electrolysis are around 80% [36]. This is expected to increase to between 82–86% [37] before 2030.

From a logistical perspective, green hydrogen can be produced either in a centralized plant or on-site, closer to the distribution point (see Fig. 2.1). A centralized electrolyzer plant offers numerous benefits with easier maintanence and control of the electrolyzers. This solution can also process the hydrogen more efficiently from its low pressure state to its final storage form (compressed or cryogenic). The main drawback is that it introduces transportation costs to the

distribution stations. Production of Green hydrogen directly at distribution station eliminates transport costs but can be problematic from a maintanence, control and safety perspective. Many projects are considering centralized distribution hubs were it is possible to refuel city taxis, busses and ferries from a centralized plant placed strategically in a urban area [38].

Figure 2.1: Hydrogen production and refueling station in the city of Aberdeen, Scotland

2.3 Balance of plant components

Auxiliary components are necessary to generate electrical power with a fuel cell stack (see Fig. 2.2). These components make up a large portion of the system in terms of footprint compared to the space occupied by the stack itself. A key element to take into consideration with respect to auxiliary components is the reliability and durability, as their malfunctioning compromises the ability of the fuel cell to operate within operational parameters. In this section is presented a brief overview on the auxiliary systems necessary to run a fuel cell system.

The goal for auxiliary components is to keep the FC stack within operational parameters. The FC stack itself is a chemical reactor with no moving parts, so it does not experience degradation related to the component's friction. The degradation the stack comes mainly in the form of mechanical degradation, thermal degradation and electrochemical degradation of the polymer electrolyte membrane [39]. In addition to membrane degradation, a deterioration in performances is experienced by the electrocatalyst and catalyst layer aswell, where Pt and binary, ternary, or even quaternary Pt-transition metal degrading much faster under harsh conditions.

The fuel cell system includes also a series of traditional components that can be classified as high temperature components or low temperature components. One high temperature components is, for example the heat exchanger included in

the cooling system. Other high temperature components are the inter-cooler in the air supply system and the gassifier connected to a cryogenic hydrogen tank. Low temperature components include pumps blowers and compressors used to supply fuel and oxidant to the fuel cell stack. Other low temperature components include valves, system actuators, pressure regulators and fans. Many auxiliary components, both classified as high or low temperature have a design similar to the one included in traditional systems. The cooling system to and from the fuel cell stack, for example, resembles the one installed with an internal combustion engine and operates practically in the same temperature range. These components shared with traditional systems have been studied for years in terms of reliability and durability and are optimized to achieve the longest lifespan possible.

There are also components that are specific to the hydrogen system, such as pumps able to recirculate hydrogen, and valves able to withstand low density and high pressure hydrogen gas [40]. Many auxiliary components consume parasitic power and the extra fuel consumption needs to be taken into account.

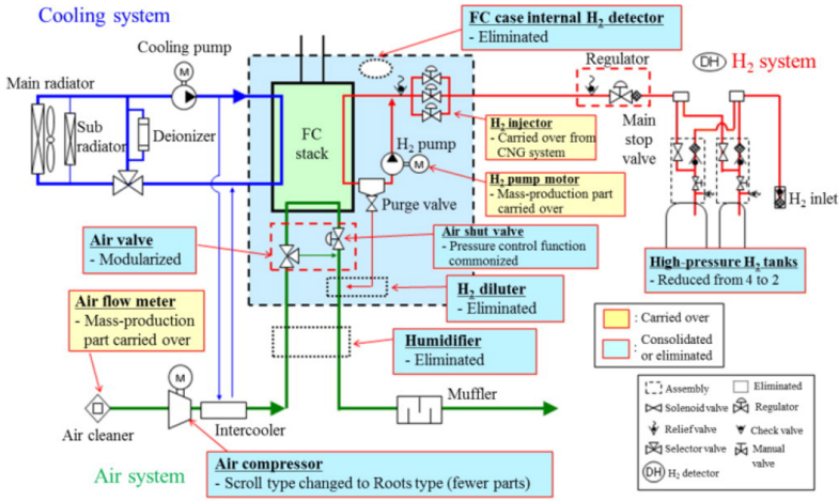

Figure 2.2: Hydrogen powerplant system for automotive applications from the schematics of the Toyota Mirai. The system includes the balance-of-plant components required for the fuel cell

2.4 Hydrogen safety

In every sector of the transportation industry the safety aspect related to the fuel storage plays a key role, especially when considering the transport of passengers. The maritime industry currently uses LNG or other high-flammable compressed or cryogenic gasses to power ships, but pure hydrogen poses additional

challenges with its chemical and physical properties being different from conventional fossil fuels.

Hydrogen can easily escape through joints and seals that would retain natural gas. These joints and seals have to be therefore specially designed, maintained on frequent schedule, and closely inspected at the beginning of every bunkering operation. The thickness of insulation around the tank is also a key difference when considering the cryogenic form. Normal 40cm LNG insulation is not enough to maintain a stable temperature of -253°C and while a moderately large LNG tank could lose 0.2% of its total volume a day if stored in the same kind of tank the LH2 actually lost would be around 5% [41].

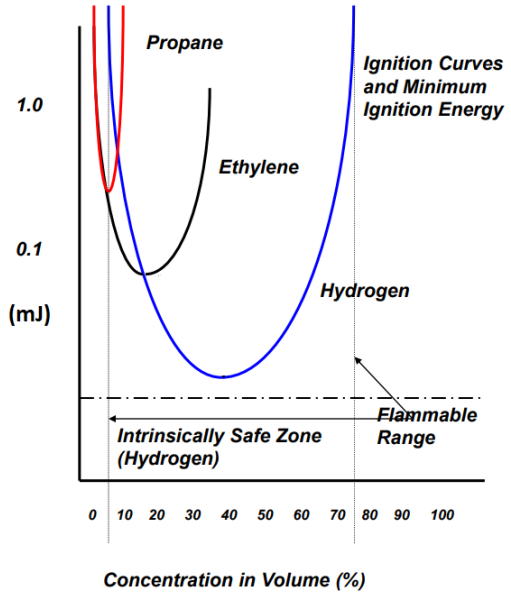

Figure 2.3: Minimum ignition energy curves for propane, ethylene and hydrogen compared as a function of the concentration in atmospheric air [Source: JSS Technical service]

Hydrogen has a wide range of flammability in air compared to natural gas, with concentrations ranging between 4% and 75%, compared to 2% to 10% of propane and 5% to 15% of methane. This, combined with the low minimum ignition energy of 0.02 mJ, compared to the 0.25 mJ of propane in 5.2% O_2, can create serious safety hazards in uncontrolled releases (see Table 2.3). A consequence of the wide flammability range and low ignition energy can be observed in Figure 2.3, where the ignition curve for hydrogen spans on a much wider range with respect to both propane and ethylene, resulting in an increased likelihood of ignition and explosion, if released. If ignited, hydrogen is odorless and burns with a color-

less flame [42]. A hydrogen fire is recognisable from the distance only by using a thermal camera. This difference between fossil fuels and hydrogen is highly relevant during the design phase of the vessel when considering the placement of the hydrogen tanks.

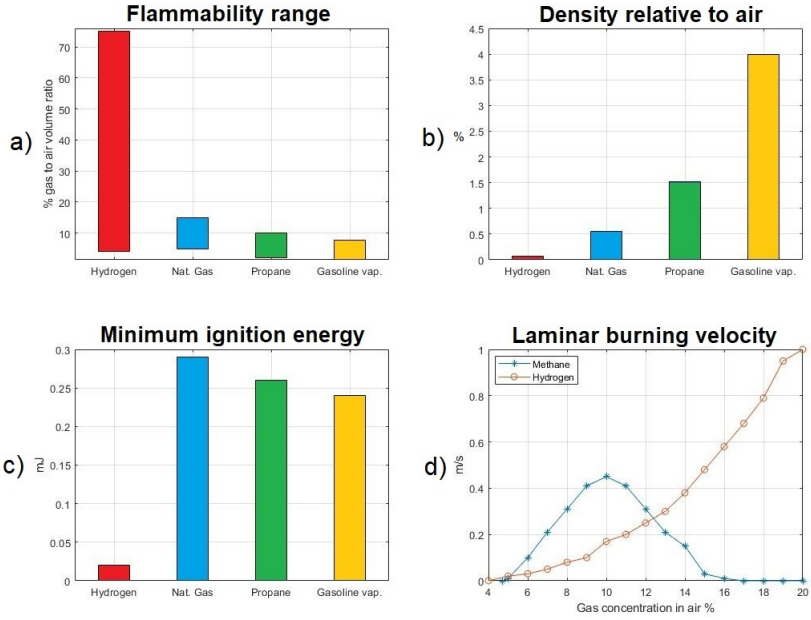

Figure 2.4: The a,b,c graph compare the characteristics of hydrogen, natural gas, propane and gasoline vapor.(a) Flammability range expressed as a function of the % of gas to air volume ratio, (b) Density of the flammable sources relative to atmospheric air, (c) minimum ignition energy expressed in mJ. (d) Laminar burning velocity in m/s comparison between hydrogen and methane as a function of the concentration in atmospheric air

Some of the safety concerns when dealing with hydrogen are counterbalanced by some positive aspects. The low density of hydrogen allows for a much faster dispersion rate compared to natural gas (table 2.2), provided that enough ventilation is available. In addition, electric current carrying capacity is also smaller than in natural gas with charge buildup not being a concern for flowing liquefied H_2 [43].

Safety aspects related to the use of hydrogen onboard a maritime vessel were studied in Article 3 and 6 (see Section 7). In these articles the Barrier and Operational Risk Analysis (BORA) method is applied [44, 45]. This method, used in the Oil and Gas industry has been applied to a case considering the release of cryo-

genic hydrogen onboard a vessel. The articles describe respectively a qualitative and quantitative risk analysis analyzing the safety barriers identified. The work highlights possible weaknesses in some technical and administrative aspects that can be considered by the designers of the vessel or the crew operating it.

Table 2.2: Buoyancy behaviour of hydrogen at different temperatures [46]

Property	Hydrogen
H2 at 20°C	Very buoyant
H2 at -253°C	Neutral
H2-Spray	Dense gas behaviour

Table 2.3: Stoichiometry, detonation and explosion limits comparison for hydrogen and methane

Property	Hydrogen	Methane
Explosion Limits	4% to 75%	5% to 15%
Detonation Limits	15% to 60%	5% to 15%
Stoichiometry	29,6%	9,5%

2.5 Energy density and storage solutions

The energy density and storage problem is a key challenge in the transition from fossil fuels to hydrogen for the production of electrical power onboard a vehicle. While the gravimetric energy density of hydrogen is much higher than any fossil fuel commonly used in the transport industry, its volumetric energy density is low (see Fig. 2.5). This is one of the reasons why hydrogen is still not usable as a direct replacement for fossil fuels, and it is relegated to specific zero-emission applications. As a result, one of the most important factors for the adoption of hydrogen systems is the creation of new storage solutions that can increase the volumetric energy density and ensure that the hydrogen is stored safely.

The limitation regarding the volumetric energy density of hydrogen is one of the factors that defined the power range for the maritime vessels considered in this thesis. Long-range routes operated by cargo and container ships, equipped with high efficiency 2 stroke engines, cannot be currently operated by hydrogen powered ships unless a considerable portion of the cargo area is dedicated to hydrogen storage. At the same time, for systems below 1 MW, the initial investment and running costs required for systems using hydrogen are high, and aren't currently competitive solutions, while achieving a very small reduction in emissions.

There are currently multiple hydrogen storage solutions on the market, both for the storage of pure hydrogen and for the storage of hydrogen carriers, liquid and solid. Each technology has its own advantages and disadvantages in terms of energy density and safety (see Table 2.4).

Table 2.4: Energy density for hydrogen and considered energy carriers

Form of Storage	En. den. by weight [kWh/kg]	En. den. by volume [kWh/l]
Gas (30 MPa)	33.3	0.75
Gas (70 MPa)	33.3	1.386
Liquid (-253°C)	33.3	2.36
Metal hydride	0.58	3.18
Ammonia (NH_3)	2.44	3.6
$Mg(NH_3)_6Cl_2$[23]	2.44	3.6
LOHC (Dybenzyltoluene)	1.9	1.9

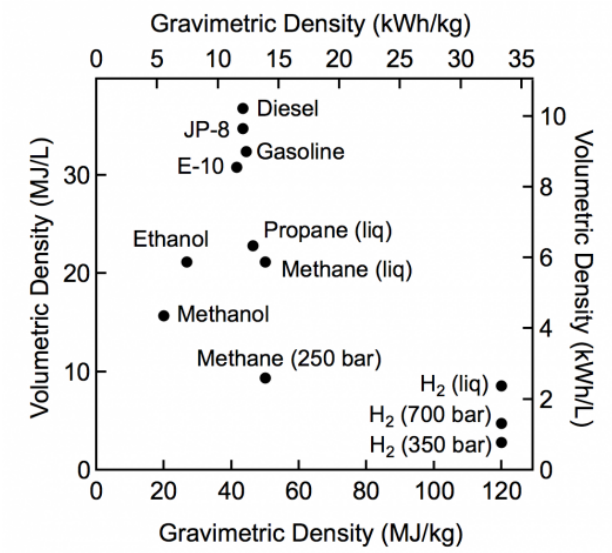

Figure 2.5: Volumetric and gravimetric energy density for commercial fossil fuels, alcohol based fuels, and hydrogen

Chapter 3

Maritime electrical installations and hybrid systems for maritime propulsion

Today electric propulsion is widely adopted in the maritime sector and found on numerous vessels belonging to different types and classes. This type of propulsion allows for higher efficiency and lower fuel consumption in specific applications, such as during low load conditions or dynamic positioning operations (DP) [47]. This is possible by mechanically decoupling the source of power (prime mover, usually an ICE) from the propeller. The connection that was previously realized with a propeller shaft, is now substituted by an electrical grid that transfers electrical power from the generators to the motors.

Further optimization of operations can be achieved by combining multiple components able to produce, release or store electric power, realizing a hybrid system [48]. Hybrid systems, in the maritime sector, have seen increasing adoption as they are able to solve technical challenges, such as zero-emission navigation. Hybrid systems increase complexity in a maritime powerplant and its initial cost, but offer a reduced vulnerability to single failures of the components, a lower fuel consumption through the use of smart load sharing strategies, and can improve performances using each components in its best output range.

In this chapter are presented informations regarding the diesel-electric configuration, and the hybrid configurations including batteries and hydrogen fuel cells. The state-of-the-art for these two types of configuration is described, including a characterization of the types of electrical grid and components required

for efficient operations. The configurations presented provide a scientific background used for the development of the models described in the articles enclosed in this thesis. The possibility to compare the older architecture, based on ICEs, with the one utilizing hydrogen fuel cells and batteries helps to better understand challenges and opportunities provided by this transition for the transport industry, including, but not limited to zero-emission propulsion.

3.1 Conventional and diesel-electric propulsion

Conventional propulsion systems, in the majority of cases, include an internal combustion engine that burns marine diesel or heavy fuel oil and is connected to the propeller shaft directly, or through a gearbox with different reduction ratios. In this configuration, the connection between the prime mover and the propeller is mechanical and the rotational speed of the propeller is a function of the rotational speed of the engine's crankshaft. The electrical power needed for auxiliary and hotel load is provided by generators, usually diesel engines of smaller size, connected to the vessel's electrical grid. This layout provides limited flexibility and does not allow load sharing between the main diesel engine and the generators.

In diesel-electric propulsion one or more diesel generators are connected to a central switchboard that distributes power to both propulsion motors and inboard loads [47] (see Fig. 3.1). Diesel-electric powertrain configurations normally use alternating current (AC) for power distribution within the vessel's electrical grid. The propellers are not driven by a shaft connected to the engine but by electric motors. The propellers can be connected to the electric motors using a transmission, or directly, as it is done in azimuth thruster pods. The rotational speed of the propeller, in this case, is not a function of the rotational speed of the engine anymore, allowing for greater load regulation.

There are multiple advantages when adopting this configuration compared to the conventional layout, both in terms of performances, footprint usage and reliability. The first advantage is given by the connection of all the components to a single controlled electrical grid, allowing more flexibility with respect to load delivery. With all the components connected, the propulsion system can be based around high/medium speed diesel engines that create less vibrations and have faster response time in load transients. No additional diesel generator is required for the delivery of hotel loads. Another advantage is the improved maneuverability and the possibility for efficient station-keeping when azimuth podded propellers are used. This also create less propulsion noise and increases efficiency. From a footprint perspective a diesel-electric drive occupies less space than the equivalent conventional geared drive allowing the aft section to be slimmer and giving better flow over the propeller. Not only is the diesel-electric drive train lighter than a

large two-stroke engine, but also its weight can be distributed more evenly.

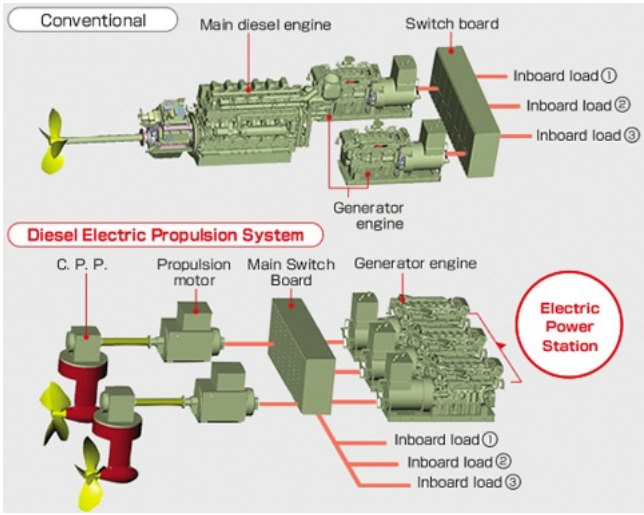

Figure 3.1: Conventional configuration based on direct propulsion (top) and diesel-electric propulsion system (bottom) [Source: yanmar.co.jp]

Diesel-electric layouts are the configuration of choice for ship with high inboard loads, ships that spend extended amount of time in dynamic positioning mode, ships with high load transients or that do a lot of maneuvering [49]. Vessels like drill ships, where the main propulsion system is used only in transit, are one ideal case for this configuration as they require large amounts of energy even when stationary. Icebreakers are also a special case. Here diesel-electric propulsion is a favourite configuration since it meets the requirements for maximum output at very low speeds. For vessels such as floating production storage offloading (FPSO), the choice of diesel-electric drive is almost automatic, since about 80 percent of time is spent on production at low power while in station-keeping mode. The remaining time is split between transit, offloading, standby and production at variable loads. The last vessel type that uses almost exclusively diesel-electric layouts is the cruise ship. In this type of ship there is a primary need of limiting the vibration for the comfort of the passenger. It is also relevant that these ship hop from one port to the other, with short periods at sea eliminating some of the advantages given by the low speed 2 stroke diesel engines. This kind of vessel has also very high hotel loads (inboard loads) compared to propulsion loads and having multiple efficient motor both taking care of the propulsion motor and the inboard load is a more efficient solution than separating the main engine from generator engines.

The transition from a conventional system to a diesel-electric system allows the ship operator to deliver the load more efficiently by switching on/off generat-

ors according to the load requirements, with the aim of remaining for the longest amount of time possible within the zone of maximum efficiency (see Fig. 3.2).

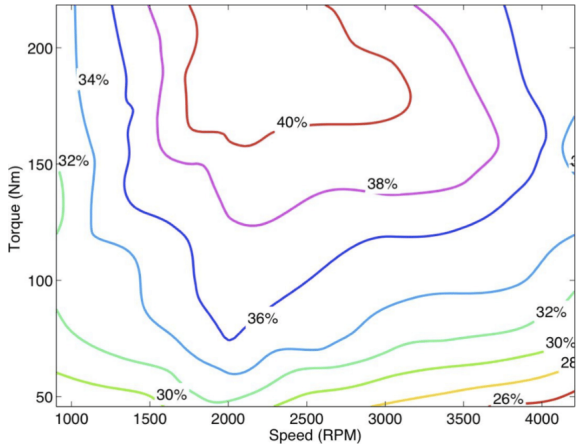

Figure 3.2: Efficiency map (hill diagram) of a generic mid-speed diesel engine as a function of rotational speed of the crankshaft and torque produced

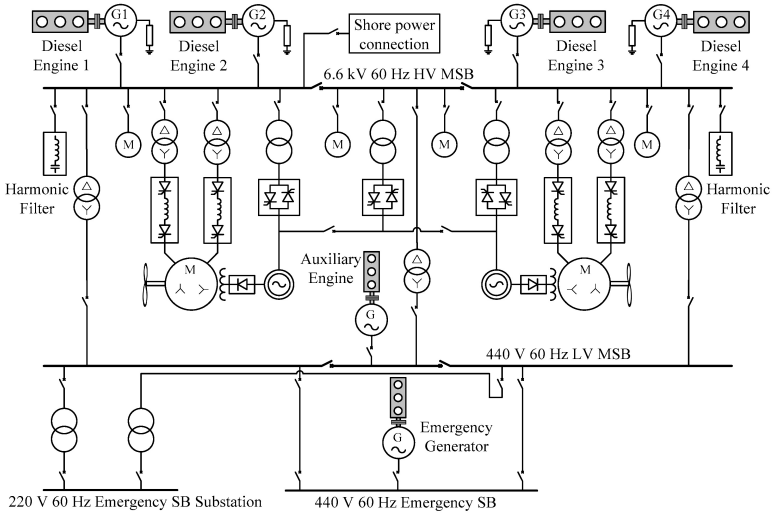

Figure 3.3: Single line diagram detailing the components of the diesel-electric system equipped with a radial AC distribution system (M: motor, MSB: main switchboard, VSD: variable speed drive) [50]

With this configuration it is possible to use fixed pitch propellers at a controlled speed, independent from the engine, and avoid the used of controlled pitch pro-

peller that experience much higher losses in low load conditions.

3.2 Diesel-electric propulsion with energy storage

The electrification of the powertrain using the diesel-electric configuration opens the possibility to further improve the system's efficiency with the installation of one or more energy storage unit [51]. The most common energy storage solution is the battery (Li-Ion, Ni-Mh, AGM), but supercapacitors may also be used in specific applications, when a very short response time to transient loading conditions is needed (see Fig. 3.4). In this hybrid configuration, the electrical power can be distributed using either an alternating current (AC) or a direct current (DC) grid. With gains on the overall weight and complexity of the system, but drawbacks with respect to additional safety equipment and challenges, the choice of DC over AC ultimately comes down to the quantity of DC producers/users on the grid. The choice is also influenced by the difference in initial investment between the two solutions.

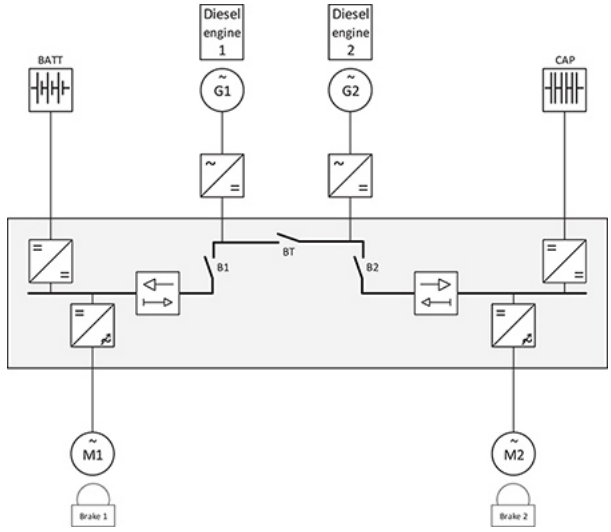

Figure 3.4: Single line diagram of system including diesel engines, batteries and supercapacitor [Source: ABB]

The grid of a maritime vessel is an isolated grid, where the energy has to be balance at all times, with unused energy disposed off as heat. The introduction of an energy storage solution can greatly reduce fuel consumption and emissions by allowing the storage of the energy surplus, for it to be released during periods of energy deficit [52]. With the system controlled by a smart energy management strategy, high frequency transient loading conditions can be greatly reduced,

maintaining the diesel generators, for as long as possible, within their output range of peak efficiency, and without the need to switch them on and off [53]. High frequency transients are compensated by the battery that has generally lower response time and a faster dynamic response than a diesel engine. A secondary advantage of adding battery to the system is the increased redundancy achieved in relation to power generation. Even during a failure of the diesel engines, the battery is able to provide electrical power to important systems making the ship more blackout-proof.

The control of a hybrid diesel-electric system with energy storage is non-trivial as the different components generating or storing power have different technical limitations and a different dynamic behavior. The control of a hybrid system such as the one seen in Fig.3.4 needs careful analysis of the technical components, the operational profile of the vehicle and the definition of the key factors for the optimization of the powertrain design [50]. The challenges encountered in the formulation of smart control strategies are a key topic of this thesis, together with the problem of component sizing.

3.3 Hydrogen fuel cell and battery configurations

The hybrid configuration studied in this thesis consists of a combination of proton exchange membrane fuel cells and batteries (see Fig. 3.5). In the considered powertrain, fuel cells are tasked with the onboard power generation, replacing the diesel generators entirely. The batteries included in the system are needed for the start-up procedure of fuel cells and BOP components, and perform as an energy storage during normal operation, similarly to what is described in the previous section 3.2. This hybrid configuration ensures zero-emission navigation with medium range capabilities thanks to the higher energy density of hydrogen when compared to batteries.

Considering a series of technical and economic factors, the type of fuel cell chosen for this powerplant is the proton exchange membrane fuel cell (PEMFC). Section 5.1 provides more detail on the choice of this type of fuel cell. The battery chosen for this application is of the Lithium-Ion type as described in section 5.2. With both the PEMFCs and batteries having a direct current (DC) output, the type of grid considered is using DC. The adoption of DC grids in the maritime industry has increased thanks to the offered weight saving, increased efficiency thanks to lower electrical conversions, and improved dynamic response. Drawbacks of this type of grid include the technical difficulty of interrupting safely a DC current and the need for a much faster fault detection system. More information on the grid are provided in Chapter 5.

While internal combustion engines have been used for decades in the maritime industry, allowing the refinement of the architecture for maritime use, PEMFCs are at a lower technology readiness level (TRL), with only a few installation onboard vessels. The lower TRL and market adoption determines a general lack of data for factors such as PEMFC degradation, to determine the real operational life of the unit, as these studies require long-term testing or the monitoring of units in commercial applications during, and at the end, of their life cycle. The installation of PEMFCs in maritime vessels poses additional challenges when compared to road or rail vehicles. Some of these challenges include the need to satisfy the requirements of high power density related to weight and size, tolerance to salt air, shock resistance, and load responding characteristics [54].

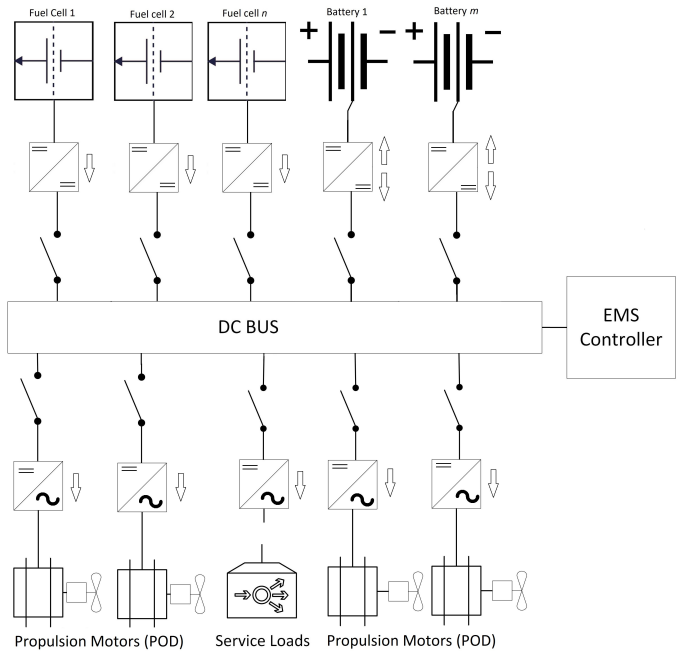

Figure 3.5: Hybrid configurations with PEMFCs and batteries, simplified single line diagram of DC grid

To target the power density problem, PEMFCs stacks or modules (defined as connected stacks) of increasing size are being built by multiple companies around the globe to satisfy the needs of the maritime industry. These modules normally are considered as a complete solution and include the BOP components and offer good power density and load responding characteristics similar to the ones of a large diesel engine. Such systems can be scaled up to the megawatt scale to satisfy the power requirement of larger vessels.

Air filtration is another key factor in avoiding reduction in efficiency and life, as a result of poisoning of platinum catalysts by airborne contaminants [55]. In addition to the standard filtration of contaminants, the air filters installed in a maritime system have to take into consideration the presence of sea spray. Sea spray are aerosol particles formed from the ocean, mostly by ejection into Earth's atmosphere by bursting bubbles at the air-sea interface [56]. Sea spray contains both organic matter and inorganic salts that form sea salt aerosol (SSA) that needs to be filtered out for the correct operation of the PEMFC. Shock and vibration resistance and other reliability factors are extremely important for this new technology as the grid of the ship is an isolated grid and the failure of multiple units could lead to the ship blackout. Regulations for hydrogen systems onboard ships have been formulated by maritime classification societies [57, 58] and are in constant evolution to ensure that the designed systems have the appropriate active and passive redundancy features for maritime operations.

Chapter 4

Onboard powerplant balancing software

The design phase of a hybrid powerplant for a maritime vessel utilizing fuel cells powered by hydrogen, and batteries, consists in defining the composition of such a powerplant and how it is controlled. The composition of the powerplant is defined by calculating the number of components required to satisfy the power demand of the considered vessel, in addition to the definition of component's technical characteristics and performances. This activity is referred to as component sizing (CS). The control of the powerplant is performed using an energy management strategy (EMS). The EMS controls the power production and distribution within the vessel's electrical grid. The definition of CS and EMS needs to be performed concurrently as the definition of one influences the other and vice-versa.

In this chapter, a software built as a Matlab application is presented. The software based application is built using a quasi-static model of the hybrid powerplant, focusing on power generation, storage, and distribution inside the vessel's electrical grid. The use of a quasi-static model allows for the observation of a system with time dependent variables over an interval of time, while considering that the system, in this case the electrical grid, operates in a state of equilibrium. The model considers each instant as separate and the previous or following instants do not influence the simulation. Calculations performed with this software named ZEPCo for Zero Emission Powerplant Configurator, allow for the quick configuration of the powerplant. The software calculates possible combinations of CS once an EMS is selected by the user.

The work described in this chapter is reported in Article 5, with an earlier

version of the application described in Article 1 (Chapter 7). The software is developed in Matlab and provides and efficient tool, with respect to computational resources, to calculate CS configurations that comply with the requirements specified by the user during setup. The use of Matlab for this software makes the integration with the Simulink dynamic models described in Chapter 6 easier. The model of the hybrid system, used as a base for the software, is developed with versatility in mind, and allows to perform the CS for maritime vessels, but also for other types of vehicles such as road heavy duty transport. This versatility is made possible by the nature of the hybrid powerplant, that consists of many individual modules that can be connected in parallel to achieve the required power level.

4.1 Algorithm logic and boundary conditions

The configuration of the hybrid fuel cell and battery powerplant is carried out through the definition of four factors:

- **Energy management strategy (EMS)**: Set of rules or conditions that allow to regulate the energy production, consumption, distribution and storage in a vessel's electrical grid. The EMS defines the load sharing strategy between the fuel cells P_{fc} and battery P_{b}.
- **Fuel cells technical data**: Data that allows the characterization of the components considered. This type of data can usually be obtained from the datasheet of the commercial model considered. These include the fuel cell maximum power, rated power, efficiency variation.
- **Battery technical data**: Data that allows the characterization of the battery module or battery cell depending on the case considered. These data include battery capacity, rated discharge/recharge current, and C-Rate.
- **Number of units**: The number of fuel cells (n_{fc}) and batteries (n_b) required to satisfy the power demand during operations.

To complitely define a hybrid powerplant, all four of the above mentioned factors have to be determined during the design phase. Because the combination of factors that satisfy a specific use case are mathematically infinite, some boundary conditions need to be put into place to create an efficient algorithm for the software based application, that is able to solve the design problem for efficient vessel's operations.

The design problem is a non-trivial problem as the number of units and their technical data defines the EMS required to carry out efficient operations, while

the definition of the EMS determines a the number of components and the required characteristics. Because of this reciprocal relationship, the configuration of the powerplant carried out using the software based application described in this chapter starts from the definition of the EMS and calculates the remaining factors.

The composition of the powerplant is defined based on the power demand (P_{op}) during the operational interval considered. The power demand, also referred to as operational profile (OP), is required as a model input at the beginning of the calculations. The number of components, intended as the number of proton exchange membrane fuel cells (n_{fc}) and the number of batteries (n_{b}), required to satisfy the OP is calculated as a function of the technical data provided for the components. The total power rating of the vessel's powerplant can be reached by considering multiple fuel cell stacks and battery modules as connected in parallel. In this case, all the fuel cell stacks are considered identical between each other and are characterized using the technical data provided by the datasheet of the unit. The same approach used for the fuel cell can be also considered applied for the batteries, with modules installed in the system being identical between each other and with the same technical characteristic. The technical data for the fuel cell stacks and for the battery cells are obtained from commercially available components.

The software execution steps for a case where the proton exchange fuel cell (PEMFC) data are provided as input are represented in the flowchart in Figure 4.1.

4.2 Operational profile selection

To perform the calculations required to determine the composition of the powerplant, the operational profile, representing the power demand during the interval considered, needs to be known. The operational profile is provided as input by the user as an array of power values with a known sampling rate.

The operational profile of the vessel can be obtained by sampling the power produced by the vessels or estimated using data-mining. For a retrofit operation, it is possible to sample the power output of the vessel operating under the conventional propulsion system. The sampled values provide a target for the power delivery of the fuel cell and battery system. The hybrid system has to replicate the power delivery of the conventional propulsion system to ensure the same level of performances. For a new ship design, the operational profile needs to be built, prior to the software execution considering factors such as length of the route, hydrodynamic performances of the hull (or foils), typical meteorological conditions on the route and many more. This case proves non-trivial as large databases needs to be analyzed to have an accurate estimation of the power demand over time.

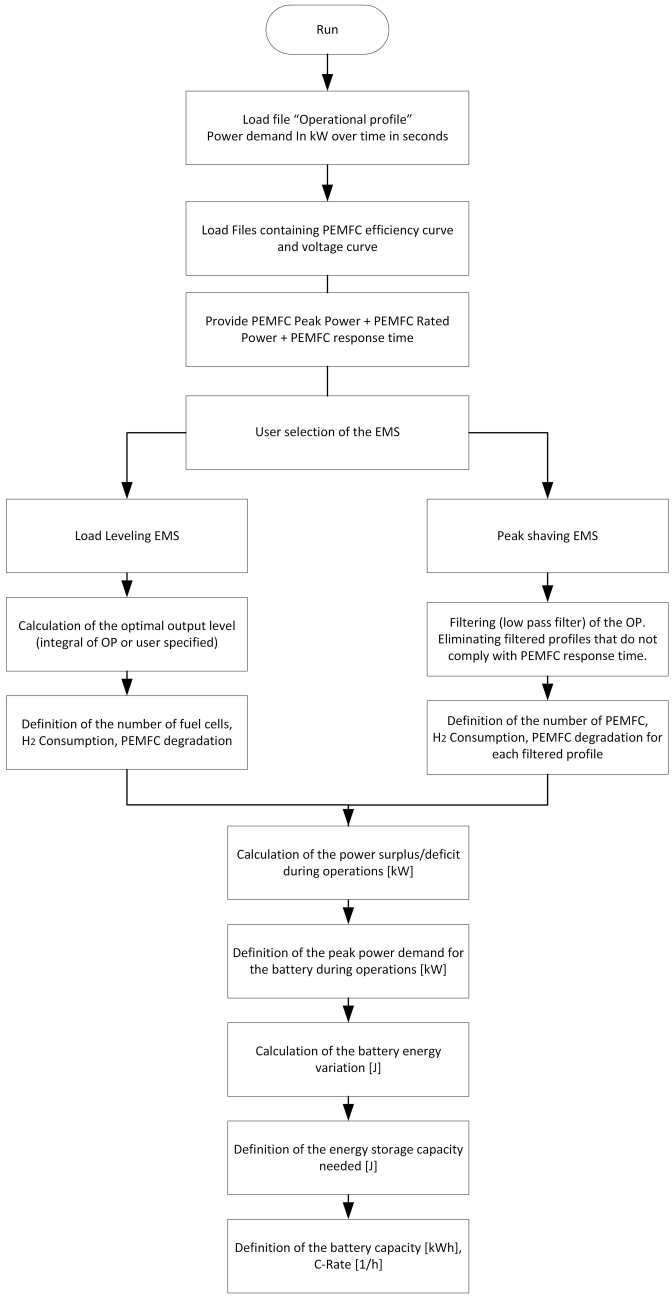

Figure 4.1: Flowchart describing the algorithm of the MATLAB application ZEPCo

In this thesis all the vessels considered are currently operational and use a

powerplant where the prime movers are internal combustion engines (see Section 1.5.2). The layout and type of powerplant installed on these vessels needs to be taken into consideration when defining the approach used approach used for the collection of the power output values. The double-ended ferry operates using a diesel-electric configuration, and AC grid distribution, while the harbor tugboat uses a conventional configuration with two diesel engines and a gen-set. Taking these differences into consideration, the operational profiles used in this thesis and enclosed articles are built by summation of the output of all the individual internal combustion engines installed in the system. In the case of the double ended ferry the power is considered to be the output of the AC generators coupled with the diesel engines (see Fig. 4.2). In the case of the harbor tugboat the power output is obtained by adding the output of the two main diesel engines and the one of the generator, prior to the distribution into the grid to the propulsion or auxiliary systems. This approach means that the operational profiles considered set a target for the power delivery at the DC-bus level, where the load is directly simulated.

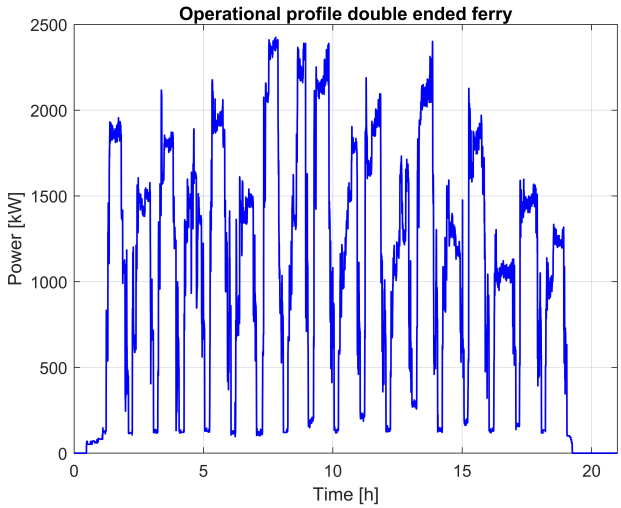

Figure 4.2: Operational profile of the Langelandslinje ferry during one day of operation

4.3 Energy management strategy

The energy management strategy (EMS) is the first of the four factors identified in Section 4.1 that defines the powerplant configuration and operation. The EMS defines how the power is generated within the vessel's grid, and how the energy storage capabilities are managed during operations. The EMS's task is to use the components of the powerplant, following a series of rules or parameters, to satisfy the power demand determined by the operational profile.

The category EMSs onto which focus was placed at this stage of development was the one defining deterministic rule-based EMSs. This type of EMS operates using a series of pre-determined rules and conditions that define the different state of the systems during operations, and the output (or input) of each component at every instant. Rule-based EMSs are considered robust and easy to implement. The computational resources needed to run a rule-based EMS in a vessel's control unit are very low.

Two types of rule-based EMS are considered in this chapter: a load leveling EMS, and a peak shaving EMS. Load leveling is an approach commonly found in land-based grids or powerplants with large power ratings. When using this EMS, the main energy source, in our case the PEMFCs, are set to a constant power level (P_{L}). A constant power output by the PEMFCs allows to complitely eliminate transient loading conditions, eliminating problems related hydrogen or air starvation, or conditions that cannot be realized due to the slowness of electrochemical reactions inside the PEMFC. A constant output also reduces the degradation of the PEMFC. Load variations are compensated by storing power during periods of low demand and delivering it during periods of high demand. This strategy therefore requires large battery packs to operate efficiently.

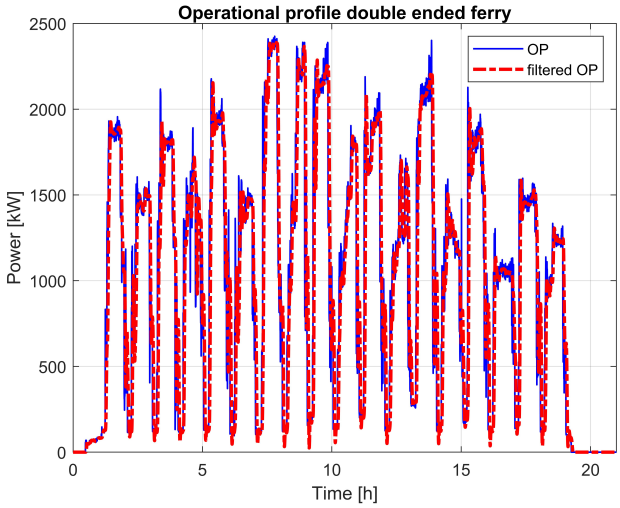

Figure 4.3: Filtered operational profile (red) and original profile (blue) for the Langeland double ended ferry. The profile considers a full day of operations, with 18 crossings

The peak shaving strategy is a rule-based strategy that uses a low pass filter on the operational profile, filtering-out high frequency load transients. The filtered profile defines the output of the PEMFCs installed in the system, while the power

surplus/deficit is managed by the battery. The filters considered in this thesis and included in the software based application are Butterworth, Gaussian and Chebyshev. Each filter is defined by a series of parameters that are considered as variables:

- **Butterworth filter**: Order and Cut-Off frequency.
- **Gaussian filter**: Smoothing kernel and standard deviation (default is 0.5)
- **Chebyshev filter**: Normalized pass-band edge frequency (Wp) and decibels of peak-to-peak pass-band ripple (Rp).

Each filter provides a different frequency response (see Fig. 4.4) when the parameters that defined it are changed. This allows the user to define the smoothing of the operational profile, and consequently the amount and intensity of transient loading conditions for the PEMFC. Iterating through different parameters allows the user to find a configuration that complies with the technical specifications of the selected model of PEMFC.

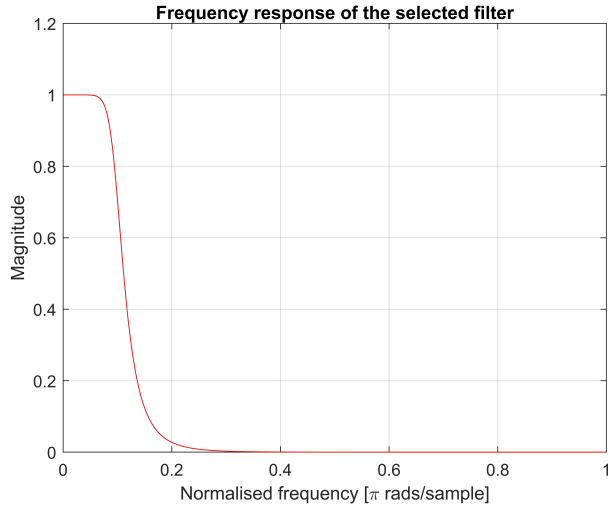

Figure 4.4: Example of frequency response of a Butterworth filter with order 5 and cut-off frequency of 0.1. This filter is the one applied to the operational profile in Figure 4.3

4.4 Powerplant components model

The proton exchange membrane fuel cell is modelled as a serial circuit of an ideal voltage source V_{fc}, and a total internal resistance R_{fc}. The performance of the fuel cell is characterized using the data of Table 4.1, in addition to the efficiency

η_{fc}, and voltage V_{fc} data provided as a function of the current output (see Fig. 4.5). The definition of the voltage curve allows the calculation of the PEMFC power curve, determining the power output for every operational point, and the definition of the efficiency curve allows the calculation of the hydrogen and oxygen consumption.

$$P_{\text{fc}}(t) = V_{\text{fc}}(t)\, I_{\text{fc}}(t) = V_{\text{fc-ideal}}(t)\, I_{\text{fc-ideal}}(t)\, \eta_{\text{fc}} \tag{4.1}$$

The number of points provided in the form of tabulated data for the definition of the two curves V_{fc}, and η_{fc} determines how accurate of a behavior characterization it is possible to replicate. The data for both efficiency and voltage is interpolated to perform the calculations.

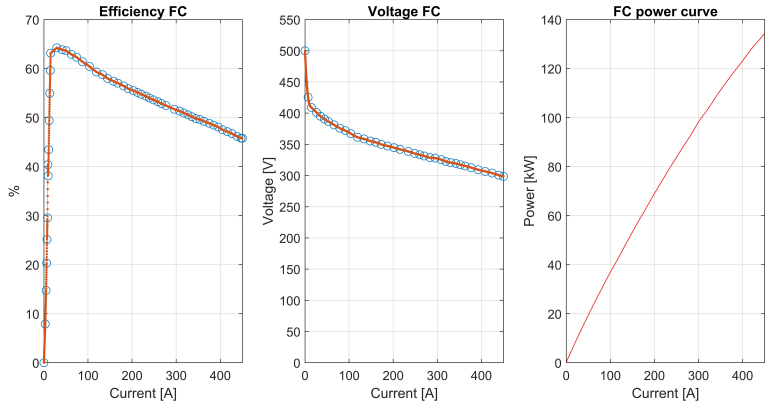

Figure 4.5: Curves representing η_{fc}, V_{fc} and relative power curve P_{fc}

Table 4.1: Parameters from a commercial PEMFC model used to define the operational capabilities of the unit in the quasi-static model

Rated power ($P_{\text{fc-rated}}$)	100kW
Gross output at rated power	320 V / 350 A
Peak power EOL,OCV @BOL	250,500 V
System efficiency (Peak, BOL)	62%
System efficiency (BOL)	50%
Response time (t_{fc})	8s

The PEMFC (or stack) experiences a performance degradation that is influenced by many internal and external factors, such as fuel cell design and assembly, application of materials, operational conditions, and impurities or contaminants. The degradation is measured by observing a reduction in the voltage per cell output and current density of the cell. The estimation of the degradation experienced

by the fuel cell during operations is necessary to determine the durability of the component under specific conditions and its viability. The degradation of the fuel cell is modelled using a set of numerical values that determine the reduction in voltage with respect to time, transient loading conditions or number of cycles. Choosing the correct set of values for the specific use case is challenging as there are only a limited amount of studies defining these values, usually obtained in laboratory conditions on models with low power output. This is mainly due to the fact that PEMFC technology has not yet reached widespread adoption and data from marine applications is very limited. The reviews from Wu et al. [39] and Zhao et al. [59] present a series of values obtained in experiments carried out both by academic and industry researchers. A set of presented values defines the degradation obtained by measuring voltage in long duration static tests of different fuel cells, while a second set describe the results obtained in accelerated durability tests. Of the analyzed cases, articles [60, 61, 62, 63] focus on different cases where dynamic loading conditions are applied to a PEMFC. All the experiments are carried out with stacks of output far lower than the one considered in this case (see Table 4.1). Fletcher et al. [64] presents a set of values used for the calculation of the degradation of the single fuel cell. The stack considered has a 4.8 kW nominal power output. The value of the start/stop cycle is obtained from the PEMFC manufacturer datasheet, while other values are obtained from the literature (see Table 4.2).

Table 4.2: Degradation values from Fletcher et al. [64]

Operating Conditions	Degradation Rate
Low power operation (80 < % Load)	10.17 μVh^{-1}
High power operation (> 80 % Load)	11.74 μVh^{-1}
Transient loading	0.0441 μV/ΔkW
Start/stop	23.91 μV/cycle

Values measured for a 10 kW PEMFC installed on a city bus, and tested in a lab, are presented in Chen et al. [65]. In this article, values defining each operational condition are presented. The transient loading degradation is identified using a value that defines the degradation produced at each cycle when passing from idling (10 < % Load) to high power load conditions ($\sim$ 100 % Load). Considering the nominal power of the stack (10 kW) and the load variation it is possible to obtain a value of 0.045 μV/Δkw in this application.

Considering the studies and values reported in the scientific literature, the values used to estimate the degradation of the fuel cell in the model presented in this Chapter are reported in Table 4.3. The values are the one presented by

Table 4.3: Degradation values used in the developed model for the 100 kW PEM fuel cell

Operating Conditions	Degradation Rate
Low power operation (80 < % Load)	10.17 μVh^{-1}
High power operation (> 80 % Load)	11.74 μVh^{-1}
Transient loading	0.0042 μV/ΔkW
Start/stop	23.91 μV/cycle

Fletcher et al. with the exception of the one used to estimate the degradation of the transient loading conditions. To evaluate the transient loading degradation it is necessary to take into consideration the difference between the nominal power output of the fuel cells used by Fletcher et al. (4.8 kW), Chen et al. (10 kW) and the model considered here (100 kW). The value of degradation per cycle obtained by Chen et al. [65] is considered as a starting point for the calculation of a new value coherent with the 100 kW stack. It is observed that the loading cycle in Chen et al. determines a change in PEMFC output from idling conditions to the nominal rated output and vice versa. As it is possible to assume that the 100 kW stack considered in this chapter is built combining multiple identical cells with the same current density as the one utilized for the stack with a 10 kW output, the value for transient loading degradation is recalculated. The new value has to take into consideration that the nominal power output of the PEMFC considered in Table 4.1 is 10 times higher, modifying the ΔkW range. With this considered it is possible to determine a value over the new range that is equal to 0.0042 μV/Δkw.

The model for the battery, similarly to the one of the fuel cells, is a simplified model. The model considers the battery as an ideal energy storage, capable of storing and delivering power with an instant response time. This assumption is motivated by the relatively low response time of the battery when compared to the PEMFC. No serial resistance is considered in this case determining an Ohmic efficiency of 100%. Coulombic efficiency, considered as the ratio of the current entering the battery to the current that is possible to retrieve, is also considered equal to 100%. No thermal effects are considered. The choice of assuming the battery as an ideal energy storage was determined by the intention to not tie the calculation to any specific battery technology, as each technology (e.g. Ni-Mh, Li-Ion, AGM) has different internal characteristics and efficiency values.

The electrical grid of the vessel includes DC/DC converters, a switchboard, DC/AC converters, and induction motors. It was defined in Section 4.2 that the operational profiles taken into consideration in this thesis are considered as the power demand at the DC-Bus level. For this reason the efficiency of components such as

the switchboard, the DC/AC converters and induction motors can be disregarded when formulating the equation representing the balance of power in the electrical grid. The DC/DC converters that connect the PEMFC and battery to the grid are instead considered in the overall power balance as they are placed between the DC-Bus and the power generation/storage components. The values of efficiency used for these components are considered constant during operations and are determined using the efficiency of components in the analyzed power range. The values relative to the efficiency of the boost converter (η_{bc}), connecting the PEMFC to the grid, and relative to the bi-directional converter ($\eta_{\text{bi-dir}}$), are respectively 0.98 and 0.95. These values are obtained as and average between conditions at low load, determining low efficiency, and conditions at high load, determining high efficiency.

4.5 Powerplant configuration model

The model of the powerplant, considering energy generation, storage and distribution is based on the assumption, represented by the system of equations 4.2, that the power demand imposed by the operational profile in each time-step $P_{\text{op}}(t)$, is equal to the sum of the PEMFCs and batteries output. This assumption is based on the consideration that the vessel's electrical grid is isolated.

$$\begin{cases} P_{\text{op}}(t) = P_{\text{fc-tot}}(t)\ \eta_{\text{bc}} + P_{\text{b-tot}}(t)\ \eta_{\text{bi-dir}} \\ P_{\text{fc-tot}} = P_{\text{fc}} n_{\text{fc}} = (P_{\text{fc-ideal}}\ \eta_{\text{fc}})\ n_{\text{fc}} \\ P_{\text{b-tot}} = P_{\text{b}} n_{\text{b}} = (P_{\text{b-ideal}}\ \eta_{\text{b}})\ n_{\text{b}} \\ 0 \leq P_{\text{fc}} \leq P_{\text{fc-rated}} \end{cases} \tag{4.2}$$

The EMS strategy selected by the user is used to calculate the value of $P_{\text{fc-tot}}$. The value of $P_{\text{fc-tot}}$ determines the share of load assigned to the fuel cell stacks installed in the hybrid system. When considering the load-leveling strategy the value of $P_{\text{fc-tot}}$ can be either set by the user as a constant value P_{L} or calculated using Equation 4.3 to ensure a balanced load sharing between battery and PEMFC. In the case of the peak-shaving strategy the value of $P_{\text{fc-tot}}$ is not constant, and is determined by applying a low pass filter to the OP (see Equation 4.4).

$$P_{\text{fc-tot}} = P_{\text{L}} = \frac{1}{t_{\text{tot}}} \sum_{t=0}^{n} (P_{\text{op}}(t)\ t_{\text{s}}) \tag{4.3}$$

$$P_{\text{fc-tot}}(t) = P_{\text{f}}(t) = filter(P_{\text{op}}(t)) \tag{4.4}$$

The definition of $P_{\text{fc-tot}}$ allows the calculation of the number of PEMFCs required to satisfy the load share defined. This value is obtained using Equation 4.5, assuming that the PEMFC's maximum allowed output is equal to the rated value $P_{\text{fc-rated}}$ provided in Table 4.1. The number of fuel cells needs to be an integer, and to provide a conservative solution the number is always rounded to the nearest integer greater than or equal to that element.

$$n_{\text{FC}} = ceil(max(P_{\text{fc-tot}})/(P_{\text{fc-rated}})) \tag{4.5}$$

The definition of the number of PEMFCs n_{FC} can be used to define the power output of the single PEMFC P_{fc}. This allows the estimation of the degradation for the single PEMFC unit. This calculation is based on the values presented in Table 4.3. In this table, the low power operation interval is identified by values that are below 80% of the selected PEMFC rated load. The calculation of the degradation using Equation 4.6 is done considering the low power degradation interval, the high power degradation interval and transient loading degradation. The total degradation value at the end of the considered time interval is equal to the sum of the three components. No start/stop phase is considered.

$$d_{\text{fc}} = Hpo\, t_{\text{hp}} + Lpo\, t_{\text{lp}} + \sum_{t=0}^{n}(|P_{\text{fc}}(t) - P_{\text{fc}}(t-1)|\, Tl) \tag{4.6}$$

The hydrogen consumption of the single PEMFC can be estimated using Equation 4.7. The efficiency data provided as input are interpolated and used to calculate the efficiency value at which the PEMFC operates at each time-step (η_{fc}) of the simulation. The value of the hydrogen energy density, equal to 120 MJ/kg or 33.6 kWh/kg, is used to estimate the consumption for each time-step.

$$Cons_{\text{H}_2} = \sum_{t=0}^{n} \frac{P_{\text{fc}}(t)}{H_2\ Energy\ Density}\ \frac{t_{\text{s}}}{\eta_{\text{fc}}(t)} \tag{4.7}$$

The battery capacity that needs to be installed in the powerplant to satisfy the power demand at each time-step is calculated as a function of the PEMFC output. The battery compensates for operational conditions where the PEMFC output determines a power deficit by releasing power, and for conditions where the PEMFC output determines a power surplus by storing power. The value for battery power P_{b} at each time-step, calculated using Equation 4.8 can be either positive or negative according to conditions of power surplus or deficit, determining a recharge state or a discharge state.

$$P_{\text{b}}(t) = \frac{P_{\text{op}}(t) - P_{\text{fc-tot}}(t)\ \eta_{\text{bc}}}{n_{\text{b}}\ \eta_{\text{bi-dir}}} \tag{4.8}$$

The value representing the quantity of energy stored inside the battery at each time-stem during operations is calculated using Equation 4.9.

$$E(t) = \sum_{t=0}^{n} (P_{\text{b}}(t)\ t_{\text{s}}) \tag{4.9}$$

The minimum battery capacity C_{b} required to satisfy the power demand imposed by the operational profile is calculated using Equation 4.10.

$$C_{\text{b}} = max(E(t)) + |min(E(t))| \tag{4.10}$$

Knowing that the energy stored inside the battery cannot be negative, it is possible to calculate the amount of energy that has to be stored in the battery at the beginning of operations (E_{start}). This value determines the minimum initial state of charge (SOC) of the battery.

$$|min(E(t))| = E_{\text{start}} \tag{4.11}$$

An optional function is included in the model to verify that the load variation happening during a time-window that is equal to the PEMFC response time (R_{t}), is compatible with the technical limits of the unit imposed by the manufacturer, and specified by the user. This option is used only with the peak-shaving strategy as the output of the PEMFC with the load-leveling strategy is constant, and therefore the load variation is zero. To perform this evaluation the condition represented in Equation 4.12 needs to be satisfied. This means that 2 or more power-data samples need to be available within the time-window considered to analyze the load variation ($U(n)$).

$$2 \leq \frac{R_{\text{t}}}{t_{\text{s}}} = y \tag{4.12}$$

If the calculation of y does not return an integer number, it is assumed that the result is rounded to the nearest higher integer. This produces a conservative evaluation with respect to the PEMFC response as the length of each time window

where U is evaluated is longer than the actual PEMFC response time. The load variation during the time-window defined by R_{t} is calculated using Equation 4.13.

$$U(n) = |P_{\mathrm{fc}}(y+n) - P_{\mathrm{fc}}(n)| \tag{4.13}$$

Every element of the $U(n)$ array has to be lower than the maximum acceptable U value specified by the user for the case study, between 0 and the rated $P_{\text{fc-rated}}$, for the solution to be considered valid.

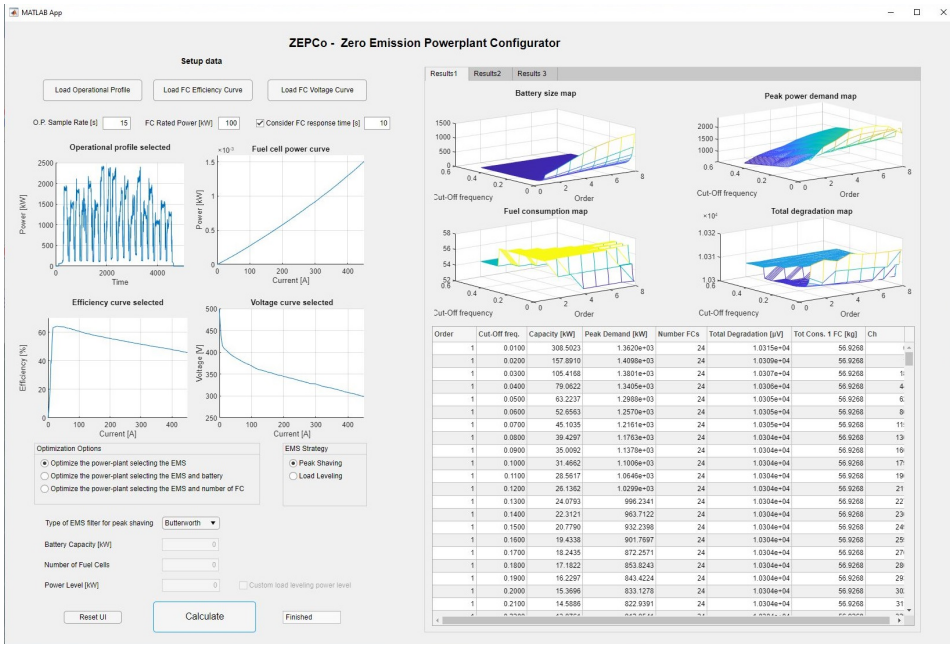

Figure 4.6: Graphic user interface of the ZEPCo application

4.6 Software based application

The conditions and equations described in the previous section are used as a reference for the creation of a software base application in Matlab. The application uses a graphic user interface (GUI) (see Fig. 4.6) for ease of use.

The operational profile and component's technical data are loaded on the left side of the GUI using buttons or editable fields. The EMS selection can be carried out on the bottom-left part of the GUI. Results are displayed on the right-side of the GUI. The results section includes 3D maps for the evaluation of the battery size, C-rate (peak battery power demand), hydrogen consumption and PEMFC degradation as a function of the filter's parameters when using the peak shaving strategy.

A table contains all possible configurations calculated for the configuration of the powerplant. If a load leveling strategy is selected, only one configuration is calculated, based on the value of P_{L} defined in Equation 4.3 or one specified in the setup phase inside the "Power Level" editable field.

The results produced by the application can be used to determine the footprint required for the hybrid powerplant, knowing the dimensions of the components, and the initial investment cost knowing their price. Maintenance costs can also be estimated by considering maintanence intervals determined by the degradation, and running costs can be estimated knowing the hydrogen consumption.

Chapter 5

Hybrid powerplant components: Analysis and modelling

In this Chapter the models developed to represent the components used in the powerplant dynamic model are described. The models are developed in Simulink. The description includes the component's basic construction characteristics and operational modes.

The approach used to model the components for the powerplant dynamic model in Simulink differs substantially from the approach used for the powerplant balancing software in Matlab, described in Chapter 4. The type of model considered in this Chapter is dynamic because it describes how system properties change over time. The dynamic model describes those aspects of a system concerned with time and the sequencing of operations: events that mark changes, sequences of events, and the organizing of events and states. The dynamic model does not consider what the operations do, what they operate on, nor how they are implemented [66]. In this model the state of the system in past time instants influences the state of the system at the current instant.

The dynamic model is built using multiple dynamic sub-models representing the single components such as PEMFCs, Li-Ion batteries, switchboard, and converters, allowing the user to study the inputs and outputs of each individual component and observe its behavior during operations. The modeling of individual components provides the possibility to study multiple configuration when it comes to components connection to the ship's electrical grid, and their control by a simulated energy management systems.

While the Simulink model's aim is to simulate the behavior of the real-world

counterpart with a good degree of accuracy, limits in computational resources and time rendered necessary the introduction of simplifications in the components representations and control. Such simplifications were tested, validated and selected after multiple simulations using real-world data.

5.1 Proton exchange membrane fuel cell

The proton exchange membrane fuel cell (PEMFC), also referred to as polymer electrolyte membrane, is introduced in section 2.1 as the selected electrical power generator for the powerplants considered in this thesis. This choice was defined during the early stages of the project considering a series of technical and economic factors including performances, cost and availability of PEMFC units certified for maritime use. The LT-PEMFC (low temperature PEMFC) is currently the preferred type of fuel cell for applications in the transport industry for zero-emission vehicles. PEMFC has achieved good power density, satisfactory transient performances [67], and the possibility for quick start-up. This type of fuel cell also has an operational temperature range between 65 and 85 degrees Celsius, similar to an ICE, and compatible with the heat exchangers installed in many transport vehicles. PEMFCs do require high purity hydrogen to operate, and air needs to be filtered to eliminate impurities of, in maritime application, sea salt aerosol.

The technical characteristics of the PEMFC considered during the construction of the model are reported in this section. While focusing mainly on electrical power generation and hydrogen consumption, the study of the fuel cell model includes a brief overview of the electro-chemical processes that lead to the generation of current and the depletion of hydrogen.

5.1.1 Components and characterization

The PEMFC is a chemical reactor with no moving parts that is able to convert the chemical energy stored in hydrogen directly and efficiently to electrical energy. In a single cell we can identify components including plates, membrane and gaskets sandwiched together to form a single rectangular or square unit. In order, from anode to cathode, it is possible to identify the following components:

- Anode side current collector plate
- Hydrogen fuel bipolar flow plate
- Anode-side gasket
- PEM membrane
- Cathode-side gasket
- Oxygen side bipolar plate

- Cathode side current collector plate

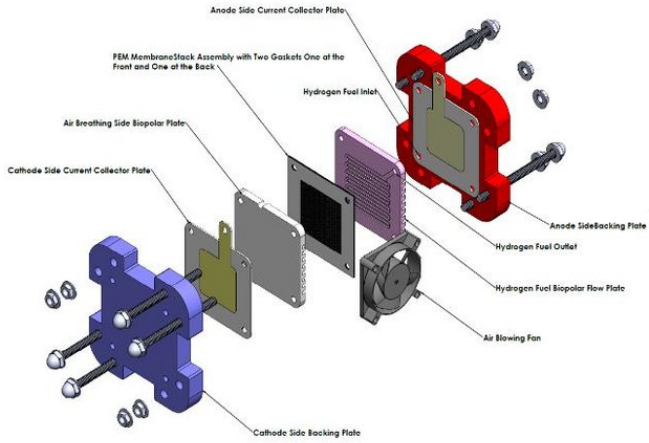

Figure 5.1: Fuel cell exploded view [68]

The hydrogen fuel bipolar flow plate contains a series of gas flow channels that lets hydrogen flow through and excess hydrogen exit from the other side. Similarly the oxygen side bipolar plate contains a series of channels that lets oxygen flow through and excess oxygen exit from the other side. While small PEMFC units used in laboratories are not cooled, in transport applications the flow plates are cooled (usually water cooled) to maintain the perfect thermal conditions for the reactions. The membrane electrode assembly (MEA), more specifically, includes the membrane, catalyst layer, gas diffusion layer, and micro-porous layer. The polymer electrolyte membrane is based on synthetic polymers (notably sulfonated tetrafluoroethylene or NAFION) as a proton conductor [69]. The membrane has to have high proton conductivity, low methanol/water permeability, good mechanical and thermal stability and moderate price. The type of catalyst used belongs to one of three possible categories:

- **Pt-Based Catalyst:** Excellent characteristics of high activity for fuel cell reactions. High price and relatively low stability.
- **Modified Pt-Based Catalyst:** Low price and high durability under special conditions. Indefinability for long term performances.
- **Non PT-Based Catalyst:** Low price and un-exhausted resources. Relatively low activity.

During normal operations the hydrogen flowing through the flow plate (anode side) is split into electrons and protons using the catalyst. The MEA lets the protons pass immediately from the hydrogen side to the oxygen side. The electrons are forced through terminals connecting the two chambers, and flow from the anode side to the cathode side as the atoms need a balancing charge, generating electricity. The hydrogen and oxygen combine producing water.

The multi-physics, highly coupled and nonlinear transport and electrochemical phenomena taking place inside the PEMFC can be explained in a simplified way using the reactions listed below. Fundamental models to examine more in detail the transport processes can be examined in [69]. The reaction for the anode is:

$$H_2 \rightarrow 2H^+ + 2e^- \tag{5.1}$$

While the reaction at the cathode is:

$$\frac{1}{2}O_2 + 2H^+ + 2e^- \rightarrow H_2O \tag{5.2}$$

The overall reaction is:

$$H_2 + \frac{1}{2}O_2 \rightarrow H_2O \tag{5.3}$$

From the products of this chemical reaction it is always possible to re-obtain hydrogen molecules. The reaction in itself is not reversible but the products can be processed into an electrolyzer to split the water into hydrogen and oxygen. This means that hydrogen is infinitely renewable as long as it is possible to source some energy to separate it from other elements in a molecule.

Since fuel cells are electrochemical systems, electrode processes play a central role in their performance and durability. For this reason, common electrochemical techniques, such as polarization curves, have become standard methods for fuel cells characterization [70]. The polarization curve for a PEMFC can be observed in Figure 5.2. The measurement to plot the curve is usually performed in a quasi steady-state in which the current is held at specified points until the voltage stabilizes. A typical PEMFCs produces a voltage around 0.6 V at rated load. Voltage decreases as current increases, due to several factors [71]:

- **Activation loss**: the FC potential drops significantly due to the slow kinetics of the oxygen reduction reaction.

- **Ohmic loss**: voltage drops due to resistance of the cell components and interconnections. The ohmic resistance that affects this region of the curve regards both the electronic transport through the electrodes and the protonic one through the electrolyte.

- **Mass transport loss**: depletion of reactants at catalyst sites under high loads, causing rapid loss of voltage.

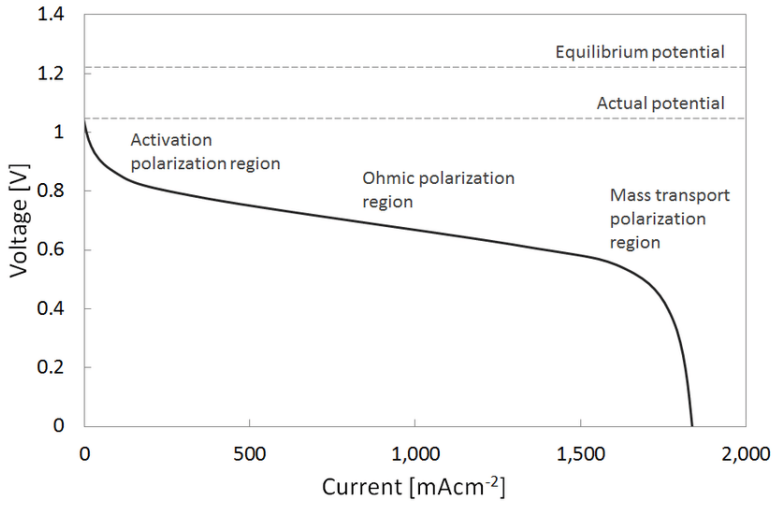

Figure 5.2: Typical polarization curve for PEM fuel cells. The curve is expressed as a variation of the voltage as a function of the single cell current output [70]

Other common electrochemical techniques, such as cyclic voltammetry (CV), CO stripping voltammetry, electrochemical impedance spectroscopy (EIS), and linear sweep voltammetry (LSV) can be used for the characterization of the PEMFC but such techniques were not taken into consideration during the PEMFC characterization performed in this dissertation.

As specified in Chapter 4 the single cells can be connected to reach the desired electrical power output. Such a design is called a fuel cell stack. The cell surface area can also be increased, to allow higher current from each cell. Within the stack, reactant gases must be distributed uniformly over each of the cells to maximize the power output. These solutions are applicable within technical limits posed by the PEMFC or the BoP components.

5.1.2 Fuel cell model

Fuel cell models described in literature can be classified as chemical, experimental or electrical representations. Focusing on the simulation of the electrical power generation, storage and distribution, the type of model chosen is an electrical representation. The model selected for this application was developed by Njoya et al. [72]. The use of a pre-existing model from the literature was deemed adequate as the creation of a detailed electrochemical model for the fuel cell was outside the scope of the main research question. The selection of this model was motivated by three factors. The first reason is the accuracy obtained in the results described in the paper, where it is declared that, during the simulations, the authors obtained a range of error of just $\pm 1\%$ both for steady and transient state, provided a controlled stack humidity. The second reason is the compatibility with the available inputs and the desired outputs from the model. The third reason is the ease of use of this model, providing instruments for easy reconfiguration.

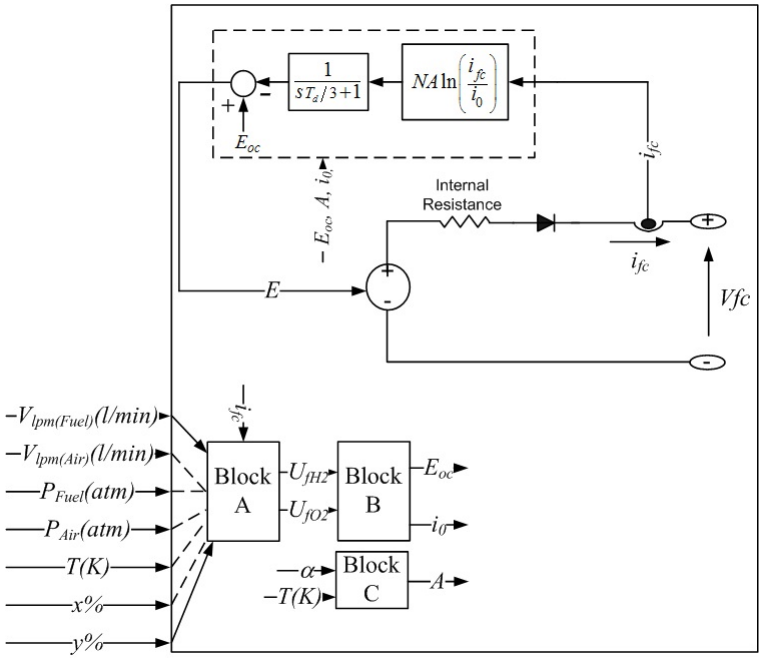

Figure 5.3: Fuel cell model representation using Simulink blocks [72]

Two generic fuel cell models are presented in the Article from Njoya et al., a simplified version of the fuel cell model and a detailed version of the fuel cell model. The detailed version of the model (see Fig. 5.3), configured as a proton exchange membrane fuel cell is used in the simulations performed. The config-

uration is carried out using the fuel cell data (see Table 5.1) available from the producer. By defining the power demand at the DC-Bus, the detailed model is used to calculate the following factors relative to the PEMFC stack operations:

- Current output
- Voltage output
- Efficiency
- Hydrogen and air consumption

The datasheet of the PEMFC model used in the simulation does not specify a response time. The response time considered in this study is set equal to 15 second. This value defines a conservative PEMFC behavior, with response times, even of large stacks, being lower [14].

Table 5.1: Parameters from a commercial PEMFC model used to define the operational capabilities of the unit in the Simulink model

Rated power (net)	100kW
Gross output at rated power	320 V / 350 A
Peak power EOL,OCV @BOL	250,500 V
System efficiency (Peak, BOL)	62%
System efficiency (BOL)	50%
Max waste heat	120 kW
Coolant outlet temperature	80C
Fuel inlet pressure	8-12 bar(g)
System pressure	1.6 bar(g)
Ambient temperature	-20 to +50C
Ambient relative humidity	5-95%, non-condensing
Weight	120-150 kg
Volume	300 l
Fuel quality	ISO 14687-2, SAE J2719
IP classification	IP54

The degradation of the fuel cell during operations is taken into consideration in also in the dynamic model. The considerations listed in Section 4.4 for the quasi-static model are also valid for the dynamic model. The value representing the degradation is obtained in the same way as it is obtained in the quasi-static model, considering the time spent at high or low load operations and during transients (see Equation 4.6). As the study of detailed degradation mechanisms is outside the scope of this thesis, the values used in Article 2 and 4 are based on the ones reported by Fletcher et al. [64]. (see Table 4.2). Further considerations on this topic have lead to the modification of the value representing transient load degradation as reported in Table 4.3.

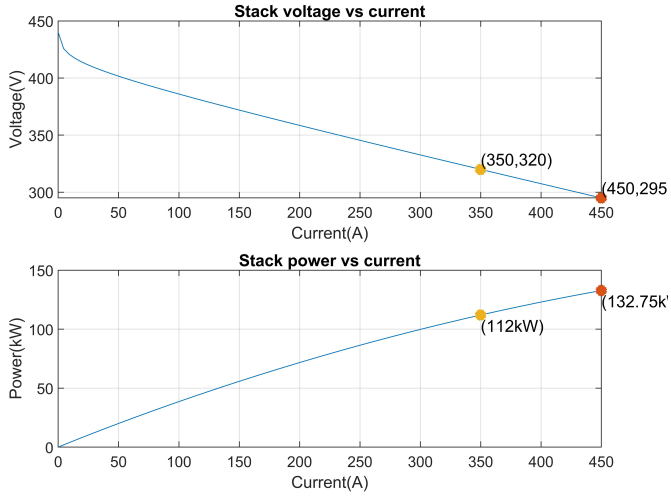

Figure 5.4: PEM fuel cell characterization curves obtained using the values specified in Table 5.1 into the dynamic model

5.2 Energy storage system

A hybrid system is defined as a system that combines two or more different components to produce power. In power engineering the term hybrid is often used to describe the combination of a power generation system and and energy storage system. In the transport industry, multiple energy storage technologies have been tested for the integration into hybrid systems [73]. While batteries are the most widespread solution, supercapacitors are also used for transport applications due to their high power density and low response time. Mechanical energy storage has also been adopted on vehicles in the form of flywheels [74]. In this thesis, the focus is limited to batteries and their integration into the ship's electrical grid.

There are currently many different battery technologies on the market and many others under development [75, 76]. It is nonetheless clear that at this time the technology that provides the best compromise between cost/kWh, energy density, power density and performances is the lithium ion (Li-Ion) battery. The studies and simulations carried out here are therefore focused on the Li-Ion technology

5.2.1 Scientific background

Li-ion batteries use an intercalated lithium compound as the material at the positive electrode. The most common technologies include cathodes made with $LiCoO_2$, $LiNi_xMn_yCo_zO_2$, $LiMn_2O_4$, $LiFePO_4$. The positive electrode (cathode)

half-reaction, when considering a lithium-doped cobalt oxide substrate is [77]:

$$\mathrm{CoO_2} + \mathrm{Li^+} + \mathrm{e^-} \rightleftharpoons \mathrm{LiCoO_2} \tag{5.4}$$

The negative electrode (anode) half-reaction for the graphite is:

$$\mathrm{LiC_6} \rightleftharpoons \mathrm{C_6} + \mathrm{Li^+} + \mathrm{e^-} \tag{5.5}$$

The full reaction (left to right: discharging, right to left: charging) being

$$\mathrm{LiC_6} + \mathrm{CoO_2} \rightleftharpoons \mathrm{C_6} + \mathrm{LiCoO_2} \tag{5.6}$$

The overall reaction has its limits. Over-discharging supersaturates lithium cobalt oxide, leading to the production of lithium oxide [78], possibly by the following irreversible reaction:

$$\mathrm{Li^+} + \mathrm{e^-} + \mathrm{LiCoO_2} \longrightarrow \mathrm{Li_2O} + \mathrm{CoO} \tag{5.7}$$

Overcharging up to 5.2 volts leads to the synthesis of cobalt(IV) oxide, as evidenced by x-ray diffraction [79]:

$$\mathrm{LiCoO_2} \longrightarrow \mathrm{Li^+} + \mathrm{CoO_2} + \mathrm{e^-} \tag{5.8}$$

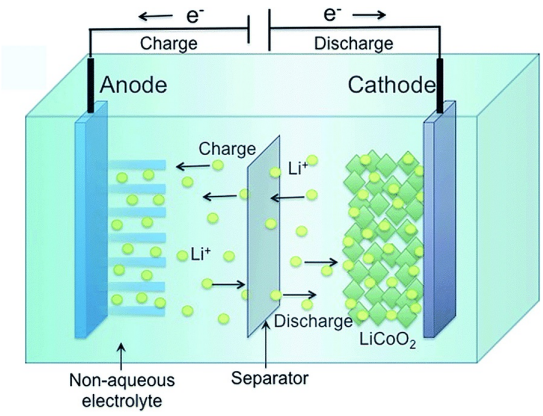

Figure 5.5: Lithium Ion battery simplified representation

An important factor regarding the construction process are the additives introduced into the electrolyte. The electrolyte in Li-Ion batteries consist of one, or more, conducting lithium salts dissolved in a single or mixtures of non-aqueous solvents. The use of electrolyte additives is the most economical and efficient method to improve Li-Ion battery performance. The electrode's surface morphology can be improved by the addition of small amounts of additives, as they are usually preferentially involved in the interfacial redox process, i.e. prior to the electrolytes. Electrolyte additives in lithium ion systems improve not only the properties of the solid electrolyte interphase (SEI) on the electrodes' surfaces, but also the ionic conductivity and safety of the electrolyte. The additives should reduce irreversible capacity and gas generation, improve the thermal stability and protect the cathode material from dissolution and overcharging [80].

Batteries experience electrochemical degradation over time. The longevity of a battery can change dramatically with variations of factors such as temperature, speed of the cycle, and depth of discharge.

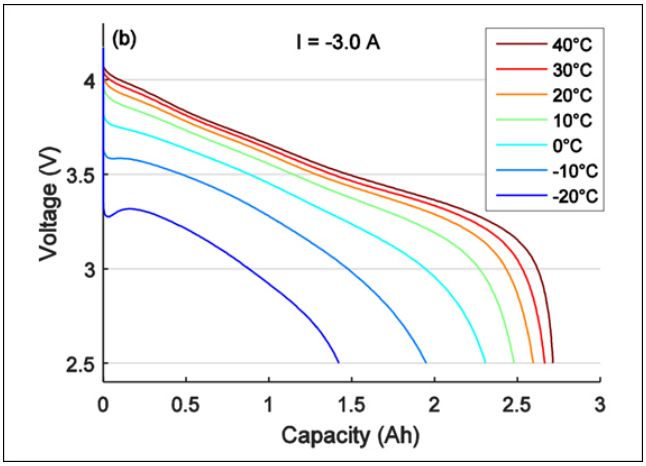

Figure 5.6: Discharge voltage of an 18650 Li-ion cell at 3A and various temperatures [81]

To address the temperature problem the battery must be equipped with a cooling system or heat management system to cool down the cells or warm them up for them to be always in the optimal temperature range (see Fig. 5.6). This temperature should be kept around 20 °C at all times during operation, and preferably also during storage. The speed of the charge/discharge cycle is also a key factor in the battery operational life. The extended length of these cycles can determine the start of time-dependent parasitic chemical reactions that reduce battery life. These reaction speed up when the battery is hot, so the fist step into this problem is to dimension the heat management system to keep the battery at the optimal

temperature. Of course, in the real world, designing a system that operates under laboratory conditions is impossible. Batteries in lab experiments are charged in 40 minutes and discharged in 20 minutes on a continuous cycle for 30 days, beating the clock on those parasitic chemical reactions and giving a biased result on the life expectancy. A system like this installed on a vehicle would allow the user no flexibility if the expected result wanted is the same as in the lab. The use of the battery under normal conditions would lead anyway to a buildup in solid electrolyte interphase and reduction in capacity. The range of charge across wich the battery operates is also an important factor in the battery lifespan. Similarly to the conditions explained above, we can operate a battery in a limited range (e.g. 40% to 60% SOC) to mimic the conditions of the lab of rapid discharge and charge but including additional capacity that gives versatility to the system.

5.2.2 Battery characterization

Li-Ion batteries are defined using a series of factors that determines their level of performance. The evaluation of such factors is instrumental in defining the correct battery size and rating for the use-case taken into consideration. The first factor that is taken into consideration is energy density. Li-Ion batteries generally offer a volumetric energy density between 250 and 375 Wh/L and a gravimetric energy density between 90 and 220 Wh/kg (see Fig. 5.8). These values are steadily increasing with many research and development project both carried out in academia and industry alike. The second factor taken into consideration is the power density. Power density measures how quickly the battery can deliver the required energy. In other words, it's equivalent to the maximum current it is possible to draw from a battery of a given size. Units are W/kg or W/m^3. The power density of the battery defines the C-Rate at which the battery operates and is limited to. The C-rate is a measure of the rate at which a battery is being charged or discharged. It is defined as the current through the battery divided by the theoretical current draw under which the battery would deliver its nominal rated capacity in one hour (see Equation 5.9). This parameter defines the electric power that can be delivered or absorbed by the battery at each instant, influencing the power distribution in the vessel electrical grid. The C-Rate at which the battery is limited to is usually a function of the size of the battery pack. While small Li-Ion batteries can reach C-Rates up to 25C, it is reported that in the automotive industry the battery packs are limited to 4C or lower. In maritime applications considered here, the battery packs taken into consideration are normally of large capacity (100 kWh or more), determining that the maximum C-Rate is limited to values around 2C or lower.

$$C\ Rate = \frac{Charge\ or\ Discharge\ current}{Rated\ capacity\ [A/h]} \tag{5.9}$$

As for the PEMFC, there are multiple electrochemichal techniques to characterize the performances of the battery during operations. In this study the focus is on the polarization curve of the battery. A polarization curve is a plot representing the variation of current density (I) versus voltage (V) and can be measured for the single cell or the battery pack. The voltage decreases in the case of a battery is determined by [82]:

- **IR drop:** This drop in cell voltage is due to the current flowing across the internal resistance of the battery.
- **Activation polarization:** This term refers to the various retarding factors inherent to the kinetics of an electrochemical reaction, like the work function that ions must overcome at the junction between the electrodes and the electrolyte.
- **Concentration polarization:** This factor takes into account the resistance faced by the mass transfer (e.g. diffusion) process by which ions are transported across the electrolyte from one electrode to another.

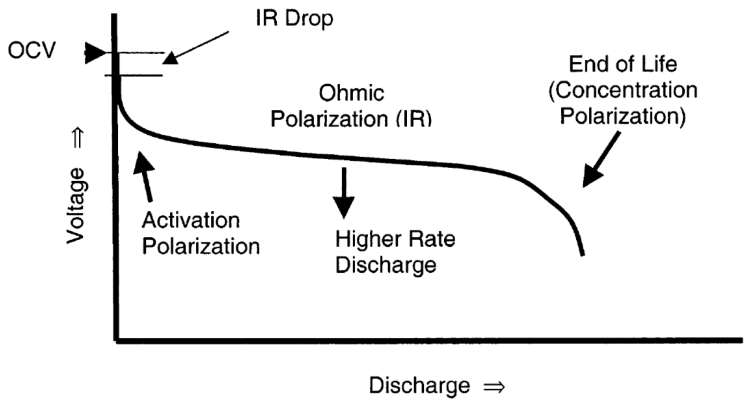

Figure 5.7: Typical polarization curve of a battery showing the three main regions of functionality: activation, ohmic polarization and concentration. The curve is expressed as a variation of the voltage as a function of the state of charge [83]

The Li-Ion battery in particular defines a region of ohmic polarization with a low voltage drop. The resulting effect of this characteristic is that the voltage of the battery remains almost constant, ensuring good performance during operations when the state of charge (SoC) is limited in order to avoid Activation and Concentration polarization areas.

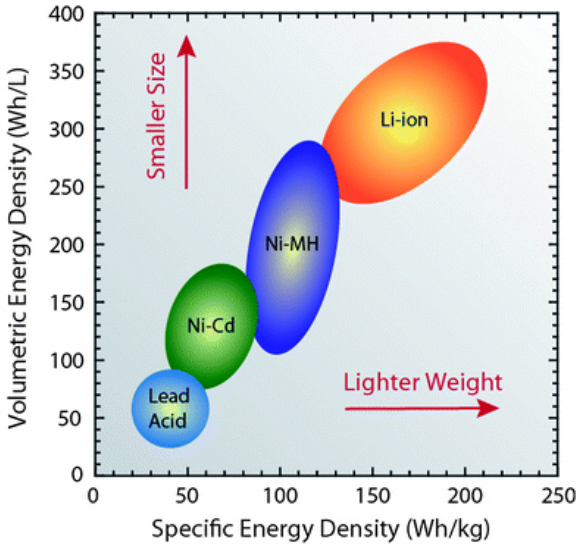

Figure 5.8: Comparison between energy density capabilities for the main commercially available battery technologies [Source: EPEC]

5.2.3 Battery model

Battery models described in literature can be classified as circuit-based, experimental or electro-chemical representations. The type of model chosen in this study is a circuit-based representation. The model selected for this application was developed by Sheperd [84], and modified by Tremblay et al. [85] to use the polarisation voltage instead of the polarisation resistance in order to remove the algebraic loop that, in simulations, uses lots of computational resources. The battery model is obtained by merging a discharge model and a recharge model that are battery type dependent. The model includes a low-pass filter term to simulate the battery dynamic behavior and a polarization voltage term to calculate the SOC. The use of a pre-existing model from the literature was deemed adequate as the creation of a detailed electrochemical model for the battery was outside the scope of the main research question. The model was selected as it can replicate the battery's behavior with good computational efficiency. The battery size and rating, for the applications considered in this thesis, are considered as a variables of the load share assigned to the battery. The battery load share is again a function of the PEMFC load share determined by the EMS, as described in Section 4.5. Once the Battery load share is calculated, it is possible to configure the model using the nominal voltage [V], rated capacity [Ah], initial state-of-charge [%], and the battery response time [s]. The model is used to calculate the current and voltage

input or output of the battery at each instant of the simulation. The battery SOC is also calculated even for variable charging and discharging currents thanks to the improvements carried out by Tremblay et al.

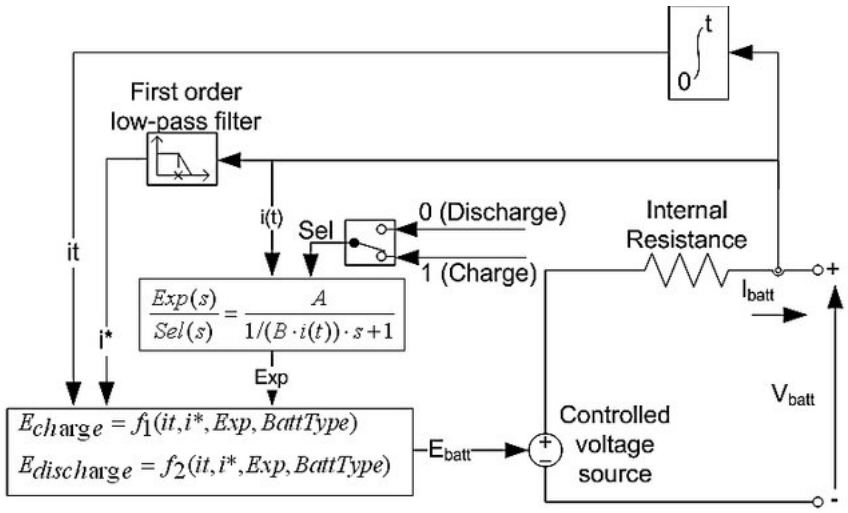

Figure 5.9: The battery model represented using a block diagram within Simulink, which in itself implements a generic model of Lithium-Ion battery [85]

The model assumptions and limitation described in Tremblay's paper do not negatively affect the results obtained during the simulations of the maritime hybrid system at this stage. It is anyway especially important to evaluate this aspect in future developments of the model if new battery models are considered where the charge and discharge characteristics are substantially different or if thermal aspects are considered.

The battery is added to the system to store excess energy from the PEMFC and deliver it during periods of energy demand. While degradation of the battery pack has an important impact in the technical and economic evaluation of a specific hybrid configuration, degradation effects on the battery are, in this study, not considered.

5.3 Electrical grid characteristics

The electrical grid is an interconnected network for electricity distribution between the power producer, power storage and power consumers. In the case of a maritime vessel (or a vehicle in general), the electrical grid is designed to operate autonomously as an isolated system, meaning that the entirety of the power produced is used, stored or dissipated. The vessel grid can be configured to connect

to the land based grid during periods of off-time, allowing the recharge of battery or providing power for hotel loads.

Electrical grids onboard maritime vessels need to be designed according to regulations imposed by maritime classification societies. Such regulations are written following parameters such as reliability, redundancy, and define the creation of redundancy groups [86, 87]. The main difference between a land based grid and a maritime grid is the short distance between power producers and consumers. This condition opens the possibility for the use of both alternate current (AC) or direct current (DC), unlike in land based grids were connections are made between long distances making DC current distribution uneconomical. The choice between an AC grid and a DC grid is generally based upon the outputs of the units assigned to electric power generation or storage. Another factor taken into consideration is the type (AC or DC) and amount of power users connected to the grid. The choice is ultimately performed evaluating the technical and economic feasibility of the two options based on the operations of the vessel. In this study a DC grid will be considered over an AC grid, as both the PEMFC and batteries produce DC current. With DC power systems there is less need for electricity conversion across the whole grid. Even if AC converters are cheaper than DC converters considering the same size, less components overall produce a smaller initial investment, less footprint usage and also less weight (switchboard and propulsion drives are much less heavy for DC grids). Some pros for DC grids with respect to AC grids are:

- Higher power quality by eliminating harmonic mitigation equipment. This equipment is instead required in AC grids due to the extensive use of converters.
- Reduced weight and volume used by eliminating total harmonic distortion (THD) filters.
- Increased compatibility with DC components such as batteries and fuel cells.
- No need for large low frequency (60Hz) transformers.
- No need for synchronization of different generators when they are switched on.

The On-board DC Grid fully complies with rules and regulations for selectivity and equipment protection. Further; any fault current will be cleared within maximum 40ms. This results in a drastic reduction in On-board DC Grid fault energy levels as compared with traditional AC protection circuits where fault duration can reach up to 1s [88].

5.4 Power converters

Power converters are used to convert electric power from one form into another desired form optimized for the user. The architecture of converter, including the choice and placement of active and passive components, depends on the type of input and output desired.

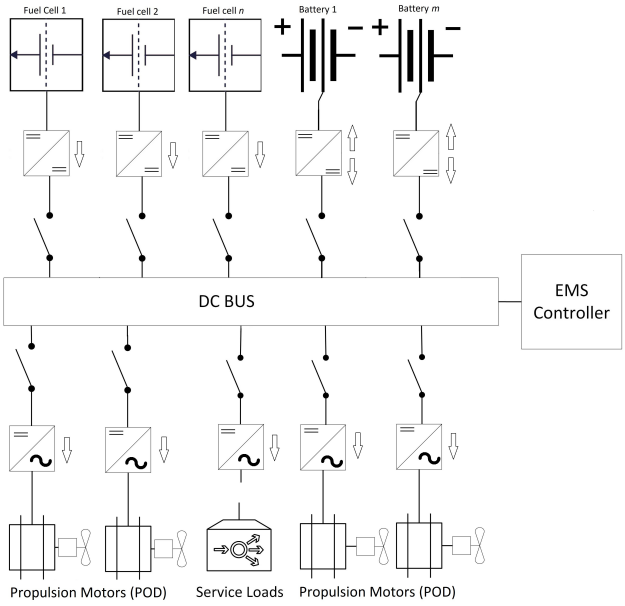

Figure 5.10: Hybrid configurations with PEMFCs and batteries, simplified single line diagram of DC grid

In the hybrid system considered in this study, both the PEMFC and the battery produce a direct current (DC) output, and are connected to a DC electrical grid. For this reason DC-to-DC converters (DC/DC) are used for power regulation between the power source and the DC-Bus. The current is distributed within the grid in DC form, but it is transformed to alternate current (AC) for a variety of users including the propulsion system, using induction motors to transform the electrical power into torque on the propeller shaft. For this application DC-to-AC converters (inverters) are used. The placement of the converters can be observed in Figure 5.10 where a single line diagram for a maritime vessel utilizing a hybrid system with DC Grid, PEMFCs, and batteries is represented.

In the models developed in this thesis and enclosed articles, the electrical power users visible in Figure 5.10 (propulsion motors and service loads) are not modelled individually but are represented using a "controlled current sink" (CCS)

to simulate the power demand. The CCS's power demand (power "absorption") is equal to the sum of all the electrical loads required by the user for each operational timestep, that is represented by the the operational profiles (OP) used in this thesis. This simplification means that the main focus is on the DC/DC converters connected to the energy source and storage, while the AC/DC converters are not modelled.

5.4.1 DC/DC boost converter model

The DC/DC boost converter is a type of converter used to increase the voltage output of the supply (input) to match the level required by the user (output). This type of converter is mono-directional, meaning that the electrical power flows only from the supply to the user but not vice-versa. The PEMFC uses this converter to step-up the voltage to the level required for the connection to the DC-Bus.

The topology of converters applied to systems that are in the power range considered in this thesis is extremely complex. The physical circuit implementation and control of such converters is considered out of the scope of this thesis. A simplified representation of the converters is presented, retaining the basic core function of the more complex unit. Three different types of boost converter are considered in this thesis to perform the voltage increase required. Each type is realized using a different component's topology, determining specific limits on the power output, efficiency, volume and cost [89].

The first type of boost converter developed is the single-phase boost converter. It was evaluated that this type of converter is suitable for the applications studied in this thesis because of the low voltage conversion ratio required between the PEMFC and the DC-Bus. This topology is simple, low cost and easy to control with only one switching component. Drawbacks include low voltage gain and the need for large passive components determining low compactness and higher costs. The single-phase boost converter (SPBC) topology can be observed in Figure 5.11. The sizing of the passive components in this topology is calculated using the simplified equations presented in the application report [90] from Texas Instruments. The application report considers simplified formulas for Low Power DC/DC application, but was used here to dimension the components, with simulations showing a satisfactory behavior with efficiency values similar to the ones specified for the high power converters. The inductor ripple current is calculated using Equation 5.10, where I_{max} is the maximum current output of the power source. Plotting efficiency vs. load current, it is possible to observe higher efficiencies when the inductor ripple current is between 20% and 40% of I_{max}. The efficiency is determined by core loss due to low inductance and high current ripple.

$$\Delta Il = (0.2\ to\ 0.4)\ I_{\max} \tag{5.10}$$

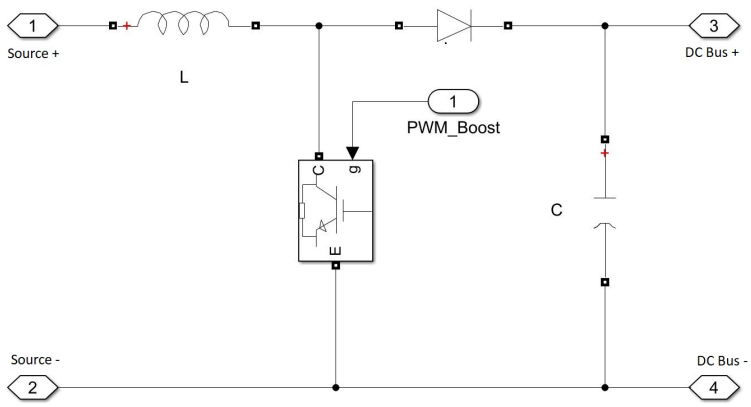

Figure 5.11: Base electrical circuit representing a single-phase boost converter connecting a voltage source and a load

The inductor ripple current ΔIl is used to define the inductor rating in Henry. V_{out} defines the voltage used by the DC grid, and V_{in} is defined as the average value calculated using voltage range of the power source. fs defines the switching frequency of the switch.

$$L = \frac{V_{\text{in}}\ (V_{\text{out}} - V_{\text{in}})}{\Delta Il\ fs\ V_{\text{out}}} = \frac{V_{\text{in}}\ D}{\Delta Il\ fs} \tag{5.11}$$

The duty ratio D is defined using Equation 5.12, where $V_{\text{in min}}$ defines the minimum voltage value given as input to the converter during operations. η_{conv} represents the efficiency.

$$D = 1 - \frac{V_{\text{in min}}\ \eta_{\text{conv}}}{V_{\text{out}}} \tag{5.12}$$

The output capacitor rating in Farad is calculate using Equation 5.13, where $I_{\text{out max}}$ defines the maximum current value provided to the converter by the power source. ΔV_{out} represents the acceptable output voltage ripple.

$$C_{\text{out}} = \frac{I_{\text{out max}}\ D}{fs\ \Delta V_{\text{out}}} \tag{5.13}$$

The converter can be equipped with an input capacitor. The minimum value for the input capacitor is normally given in the data sheet. This minimum value is necessary to stabilize the input voltage and avoid that the switching dynamics impact the PEMFC voltage output. The value can be increased empirically if the input voltage is noisy. In the case-study considered in this thesis the input capacitor is equipped, and the value is equal to the value used for the output capacitor.

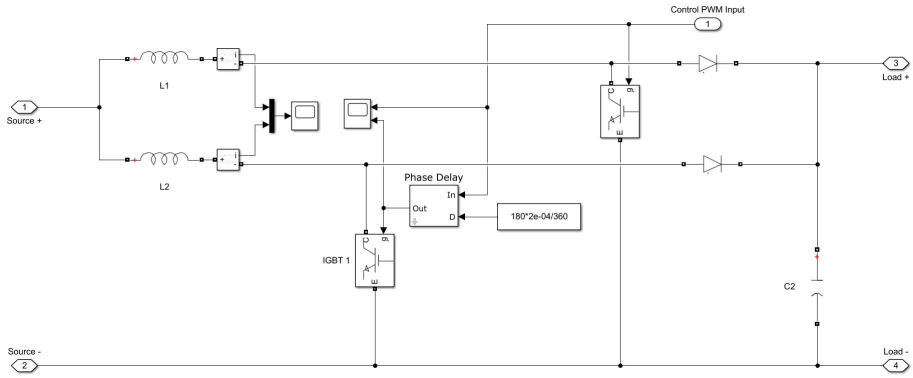

Figure 5.12: Base electrical circuit representing a double-phase boost converter connecting a voltage source and a load

The second topology developed in this thesis is the multi-phase boost converter, precisely the double-phase boost converter (see Fig. 5.12). This topology has several advantages over the single-phase topology. The first advantage of the double-phase converter is an advantage in thermal performances. The thermal performance related to conduction losses of the power source are proportional to the current squared.

$$P = I^2\, R \tag{5.14}$$

If two phases are used, power due to conduction losses is cut in half. The conduction losses are only a portion of the total losses in a power supply, but at higher currents these losses can be significant.

$$\frac{1}{2}P = 2\,((\frac{1}{2}I)^2\, R) \tag{5.15}$$

The second benefit that can be considered is the ripple current reduction (cancellation with 50% duty cycle). The ripple current reduction can reduce the root mean square (RMS) current in the input or output capacitors (see Figure 5.13). Other

benefits of this topology are the improved response during transients, due to the smaller capacitors, and the improved thermal performances.

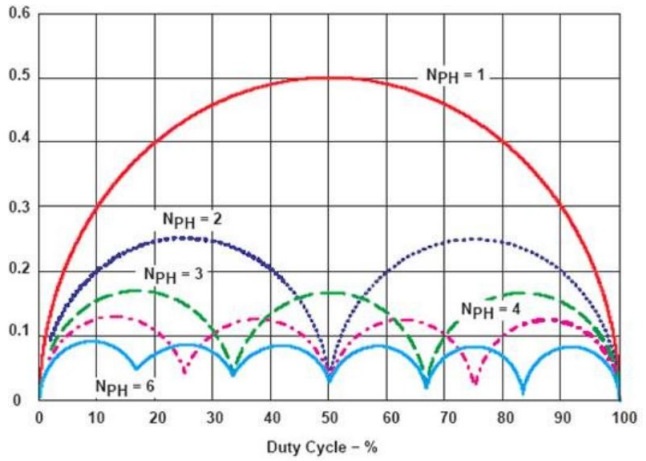

Figure 5.13: Normalized plot for RMS current reduction through the capacitor based on the number of phases and duty cycle [Source: Texas Instrument]

The approach recommended for the sizing of the multi-phase converter is to divide the maximum current ($I_{\text{out max}}$) for the number of phases, and use the same equations used for the single-phase converter. Because the PEMFC is not a constant voltage power source, the ripple reduction effects are dependent on the duty ratio at which the system is operating, and often it is impossible to eliminate the ripple complitely [91]. For this reason, the values values obtained in the dimensioning need to be slightly increased by an empirical factor that is a function of the voltage variation of the PEMFC during operations.

The third topology developed is the isolated full-bridge boost converter. The isolated power converter isolates the source from the user by electrically and physically dividing the circuit into two sections preventing direct current flow between input and output, typically achieved by using a transformer (see Figure 5.14). The physical separation of the two circuits allows for increased safety compliance, especially when transmitting high voltages as in the electrical DC-Grids considered in this thesis. A secondary benefit of this topology is the possibility to break up ground loops. This possibility benefits circuits that are sensitive to noise and can benefit by having their ground separated from noisy circuits. Drawbacks for this topology, observed also in the simulations, are high conduction losses and lower efficiency compared to the single and double-phase converters. An additional drawback is the need to monitor the current during the control of the converter

to avoid transformer saturation. The values needed for the sizing of the converter are based on the study of Nymand et al. [92], where the input parameters for the calculations are modified for the case-study considered in this thesis.

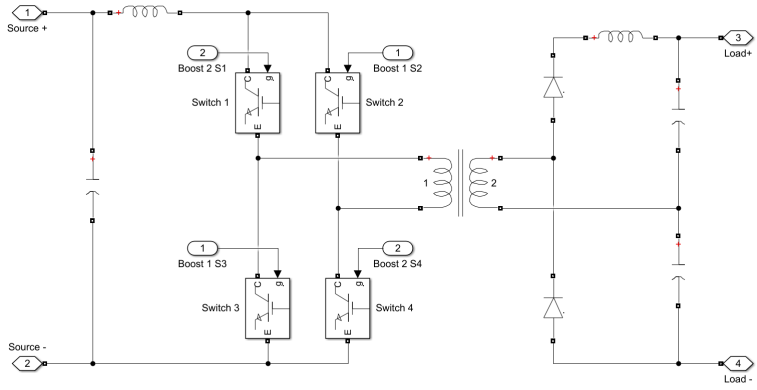

Figure 5.14: Base electrical circuit representing a isolated boost converter connecting a voltage source and a load

5.4.2 DC/DC boost converter control

Two types of control are considered for the boost converter connected to the PEMFC, voltage control mode and current control mode. The PEMFC, during operation, has a variable output voltage determined as a function of the output current (see Fig. 5.15). In voltage control mode the converter's variable input voltage, coming from the PEMFC, is transformed into a stable output voltage matching the value specified for the DC-Bus. The voltage step-up and control is realized using a feedback loop with a PID controller (see Figure 5.16). The feedback loop uses the voltage measured on the DC-Bus to calculate the error with the reference voltage, feeding this to the PID that determines the duty ratio for the PWM generator. The PWM generator's output is connected to the converter's switching element (or elements) to control the voltage output to the DC-Bus. The PID tuning and the values selected for inductance and capacitance need to ensure a non-oscillatory voltage rise with an acceptable level of voltage ripples[1]. The switch used for all the boost-converters is an IGBT with a switching frequency of 5kHz. This switching frequency directly determines the maximum timestep that can be used in the system's simulation [2]. This type of switch is selected after evaluating the power and current

[1]The value used for P is 1.1594e-5, for I is 0.0116, and for D is 5.7971e-6.

[2]The simulations that include a converter with switching elements are performed with discrete 1e-6 s time-steps.

range for the case studies considered in this thesis, the switching frequency used, and the voltage level specified for the DC-Bus (see Fig. 5.17).

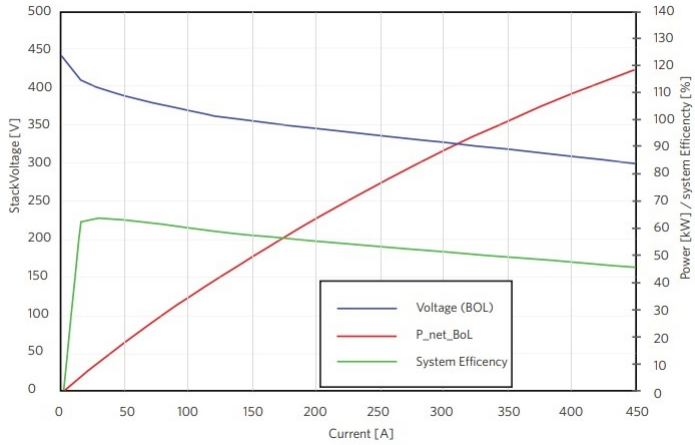

Figure 5.15: Fuel Cell voltage, power and efficiency characterization curves. [Source: Powercell Data-sheet MS100]

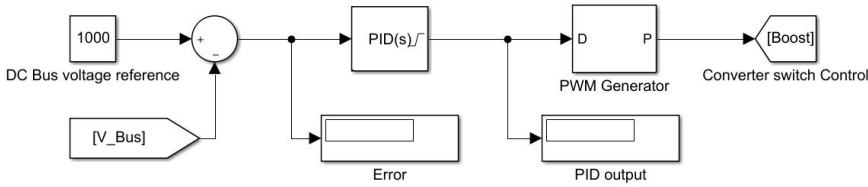

Figure 5.16: Feedback loop controlling the PWM generator of the converter in voltage control mode

The dual-phase and the insulated boost converter are controlled using the same feedback loop when in voltage control mode. In the dual-phase converter the switch on the second phase is controlled using the same pulses, but shifted of a constant 180 degrees. Similarly to the dual-phase converter, the insulated converter controls switch 1 and switch 4 with the original signal and switch 2 and 3 with the phase shifted signal.

In current control mode the current output of the PEMFC is actively controlled using the converter's switch. This type of control was implemented for the single and double-phase boost converters. The control is implemented with a feedback loop using a PID controller (see Fig. 5.18). In the single-phase boost converter the measurement of the output current is carried out on the branch containing the inductor. In the double-phase converter, because of the two inductors,

the measurement of the output current is carried out before the input capacitor of the converter. In both cases the error is fed to the PID controller that determines the duty ratio for the PWM generator. The PWM generator then controls the IGBT switch implementing the current control on the user side. This approach leads to the control of the circuit where the inductor acts as a controlled current source.

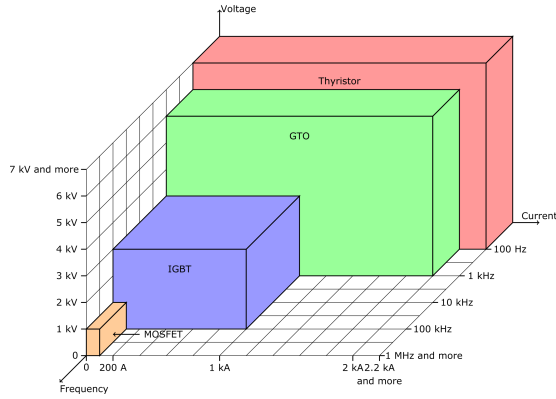

Figure 5.17: Current, voltage and frequency range for switches in power electronics components [Source: Electronics stack exchange]

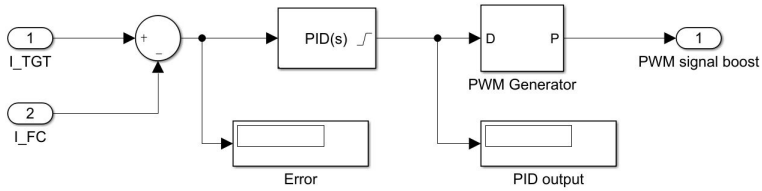

Figure 5.18: Feedback loop controlling the PWM generator of the converter in current control mode

It is possible to realize a combined control feedback loop that regulated both current and voltage output. This type of feedback loop can be realized using an inner and outer loop feedback with cascade PID controllers. This type of control is not studied in this thesis and is part of future developments.

5.4.3 DC/DC bi-directional converter model and control

The battery is connected to the DC-Grid using a single-phase bi-directional DC/DC converter. This topology allows the flow of electric current from power source to user and vice versa, allowing the discharge or recharge of the battery depending on operational conditions (see Fig 5.19).

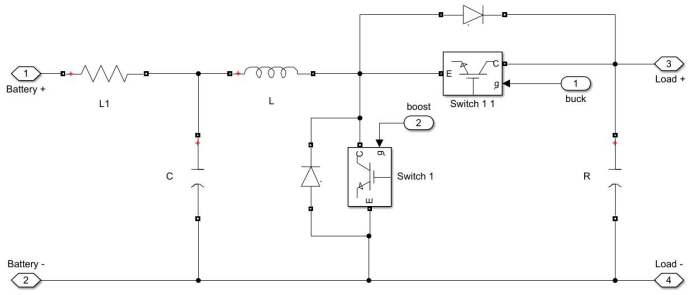

Figure 5.19: Base electrical circuit representing a bi-directional converter connecting a battery and a load

The sizing of the inductance and capacitance follows the same equations described for the single-phase boost converter in Section 5.4.1. The calculated values need to be tested to ensure low levels of voltage ripple both during discharge and recharge. The switches used in this case are IGBT's, as in the case of the boost converter, due to considerations on the power range, switching frequency and output voltage.

The bi-directional converter control can be defined for two separate phases: discharge phase and recharge phase. In the discharge phase, switch 1 (see Figure 5.19), is left open with the current passing through the diode. Switch 2 is controlled using the same method defined for the boost converter in Section 5.4.2, either in current control mode or in voltage control mode. With switch 1 open, the bi-directional converter acts as a single-phase boost converter and the feedback loops used are identical. During the recharge phase multiple approaches can be adopted. The battery recharge conditions have an effect on the longevity of the unit [93] and need to be carefully evaluated to present a good trade-off between operational flexibility and degradation. In this case two recharge approaches have been adopted. The first approach is the most conservative and imposes a constant current recharge until the maximum cell voltage is reached, and then a constant voltage recharge until the SOC of the battery is equal to 100% (see Figure 5.20). This dual recharge mode is realized with a combination of a current feedback loop for the constant current (CC) recharge, and a voltage feedback loop for the constant voltage recharge (CV) (see Figure 5.21). The feedback loops include two PID controllers[3]. The connection to the system of each one of the two is controlled by a switch that measures the voltage on the battery. With the two loops connected alternatively to the system, it is important to include an external reset for the PID

[3]The values used for a battery of 400V and 1750Ah in the discharge loop are: P = 1e-6, I = 5e-3, D = 1e-5. In the recharge loop are: P = 5e-3, I = 0.1, D = 1e-8.

controlled during the connection of the loop to to discharge the controller's internal integrator. The second recharge mode is less conservative and is realized using a single voltage control loop, similar to the one used for the PEMFC (see Fig. 5.16). This mode of operation recharges the battery with a variable current, determining less ideal conditions, and therefore more degradation, but allowing all of the PEMFC surplus power to be stored inside the battery providing more operational flexibility. This is the approach used in the load leveling strategy presented in Article 4, when CC/CV recharging is not possible.

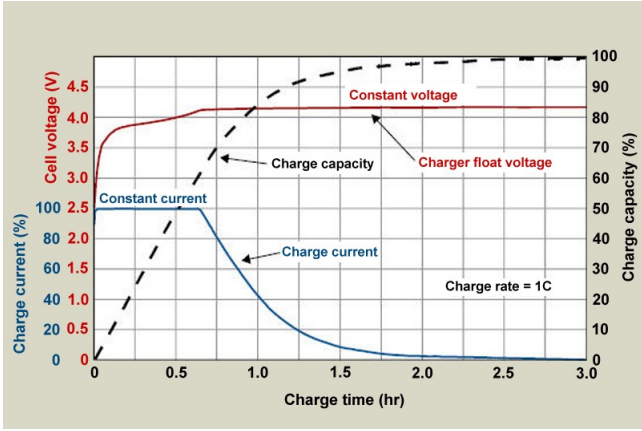

Figure 5.20: Recharge curves for the battery model when using the CC/CV recharge approach

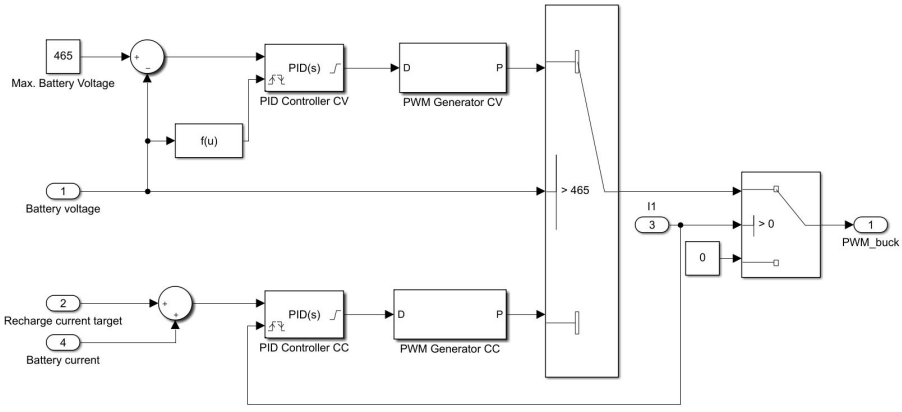

Figure 5.21: Feedback loop for 2-mode battery recharge CC/CV

5.4.4 DC/DC buck and boost converter average model

All the converters modelled in the previous sections include one or more switching elements, in the form of IGBT switches. The simulation of these switches is necessary when the user wants to study the switching dynamics of the converters and test realistic PWM control system for the converters. The use of switching elements makes the model more realistic, but increases the computational cost of the simulations. The first factor that contributes to the increase in computational cost is the need for small simulation time-steps (s_r) in a cycle-by-cycle simulation. The appropriate timestep is calculated as a function of the switching frequency (s_r) and should not exceed the value calculated using Equation 5.16.

$$s_r = \frac{1}{2\, f_s} \tag{5.16}$$

The second factor that increases the computational cost is the use of feedback loops with PID controllers for the control of the converters, checking the reference value at each time-step and correcting the output.

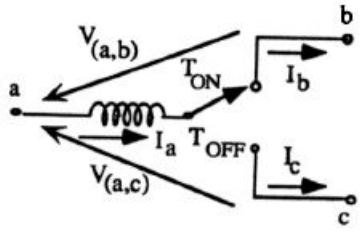

Figure 5.22: Switched inductor representation [94]

If the user is mainly interested in the power generation and distribution inside the vessel's grid, and it is possible to assume that the switching dynamics do not influence the results in a relevant way, it is possible to use an average model for the converters included in the system. The difference between an average model and a realistic model is detailed in the work of Ben-Yaakov [94]. In an average model the switched assembly, including switch, diode and inductor is replaced with a switched inductor (see Figure 5.22). The switched inductor can be modelled using three current dependent sources G_a, G_b, G_c (see Figure 5.23) defined using Equation 5.17.

$$G_a = \bar{I}_l \; ; \; G_b = \bar{I}_l * D_{on} \; ; \; G_c = \bar{I}_l * D_{off} \tag{5.17}$$

$$\frac{dI_1}{dt} = \frac{V_1}{L} \tag{5.18}$$

$$\bar{V}_1 = \frac{V(a,b) * T_{\text{on}} + V(a,c) * T_{\text{off}}}{T_{\text{on}} + T_{\text{off}}} = V(a,b) * D_{\text{on}} + V(a,c) * D_{\text{off}} \tag{5.19}$$

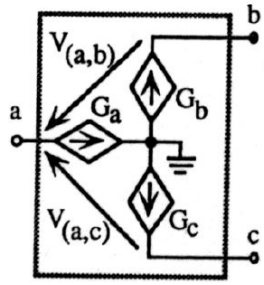

Figure 5.23: Switched inductor model [94]

With this modelling approach it is possible to simulate the function of the converter using controlled voltage and current sources, instead of switches, reducing substantially the computational time. The average converter model can be controlled using the equations defining the duty ratio for the buck or the boost converter without the need for PID controllers. The average model is implemented in Simulink using the described approach and using the work of Motapon et al. [95] as reference for the integration in the hybrid system.

5.5 Other components

The remaining components included in the model are the switchboard and the load, also defined as "current sink". Considering the adoption of a distributed DC On-board grid, each power converter is located as close as possible to the respective consumer or producer. Each production unit has the possibility of an integrated converter mounted directly on the unit itself or alternatively in a separate cabinet close by. There are no needs of collecting all these units in a centralized “switchboard room” as in a classic AC-Grid design. For these reasons the model of the switchboard is very simple and includes a series of ideal switching connecting the components to the grid.

The electrical load is modelled using a controlled current source with negative input values so that the current is absorbed by the component, turning it into a

load sink. Such component is considered ideal and does not take into consideration the more complicated effects encountered in the vessel's electrical grid when induction motors, or other power users, are connected. The replacement of such an ideal load model with a realistic model of the load side of the vessel's grid is considered for future development.

Chapter 6

Hybrid powerplant dynamic model

The components described in Chapter 5 are used to realize a dynamic model in the block diagram environment Simulink to simulate a vessel's powerplant system during operations. Particular interest is placed on the power generation, storage, and distribution within vessel's electrical grid. Two different modelling approaches are described in this Chapter. The two approaches use the same component's sub-models, but differ in aspects such as component's connection and control.

6.1 Modelling methods

The creation of a hybrid powerplant model that can simulate the operations of a maritime vessel of new design, or one that currently operates with a conventional propulsion system and will be retrofitted with a hybrid system, starts by analyzing the energy requirements of the vessel. When considering a new vessel, such energy requirements can be estimated by analyzing factors related to the vessel's design and the operated route. For a vessel currently in operation with a conventional propulsion system, being retrofitted with a hybrid system, the energy requirements are obtained by sampling the power demand during operations with the conventional powerplant. The energy requirement analysis leads to the definition of the operational profile (OP), that provides a power delivery target for the hybrid powerplant in each operational instant. The OP in this thesis is considered as the power demand measured at the DC-Bus, prior to being reconverted to AC and distributed to motors and auxiliary loads. The definition of the OP is a starting point for the calculation of the component sizing, and formulation of the energy management strategy. Both of the presented models utilize the OP as the initial

input.

The scalability of hybrid systems, where multiple identical components can be connected in parallel to achieve the desired power output, means that many different types of powerplants configuration, belonging to different vessel classes, can be represented using the components described in Chapter 5. An example of powerplant configuration is studied in both Article 2 and 4 (see Section 7), proposing a hybrid powerplant with PEMFCs and Li-Ion batteries for the double ended ferry described in Section 1.5.2. The model, independently from the type of vessel considered, should be configured to satisfy the conditions listed below.

- The proposed hybrid configuration, utilizing PEMFCs and Li-Ion batteries, should be able to satisfy the power demand (OP) of the vessel during the considered operational interval, ensuring satisfactory performances when compared to a conventional propulsion system (ICE or turbine).
- The proposed hybrid configuration should ensure the same level of operational flexibility, when compared to the conventional propulsion system. Operational flexibility is defined using factors such as hydrogen consumption, aiming to eliminate the need for refueling during day operations, or monitoring the power consumption to eliminate the need for land-based recharging during Ro-Ro operations.

These goals are obtained using a combination of effective component sizing (CS) and energy management strategy (EMS), where these are developed in a combined package. While a first attempt solution at defining the optimal CS and EMS combination can be carried out using the software presented in Chapter 4, a dynamic model is necessary for the validations of the obtained results. Two possible approaches were identified and used for the realization of a dynamic powerplant model. The use of such approaches has led to the development of two different models to represent the ferry's powerplant:

- Model using load separation
- Model using load combination

The two approaches have different structures, determining the model's limitations, and are based on different assumptions. The computational cost of carrying out simulations with the two models is also different, depending on the simplifications selected. Both models use the same base sub-models for all PEMFCs, batteries, converters and current sink, the only difference is in the number and connection between these components.

6.1.1 Model using load separation

The first model developed for the project is the model using the "load separation" approach. This model is the one used in Article 2 and 4 (see section 7) for the simulations of the hybrid system. This type of model was developed to simulate the hybrid powerplant at a relatively low computational cost, introducing a series of assumptions that allow the user to limit the number of components necessary to simulate the system's dynamic behavior.

In this model, each individual PEMFC and Li-Ion battery model is connected to an independent DC-Load block after the power conversion using either the boost or bi-directional converters. This model is compatible with all the converters presented in Section 5.4, with average converter models being used in continuous simulations and other models being used for discrete simulations. The electrical connections in this topology are represented by black lines in Figure 6.1, and control connection are represented by red lines. It is possible to observe that no electrical connection is present between the individual DC-Load blocks.

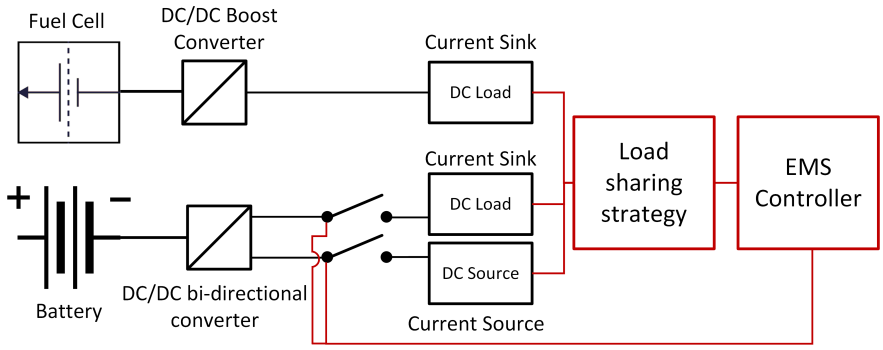

Figure 6.1: Simplified block diagram representing the load separation model logic

$$P_{\text{op}}(t) = P_{\text{fc-tot}}(t)\ \eta_{\text{bc}} + P_{\text{b-tot}}(t)\ \eta_{\text{bi-dir}} \tag{6.1}$$

The model using load separation is built on two conditions. The first condition is that Equation 6.1 is valid for each timestep of the simulation. The second condition is that the converter's control system is able to keep the voltage output to the DC-Load blocks stable at the reference set by the user.

The first condition, involving Equation 6.1, is necessary for the correct simulation of the system when considering the load sharing strategy used to control the DC-Load blocks. The power demand at the DC-Bus P_{op} is split between PEMFCs $P_{\text{fc-tot}}$ and batteries $P_{\text{b-tot}}$. The term $P_{\text{b-tot}}$ can be either positive, during discharge,

or negative during recharge. Using individual DC-Load blocks in this model opens the possibility to reduce the number of components required to simulate the powerplant. PEMFCs and batteries respectively can be grouped together and represented as a single unit, subjected to a DC-Load that is equal to the load of the group divided for the number of units in the group. This is based on the assumption that the dynamic behavior of all the PEMFCs or batteries in a group is identical. This simplification can be extended, representing the entire system using just one PEMFC group and one battery group. In this case, for example, the power demanded from each component group is equal to the total power demand assigned to a type of component ($P_{\text{fc-tot}}$, $P_{\text{b-tot}}$), and it is divided for the respective number of unit present in the system (n_{fc}, n_{b}), to be assigned to the DC-Load connected to either the PEMFC or battery. The behavior of PEMFC, and battery, is observed thanks to the output of the dynamic sub-models described in Chapter 5. The results obtained from of the single components are then multiplied again for the number of units to simulate the response of the complete system. This approach reduces substantially the computational resources needed for the simulation, but introduces the limitations. The first limitation is the impossibility to control the current output of the PEMFCs independently, leading to the load always being always considered split equally between the components that are considered grouped together. The second limitations is the impossibility to complitely disconnect one or more PEMFCs during operations.

The second condition is based on the converter's operations. The converters ensure that, after the component's start-up phase, the voltage on the DC-load blocks side is kept stable at the user's set reference $V_{\text{DC-Bus}}$. Maintaining all the DC-load blocks at the same voltage, stable throughout operations, is a key conditions for using this model for two reasons. The first reason is that, with no electrical connections between the load blocks, there is no possibility of observing the effects of a deviation from stable a voltage of one component onto the other components. The second reason is that all the components in this topology are controlled using just voltage control mode with feedback loops using one PID controller. In this configuration the current output of the PEMFC or battery is defined indirectly by the DC-Load (see Equation 6.2 and 6.3). A voltage instability on one DC-Load block would lead to the calculation of inaccurate results and the failure to correctly simulate the system. A stable voltage throughout operations, with a small range of acceptable variation during transients, is the only way to correctly implement a sort of simulated DC-Bus, not physically present in this model's topology but realized through the control system.

$$P_{\text{fc-tot}}\,\eta_{\text{bc}} = V_{\text{fc}}\,I_{\text{fc}}\,n_{\text{fc}}\,\eta_{\text{bc}} = V_{\text{DC-Bus}}\,I_{\text{demand-fc}} \tag{6.2}$$

$$P_{\text{b-tot}}\,\eta_{\text{bi-dir}} = V_{\text{b}}\,I_{\text{b}}\,n_{\text{b}}\,\eta_{\text{bi-dir}} = V_{\text{DC-Bus}}\,I_{\text{demand-b}} \tag{6.3}$$

Equation 6.2 and 6.3 show respectively the relation between $P_{\text{fc-tot}}$ and $P_{\text{b-tot}}$ and the current value ($I_{\text{demand-fc}}$,$I_{\text{demand-b}}$) assigned to the DC-Load blocks connected to either the PEMFC or the battery. The battery can be discharged or recharged in this model as it would be possible in the complete system. If the EMS imposes a value for $P_{\text{fc-tot}}$ that results in a negative value for $P_{\text{b-tot}}$ in Equation 6.1, the battery is in recharge mode. The DC-Source connected to the battery produces a current value equal to the surplus current absorbed by the DC-Load connected to the PEMFC. The limitation in this case is that it is assumed that the simulated DC-Bus is kept at a stable voltage, even during recharge, by the boost converter connected to the PEMFC.

To summarize the characteristics of the model using load separation it is possible to list the assumptions that the model is based upon:

- All the components grouped together, with the same technical characteristics, and represented as a single unit have the same dynamic behavior when delivering the same electrical load.
- It is not necessary to simulate the DC-Bus while the voltage is kept stable at the same value for all of the DC-Load blocks.
- The voltage on the the simulated DC-Bus is considered constant even during the recharge phase of the battery.

And the limitations:

- The electrical load can only be split equally among the components of a group, as they are represented by a single unit in the model.
- It is not possible to observe the effects of voltage instabilities on the DC-Bus affecting other components in the system, if the control of one component fails.
- During the recharge phase of the battery the surplus of current used is not flowing from the PEMFCs to the batteries through an electrical connection but a separate current source is used. This approach ignores losses within the recharge circuit and prevents the user to detect anomalies in the dynamic behavior of the system that may appear in the complete system.

6.1.2 Model using load combination

A second model has been developed to carry out more computationally heavy, yet realistic, simulations of the powerplant system. The second model uses an approach defined as "load combination", in contrast with the "load separation" of the previous section.

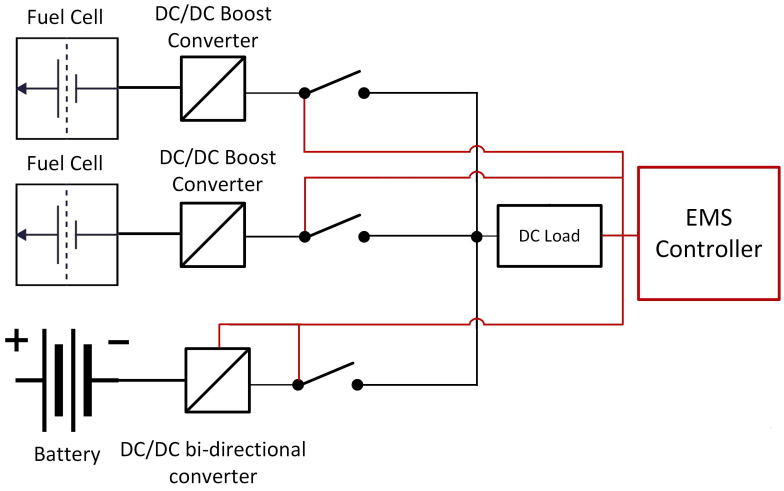

Figure 6.2: Simplified block diagram representing the load separation model logic

The dynamic models used to represent the components in the system are the same as the one described in Chapter 5, and also used in the load combination model, but the connections between them are different, introducing new capabilities in the simulations. This model is compatible with all the converters presented in section 5.4, with average converter models being used in continuous simulations and other models being used for discrete simulations.

The structure of the model can be observed in Figure 6.2. In this model the total electrical load is represented using a single DC-Load block controlled by the EMS. The DC-Load block represents the only current sink of the system, and is in charge of simulating the total power demand. The current demand I_{demand} assigned to this DC-Load block at each time-step is calculated using Equation 6.4.

$$P_{\text{op}} = V_{\text{DC-Bus}}\, I_{\text{demand}} \tag{6.4}$$

The DC-load is connected to the PEMFCs and batteries through a point of connection that simulates the DC-bus. The connection of multiple components to

a simulated DC-Bus allows the observation of possible voltage instabilities generated by one component and the effects on other components. Voltage instabilities can be detected if the components are operating outside the recommended power output range or if the control system is not able to quickly respond to a sudden change of load.

The components in this topology cannot be grouped, but can be individually disconnected from the system using the switches between the DC/DC converters and the DC-Load. The EMS monitors the power output of each PEMFC and controls the switches connecting the components to the DC-bus. The EMS also controls the switches inside the bi-directional converter of the battery, determining if it is discharging or recharging. If a power surplus is detected by the EMS, the PEMFC creating this condition can be temporarily disconnected from the grid, or the power surplus can be sent to the battery pack for energy storage. Similarly, if a power deficit is detected, the battery can be connected to the system to satisfy the power demand while in discharge mode.

The validity of Equation 6.1 is ensured by the electrical connections in an isolated grid. The power generated by the PEMFCs and batteries is either used by the DC-Load or lost due to the efficiency parameters of the components. The power recharging the battery is always equal to the power surplus of the PEMFC's as the system is isolated with only a controlled DC-load source as an alternative power-sink.

The PEMFCs and batteries utilized in this model can be controlled either in voltage control mode or on current control mode. It has to be specified that at least one component needs to be controlled using voltage control mode to maintain the DC-Bus at a stable voltage level. Preferably the component used in voltage control should have a low response time (secondary battery or super-capacitor).

The creation of the load combination model requires the formulation of new assumptions. These assumption can be summarized as:

- The total power demand during the vessel's operations can be represented by a single controlled DC-Load block, neglecting the effects of the remaining powertrain components.
- During the simulation, the components connected to the DC-grid can be disconnected or reconnected instantly and safely.

The development also leads to the observation of new limitations:

- Computational cost is higher as the component cannot be grouped, but have

to be represented individually.

- The energy management strategy is more complex to create, with more variables to monitor and control.

6.2 Powerplant model monitoring and control

Every maritime powerplant nowadays is equipped with an integrated control, monitoring and protection system to regulate power generation and distribution. Considering the control hierarchy for a maritime powerplant, it is possible to identify three different levels: the user interface consisting of the operator stations, the system control level including the power management system (PMS), and the distributed control layers. The focus of this thesis is on the system control level. The PMS is tasked with different functions such as energy management, blackout prevention, and powerplant startup. The energy management function, implemented thanks to one, or more, energy management strategies (EMS) needs to ensure that power production is in line with the vessel's power demand at any time. In hybrid systems, with one, or more, energy sources and energy storage solutions, the energy control becomes a non-trivial task as there are many possible solutions to satisfy the imposed power demand using the different components. For this reason, the EMS of a hybrid system needs to be built and tested to optimize the energy production, consumption, distribution and storage in a grid system.

6.2.1 Energy management strategies

The EMSs suitable for hybrid powerplants utilizing proton exchange membrane fuel cells and lithium ion batteries were identified through a literature review and subsequent study. The literature review included the papers considering maritime applications, but was also focused on the automotive industry, as scientific publications for this field are readily available. A good overview of possible EMSs strategies is presented in the publication of Huang et al. [10].

The EMSs identified can be either defined as offline or online. Offline strategies are map-based methods that define the load sharing strategy between components using static performance maps compiled after laboratory tests. Such maps are based on the consideration of parameters such as fuel consumption or required speed. Online methods are capable of real-time definition of the load-sharing strategy as they use different analytical methods to evaluate input parameters from the system. As the activity of this thesis is dedicated to system modelling with no experimental activity, the EMSs considered for testing on the developed Simulink models are of the Online type.

The development of EMSs to conduct tests with the Simulink models started

from the less complex rule-based EMSs. These rule based EMS use a set of predefined instructions that, according to the system parameters, define the load sharing strategy at each instant. Following the development of rule-based EMSs, optimization based EMSs such as the equivalent consumption minimization strategy (ECMS), were developed.

6.2.2 Model implementation for rule-based EMSs

The use of Online EMSs is determined by the need to simulate the response of a system that changes its state as a function of physical time. Online systems are defined here as systems that are not dependent upon just logical results of computations but also on the instant that the event takes place. Rule-based EMS's have been selected, in this case, as the first EMSs to be studies due to faster implementation in the testing of a newly developed model. Rule-based approaches rely on a set of predefined rules that define the power distribution at each time instant based on the inputs received by the EMS. The selected rule-based approaches are described in detail in Article 2 and Article 4 of Chapter 7.

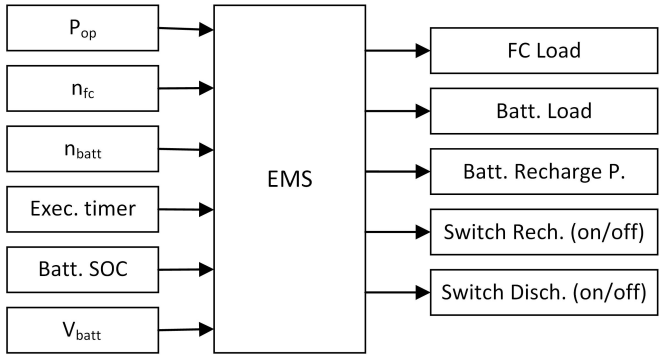

Figure 6.3: Block diagram representing the I/O of the EMS in the load separation model

In the model using load separation the EMS uses Equation 6.1 as a target for each operational point. A small range of variation is taken into account during transient loading conditions. The power distribution is regulated by controlling the switches connecting the battery to the recharge or discharge circuit, and assigning a DC-load to each individual current sink. The DC-load assigned to each individual current sink is defined by the load sharing strategy calculated by the EMS based on system parameters such as the battery SOC. The battery voltage (V_b) is also used, in this case, to define the battery recharge power and how this is carried out, as the DC/DC converter can operate both in constant current (CC) or in constant voltage (CV) recharge mode.

In the model using load combination, the EMS controls the connection of all

the components to the DC-Bus, and controls if the battery is charge or discharge mode. In this model there is the option of controlling all the components in voltage control mode, not imposing a load sharing strategy, and using the battery to simply store/release energy to compensate with the battery response time. It is also possible to control a series of components in current control mode to define the power output and, in case of the PEMFCs, the hydrogen consumption at any given time (see Fig. 6.4).

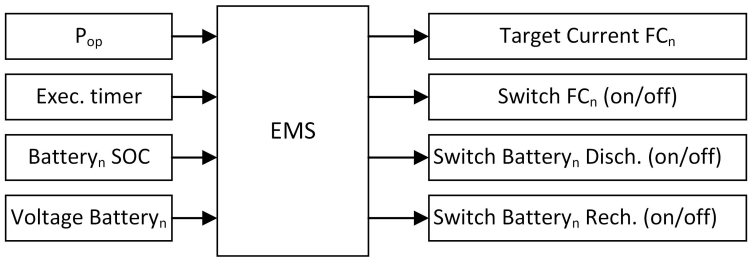

Figure 6.4: Block diagram representing the I/O of the load combination EMS, if one or more PEMFCs are controlled in current control mode

The inputs and outputs in this case are fewer than in the load separation model. This is because it is not necessary to simulate the current flow between the components, as this happens in the electrical connections representing the vessel's grid. The subscript *n* for the fuel cell and the battery inputs or outputs indicates that the EMS needs one of these inputs or produces one of these outputs for each unit included in the system. The EMS needs to ensure a satisfactory performance level in addition to ensuring a reliable power delivery.

6.2.3 Model implementation for optimization-based EMSs

Optimization based EMSs are able to address constrained multi-variable problems in real-time, improving on the capabilities offered by rule-based EMSs. Optimization based EMSs considered in this thesis are adaptive EMSs, meaning that the evaluate a series of parameters of the system at each operational instant and calculate the optimal strategy for power production and distribution. In the model the optimal solution is often impossible to achieve due to the component's phisical and technical limitations, but sub-optimal solutions are often adopted when taking these conditions into consideration. The optimization based strategy developed is the equivalent consumption minimization strategy (ECMS). This strategy was tested on the model using load combination with average converter models for a fast computational time. The strategy was developed based on the study of Motapon et al. [95] with relative cost function formulation.

The implementation is done on the model where the PEMFCs are all in cur-

rent control mode while the battery operates in voltage control mode. The load sharing strategy calculation is carried out starting from the parameter α defining the penalty coefficient of battery power in Equation 6.6 based on the battery SOC at each instant. μ is a constant value during the simulation that can be tuned for applications in different systems.

$$\alpha = 1 - 2\mu \frac{SOC - 0.5(SOC_{\text{max}} - SOC_{\text{min}})}{SOC_{\text{max}} + SOC_{\text{min}}} \tag{6.5}$$

$$f(P_{\text{fc}}, \alpha, P_{\text{b}}) = P_{\text{fc}} + \alpha * P_{\text{b}} \tag{6.6}$$

The cost function f is calculated at each instant for the values that satisfy the conditions imposed in the system of equation represented in 6.7

$$\begin{cases} P_{\text{fc}} + P_{\text{b}} = P_{\text{load}} \\ P_{\text{b-min}} \leq P_{\text{b}} \leq P_{\text{b-max}} \\ 0 \leq \alpha \leq 1 \end{cases} \tag{6.7}$$

The power output of the PEMFC is then limited, for technical reasons using Equation 6.8.

$$P_{\text{fc-min}} \leq P_{\text{fc}} \leq P_{\text{fc-max}} \tag{6.8}$$

The calculated value for P_{fc} is then used as a target output for the PEMFCs, with the power split equally in this case between all the units of the system. The battery is kept in voltage control mode to compensate for quick variations in the load and the delivery of power where the PEMFCs cannot deliver the total power demand.

Chapter 7

Summary of results

This chapter summarizes the purpose, methodology, and results of all articles enclosed in this Thesis. The summary focuses on the enclosed publications. The articles are presented in chronological order of publication (or submission).

All the articles enclosed in this thesis are developed following the objectives defined in the research plan (see Section 1.3). While Article 3 and Article 6 have been developed as part of the coursework, and address safety challenges identified during the literature review defined objective 1, all other articles target directly the main research question.

7.1 Article 1: Study on the architecture of a zero-emission hydrogen fuel cell vessel power-generating unit

7.1.1 Purpose and novelty

The purpose of this article is to describe the development process of a Matlab application for the sizing of a maritime powerplant utilizing PEMFCs and Li-Ion batteries. The powerplant's sizing and composition is determined as a function of the energy management strategy selected by the user. This application was developed from the ground up, with the aim of building a software that could automate the sizing process, providing design guidelines based on user input with a relatively short computational time. The application includes a graphic user interface for ease of use. Equations describing the model, Calculations of the component sizing, and the logic of the algorithm are described in the paper.

The development of this application is motivated by the need to produce a first attempt solution for the component sizing of the powerplant. This need is

present both in industry and research. In research the powerplant configuration can be the starting point for setup of simulations with a dynamic model. In the industry the configuration can be considered as a base for the calculation of the technical and economic feasibility of a hybrid solution.

The work is carried out as a part of objective 2 from the research plan, where the main focus is on investigating the formulation of design criteria for hybrid powerplants utilizing proton exchange membrane fuel cells and batteries. The Matlab application provides a software tool to define such design criteria, producing results that can be used for the optimization of operations based on the shipowner priorities.

7.1.2 Methodology

The article starts with a literature review on the state-of-the-art of maritime hybrid systems, energy management strategies, and the main system's components. Once familiarized with the system topology, the components of the powerplant are characterized. The component's technical characteristics are selected based on the size and power output of the vessel considered in the case study. In this paper, the vessel selected for the case study is the double ended ferry described in Section 1.5.2, with a diesel-electric configuration, and capable of a power output equal to 4MW. The PEMFC selected is a unit with a power output of 100kW, and it is characterized according to the data available on the technical documentation provided by the manufacturer. The characterisation includes the power output curve, the maximum power output value, and efficiency values for different operational points. The battery is characterized as an ideal energy storage, to simplify the calculations, with the ability of storing and delivering power without limitations when operating within the SOC limits imposed.

The algorithm that identifies the sequence of calculations performed to achieve the case study results is presented in the article. This algorithm is used to also define the structure of the code. The results are obtained applying a series of equations to determine the power generation and distribution in the vessel's electrical grid when the EMS selected is of the load-leveling type.

The approach adopted during the modelling phase can be defined as quasi-static. During the simulation of the system multiple time-dependent variables are considered, but each timestep is calculated independently and is not influenced by the system's condition in previous or following time-steps. It is assumed that the electrical grid operates in a condition of equilibrium.

7.1.3 Results

The application is used to calculate one the possible configurations for a hybrid powerplant to substitute the diesel-electric configuration currently adopted on the vessel considered in the case study. The main output of the application is the definition of the powerplant size through the calculation of the number of PEMFCs, and the battery energy storage capacity required. Other outputs, such as the consumption of hydrogen, and the estimated PEMFC degradation can help the used user to estimate the feasibility of the selected solution.

Overall the application presents itself as simple and intuitive, thanks to the developed GUI, to calculate values necessary during the vessel's preliminary design. This version of the application has large room for improvement with the possibility to include new functionalities, and new EMSs. It is for this reason that Article 5 expands the work carried out in this first publication, producing a more polished and complete version of the Matlab application.

7.2 Article 2: Modelling and simulation of a zero-emission hybrid power plant for a domestic ferry

7.2.1 Purpose and novelty

The purpose of this article is to describe the development and testing of a dynamic model representing a hybrid powerplant utilizing proton exchange membrane fuel cells and lithium ion batteries. The model is developed in Simulink and it is based on the load separation approach presented in Section 6.1.1. The hybrid powerplant considered in the case study is proposed as a replacement for the diesel-electric configuration currently powering the double ended ferry described in Section 1.5.2.

The load separation model was developed from the ground up and presents itself as a novel approach for the simulation of a hybrid powerplant. While assumptions and simplifications are introduced to reduce the computational complexity, this dynamic model allows the user to observe the response of PEMFCs and Li-Ion batteries during operations. The results obtained of the case-study are analyzed and presented, to show the capabilities and limitations of such a model.

The dynamic model presented in the article was developed as a part of objective 4 of the research plan. The main focus is to optimize the system's operations based on the dynamic behavior observed for the components of the electrical grid. In this case, a benchmark for the operations parameters is set with the simulation using a load-leveling EMS.

7.2.2 Methodology

The paper starts with the detailed description of the ferry's powerplant and its daily operations. The time interval considered for the simulations is equal to 1 hour. In this time interval the ferry performs one out of eighteen crossing from its fixed daily schedule. As all the crossings show a very similar pattern in the power demand, it is considered sufficient, for this study, to consider a single crossing.

The dynamic models used to represent the components of the powerplant are presented. The model representing the PEMFC and Li-Ion battery are obtained from the literature, while the converters and their control system are modelled from the ground up. The proposed hybrid configuration, tested in the case study, uses a powerplant with 15 PEMFCs and 2 Li-Ion batteries for a nominal power output of 3500 kW. The power demand for this powerplant is defined by the operational profile, characterizing the power absorption at the DC-Bus level. The sub-models representing the components are connected inside the Simulink simulation environment using the load-separation approach described in Section 6.1. A simulation in the discrete domain using a 1e-6 seconds timestep is performed. The EMS selected for this case study is of the load-leveling type.

7.2.3 Results

The simulation using the dynamic model produces a series of outputs in the form of data-points that can be plotted to observe the dynamic behavior of the powerplant components during the time interval considered. The outputs include the voltage and current of both PEMFC and Li-Ion battery, the voltage and current values on the DC-Load side, the SOC of the batteries, and the hydrogen consumption. The calculation of the degradation is performed based on the power output values of the PEMFC during the simulation.

The first step of the results analysis is the comparison between the power delivery of the hybrid system and the power delivery of the diesel-electric system currently installed on the vessel. A range of variation was set prior to the simulation to account for a different dynamic behavior during constant and transient loading conditions. The power delivery calculated for the hybrid system is within the limits determined prior to simulations. The results analysis follows with the observation of the voltage on the DC-load side. The voltage regulation of PEMFCs and batteries is satisfactory, but shows room for improvement, especially in the elimination of voltage instabilities during the connection and disconnection of the battery recharge circuit. The value representing the SOC of the battery is analyzed to verify that the battery capacity included in the system is of adequate size and C-rating. The hydrogen consumption of the PEMFC is analyzed to define the

size of the hydrogen storage that needs to be installed onboard and the estimated fuel costs per crossing.

The results help to evaluate the choice of powerplant and EMS for this specific use-case. If the configuration results obtained are deemed satisfactory by the the ship designer, it is possible to proceed with the system's implementation or opt for further refinement of the solution, or even test a different EMS.

7.3 Article 3: Towards safety barrier analysis of hydrogen powered maritime vessels

7.3.1 Purpose and novelty

The purpose of this paper is to perform a qualitative safety barrier analysis for a hydrogen powered maritime vessel. The topic of the article was selected to familiarize with possible safety challenges related to the use of hydrogen as an energy carrier in the maritime industry (see Section 2.4). The article focuses on vessels powered by cryogenic hydrogen, specifically vessels with a storage placed below deck, in a ventilated yet enclosed space. The scenario considered in the case study examines the effects of a leak of hydrogen from the cryogenic tank, defining a series of safety barriers that need to be put in place to avoid ignition, explosion, detonation or other critical scenarios.

The work carried out in this article describes a study carried out during the PhD coursework. The topic has been selected in relation to the safety challenges of hydrogen systems encountered during the literature review performed in objective 1 of the research plan.

7.3.2 Methodology

The method used in the study is the Barrier and Operational Risk Analysis (BORA) method. The BORA method is generally used in the oil and gas industry to evaluate the risks related to the leak of hydrocarbons, but is adapted to carry out a safety barrier analysis considering a leak from a hydrogen storage system onboard a vessel. This article focuses on the qualitative part of the BORA method, developing 4 out of the total 8 steps. The qualitative part of the BORA method developed in the case study provides a generic framework for the evaluation of safety barrier analysis in vessels using cryogenic hydrogen as an energy carrier. The BORA method is structured in well defined steps and uses different well known methodologies for the safety barrier analysis, including barrier block diagrams (BBD), risk influencing diagrams (RID), and fault tree analysis (FTA).

7.3.3 Results

The qualitative safety barrier analysis performed in the article leads to the formulation of a barrier block diagram wherein the safety barriers and their functions are defined. The barriers are evaluated using FTA. Factors which may lead to the considered critical scenario are described in the risk influence diagram. The analysis of the barriers and their qualitative evaluation has identified a series of technical and administrative measures to be implemented during the design of the vessel or the training of the crew. These measures can be used in the development of a maintanence checklist, to ensure safe operations. This topic is expanded in a with a quantitative risk analysis using Bayesian networks in Article 6.

7.4 Article 4: Energy management strategies for a zero-emission hybrid domestic ferry

7.4.1 Purpose and novelty

The purpose of this article is to present three case studies, performed with the hybrid powerplant dynamic model developed in Simulink. The three case studies focus on the the influence of component sizing on the choice of energy management strategy and vice-versa. They also generate a series of results that can be used to compare the different powerplant configurations and evaluate performances. The vessel taken into consideration is the double-ended ferry described in Section 1.5.2. The work is a further development of the analysis carried out in Article 2.

The three case studies are developed following the guidelines set in objective 5 of the research plan, where the focus is on the testing of the developed models with real world data. The testing of different EMSs is also fundamental in the effort of operation optimization, with the possibility to compare the results obtained with different strategies and evaluate the most suitable for the considered conditions.

7.4.2 Methodology

The powerplant dynamic model developed in Simulink is configured according to the load-combination approach described in Section 6.2. Three energy management strategies of the rule-based category are selected: load-leveling, peak-shaving, and charge-depleting/charge-replenishing. The EMS is implemented in the EMS function block included in the model. The load-leveling strategy is a modified version of the one used in Article 2. The main modification introduced is the potential to recharge the battery at a variable current input if a power surplus is detected during transient loading. The peak shaving strategy is used to reduce high frequency load transients that may be experienced by the PEMFCs, filter-

ing the power demand of the DC-Load. The operational profile is filtered using a simple moving average with a window of 5 data points. The filtered power demand is then assigned to the PEMFCs while the battery compensates for the slower dynamic response of the PEMFC's during transients. The charge-depleting/charge-replenishing (CDCR) strategy, a variation of charge-depleting/charge-sustaining used in the automotive industry, allows the vessel to navigate under battery power for extended periods of time. The PEMFC's are, in this case, considered as range-extenders and are tasked with alternatively recharging one of the two main battery packs.

The powerplant composition, including the number of PEMFCs and Li-Ion batteries is calculated for each individual case. The reconfiguration is necessary as the choice of EMS determines the load sharing strategy during operations and how the power demand is satisfied. The component sizing is performed using the approach described in Article 5 for the load-leveling and the peak-shaving strategy. The powerplant sizing used for the CDCR strategy is defined using one one calculated for the load-leveling EMS.

All the simulations are performed in the discrete time domain with a time-step equal to 1e-6 seconds. This time-step is selected to capture the switching dynamics of the converters and observe in detail the voltage and current delivery to the DC-Load blocks.

7.4.3 Results

Each performed simulation produces a series of results, in the form of data-points, that can be used to evaluate the performance of the powerplant configuration. After plotting the results it is possible to observe the dynamic behavior of the PEMFC and Li-Ion battery under the load sharing strategy imposed by the selected EMS. The power conversion taking place inside the converter and the converter's output can be also observed. The hydrogen consumption of the PEMFC is calculated and the degradation of the single FC estimated using degradation values from the literature.

The analysis of the case studies concludes that each configuration optimizes a set of factors while giving secondary priority to another set of factors. For example, a load-leveling strategy prioritizes the minimization of the PEMFC degradation at the expenses of space and footprint used. Each solution is considered as a trade-off and the parameters to optimize need to be selected by the shipowner during the design process. All the powerplants can work with all the EMSs, but performances and range is heavily impacted. The design of the powerplant, in terms of component choice and sizing, needs to follow the choice of the EMS or

vice-versa.

The study carried out in the article paves the way for further work on optimization-based EMS's, such as equivalent consumption minimization strategy (ECMS). The study can be replicated and the results can be compared with the ones obtained with the rule-based strategies.

7.5 Article 5: Hybrid powerplant configuration model for marine vessel equipped with hydrogen fuel-cells

7.5.1 Purpose and novelty

The purpose of this article is to describe a mathematical model, and a software application built on it, that can aid the component sizing of a hybrid powerplant utilizing proton exchange membrane fuel cells and batteries. The work described in this article is an expansion of the application described in Article 1, and is developed in connection to objective 2 of the research plan.

The quasi-static mathematical model presented in this article has been modified, compared to what was presented in Article 1, to produce more precise results. Equations used for the calculation of the battery size and hydrogen consumption have been modified, and a function to monitor the response of the PEMFC to fast transient loading conditions is introduced. Multiple powerplant configurations based on two deterministic rule-based energy management strategies, either peak shaving or load leveling, can be calculated.

The development of this model, transformed into a software based application, is a response to the need of both academia and industry to determine powerplant configurations that allow efficient operations. The calculated configurations can be implemented and tested on dynamic models to validate the feasibility of the considered solution for the specific use-case.

7.5.2 Methodology

The topic presented in this article is a quasi-static model of the hybrid powerplant focusing on power generation, distribution and storage. The quasi-static definition considers that the generation and distribution of electric power inside the vessel's grid happens in a state of equilibrium. This assumption means that instabilities in the system during operations are not considered. The powerplant components including PEMFCs, batteries, and other power electronics components are modelled using simplified equations and are characterized through mapped data available from the literature or manufacturer. The technical data for these components are obtained from the datasheets of commercially available compon-

ents.

The vessel selected for the case-study is a harbor tugboat described in Section 1.5.2. This vessel performs operations with high frequency transients and it is an interesting change study when considering PEMFC propelled vessel. The operational profile was made available by the company operating the vessel.

The calculation is carried out according to the algorithm sequence and relevant equations presented in the article. The approach used is very efficient in terms of computational resources, and it allows the possibility to iterate through multiple different configurations, allowing the user to find the most suitable for the specific use case taken into consideration. The user can choose between two EMS, either load-leveling or peak-shaving, with the peak-shaving strategy including three different types of filters for the filtration of the OP. The model is used as a base for the development of a software to automate the calculation process. The software is turned into a Matlab based application with a GUI for ease of use.

7.5.3 Results

The harbor tugboat powerplant configuration is calculated using a peak-shaving EMS based on a Butterworth filter, for the filtration of high frequency transients, and the load-leveling strategy. Results relative to the component sizing for these specific use-cases are presented, allowing the comparison between the two strategies. The presented results provide important information for the evaluation of the technical performances of the system under the specified conditions. The evaluation of the hydrogen consumption allows the user to define the volume that needs to be dedicated to on-board hydrogen storage, while the value of degradation determines the required maintanence intervals.

7.6 Article 6: A Bayesian networks approach for safety barriers analysis: A case study on cryogenic hydrogen leakage

7.6.1 Purpose and novelty

The purpose of this paper is to further develop the study started in Article 3 with the presentation of a quantitative safety barrier analysis. The quantitative analysis is performed using Bayesian networks. The aim is to evaluate the performance of the safety barriers identified in Article 3, and calculate their failure rate based on data collected from the literature and the industry. In addition, it is possible to use the Bayesian network to evaluate different critical scenarios and relative consequences.

This quantitative risk barrier analysis adopts a well established methodology,

such as the Bayesian network, and uses it to define possible weaknesses in a system utilizing cryogenic hydrogen for energy generation onboard a maritime vessel. The evaluation of barrier performances is critical in a rapidly expanding sector and the identification of possible shortcomings is of the utmost importance for widespread adoption.

The work carried out in this article describes a study carried out during the PhD coursework. The topic has been selected in relation to the safety challenges of hydrogen systems encountered during the literature review performed in objective 1 of the research plan.

7.6.2 Methodology

The study begins with a review of Bayesian networks theory, including how they can be applied in risk assessments and how they can be implemented. The definition of the network's components, such as root nodes and leaf nodes is provided. The study of the Bayesian network is necessary to ensure the correct implementation of this tool during the safety barrier analysis.

The case study presented analyzes the hydrogen release from the cryogenic tanks stored below deck. The creation of the Bayesian network starts with the analysis of the event trees and barrier block diagram presented in Article 3. The failure probabilities of the considered events were derived from reliability data handbooks, and relevant literature on hydrogen systems and hydrocarbon release in Oil & Gas fields. The analysis of the Bayesian network model was carried out using Genie software developed by the Decision Systems Laboratory of the University of Pittsburgh.

7.6.3 Results

The probability of barrier failure is quantified using the Bayesian network. The ignition isolation barrier shows the highest probability of failure according to the data considered in the study. The results emphasizes the importance of avoiding procedures or equipment handling that could create static sparks and results in the ignition of released hydrogen. Of the remaining barriers analyzed, it is found that potential high-impact consequences have very low occurrence probability.

Since the model focuses on analyzing causes of safety barrier failure and their corresponding consequences, the hydrogen release is considered as an initiating event with a given likelihood. Further research should study the expansion of the model considering the technical, operational and external factors that can lead to a hydrogen leakage.

Chapter 8

Conclusions and further work

This chapter draws conclusions from the thesis and enclosed articles. Future research and development opportunities, that may contribute to the widespread adoption of zero-emission powertrain in the maritime industry, are also described in this chapter.

8.1 Conclusions

The main purpose of the PhD research work has been the study of hydrogen systems, the integration of PEMFCs in hybrid maritime powerplants, and the study of operation optimization with such systems. The work is carried out according to the objectives listed in the research plan and mainly focused on the development and testing of hybrid powerplant models to study the system behavior to set a benchmark and improve upon it.

Maritime powerplants have become increasingly complex systems over the last decades, with a shift towards electrical grids, instead of mechanical systems (propeller shaft, gearbox), for power distribution. The adoption of an electrical grid for power distribution allows a substantial increase in the efficiency of vessels operating short and medium range routes, with frequent maneuvering or dynamic positioning operations. Energy storage components, such as batteries, can be connected to the grid to further improve efficiency, storing excess power to be released in times of high demand, reducing the load of the prime mover. Hydrogen systems, including proton exchange membrane fuel cells, can also be seamlessly be integrated into the vessel's grid, allowing zero-emission power generation onboard the vessel. The use of hydrogen allows to extend the operational range thanks to the energy density of this energy carrier being higher than any available battery. Fuel

cells can replace ICEs on selected maritime routes, allowing ship operators to comply with the regulations on emissions of pollutants and greenhouse gasses from the IMO and other international organizations.

The transition to maritime hybrid powertrains utilizing PEMFCs and Li-Ion batteries needs to be carefully evaluated both from a technical and economic perspective for each specific use-case. This type of powertrain is currently suitable for a set of vessels with specific operational parameters, bridging the gap between battery operated vessels, with range limitations, and diesel-electric configurations with undesirable emissions. The software and dynamic models developed in this thesis allow the technical analysis of different possible hydrogen systems in order to select the most suitable powertrain configuration for each specific use-case, ensuring good performances and comparable costs to a diesel-electric configuration.

In Articles 1 and 5, the problem of component sizing was analyzed and a Matlab application developed. The aim was to automate the calculation of possible powerplant configurations based on the vessel's power demand, and other user-selected parameters. This application provides a series of results that can be used in the Simulink dynamic models described in Articles 2 and 4, but also in the model using the load combination approach. Multiple simulations with different combinations of component sizing and energy management were carried out to validate the models and analyze the results.

Results obtained with simulations using both the quasi-static and dynamic model can help to answer the main research question: *"How can the design of the powerplant and energy management system for hybrid fuel cell vessels be optimized with respect to overall efficient operation and lifetime of the batteries and fuel cells?"*. Different approaches are presented in the thesis and enclosed articles, with case studies producing results relative to the hybrid systems performances that can be compared to the traditional diesel-electric configuration. Results show that it is important to perform the component sizing and choose an energy management strategy concurrently to obtain the best performances possible out of the system. This is because the optimization process is effectively a balance of factors that impact the performances of the system. Each configuration created is a trade off between the priorities of the shipowner (e.g. low hydrogen consumption), at the expenses of other factors of secondary importance.

The work carried out in this thesis and the enclosed articles focuses on the assumption that by easily verifying the feasibility of hybrid solutions utilizing PEMFCs in selected maritime vessels, it is possible to aid the adoption of such systems. The widespread adoption of zero-emission systems would contribute to the reduction of pollutants and greenhouse gasses in the atmosphere, with beneficial effects

on climate change. The aim is also to reduce the transport sector's reliance on fossil fuels which are responsible for substantial emissions not only during combustion, but also during extraction and processing.

8.2 Addressing research objectives

The objectives described in this section are completed as a part of the work carried out for the H2Maritime project.

Objective 1: Introduction to fuel cells and hydrogen systems. Differences between conventional and hybrid powertrains in the maritime industry, positive and negative aspects of each technology. A general introduction to the safety challenges of hydrogen systems, maintanence, and degradation of the components.

The first objective was addressed during the first year of the PhD via both a literature review and selected coursework. The knowledge gained at this stage was deemed necessary for the development of the work carried out in the thesis. The study included topics such as the state-of-the-art of hydrogen systems, power electronic components and control.

Technical challenges related to the adoption of hydrogen systems in the maritime industry were also briefly investigated. The study of safety aspects has led to the development of a safety barrier analysis described in Articles 3 and 6.

Objective 2: Development of a Matlab tool to investigate and develop design criteria for the operation of fuel cell and battery systems for maritime vessels.

Work on the second objective of the research plan started with the creation of the first version of the powerplant model included in the Matlab application for the study of design criteria for hybrid vessels. The work is described in Article 2. This application provides a way to perform the calculations that define the composition of the hybrid powerplant, including the number and size of components. The calculations are carried out based on the EMS selected. The aim, at this stage, was to evaluate the technical and economic feasibility of the hybrid powerplant in specific use cases.

The application was later reworked with a new algorithm, and described in Article 5. This version of the application included multiple rule-based energy man-

agement systems that can be tested using the power demand data provided by the user. Multiple outputs can be plotted, including PEMFC degradation and hydrogen consumption. It was also possible to evaluate the target power for the PEMFC, determined by user conditions, and verify that it was compatible with the response time of the unit. The application provided a first-attempt solution to determine the optimal composition of the powerplant. The calculated configurations can be used as reference or input for the dynamic models developed in this project.

Objective 3: Study of existing methods for energy management systems (EMS) of fuel cell systems in existing applications. Familiarization with different control strategies from the automotive and heavy duty transport industry to optimize the power generation and distribution within the vessel's electrical grid.

Objective 3 involved a literature review on energy management strategies across different transport industries. This literature review spanned different sectors, including automotive, heavy-duty transport and maritime. Particular interest was placed on Online EMSs, which determine the real-time power generation and distribution strategies used in the dynamic models developed for the project. Rule-based EMSs were the first strategies to be tested, including deterministic rule-based and fuzzy logic approaches.

The review carried out for Objective 3 allowed the development of the detailed digital models for the hybrid powerplant described in the following Objectives.

Objective 4: Development of a detailed digital model of the hybrid fuel-cell maritime powerplant on Simulink to replicate operations for different use-cases. Testing of existing and new energy management strategies and component sizing configurations. Key parameters such as hydrogen consumption, fuel cell degradation and operational life are calculated.

Work on objective 4 started with the modelling of the individual components in the hybrid powerplant including PEMFC, Li-ion battery, converters, and DC-Load sink. These components were then connected to each other in different configurations, to realize two different types of dynamic models.

The model using the load-separation approach was described in Articles 2 and 4 and used to simulate the system, testing different rule-based EMSs. This model was based on a set of assumptions that allowed the simulation of the system

at a relatively low computational cost. The main condition to correctly simulate the powerplant with this model was to have a robust voltage control system that would ensure a stable voltage output to the DC-Load blocks for each timestep of the simulation. The model using load-combination was developed after the one using load-separation. This type of model allows the control of individual energy sources in the powerplant, at the expenses of higher computational resources. This model was tested with both rule-based EMSs and one optimization based EMSs.

Both models provided a platform to test different EMSs with minor modification to the system. The key parameters that were of interest in the study, such as hydrogen consumption and PEMFC degradation could be calculated using the model, and saved to perform comparisons or to establish a benchmark for operations optimization.

Objective 5: Test and validation of the different strategies implemented in the EMS using data sampled in real-world scenarios.

The development of the dynamic models described in objective 4 allowed the progress to Objective 5. The dynamic models were used for simulations with different powerplant configurations and energy management strategies to observe positive and negative effects of different design choices. The first analysis and comparison was published in Article 4. This article presented the simulations carried out with three different rule-based energy management strategies. The analysis enclosed in the article was based on data sampled from a double ended ferry operating in Danemark. The vessel was selected as it falls into the specified power range of interest, between 1 and 10 MW.

Additional testing has been carried out using both dynamic models, laying the groundwork for future developments and novel publications in this area.

8.3 Further work

Zero-emission mobility is a field in constant expansion due to the constant introduction of new and improved components. The improvement in performance of proton exchange membrane fuel cells and the increase in battery energy density provides new possibilities for zero-emission applications, increasing the technical and economic feasibility of such solutions for commercial use.

Further work that can be carried out as a continuation of the topics of this thesis include:

- The development of an updated version of the hybrid maritime powerplant Simulink models, decreasing the speed of execution and more efficiently using the available computational resources. These improvements can be carried out by reviewing the blocks developed in Simulink and their interactions, eliminating redundant and inefficient processes.
- The expansion of the load-combination model to include DC/AC transformers, variable speed drive and triphase load sinks to simulate the induction motors user for propulsion.
- The creation of a model for the azimuth podded thrusters and control. Such a model can help to better simulate the torque demand and the load that can be transformed in propulsive power during docking or navigation.
- The development of multiple sub-models for the balance of plant components, with relative control systems. Of particular importance is modeling components that provide the supply of hydrogen and oxygen to the fuel cells. Such a model is necessary to evaluate the system's behavior during transient loading conditions.
- Study on the integration of supercapacitors in the hybrid powerplant as an energy storage component.
- Study on the integration of additional zero-emission energy sources to the vessel electrical grid including Flettner rotors and photovoltaic systems.
- The improvement of operational efficiency with currently developed rule-based energy management strategies. The development of new optimization-based energy management strategies belonging to the category of model predictive control, robust control or intelligent control.

Bibliography

[1] Bin Lin and Cherng-Yuan Lin. Compliance with international emission regulations: Reducing the air pollution from merchant vessels. *Marine Policy*, 30(3):220–225, 2006.

[2] The effect of reducing cruise ship speed in the world heritage fjords. https://www.sdir.no/globalassets/sjofartsdirektoratet/regelverk-og-int.-arbeid---dokumenter/pollution-from-shipping-in-world-heritage-fjords/dnv-gl-report-2018-0025_-rev02_english.pdf?t=1620121799236. Accessed: 21-05-2021.

[3] NCE Maritime Cleantech. Norwegian parliament adopts zero-emission regulations in the fjords. Marie Launes, 05 2018.

[4] Shantha Gamini Jayasinghe, Lasantha Meegahapola, Nuwantha Fernando, Zheming Jin, and Josep M. Guerrero. Review of ship microgrids: System architectures, storage technologies and power quality aspects. *Inventions*, 2(1), 2017.

[5] Rinze D. Geertsma, Rudy R. Negenborn, K. Visser, and J.J. Hopman. Design and control of hybrid power and propulsion systems for smart ships: A review of developments. *Applied Energy*, 194:30 – 54, 2017.

[6] Francesco Baldi, Fredrik Ahlgren, Tuong-Van Nguyen, Marcus Thern, and Karin Andersson. Energy and exergy analysis of a cruise ship. *Energies*, 11(10), 2018.

[7] Diego Feroldi and Mauro Carignano. Sizing for fuel cell/supercapacitor hybrid vehicles based on stochastic driving cycles. *Applied Energy*, 183:645–658, 2016.

[8] Qiong Cai, Dan J.L. Brett, D. Browning, and N.P. Brandon. A sizing-design methodology for hybrid fuel cell power systems and its application to an unmanned underwater vehicle. *Journal of Power Sources*, 195(19):6559 – 6569, 2010.

[9] Alexandre Ravey, Nicolas Watrin, Benjamin Blunier, David Bouquain, and Abdellatif Miraoui. Energy-source-sizing methodology for hybrid fuel cell vehicles based on statistical description of driving cycles. *IEEE Transactions on Vehicular Technology*, 60(9):4164–4174, 2011.

[10] Yanjun Huang, Hong Wang, Amir Khajepour, Bin Li, Jie Ji, Kegang Zhao, and Chuan Hu. A review of power management strategies and component sizing methods for hybrid vehicles. *Renewable and Sustainable Energy Reviews*, 96:132–144, 2018-11.

[11] Mauro G. Carignano, Ramon Costa-Castelló, Vicente Roda, Norberto M. Nigro, Sergio Junco, and Diego Feroldi. Energy management strategy for fuel cell-supercapacitor hybrid vehicles based on prediction of energy demand. *Journal of Power Sources*, 360:419 – 433, 2017.

[12] Ameen M. Bassam, Alexander B. Phillips, Stephen R. Turnock, and Philip A. Wilson. Development of a multi-scheme energy management strategy for a hybrid fuel cell driven passenger ship. *International Journal of Hydrogen Energy*, 42(1):623–635, 2017.

[13] Ameen M. Bassam, Alexander B. Phillips, Stephen R. Turnock, and Philip A. Wilson. An improved energy management strategy for a hybrid fuel cell/battery passenger vessel. *International Journal of Hydrogen Energy*, 41(47):22453–22464, 2016.

[14] Bambang Trilaksono, Arief Syaichu-Rohman, Cees Dronkers, Romeo Ortega, and Arif Sasongko. Energy management of fuel cell/battery/supercapacitor hybrid power sources using model predictive control. *IEEE Transactions on Industrial Informatics*, 10, 11 2014.

[15] Yupeng Yuan, Jixiang Wang, Xinping Yan, Boyang Shen, and Teng Long. A review of multi-energy hybrid power system for ships. *Renewable and Sustainable Energy Reviews*, 132:110081, 2020.

[16] Huei Peng Min-Joong Kim. Power management and design optimization of fuel cell/battery hybrid vehicles. *Journal of Power Sources*, 1(165):819–832, 2007.

[17] Davide Pivetta, Chiara Dall'Armi, and Rodolfo Taccani. Multi-objective optimization of hybrid pemfc/li-ion battery propulsion systems for small and medium size ferries. *International Journal of Hydrogen Energy*, 46(72):35949–35960, 2021. Special Issue on HYPOTHESIS XV.

[18] Chiara Dall'Armi, Davide Pivetta, and Rodolfo Taccani. Health-conscious optimization of long-term operation for hybrid pemfc ship propulsion systems. *Energies*, 14(13), 2021.

[19] Nikolce Murgovski, Lars Johannesson, Jonas Sjöberg, and Bo Egardt. Component sizing of a plug-in hybrid electric powertrain via convex optimization. *Mechatronics*, 22(1):106–120, 2012.

[20] Hongliang Jiang, Liangfei Xu, Jianqiu Li, Zunyan Hu, and Minggao Ouyang. Energy management and component sizing for a fuel cell/battery/supercapacitor hybrid powertrain based on two-dimensional optimization algorithms. *Energy*, 177:386–396, 2019.

[21] Fcs alsterwasser. shorturl.at/jnwzT, BlueGrowth.org.

[22] Nemo h2 ferry. shorturl.at/doxPW, Fact Sheet n.4 Interreg Danube transnational programme.

[23] Norled mf hydra. shorturl.at/cikBI, Tu.no.

[24] Sea change ferry. shorturl.at/inoE3, Marine Insight, September 2021.

[25] Hydrogen in the maritime. https://www.ieahydrogen.org/wp-admin/admin-ajax.php?juwpfisadmin=false&action=wpfd&task=file.download&wpfd_category_id=17&wpfd_file_id=3991&token=abad9fa9a0f0a9c00152edff03825bf4&preview=1, IEA's Hydrogen TCP Task 39, October 2021.

[26] Stig Eriksen, Marie Lützen, Jens Brauchli Jensen, and Jan Corfixen Sørensen. Improving the energy efficiency of ferries by optimizing the operational practices. In *Proceedings of the Full Scale Ship Performance Conference 2018*, pages 101–111. The Royal Institution of Naval Architects, October 2018. null ; Conference date: 24-10-2018 Through 25-10-2018.

[27] Helmut Eichlseder, Thomas Wallner, Raymond Freymann, and Jürgen Ringler. The potential of hydrogen internal combustion engines in a future mobility scenario. In *Future Transportation Technology Conference & Exposition*, pages 2003–01–2267, 2003.

[28] Qing he Luo, Ji-Bin Hu, Bai gang Sun, Fu shui Liu, Xi Wang, Chao Li, and Ling zhi Bao. Experimental investigation of combustion characteristics and nox emission of a turbocharged hydrogen internal combustion engine. *International Journal of Hydrogen Energy*, 44(11):5573–5584, 2019. The 6th International Conference on Energy, Engineering and Environmental Engineering.

[29] Gregoris Panayiotou, Soteris Kalogirou, and Savvas Tassou. Pem fuel cells for energy production in solar hydrogen systems. *Recent Patents on Mechanical Engineering*, 3:226–235, 11 2010.

[30] Hydrogen production. https://www.planete-energies.com/en/medias/close/hydrogen-production, Planete Energies, 07 jan. 2015.

[31] Fully charged interview with forsea. https://energypost.eu/hard-to-abate-sectors-need-hydrogen-but-only-4-is-green/, by Patrick Molloy, Leeann Baronett, September 3, 2019.

[32] Giuseppe Bellussi, Matthias Bohnet, James Bus, Karlheinz Drauz, Helmut Greim, Klaus-Peter Jackel, Uwe Karst, Axel Kleemann (D), Gerhard Kreysa, Trevor Laird, Willi Meier, Eckhard Ottow, Michael Roper, Japie Scholtz, Kai Sundmacher, Roland Ulber, and Ulrich Wietelmann. Gas production, 2 processes. *Ullmann's Encyclopedia of Industrial Chemistry*, ISBN 978-3-527-30673-2(2), 2011.

[33] Alfredo Ursua, Luis M. Gandia, and Pablo Sanchis. Hydrogen production from water electrolysis: Current status and future trends. *Proceedings of the IEEE*, 100(2):410–426, 2012.

[34] Detlef Stolten and Berndt Emonts. Hydrogen science and engineering: Materials, processes, systems, and technology. *Wiley*, ISBN 3527674292, 2016.

[35] Marcelo Carmo, David L. Fritz, Jürgen Mergel, and Detlef Stolten. A comprehensive review on pem water electrolysis. *International Journal of Hydrogen Energy*, 38(12):4901–4934, 2013.

[36] Jan Bernholz. RWE's former, current and possible future energy storage applications. *The 2018 IERE - RWE TI Workshop*, page 16, 2018.

[37] Magnus Thomassen. NOVEL Novel materials and system designs for low cost, efficient and durable PEM electrolysers. *Fuel Cell and Hydrogen joint undertaking*, page 25, 2011.

[38] Arnaud Vasquez. Hyseas energy and the hynovar pilot project. Maritime Hydrogen Marine Energy. Florø, 09 2019.

[39] Jinfeng Wu, Xiao Zi Yuan, Jonathan J. Martin, Haijiang Wang, Jiujun Zhang, Jun Shen, Shaohong Wu, and Walter Merida. A review of pem fuel cell durability: Degradation mechanisms and mitigation strategies. *Journal of Power Sources*, 184(1):104–119, 2008.

[40] Frano Barbir and Haluk Görgün. Electrochemical hydrogen pump for recirculation of hydrogen in a fuel cell stack. *Journal of Applied Electrochemistry*, 37(3):359–365, February 2007.

[41] Stevie Knight. Liquid hydrogen could get a leg up from the industry's experience with lng propulsion. The motorship - Insides for marine technology professionals https://escolaeuropea.eu/news/environmental-news/from-lng-to-hydrogen-pitfalls-and-possibilities/, 08 2010.

[42] Yousef S.H. Najjar. Hydrogen safety: The road toward green technology. *International Journal of Hydrogen Energy*, 38(25):10716 – 10728, 2013.

[43] Ram B. Gupta. Hydrogen fuel-production, transport, and storage. 1st ed. Taylor and Francis Group, https://doi.org/10.1201/9781420045772, 10 2008.

[44] T. Aven S. Sklet and J. E. Vinnem. Barrier and operational risk analysis of hydrocarbon releases (bora-release): Part i. method description. *Journal of Hazardous Materials*, 137(2):681 – 691, 2006.

[45] S. Sklet, J. E. Vinnem, and T. Aven. Barrier and operational risk analysis of hydrocarbon releases (bora-release): Part ii: Results from a case study. *Journal of Hazardous Materials*, 137(2):692 – 708, 2006.

[46] Olav Roald Hansen. Liquid hydrogen releases show dense gas behavior. *International Journal of Hydrogen Energy*, 45(2):1343–1358, 2020. International Hydrogen and Fuel Cell Conference 2018, Trondheim, Norway.

[47] Alf Kåre Ådnanes. Maritime electrical installations and diesel electric propulsion. ABB AS, 04 2003.

[48] Miikka Jaurola, Anders Hedin, Seppo Tikkanen, and Kalevi Huhtala. Optimising design and power management in energy-efficient marine vessel power systems: a literature review. *Journal of Marine Engineering & Technology*, 18(2):92–101, 2019.

[49] Jan Fredrik Hansen and Frank Wendt. History and state of the art in commercial electric ship propulsion, integrated power systems, and future trends. *Proceedings of the IEEE*, 103(12):2229–2242, 2015.

[50] Monaaf Al-Falahi, Tomasz Tarasiuk, Shantha Gamini Jayasinghe, Zheming Jin, Hossein Enshaei, and Josep M. Guerrero. Ac ship microgrids: Control and power management optimization. *Energies*, 11(6), 2018.

[51] Viknash Shagar, Shantha Gamini Jayasinghe, and Hossein Enshaei. Effect of load changes on hybrid shipboard power systems and energy storage as a potential solution: A review. *Inventions*, 2(3), 2017.

[52] Luisa Alfieri, Fabio Mottola, and Mario Pagano. An energy saving management strategy for battery-aided ship propulsion systems. In *2019 IEEE Milan PowerTech*, pages 1–6, 2019.

[53] Satoshi Kitayama, Marina Saikyo, Yui Nishio, and Kojiro Tsutsumi. Torque control strategy and optimization for fuel consumption and emission reduction in parallel hybrid electric vehicles. *Structural and Multidisciplinary Optimization*, page 17, 2015.

[54] Yousri M.A. Welaya, M. Morsy El Gohary, and Nader R. Ammar. A comparison between fuel cells and other alternatives for marine electric power generation. *International Journal of Naval Architecture and Ocean Engineering*, 3(2):141–149, 2011.

[55] Daniel M. Kennedy, Donald R. Cahela, Wenhua H. Zhu, Kenneth C. Westrom, R. Mark Nelms, and Bruce J. Tatarchuk. Fuel cell cathode air filters: Methodologies for design and optimization. *Journal of Power Sources*, 168(2):391–399, 2007.

[56] Lewis. Sea salt aerosol production : mechanisms, methods, measurements and models : a critical review, 2004. Archive: /z-wcorg/ISBN: 9781118666050 1118666054 Library Catalog: http://worldcat.org Place: Washington, DC Publisher: American Geophysical Union.

[57] Handbook for hydrogen-fuelled vessels. https://www.dnv.com/maritime/publications/handbook-for-hydrogen-fuelled-vessels-download.html, Accessed 07/12/2021.

[58] DNV GL AS. Part 6 additional class notations; chapter 2 propulsion, power generation and auxiliary systems. Rules for classific-

ation, https://rules.dnv.com/docs/pdf/DNV/RU-SHIP/2018-01/DNVGL-RU-SHIP-Pt6Ch2.pdf, 01 2018.

[59] Jian Zhao and Xianguo Li. A review of polymer electrolyte membrane fuel cell durability for vehicular applications: Degradation modes and experimental techniques. *Energy Conversion and Management*, 199:112022, 2019.

[60] D. Liu and S. Case. Durability study of proton exchange membrane fuel cells under dynamic testing conditions with cyclic current profile. *Journal of Power Sources*, 162(1):521–531, 2006.

[61] Bouchra Wahdame, Denis Candusso, Xavier François, Fabien Harel, Marie-Cécile Péra, Daniel Hissel, and Jean-Marie Kauffmann. Comparison between two pem fuel cell durability tests performed at constant current and under solicitations linked to transport mission profile. *International Journal of Hydrogen Energy*, 32(17):4523–4536, 2007. Fuel Cells.

[62] Languang Lu, Minggao Ouyang, Haiyan Huang, Pucheng Pei, and Fuyuan Yang. A semi-empirical voltage degradation model for a low-pressure proton exchange membrane fuel cell stack under bus city driving cycles. *Journal of Power Sources*, 164(1):306–314, 2007.

[63] R. Lin, B. Li, Y.P. Hou, and J.M. Ma. Investigation of dynamic driving cycle effect on performance degradation and micro-structure change of pem fuel cell. *International Journal of Hydrogen Energy*, 34(5):2369–2376, 2009.

[64] Martin Watkinson Tom Fletcher, Rob Thring. An energy management strategy to concurrently optimise fuel consumption & pem fuel cell lifetime in a hybrid vehicle. *International Journal of Hydrogen Energy*, 41(46):21503 – 21515, 2016.

[65] Huicui Chen, Pucheng Pei, and Mancun Song. Lifetime prediction and the economic lifetime of proton exchange membrane fuel cells. *Applied Energy*, 142:154–163, 2015.

[66] Dynamic modeling overview. shorturl.at/aqrAJ. Accessed: 13-06-2022.

[67] L. van Biert, M. Godjevac, K. Visser, and P.V. Aravind. A review of fuel cell systems for maritime applications. *Journal of Power Sources*, 327:345 – 364, 2016.

[68] Abdulrahman Alanazi, Emmanuel Ogungbemi, Awortwe Wilberforce, Oluwatosin Ijaodola, Parag Vichare, and Abdul Ghani Olabi. State-of-the-art manufacturing technologies of pemfc components. In *10TH International Conference on Sustainable Energy and Environmental Protection*, pages 189–198, 07 2017.

[69] Yun Wang, Ken S. Chen, Jeffrey Mishler, Sung Chan Cho, and Xavier Cordobes Adroher. A review of polymer electrolyte membrane fuel cells: Technology, applications, and needs on fundamental research. *Applied Energy*, 88(4):981–1007, 2011.

[70] Francesco Valle. *Electrocatalyst degradation in high temperature PEM fuel cells*. PhD thesis, University of Trieste, 04, 2015.

[71] H. Li H. Wang, X. Yuan. Pem fuel cell diagnostic tools. CRC Press, 08 2011.

[72] Souleman Njoya Motapon, O. Tremblay, and L. Dessaint. A generic fuel cell model for the simulation of fuel cell vehicles. In *2009 IEEE Vehicle Power and Propulsion Conference*, pages 1722–1729, 2009.

[73] Yasaman Balali and Sascha Stegen. Review of energy storage systems for vehicles based on technology, environmental impacts, and costs. *Renewable and Sustainable Energy Reviews*, 135:110185, 2021.

[74] S.M. Mousavi G, Faramarz Faraji, Abbas Majazi, and Kamal Al-Haddad. A comprehensive review of flywheel energy storage system technology. *Renewable and Sustainable Energy Reviews*, 67:477–490, 2017.

[75] Fiorentino Valerio Conte. Battery and battery management for hybrid electric vehicles: a review. *e & i Elektrotechnik und Informationstechnik*, 123(10):424–431, October 2006.

[76] Rakesh Chandra Agrawal and Gaind P. Pandey. Solid polymer electrolytes: materials designing and all-solid-state battery applications: an overview. *Journal of Physics D: Applied Physics*, 41(22):223001, oct 2008.

[77] Peter H.L. Notten Henk Jan Bergveld, Wanda S. Kruijt. Battery management systems: Design by modelling. Springer, pp. 107–108, 113. ISBN 978-94-017-0843-2, 08 2002.

[78] Hyun Chul Choi, Young Mee Jung, Isao Noda, and Seung Bin Kim. A study of the mechanism of the electrochemical reaction of lithium with co by two-dimensional soft x-ray absorption spectroscopy, 2d raman, and 2d hetero-spectral xas-raman correlation analysis. *The Journal of Physical Chemistry B*, 107(24):5806–5811, 2003.

[79] Lisa C. Klein Glen G. Amatucci, Jean-Marie Tarascon. Coo2, the end member of the lixcoo2 solid solution. Journal of The Electrochemical Society, Volume 143, Number 3, 08 1996.

[80] Atetegeb Meazah Haregewoin, Aselefech Sorsa Wotango, and Bing-Joe Hwang. Electrolyte additives for lithium ion battery electrodes: progress and perspectives. *Energy Environ. Sci.*, 9(6):1955–1988, 2016.

[81] Discharging at high and low temperatures. https://batteryuniversity.com/learn/article/discharging_at_high_and_low_temperatures. Accessed: 10-09-2019.

[82] Bhaskar Saha, Patrick Quach, and Kai Goebel. Exploring the model design space for battery health management. *Proceedings of the Annual Conference of the Prognostics and Health Management Society 2011, PHM 2011*, 01 2014.

[83] Dervis Emre Demirocak, Sesha S. Srinivasan, and Elias K. Stefanakos. A review on nanocomposite materials for rechargeable li-ion batteries. *Applied Sciences*, 7(7), 2017.

[84] Clarence M. Shepherd. Design of primary and secondary cells ii . an equation describing battery discharge. *Journal of The Electrochemical Society*, 112:657–664, 1965.

[85] Olivier Tremblay and Louis-A. Dessaint. Experimental validation of a battery dynamic model for ev applications. *World Electric Vehicle Journal*, 3:289–298, 2009.

[86] Dnv gl rules for classification. https://rules.dnvgl.com/docs/pdf/DNVGL/RU-SHIP/2015-10/DNVGL-RU-SHIP-Pt6Ch3.pdf.

[87] International guidelines for the safe operation of dynamically positioned offshore supply vessels. shorturl.at/dqxIJ, 2018.

[88] The step forward - onboard dc grid, abb 2011. https://new.abb.com/docs/librariesprovider91/articles/lm00614-onboard-dc-grid-brochure_june2014_1.pdf.

[89] Mohammad Kabalo, Benjamin Blunier, David Bouquain, and Abdellatif Miraoui. State-of-the-art of dc-dc converters for fuel cell vehicles. In *2010 IEEE Vehicle Power and Propulsion Conference*, pages 1–6, 2010.

[90] Brigitte Hauke. Basic calculation of a boost converter's power stage. Application Report - SLVA372C, 01 2014.

[91] Milos Zivanov, Boris Sasic, and Miroslav Lazić. *Desing of Multiphase Boost Converter for Hybrid Fuel Cell/Battery Power Sources*, chapter 1. Paths to Sustainable Energy, 11 2010.

[92] Morten Nymand and Michael A. E. Andersen. High-efficiency isolated boost dc–dc converter for high-power low-voltage fuel-cell applications. *IEEE Transactions on Industrial Electronics*, 57(2):505–514, 2010.

[93] Benedikt Lunz, Zexiong Yan, Jochen Bernhard Gerschler, and Dirk Uwe Sauer. Influence of plug-in hybrid electric vehicle charging strategies on charging and battery degradation costs. *Energy Policy*, 46:511–519, 2012.

[94] Sam Ben-Yaakov. Average simulation of pwm converters by direct implementation of behavioural relationships. *International Journal of Electronics*, 77(5):731–746, 1994.

[95] Souleman Njoya Motapon, Louis-A. Dessaint, and Kamal Al-Haddad. A comparative study of energy management schemes for a fuel-cell hybrid emergency power system of more-electric aircraft. *IEEE Transactions on Industrial Electronics*, 61(3):1320–1334, 2014.

PAPER I

Proceedings of the ASME 2020 39th International Conference on Ocean, Offshore and Arctic Engineering
OMAE 2020
June 28-July 3, 2020, Fort Lauderdale, FL, USA

OMAE 2020 - 18093

STUDY ON THE ARCHITECTURE OF A ZERO EMISSION HYDROGEN FUEL CELL VESSEL POWER GENERATING UNIT

Lorenzo Balestra*
Department of Marine Technology
Norwegian University of Science and Technology
NO-7491, Trondheim, Norway

Ingrid Schjølberg
Department of Marine Technology
Norwegian University of Science and Technology
NO-7491, Trondheim, Norway

ABSTRACT

This study focuses on providing design guidelines for a vessel's power-plant in the multi-megawatt range, equipped with a hybrid fuel cell and battery system. Background information is provided on the challenges to realizing such a system, spanning from a literature review on studies looking into energy management, to the technical limitations of state-of-the-art fuel cells and batteries. The central part of the work consists of the description of the model used to calculate the size of the hybrid power generating unit, including a case study on a single, real-world scenario. The Plant Analysis Balance with Operational Profile (PABOP) model, developed by the author and presented in the paper, is used to calculate the resources needed to retrofit a vessel operating on fossil fuels with a hybrid zero-emission power-plant. The model aim is to achieve a 1:1 replacement for diesel-electric configurations, both in terms of range and power, using fuel cell and battery power. In the case study, the model is applied to analyze the operational data of a double-ended ferry operating with diesel-electric propulsion. Emphasis is put on the I/O needed and produced by the model, and how this tool can be used by shipyard engineers to estimate the footprint required, the necessary storage capacity, lifetime of components and other parameters. The presented solutions could help manufacturers estimate the economical viability of hydrogen vessels, filling a gap in current maritime fleets where zero-emission systems are gaining increasing importance.

*Address all correspondence to this author.

INTRODUCTION

Zero-emission propulsion systems for marine applications are today a central topic in the industry due to new resolutions by the International Maritime Organization (IMO) to reduce greenhouse gas (GHG) emissions and air pollution by 2050 [1,2]. The resolutions have been complemented in many countries by national legislation, with Norway pledging to have an emission-free zone in its world heritage fjords no later than 2026 [3]. Norway's peculiar shoreline conformation creates the need for hundreds of ferries for fjord crossing, to allow for the fast transport of passengers by sea. The passenger vessel and ferry operators, with routes in zones that will be under emission control, are looking into retrofitting their vessels with environmentally friendly onboard power-plants and developing new designs to comply with regulations. Zero-emission ferries, like the MF Ampere [4], are already operating using batteries as the sole energy storage, however this solution greatly limits the possible applications of the vessel due to range concerns [5]. Where more flexibility is needed, multiple fuel cell stacks could be used as a range extender, providing the necessary power for operation on longer routes. Fuel cells may reduce the recharge time, with the target of achieving a perfect 1:1 replacement of fossil fuel propulsion with respect to both power and range.

Design requirements for diesel or hybrid diesel-electric ships have been developed for years, with hundreds of technical papers and comparative studies analyzing every aspect of this architecture. The same cannot be said for hydrogen powered vessels, as only a couple of pilot projects are available today for study and data collection, and the majority have less than 1MW of total

power installed.
The scope of this paper is therefore to present an engineering toolbox that can help size and balance the on-board powerplant for powers up to to 10 MW, providing a preliminary calculation of the resources required at the beginning of life (BOL) to operate with zero-emission power generation.
First, the characteristics of the components used in the toolbox are defined, providing an overview on the main input values. State of the art components have been selected to provide results that reflect the technological development achieved in the Polymer Exchange Membrane (PEM) fuel cell field in the last years. The rule-based toolbox adopts a streamlined approach to reduce computational load. The dynamics of other power electronics components (e.g. converters and transformers) is assumed as ideal, thus the focus is only on the fuel cell and battery.
With these boundary conditions defined, it is possible to specify how the toolbox operates. The first step is a configuration phase by the user, during which parameters are selected and input files are loaded. These input files are relative to the operational profile, the fuel cell stacks, and the battery pack. When the first step is completed it is possible to run the software and obtain the requested configuration. This configuration will be a 1:1 replacement of the fossil fuel setup, operating on fuel cell and battery pack, able to sustain the power requirement imposed by the operational profile (given the boundary conditions of the study). Operational profiles can be sampled from vessels that currently operate on conventional fossil fuels configurations along the routes set to be under emission control.
It should be noted that there is no singular configuration that can sustain the load and a multitude of different solutions may be available. The only factor restricting the number of solutions is the configuration setup provided by the user. During this phase, it is possible to decide which parameters should be maximized or minimized (e.g. battery life, fuel cell life, hydrogen consumption), defining an operational point or a range of values for the battery and fuel cell system. The operational range specified in the setup can lead to the estimation of life-cycle costs taking into account the degradation of the components produced by heavy loads. This is possible as the toolbox allows the user to visualize the value of PEM fuel cell degradation in μV/h as well as the number of battery cycles with high degradation during the considered time interval. Actions to mitigate the unprioritized parameters can be dealt with at a later stage, when defining the software of the energy management system of the vessel.
The ultimate goal for the developed tool is to provide a preliminary estimate of the resources needed to retrofit a fossil fuel vessel. The definition of the required resources allows the operators to estimate the initial cost, with values for degradation and hydrogen consumption to quantify the running costs. This will allow companies to measure the feasibility of this solution and explore different configurations for a vessel to see if better results can be achieved by prioritizing some factors over others. If the conversion results are feasible, more in depth studies on the fuel cell and battery hybrid system can be carried out, making the adoption of this vessel power plant not just an environmental decision, but one backed up by financial considerations.
In the case study the first version of the software is used to analyze the operational profile of a double-ended ferry currently in operation. The ferry, in its original configuration, is powered by a diesel electric power plant and is capable of transporting 122 cars and 600 passengers. The configuration of the power plant is performed by the user inputting the operational profile during a time-frame (24h recommended, depending on the computational power) into the tool, with the same base option setup, and verifying that the configuration picked can provide enough power for each day.
This paper is organized according to the IMRAD format. The required background informations on the components, an overview of the developed software tool followed by a case study applying the given tool are presented. Result and discussions are in the final section of the paper, with a brief explanation of the values obtained.

HYDROGEN IN THE MARITIME INDUSTRY

Around the world it is possible to see hydrogen systems development in the automotive and heavy-duty transport industry due to increased awareness of the importance of environmental protection [6, 7]. Fuel cell powered systems are still at a lower technology readiness level (TRL) with respect to electric vehicles, but their economical feasibility is increasing with new technological developments and greater hydrogen production.
In the maritime sector, new solutions are being developed as emission control restricts the access of fossil fuel vessels to certain areas [8,9]. To maximize fuel economy and component lifespans in a hybrid fuel cell system, optimal component sizing and power management are two key aspects to consider during the design process. Several researches investigate the problem of energy management in vehicles [10, 11] while others focus on small vessels [12, 13]. Few studies cover sizing and energy management as a single package [14].
The idea behind this paper is to reverse the approach taken in the aforementioned energy management studies, considering the operational profile of the vessel as input and estimating the resources required, in terms of power delivery, to operate on a combined fuel cell and battery power plant.

COMPONENT CHARACTERIZATION

Fuel cell technology has made constant progress in the recent years with manufacturers lowering production costs by reducing the amount of precious metals needed and increasing their recycling effort. The market's increasing demand seems to push producers into further technological development, with Ballard

announcing the World's First PEM Fuel Cell product using a non-precious metal catalyst [15].

TABLE 1. Fuel cell data used in the model

Rated power (net)	100kW
Gross output at rated power	320 V / 350 A
Voltage range	250…500 V
System efficiency (@Peak, BOL)	62%
System efficiency (@Rated P. BOL)	50%
Weight	120-150 kg
Volume	300 l
Fuel quality	ISO 14687-2

TABLE 2. Degradation from Fletcher et. al. [16]

Operating Conditions	Degradation Rate
Low power operation (<80%)	10.17 μV/h
High power operation	11.74 μV/h
Transient loading	0.0441 μV/Δkw
Start/stop	23.91 μV/cycle

All of these efforts increase viability for the introduction of fuel cells in the maritime sector [17]. Among the different Fuel Cell (FC) technologies, the low temperature PEM fuel cell seems to be the one with the most suitable characteristics for maritime propulsion. Studies on the possible use of this fuel cell (FC) type aboard sea-going vessels have been already carried out by manufacturers like Ballard and Powercell, ensuring that the units can withstand the environmental conditions presented by the sea. In the presented model we consider a state-of-the-art, low temperature PEM with characteristics similar to some commercial units seen today in the 100kW range. The data taken into consideration is listed in Table 1, while the data regarding the degradation is listed in Table 2. These values are obtained from the studies conducted by Fletcher et.al. [16] and may, at a later stage, be replaced to take into account any new technological developments or more specific studies on long-term degradation.
The battery pack considered in the software is assumed to be a generic Lithium Ion battery pack capable of a fast charge/discharge cycle. These batteries were selected for their high energy density and because of the availability of studies looking into their degradation mechanisms.

TABLE 3. Single battery pack data used in the model

Burst discharge (up to 15-sec.)	3C
Max continuous charge	2C
Round Trip Efficiency	90%

The total power, voltage, and Ampere of the battery pack are not listed as these parameters can be considered flexible. Cells can be arranged in multiple ways to achieve different voltages and current values to fit the power requirement found in the results of the developed engineering toolbox.
Data regarding the fuel cell and the battery are collected in a text file that can be read by the software. This means that multiple types of batteries equipped with different cells can be tested, given that the file is arranged according to the creator's guidelines. This data is one of the main input of the system, defining the performances of the power delivery system.

THE PABOP SOFTWARE FOR ON-BOARD POWER PLANT BALANCING

The "Plant Analysis and Balance with Operational Profile" PABOP software developed by the author provides a tool to calculate the resources required, in terms of power delivery, to equip a ship with an effective hybrid, zero-emission, power generating unit. The vessel power plant under consideration is one comprised of multiple fuel cell stacks (Table 1) and battery packs (Table 3).
PABOP, as the acronym suggests, begins with the analysis of the operational profile on a given route of interest. The operational profile represents the total power consumption of the vessel.

$$op.profile = hotel\ load + propulsion\ load \tag{1}$$

The first step when using the software is selecting the options in the graphic user interface. All the options in the setup phase are selected with "radio button" menus for an easy to understand UI (top section of Figure 1). In this first version of the software, the setup options are still limited, but it is already possible to get a preliminary estimate of how much power is required on-board and how much the fuel consumption and degradation will be given the input files.
The first option presented to the user is regarding the fuel cell stack usage. This determines the operational point of the stack. Fixed operational points for the FC stacks can help minimize

degradation, but create the need for larger battery packs to be installed.

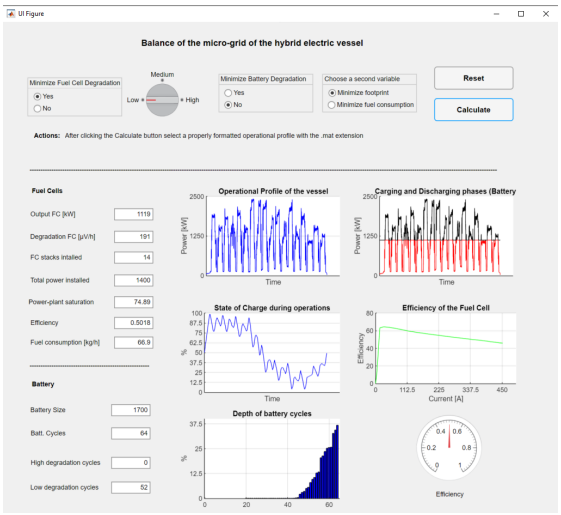

FIGURE 1. PABOP User Interface

1. Minimize fuel cell degradation?

• **1.1 YES**: The fuel cell output is set to a constant value requiring a larger battery pack to compensate for fluctuations in the load.

• **1.2 NO**: Fuel cell units have variable output power following the energy requirements. Smaller battery packs are needed. When this option is chosen three levels of degradation intensity can be selected:

1.2.1 HIGH: The units follows the OP fluctuations with rapid changes in power output. Fluctuations can span between plus or minus 40% w.r.t. the mean value set for optimal FC output.

1.2.2 MEDIUM: The units follows the OP fluctuations with average changes in power output. Fluctuations can span between plus or minus 25% w.r.t. the mean value set for optimal FC output.

1.2.3 LOW: The units follows the OP fluctuations with slow changes in power output. Fluctuations can span between plus or minus 10% w.r.t. the mean value set for optimal FC output.

The second option is regarding the battery pack. The depth of the charge and discharge cycles plays an important role in the battery degradation process. This option allows the user to set the state of charge (SoC) upper and lower limit to pre-set values, increasing the battery lifespan, or to use the entire storage capacity limiting the footprint required for the packs.

2. Minimize battery degradation?

• **2.1 YES:** The battery SoC depth is limited inside an optimal range to maximize the battery's lifespan.

• **2.2 NO:** The entire power stored in the battery is available during charge and discharge .

The third and final option is regarding the hydrogen consumption. The fuel cell has different efficiency values across the operational range that define the hydrogen consumption. Working at rated load does not mean working at the highest efficiency value possible. With the third option the user selects if they want to work at rated load, with reduced efficiency but saving footprint, or work at maximum efficiency sacrificing space.

3.Minimize fuel consumption?

• **3.1 YES**: The FC operates at maximum efficiency but not at rated load. More footprint required.

• **3.2 NO**: The FC operates at rated load.

With the options selected by the user in the UI, they can press the button "calculate" to launch the script. Before starting the calculation a file selection window will appear asking the user to select, in succession, the operational profile data, the fuel cell and the battery specifications. These informations is contained in appropriately formatted text files produced by the user. Once these are selected the software will have all the elements to proceed with the calculation.

The configuration selected by the user produces one of sixteen different scenarios, providing a preliminary estimate of the assets required to realize such scenario. The output values produced by the model are:

For the Fuel Cell stacks:

▷ Fuel cell power output required [kWh]
▷ Total degradation over the period considered [μV/h]
▷ Number of fuel cells required to sustain the load
▷ Fuel cell power effectively installed
▷ Saturation of the fuel cell unit
▷ Efficiency of the fuel cell unit
▷ Specific consumption of hydrogen [kg/h]

For the battery pack

▷ Battery size [kWh]
▷ Number of battery cycles over the period considered
▷ Number of cycles that lead to heavy degradation
▷ Number of cycles in the low degradation area

These values represent the preliminary estimate of the resources required to retrofit a fossil-fuel powered vessel with the given operational profile, with a hybrid zero-emission power plant. It should be taken into consideration that while choices are presented in a yes/no fashion, optimizing all the parameters

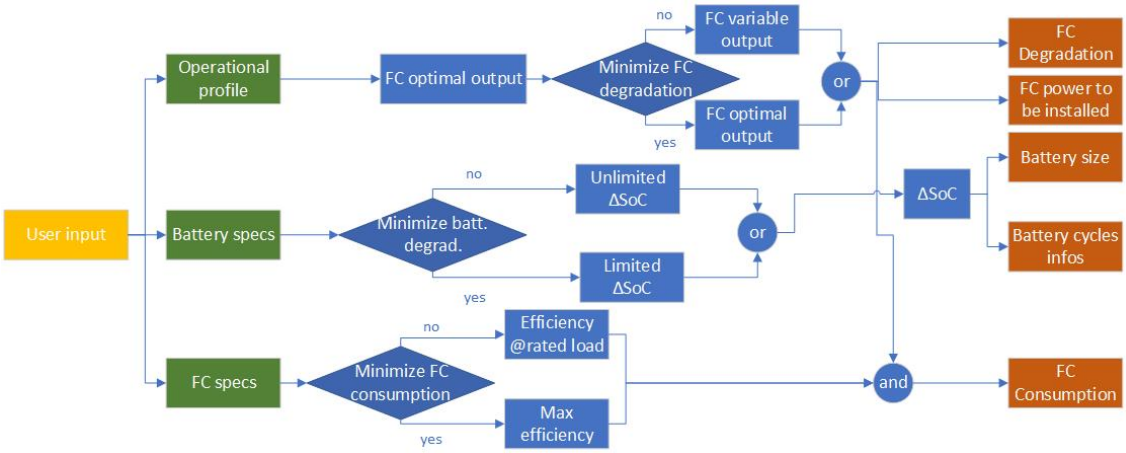

FIGURE 2. Flowchart representing the PABOP software steps

produces the solution utilizing the most footprint, therefore still consuming a valuable resource. Consequently the results need to be interpreted by someone with knowledge of the system in order to verify that the output values produced by the model fit the design requirements. This is important as the model does not include any specific reference to the vessel, but only focuses on the power generating and storage unit architecture.

CASE STUDY USING THE PABOP SOFTWARE

The case study exemplifies the potential of this tool by testing the software on the operational data of a double-ended ferry capable of transporting 122 cars and 600 passengers. The ferry operates 18 crossings per day, with a duration of approximately 45 minutes.

FIGURE 3. Example of double-ended ferry

The repetitive nature of the operation plays an important role in the optimization of the vessel power plant, as the power requirements are more or less constant each day. Therefore possible variations in power requirements are not determined by operating at longer or shorter ranges, but mainly just by different atmospheric conditions (e.g. wind, waves, current). To calculate the first-attempt solution we use an operational profile from a 24h time-frame. The software automatically eliminates the section were the vessel is inactive. The operational profile is selected randomly from 6 months of data. A scenario that realizes the following configuration is selected:

1.1 Minimize fuel cell degradation (Constant FC output)
2.2 Do not minimize battery degradation (Unlimited ΔSoC)
3.2 Do not minimize fuel consumption (FC @rated load)

The selection of option 1.1 allows the operator to maximize the operational life of the fuel cells by running them with a constant output. This allows the system to avoid high power operation peaks and transients, both conditions that would reduce the life of the PEM FC components according to the data presented in Table 2. The first step for the software is to calculate the operational point for the PEMFC units.

$$\int op.profile = FC\ operational\ p. * op.time \qquad (2)$$

The software solves equation 2 and finds the operational point for the constant operation of the FC stack. The point identified allows for the best balance between the power delivered by the fuel cells and battery. Optimizing this balance helps in

the reduction of stress on the battery, maintaining realistic cycles of charge/discharge (Figure 6) and reducing the battery size required. The fuel cell delivers a baseline constant load, recharging the battery when the power demand is lower than the one produced by the FC stack and discharging it when it is higher (Figure 4).

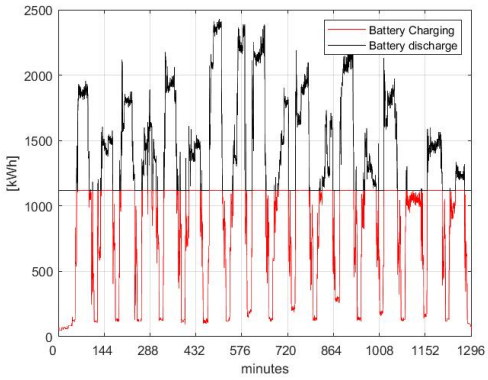

FIGURE 4. Operational profile of the vessel over 24h with no downtime

The fuel cell hydrogen consumption (option 3.2) is calculated as a function of fuel cell output and the efficiency value set by the user. By choosing not to maximize the efficiency, the value considered is automatically the one that corresponds to the rated efficiency (Table 1 and Figure 5). Knowing the efficiency value (η) of the fuel cell and the power output that needs to be produced, it is possible to roughly calculate the hydrogen consumption with Equation 3. The value for the energy density is set, in this case, to liquid hydrogen, but can be modified by the user to obtain a different configuration (Table 4).

$$H_2\ consumption = (FC\ output/\eta)/en.density\ H2 \qquad (3)$$

The battery dimension is also calculated as a function of the FC output. The battery needs to be able to cover the discharge profile of Figure 4 (black line) without going below its minimum SoC. As specified during the user input phase, the battery is allowed to use its entire range of SoC, from 0% to 100%. This situation produces very high fluctuations in the load of the battery, with rapid charge/discharge cycles. This represents an extremely heavy condition for the battery, resulting in a much shorter lifespan, but allows us to visualize the worst case scenario for operations and calculate the smallest battery size that can theoretically sustain the load.

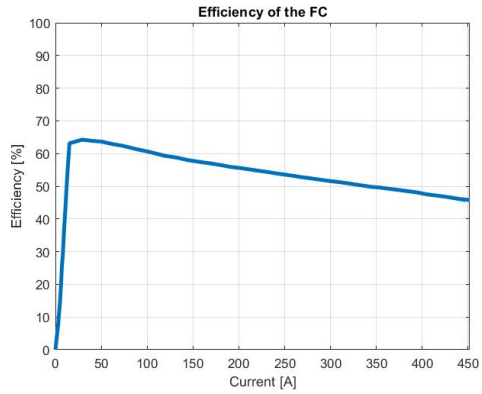

FIGURE 5. Performances of the considered PEMFC unit (Courtesy of PowerCell)

The cycles that the battery has to endure, and the depth of charge and discharge, are calculated and visualized in Figure 6. It is possible to measure the difference between the peaks and valleys of the SoC variations to quantify the depth of charge and discharge at each cycle. This data can be displayed in a histogram to help quantify the stress level of the battery pack installed.

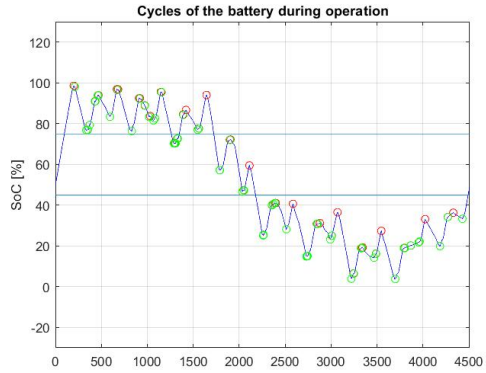

FIGURE 6. Battery pack dis/charge profile during operations

Once the script has finished its run, it is possible to analyze the results and quantify the resources needed by the vessel powerplant to deliver the required power with fuel cell and battery configuration.

TABLE 4. Hydrogen energy density for different forms

Form of Storage	[kWh/kg]	[kWh/l]
Gas (30 MPa)	33.3	0.75
Gas (70 MPa)	33.3	1.386
Liquid (-253C)	33.3	2.36
Metal hydrate	0.58	3.18
Ammonia (NH_3)	2.44	3.6

RESULTS AND DISCUSSION

The results obtained from the first run with the selected operational profile are shown in Table 5. The hybrid vessel power plant will be comprised of both fuel cell system and battery pack.

TABLE 5. First attempt solution

Fuel cell system	Value
FC Power/O opt. val.	1119 kWh
Degradation during op.	190.97 μV
Number of FC required	14 MS100 (Powercell)
Total power inst.	1400 kW
FC load	74.89%
Efficiency	50.18%
H_2 Consumption	66,90 kg/h
Battery system	Value
Min. battery size	1700 kWh
Battery cycles in op.	64
Low degrad. cycles	52
High degrad. cycles	12

In addition to these results, the software verifies that the charge and discharge cycles observed in Figure 6 match the assigned C-Rate of the battery listed in Table 3. In the case that this does not match, an error message pops up in the command window displaying the information.
At this stage, it is possible to compare the data on the load of the battery in the histogram of Figure 7 with the degradation data presented in Figure 8. In this way it is possible to obtain a preliminary estimate of the degradation produced by the cycles that have the most power intensive requirements (depth and speed of charge and discharge).
The result seems to fall within the range of requirements for a vessel of this size, even if the battery configuration produces extreme stress on the pack. It is now possible to proceed with the validation. Running the software with 5 different operational profiles of different length on other randomly selected days, with the same setup information, produced only small deviations from the solution presented in Table 5.

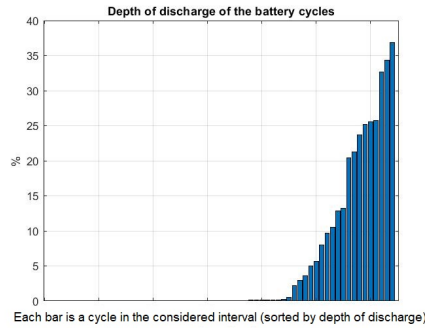

FIGURE 7. Battery cycles depth of charge

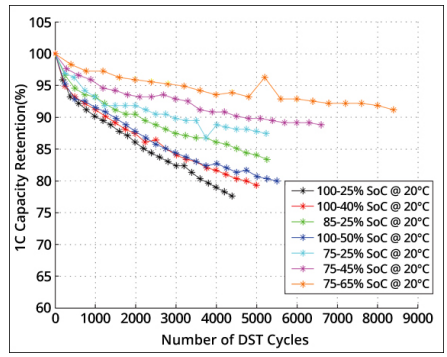

FIGURE 8. Capacity loss as a function of charge and discharge bandwidth [18]

It is important to remember that the fuel cells are not working at their full potential in the calculated configuration so there is a margin of safety if the power demand of the vessel is higher than the one estimated by the software.
The introduction of a less energy-dense form of power storage might affect the overall displacement of the vessel. The use of this software has to be accompanied by an in-depth study of the vessel's balance and displacement after the solutions are obtained. One case demonstrating that retrofitting a vessel with battery power is possible is presented by the Aurora of Helsinborg Ferry operating between Denmark and Sweden [19].

The idea for an engineering toolbox that could help designers quickly quantify the initial cost, and provide a preliminary quantification of the operational life is still in its early stages, but still marks a step forward for the maritime industry as they look to upgrade to hydrogen solutions. The clear specifications of the vessel power plant is also an important information for engineers working on energy management systems for these kind of vessels, as with this information they will be able to further optimize the systems.

CONCLUSION

This paper presentes an engineering toolbox, in the form of a Matlab/Python code, that aids in the design process of engineering a vessel with a hybrid zero emission powerplant.
Following the presented steps, it is possible to calculate the resources required to sustain the operational load using a PEM fuel cell and battery configuration. The goal of this software is to serve as a tool for sea-transport operators aiming to retrofit diesel-electric ferries with more environmentally friendly solutions to comply with emission regulations.
Future development on the software will include new functions considering the degradation mechanisms of fuel cells and battery, to produce more precise estimates of the life cycle costs. Another interesting development might include the addition of an option to select super capacitors for short term power storage.
With the maritime industry now acknowledging that more environmentally friendly fuels are needed to limit GHG emissions and pollution, providing tools to ease this transition is of the utmost importance. The goal of this work is to provide a small step in turning one of the biggest transport industry in the world towards a greener direction. In the last decade we have seen fuel cells and batteries undergo huge developments, becoming the base for power generating units of vessels of ever increasing size, so the hope is to, one day, have zero emission propulsion operating on all the feasible routes.

ACKNOWLEDGMENT

This work is supported by the Norwegian Research Council trough project number 90436501. The project is headed by IFE (Institute for Energy Technology) in Kjeller, Norway, and this work package is developed at the Department of Marine Technology of the Norwegian University of Science and Technology (NTNU) in Trondheim, Norway.

REFERENCES

[1] The International Maritime Organization. Initial imo strategy on reduction of ghg emission from ships. Annex 11, Resolution MEPC,304(72), 04 2018.

[2] N. Psaraftis Christos Kontovas Harilaos. Reduction of emissions along the maritime intermodal container chain: operational models and policies. *Maritime Policy & Management*, 38(4):451–469, 2011.

[3] NCE Maritime Cleantech. Norwegian parliament adopts zero-emission regulations in the fjords. Marie Launes, 05 2018.

[4] Kim Idar Giske. Ampere. Maritim magasin, 11 2014.

[5] S. De Breucker, E. Peeters, and J. Driesen. Possible applications of plug-in hybrid electric ships. In *2009 IEEE Electric Ship Technologies Symposium*, pages 310–317, April 2009.

[6] Leslie Eudy and Matthew Post. Fuel cell buses in u.s. transit fleets: Current status 2017. National Renewable Energy Laboratory, 11 2018.

[7] Hydrogen-powered fuel cell electric rail propulsion (hydrail). www.ballard.com/markets/light-rail. Accessed: 09-2019.

[8] Peter Gerstl Ivan Østvik, partners: Frode Skår. *Building the first hydrogen-electric ferry*, Maritime hydrogen and marine energy, 2019, Florø.

[9] presented by Mark Kammerer Dr. Joseph Pratt. Marine fuel cells and water go round. FLORØ, NORWAY, 09 2019.

[10] Mauro G. Carignano, Ramon Costa-Castelló, Vicente Roda, Norberto M. Nigro, Sergio Junco, and Diego Feroldi. Energy management strategy for fuel cell-supercapacitor hybrid vehicles based on prediction of energy demand. *Journal of Power Sources*, 360:419–433, August 2017.

[11] Yanjun Huang, Hong Wang, Amir Khajepour, Bin Li, Jie Ji, Kegang Zhao, and Chuan Hu. A review of power management strategies and component sizing methods for hybrid vehicles. *Renewable and Sustainable Energy Reviews*, 96:132–144, November 2018.

[12] Ameen M. Bassam, Alexander B. Phillips, Stephen R. Turnock, and Philip A. Wilson. Development of a multi-scheme energy management strategy for a hybrid fuel cell driven passenger ship. *International Journal of Hydrogen Energy*, 42(1):623 – 635, 2017.

[13] Ameen M. Bassam, Alexander B. Phillips, Stephen R. Turnock, and Philip A. Wilson. An improved energy management strategy for a hybrid fuel cell/battery passenger vessel. *International Journal of Hydrogen Energy*, 41(47):22453 – 22464, 2016.

[14] D. Apostolou and G. Xydis. A literature review on hydrogen refuelling stations and infrastructure. current status and future prospects. *Renewable and Sustainable Energy Reviews*, 113:109292, 2019.

[15] Ballard Energy system. Ballard to offer world's first pem fuel cell product using non precious metal catalyst. https://bit.ly/2sld0bi, 09 2017.

[16] Tom Fletcher, Rob Thring, and Martin Watkinson. An energy management strategy to concurrently optimise fuel consumption and pem fuel cell lifetime in a hybrid vehicle. *International Journal of Hydrogen Energy*, 41(46):21503 – 21515, 2016.

[17] L. van Biert, M. Godjevac, K. Visser, and P.V. Aravind. A review of fuel cell systems for maritime applications. *Journal of Power Sources*, 327:345 – 364, 2016.

[18] Bolun Xu, Alexandre Oudalov, Andreas Ulbig, Göran Andersson, and D.s Kirschen. Modeling of lithium-ion battery degradation for cell life assessment. *IEEE Transactions on Smart Grid*, 99:1–1, 06 2016.

[19] World maritime news. *HH Ferries Launches Battery-Powered Ferry Duo*, 10/2018.

PAPER II

INTERNATIONAL JOURNAL OF HYDROGEN ENERGY 46 (2021) 10924–10938

Available online at www.sciencedirect.com

ScienceDirect

journal homepage: www.elsevier.com/locate/he

Modelling and simulation of a zero-emission hybrid power plant for a domestic ferry

Lorenzo Balestra[*], *Ingrid Schjølberg*

Department of Marine Technology, Norwegian University of Science and Technology, NO-7491, Trondheim, Norway

HIGHLIGHTS

- Modelling of marine hybrid power-plant with PEM fuel cells and batteries.
- Energy management strategy for hybrid power-plant.
- Validation of the model using real world data for the double ended ferry.
- Analysis on the simulation result and optimization of the power-plant.

ARTICLE INFO

Article history:
Received 26 October 2020
Received in revised form
23 December 2020
Accepted 25 December 2020
Available online 26 January 2021

Keywords:
Hydrogen
Fuel cell
Hybrid propulsion
Digital model

ABSTRACT

This paper presents a simulation tool for marine hybrid power-plants equipped with polymer exchange membrane fuel cells and batteries. The virtual model, through the combination of operational data and dynamically modelled subsystems, can simulate power-plants of different sizes and configurations, in order to analyze the response of different energy management strategies. The model aims to replicate the realistic behavior of the components included in the vessel's grid, to asses if the hardware selected by the user is capable of delivering the power set-point requested by the energy management system. The model can then be used to optimize key factors such as hydrogen consumption. The case study presented in the paper demonstrates how the model can be used for the evaluation of a retrofitting operation, replacing a diesel electric power-plant with fuel cells and batteries. The vessel taken into consideration is a domestic ferry, operating car and passenger transport in Denmark. The vessel is outfitted with a diesel electric plant and an alternative hybrid power-plant is proposed. The hybrid configuration is tested using the model in a discrete time-domain.

Introduction

In recent years, the number of vessels transitioning from a conventional fossil fuel propulsion system to a hybrid or fully-electric system is increasing. The recent developments in battery technology and the cell's increase in energy density has encouraged the transition to hybrid power-plants, with batteries now included in a number of hybrid transport systems for energy storage purposes [1–4]. Such systems can reduce fuel consumption [5,6], reduce emissions from 10 to 35% up to 100%, and improve noise, vibration, maintainability, manoeuvrability and comfort [7]. The possibility to store

* *Corresponding author*. Otto Nielsens veg 10, Marine Technology Centre, Trondheim.
E-mail addresses: lorenzo.balestra@ntnu.no (L. Balestra), ingrid.schjolberg@ntnu.no (I. Schjølberg).

https://doi.org/10.1016/j.ijhydene.2020.12.187

excess power and release it on-demand, allows a more efficient use of a ships prime mover, enabling load leveling and peak shaving strategies [8].

While hybrid systems are able to reduce the level of emissions and fuel consumed, the next step for the maritime industry is the development of zero-emission vessels. Studies on zero-emission power generation systems for marine applications have been largely motivated by environmental goals aiming at to reduce pollution and greenhouse gas emissions. The United Nations and the International Maritime Organizations have both ratified documents planning a reduction in harmful emissions by 2050 [9,10], with local governments pledging to complement these commitments with national or regional environmentally friendly policies.

Currently, the majority of operational zero-emission vessels are equipped with battery systems. In Scandinavia, double-ended ferries such as the Aurora Af Helsingborg, the FinFerries' Elektra and MF Ampere are currently in operation facilitating the transportation of passengers and cars between coastal towns using large battery packs.

The fully electric configuration provides considerable environmental benefits, with a reduction of CO_2 emissions, for a vessel the size of the Aurora Af Helsingborg, estimated to be around 14 thousand tons per year. The vessel's power grid is also simplified when exclusively using batteries for energy storage, allowing for fewer maintanence operations. Nevertheless the full-electric configuration also presents drawbacks [11], mainly from an energy density and price perspective, that makes the transition to zero-emission challenging when considering to fully replace conventional fuel plants with battery packs for medium to long range applications. The limited amount of power stored in the pack relative to the weight and concerns regarding degradation of the battery cells, leads to a need for frequent dock recharging. To ensure low degradation of the battery pack and the highest capacity retention over the highest number of cycles, the ferry needs to discharge at a low C-Rate, if possible, and maintain a recommended value of state of charge (SOC) between 45% and 75%, depending on the specifications of the battery producer [12]. Battery systems also use a considerable amount of time to recharge, especially when considering megawatt scale applications. A ferry fast-charging during Roll on - Roll off (Ro-Ro) operations requires a dedicated infrastructure, with high voltage capabilities and values in the range of 10.000 V and 600 Amp when considering a 4 MW battery pack onboard [13]. The installation of this kind of infrastructure may be limited by financial considerations or by an inadequate and/or unstable electrical grid in remote location that still require zero-emission operations, such as remote locations in the fjord of Norway following 2026 regulation [14].

Given the limitations of batteries, not all routes that require zero-emission vessels can be operated by fully electric units. A hybrid power-plant using polymer exchange membrane fuel cell (PEMFC) technology, in conjunction with battery energy storage, can be considered as a zero-emission solution when greater range or flexibility is required [15]. The use of hydrogen, as an energy carrier, allows zero-emission operations in protected natural habitats, world heritage sites, CO_2 neutral ports and emission control areas, while maintaining an operational flexibility similar to a diesel vessel. The capability to charge batteries at sea during navigation eliminates the need for frequent dock recharging, furthermore the higher energy density of hydrogen compared to batteries, even it its pure compressed form, enables the storage of more energy on-board the vessel with considerable weight savings (Table 1).

Fuel cell technology is, in the maritime industry, at a lower technology readiness level (TRL) compared to battery technology, however the positive results with PEMFC in heavy duty transport applications, such as busses and trains, can be transferred to the maritime sector. PEMFC modules specifically designed and certified for marine use [16], have been presented in 2020, following the interest of ship operators such as Norled, in building a hydrogen vessel for passenger and car transport [17]. PEMFC have been tested aboard vessels, for example, on the FCS Alsterwasser in the EU project "zero emission ship" [18], and on a larger scale on the Viking Lady supply vessel.

The integration of fuel cells and batteries in hybrid power-plants is a non trivial task, as the operational profile and power requirements needs to be collected or data-mined, and because the operation is usually affected by the energy management system (EMS) [19]. The sizing of the powerplant decides the potential of powertrain system and affects the efficiency of the EMS. In other words, the selection of component size affects the design of the energy management strategy and vice versa.

The evaluation of the component's size and power rating should therefore be performed in a combined package with the creation of the EMS. The hybrid power-plant has to ensure a high levels of efficiency, satisfying the power demand of the vessel during operations taking into account the fuel cell and battery dynamics.

It is to aid the design process and observe the dynamic behavior of components such as battery and PEMFC in relation to the selected EMS strategy that, in this paper, is presented a model of a hybrid zero-emission power-plant. The model is developed to replicate the power-plant operation in a simulated environment, with a good degree of approximation, allowing the study of the components dynamic response to real world data inputs.

Several research approaches have been studied, considering that some limit their analysis to a predefined system and only focus on EMS [18], while others tend to ignore the EMS and focus on the optimal sizing problem [20].

This paper proposes a model that can be used to observe the effects of sizing on the EMS and vice versa, in a single software platform. This is necessary as the EMS may choose, with a smart algorithm, the optimal operational point for the power-plant and load sharing strategy, but if the hardware selected cannot realize the given strategy, different components or a different control should be chosen. The model can be adapted to different kinds of ships, and is scalable to

Table 1 – Energy density comparison.

Energy density	Pure H_2 (@700 Bar)	Li-Ion Battery
MJ/kg	120	1008
MJ/L	4.7	0.90 to 2.43

simulate power-plants up to 10 MW. The model includes converters and other power electronic components such as DC-Bus and switchboards.

To initialize the simulation the user can select or create an EMS strategy and input a series of parameters regarding the fuel cell and battery system considered. The results obtained at the end of the simulation include hydrogen consumption, which heavily impacts the vessel operating costs, as well as fuel cell degradation and battery usage. Results from different power-plants layouts and EMS strategies can be compared to choose the optimal solution for the vessel power delivery.

The model is tested using a hydrogen-hybrid configuration for a domestic double ended ferry operating in Danish national waters, currently equipped with a multi-megawatt diesel electric power-plant (see Fig. 1). The operational profile used for the initial configuration of the model was chosen to emulate a typical winter day in 2019 on the route of interest. This operational profile was one of many collected during a six month period in cooperation with the company. The case study demonstrates how the model can be used for the technical evaluation of a retrofitting operation, replacing the diesel electric power-plant with PEMFC and batteries. The power delivery values are observed and compared to the power demand in input. The power-plant sizing is validated only if the mean square error between the expected value and the produced value is below a certain threshold defined by the user, and, in general, there should be no sign of power shortages or blackouts. The technical evaluation allows further studies on the economical feasibility of the system. The data produced by the model provides figures that can be used to compare the ideal behavior of the hybrid system, the realistic behavior of the system under stress and highlight the differences with the diesel electric plant.

The study does not go into detail with respect to the changes in ship design when integrating a hydrogen system or hydrogen storage solutions such as metal amines [21,22], liquid hydrogen organic carries (LOHC) [23] or hydrides [24] that may be required to operate such power-plant. The imposed boundary condition is to assume that if a certain amount of pure hydrogen is required by the fuel cell stack, the demand can always be fulfilled by the storage.

On-board power-plant

In this section is described the original diesel-electric configuration of the ferry and the new hybrid solution proposed by the authors.

Conventional system

The ferry taken into consideration during the case-study is a double ended ferry of approximately 100 m length, with capacity for 600 passengers ans 122 cars. The route is a crossing over a 7.7 nautical miles distance with voyage time averaging 45 min and voyage interval of 1 h (Fig. 2).

The prime movers of the ferry are 5 diesel generators rated at 800 kW, powering 4 Azimuth thrusters and additional auxiliaries. The diesel generators also provide all the power for service and hotel load. No energy storage technology is installed. The system is designed to comply with class regulations and is designed with passive redundancy in mind, considering that only three generators are switched on during the crossing, out of the five installed. This is to allow maintanence activities and ensure there is always a power reserve. The single line diagram of the diesel electric configuration is represented in Fig. 3.

With the double-ended design there is no requirement to turn around in ports, directly translating to less power pulses during docking procedures compared to the single-ended counterpart. The vessel crosses a busy shipping route and often has to give way to larger commercial vessels [26]; this influences the power demand during the crossings, as the ferry deviates from the optimal route to avoid traffic. The change in meteorological condition is also a factor influencing the power demand. The variation of wind and sea current strength happens yearly, with the summer being the easiest period to operate, but also daily, with variation between the first crossing 5.15 a.m. and the last at 22.15 p.m.

The ferry operates 18 crossings in a day (see Fig. 4). The values show that once the vessel is disconnected from the

Fig. 1 – The double ended ferry considered in the study case.

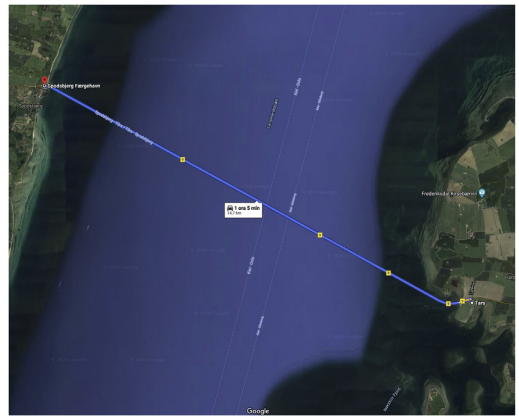

Fig. 2 – Ferry route [25].

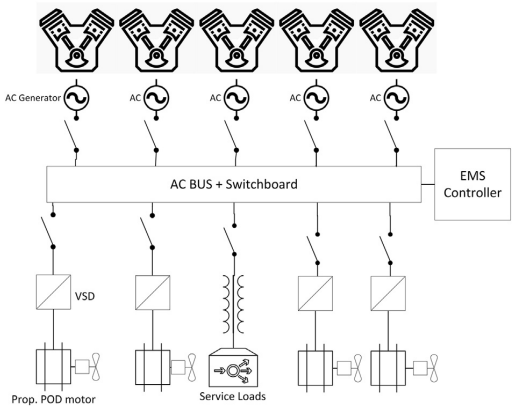

Fig. 3 – Simplified single line diagram for the diesel electric configuration.

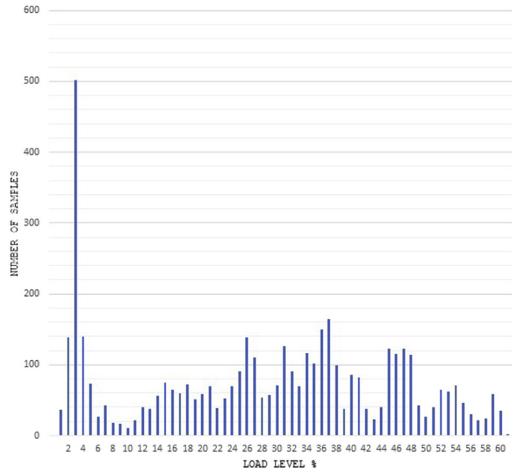

Fig. 5 – Load level distribution over one day of operations.

shore power supply, Ro-Ro operations are carried out using between 1% and 7% of the total power installed. The data collected during the crossings show that the power used for the crossing from Spodsbjerg is around 38% of the total power, while the one from Tårs is slightly higher around 48% (Fig. 5).

The observation of the power levels in Fig. 5 shows how an hybrid power-plant comprised of PEM fuel cells and batteries can eliminate pollution and greenhouse gas emissions, and also increase the overall efficiency through peak shaving or load leveling strategies.

During Ro-Ro operation for example, the load on the diesel generators is quite low (between 1% and 7% total power), forcing the units to operate at a point far from the optimal thermal efficiency [27]. This leads to a high specific fuel consumption, but cannot be prevented as the generators needs to be kept on to be ready for maneuvering.

During this phase, a hybrid propulsion plant equipped with PEM fuel cells and batteries could supply the power using some PEMFC stacks at a low load level, where the stack efficiency is higher (60%) than at rated load. This would also eliminate harmful emissions in the coastal area and the harbor [28].

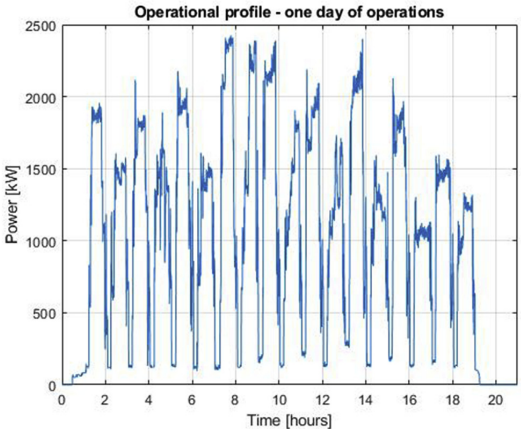

Fig. 4 – Measured power demand of the ferry over a full day of operations.

Hybrid propulsion system

The alternative, zero-emission power-plant presented for the ferry includes polymer exchange membrane fuel cells (PEMFC) and a Lithium-Ion (Li-Ion) battery packs for energy storage. Polymer exchange membrane technology has been selected for the fuel cells, in this case, after considerations on the operational requirements and good performance at relatively low temperatures [29,30]. The Lithium Ion battery pack has been selected for the high energy density and fast charging and discharging capabilities at multiple C-Ratings. The presented hybrid solution size and rating does not take into consideration vessel safety regulation for active or passive redundancy and is simply based on supplying the required power-demand. Compliance with class regulation can be achieved by increasing the number of PEMFC or batteries, but the study of the requirements was considered out of the scope of the paper. The additional PEMFCs and batteries required by the safety regulations do not impact the results obtained in this paper as they are considered switched off and disconnected from the system, only activated in case of emergency.

In Fig. 6, it is possible to observe a simplified single line diagram for the hybrid system proposed. The diagram represents the fuel cell unit unit as a single block, for the sake of clarity, with the notion that the fuel cell system is comprised of multiple stacks to reach the required rated load. The definition of the power rating for the battery and

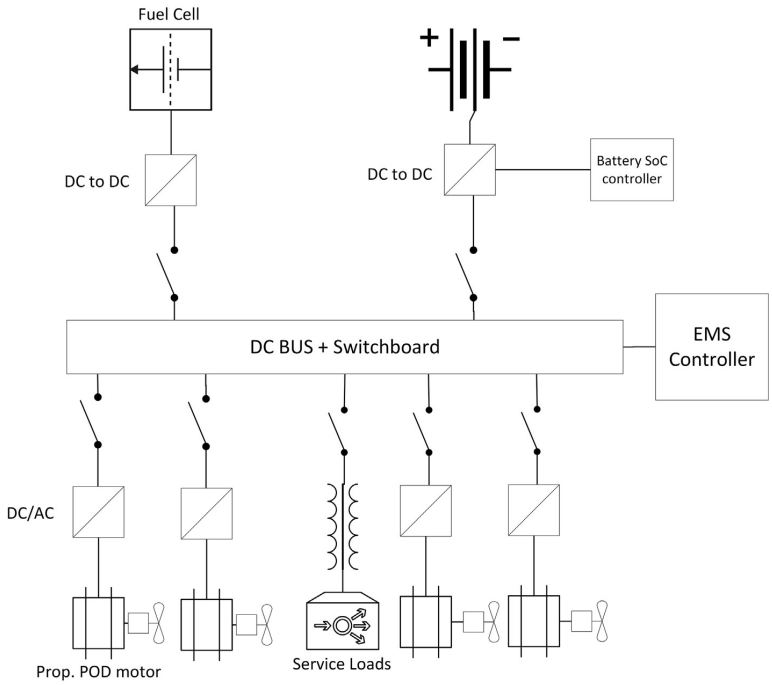

Fig. 6 – Simplified single line diagram for the hybrid configuration.

fuel cell stacks is non trivial, as the sizing defines the potential of the powertrain, influencing the energy management system, and vice versa [31,32]. In this case, both the fuel cell and the battery are intended as modular systems, meaning that a series of units can be combined in series or parallel to achieve different layout solutions and power ratings.

The first step in the sizing process is the identification of a first attempt configuration through the observation of the operational data. This configuration is, after the simulations with the digital model, either modified or validated if the results are satisfactory for the user.

The first factor that helps to define the total power rating of the battery and PEMFC system is the observation of the average power requirements during the crossing phase (Fig. 5). The power delivery capabilities of the proposed hybrid power-plant should be able to satisfy the average power demand during crossings while operating at their rated load, and be able to compensate for extra power demand if necessary.

The maximum power recorded during a crossing with the diesel electric configuration is equal to 2425 kW out of the 4 MW installed. The maximum recorded power is lower than the total installed power (4 MW) as only three out of the five diesel gen-sets are on during the crossing and the other two are considered as a power reserve. This reference value of 2425 kW provides a starting point for the dimensioning procedure of the hybrid power-plant active during the crossing. The combined output of battery and PEMFC cannot be lower than this value. To generate additional guidelines for this calculation, a power-plant design software developed by the authors has been used [33]. The hybrid configuration with batteries and PEMFC allows more flexibility when choosing power ratings compared to the selection of diesel generators. It is possible to consider that battery packs can compensate peaks in power demand with a fast response time and operating at C-Rates higher than 1, effectively allowing the increase of power delivered on demand at the expenses of a faster reduction in state of charge. Batteries also can be operated continuously and do not have to be switched off, unlike diesel generator, to perform extensive maintanence.

For the first attempt solution, the PEMFC's rating has been selected in relation to the battery size and characteristics, with the goal to provide enough power to avoid high depth of discharge cycles. The ratings are set, for the first attempt solution, to 15 PEMFC for a total of 1500 kWh and 2 batteries of 1000 kWh of batteries. The sum of the two values results a powerplant able to produce 3500 kWh at full load. Setting the rating higher limits the depth of discharge and therefore degradation. According to DC-Grid guidelines, a level of 690 V is suggested for the ship's grid in vessels with installed power up to 10 MW.

As both fuel cells and battery have a direct current (DC) output, the grid uses DC for the transfer of power, with inverters for the motors and service loads.

Model description

The model is the virtual representation of the systems illustrated in Fig. 6. The components such as fuel cell, battery and converters represented in the diagram, have been modelled to have a dynamic behavior similar to the real-world counterpart, allowing the study of their response to realistic input data. Propulsion loads and service loads are considered combined in this study, as the values sampled during operation represent the total power consumption of the vessel.

The working principle is illustrated in Fig. 7 The process starts by selecting a time interval from the database where the data are logged. The interval considered can be of variable length and can include multiple crossings, depending on the computational resources and time that the user wants to allocate for calculations. It is recommended to use a time interval between two docking operations or between two night layovers for better results. The time interval selected identifies, on the database, a list of power values in kilowatt representing the total power generated by the diesel-electric plant in the ferry's current configuration (Reference Fig. 4 for a time interval of 22 h). These power values, known as operational profile, are used as the vessel's power demand that needs to be satisfied by the new hybrid plant. The EMS contains the load sharing strategy and splits, according to the coded instructions, the total load between battery and fuel cells. Two converters control the power output of fuel cell and battery to the DC Bus, much like in the real system. The voltage is maintained constant on the DC Bus and at the recommended level using two feedback loops. A Recharging circuit is also included for the battery, giving the possibility of on-the-go recharging.

The power generated by the plant ("Produced power" in Fig. 7) is, in the end, compared with the operational profile given as input, to observe the efficiency of the EMS, and the selected components, in following the load profile. The capacity to generate the required amount of power using the hybrid plant can be seen as a validation of the components power rating and load sharing strategy.

Using as input the load profile of the diesel electric configuration for the hybrid power-plant allows for a direct comparison between the two solution. It is possible to calculate the equivalent amount of hydrogen required to carry out the same crossing and also estimate the degradation of both battery and PEMFC.

Table 2 – Fuel cell characteristics.

Rated power (net)	100 kW
Gross output at rated power	320 V/350 A
Peak power EOL…OCV BOL	250…500 V
System efficiency (Peak, BOL)	62%
System efficiency (BOL)	50%
Max waste heat	120 kW
Coolant outlet temperature	80C
Fuel inlet pressure	8–12 bar(g)
System pressure	1.6 bar(g)
Ambient temperature	−20 to +50C
Ambient relative humidity	5–95%, non-condensing
Installation environment Outdoor	Pollution degree 3
Weight	120–150 kg
Volume	300 l
Fuel quality	ISO 14687-2, SAE J2719
IP classification	IP54

Fuel cell

The fuel cell considered for this model is a polymer exchange membrane fuel cell with commercial characteristics. The reference values used in the model are reported in Table 2. The fuel cell model is a generic model parameterized to represent polymer exchange membrane fuel cells supplied with pure hydrogen and air (Fig. 8). The model is based on the work of Njoya et al. [34].

A boundary conditions of the model is set on the delivery of hydrogen and air to the fuel cell. In the model the supply of both hydrogen and air is carried out by ideal components

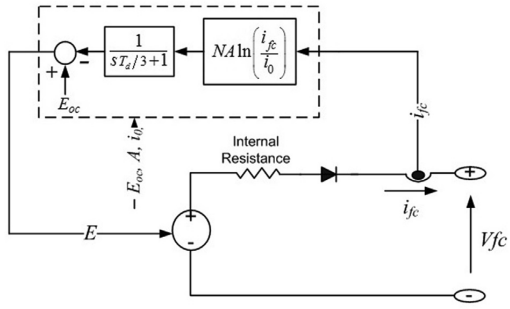

Fig. 8 – Equivalent circuit of the fuel cell included in the model [34].

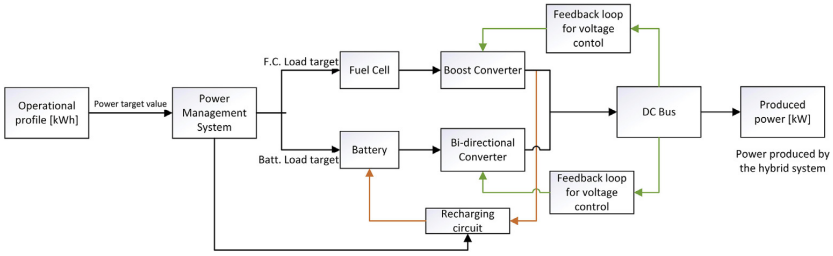

Fig. 7 – Model schematics.

(compressor and valves), eliminating problem of fuel and air starvation during dynamic loading. The assumption is made as the EMS is supposed to avoid high frequency transients on the fuel cells, limiting possible cases where air and hydrogen starvation may appear. In the model, the airflow value ($V_{lpm(air)nom}$) and the hydrogen flow value ($V_{lpm(fuel)nom}$) are calculated indirectly, based on the load power requirement (Fig. 9). This approach allows the user to quantify the hydrogen consumption at each timestep and calculate the total consumption at the end of the simulation in standard liters per minute. The degradation of the PEM fuel cell is a key aspect considered. A separate block is created to evaluate the degradation of the fuel cell over the operational time. In this case, the degradation values are based on the studies of Fletcher et al. [35] and listed in Table 3.

The equation to calculate the degradation is made up of two terms, one quantifying the degradation during constant power output periods and one for transient operations. These two values are summed to find the total value at the end of a simulation over a defined time interval.

$$Deg = \frac{Lpo}{3600}*t + \frac{Hpo}{3600}*t + \sum_{t=1}^{n} \frac{Tl*10^3}{P(t) - P(t-1)} \quad (1)$$

- Lpo = low power operation value [μV/h]
- Hpo = High power operation value [μV/h]
- τ = time sample duration [s]
- Tl = Transient loading value [μV/Δkw]
- P = Electric power μV/Δw
- Deg = degradation in μV
- t = time; n = last sim. timestamp

The calculation of the total degradation value allows the users to estimate the interval between maintenance activities and estimate the operational life of the fuel cell in relation to the implemented EMS.

Battery

The battery pack is included in the model to compensate for the slower dynamic response of the PEMFC and compensate occasional spikes in power demand during transient loading conditions. The installation of a battery also allows to include, in the energy management strategy, a peak shaving solution, reducing the overall usage of the fuel cell during high frequency transients and high power operations, therefore lowering its degradation and hydrogen consumption.

The model used for the battery is a parametric dynamic model adapted to simulate a lithium ion battery pack. The circuit is based off the work of Zhu et al. [37]. and Tremblay et al. [36] (see Fig. 10). The internal resistance is assumed to be constant during the charge and discharge cycles and does not vary with the amplitude of the current. The parameters of the model are derived from the discharge characteristics. The discharging and charging characteristics are assumed to be the same. The capacity of the battery does not change with the amplitude of the current (there is no Peukert effect).

The battery size has been calculated in relation to the 1500 kW of fuel cell capacity installed. Considering that the highest registered power demand value in the ferry's database is equal to 2425 kW, it was determined that two 1000 kWh battery packs were fitting the applications requirement maintaining the depth of discharge low. This value was calculated taking into account an efficiency of the power line of 90%. The battery selected is rated at 400 V. The nominal discharge current for one battery pack is equal to 1087 Ah and it is assumed that the battery can operate at an up to 2C. Additional characterization of the battery packs used can be observed in Fig. 11.

Converter connecting PEMFC and DC-Bus

The converter connecting the fuel cell, rated at 320 V, to the 690 V DC-bus is modelled as a conventional boost converter (see Fig. 13). The boost converter allows the increase of voltage using a IGBT, switching at 5 kHz, controlled using a PWM signal generator. The duty ratio of the PWM signal is adjusted between 0.1 and 0.9 according to the input voltage, to maintain the output voltage stable at 690 V. The duty ratio is controlled through a feedback loop with a PID controller. The values for inductance and capacitance used in the boost converter model are tuned to get a quick and non-oscillatory voltage rise with an acceptable level of voltage ripples [38].

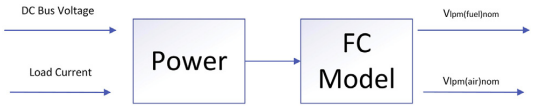

Fig. 9 – Input/output given to the fuel cell model from Njoya [34].

Table 3 – Degradation from Fletcher et al. [35].

Operating Conditions	Degradation Rate
Low power operation (<80%)	10.17 μV/h
High power operation	11.74 μV/h
Transient loading	0.0441 μV/Δkw
Start/stop	23.91 μV/cycle

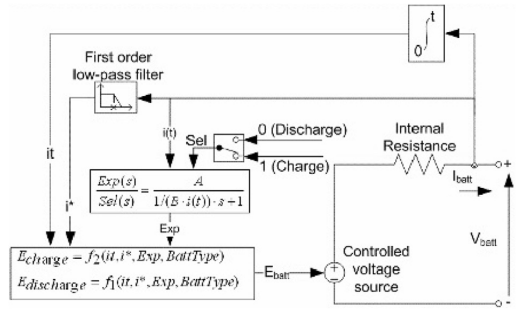

Fig. 10 – Equivalent circuit of the battery included in the model [36].

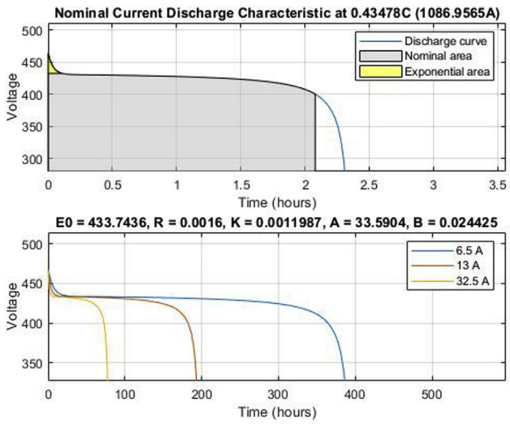

Fig. 11 – Graph representing the characteristics of the battery pack used in the model.

When tested, the model ensured a stable response well within the class limits of ±5% voltage variation during steady load and ±10% during transients. The EMS also ensures that components producing excessive or too low voltage can be disconnected from the switchboard to avoid damages to the whole system.

It has to be noted that with a switching frequency of 5 kHz and a simulation timestep in the order of the microsecond the model takes into consideration the switching dynamics and not an average model for the converter response.

Converter connecting the battery and DC-Bus

The battery is connected to the DC-Bus using a bi-directional DC/DC converter. This type of converter allows the flow of electric power in both direction (Fig. 14), allowing the discharge and recharge of the battery alternatively. The converter also provides voltage regulation, as the battery and the DC-Bus operate at different voltage levels.

The values for the inductance and capacitance of the converter have been tuned to get a non-oscillatory response with an acceptable level of voltage ripples.

The converter can operate in two distinct modes: a boost mode, used during discharge, and a buck mode used during recharge. The boost mode is used to bring the voltage on the battery side, rated at 400 V, to the level defined for the DC Bus of 690 V. The buck mode allows to lower the voltage from 690 V

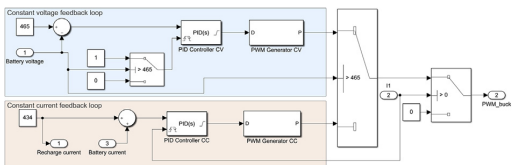

Fig. 12 – Buck mode circuit: battery recharge controller.

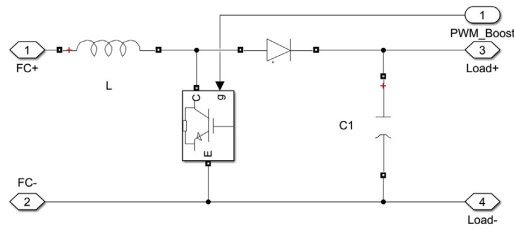

Fig. 13 – Boost converter connecting DC-Bus and PEMFC.

to a voltage level acceptable for the recharge of the battery. This voltage level is variable, according to the battery polarization curve, but higher than the rated battery voltage to allow for recharge.

The switches (IGBTs) in the bi-directional converter are controlled using a PWM source, similarly to the application in the fuel cell boost converter, with a switching frequency of 5 kHz. Also in this case the switching dynamics can be observed thanks to the simulation timestep of 1 μs. The PWM signal is generated, in both modes, using the feedback signal from a PID controller (Fig. 12 for the circuit relative to buck mode, Fig. 16 for boost mode). The PIDs are installed on feedback loops in charge of maintaining the voltage level at the desired value on the bus side during boost mode, and on the battery side during buck mode.

The buck-mode PWM signal generator can be controlled in different ways, using the EMS, to have different recharge strategies. In this study, it is considered that the battery pack is recharged at constant current at 1C when the fuel cell is able to generate the excess power needed. Once the fully charged voltage is reached, the value controlled becomes the battery voltage, kept at a constant value, using a second feedback loop, until the SOC of the battery reaches the specified upper limit (in this case 90% SOC) (see Fig. 15).

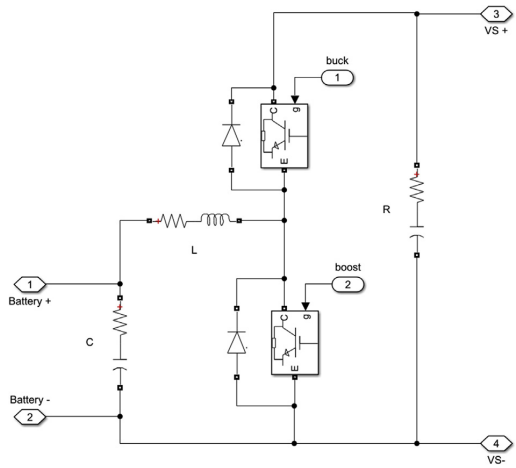

Fig. 14 – Bi-directional converter connecting the battery to the DC Bus.

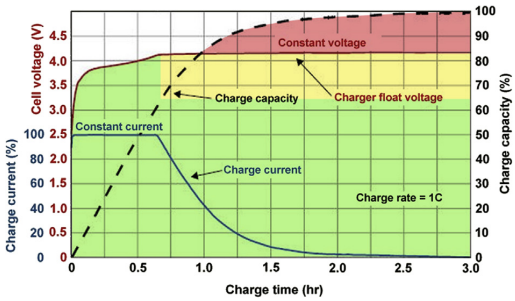

Fig. 15 – Graph representing the characteristics of the battery pack recharging.

Both PID controllers are connected to a reset switch as the battery, following the strategy of energy management system, is not permanently connected to the load. This reset switch is in charge of avoiding overshoots in the correction from the integral term of the PID.

Switchboard

The switchboard is modelled with ideal switches with a high snubber resistance (see Fig. 17). The connections realized are the one represented in the single line diagram of Fig. 6.

The connection between the bi-directional converter is modelled with two ideal switches, one dedicated to the discharge circuit and one to the recharge circuit. This differs from the single line diagram where only one switch is represented.

As the load, in this case, is modelled as a single block to include both propulsion loads and service loads, the connection between the switchboard and the load is operated by a single ideal switch.

All the switches are controlled using inputs from the energy management system.

Electrical load

The electrical load subsystem is tasked with simulating the variable power demand of the vessel over time. Once the time period that needs to be analyzed is selected, a series of power values are extracted from the database and used as input of a interpolated sequence block to create a virtual operational profile. The power values used in this study are the combination of propulsion load, auxiliaries and hotel load.

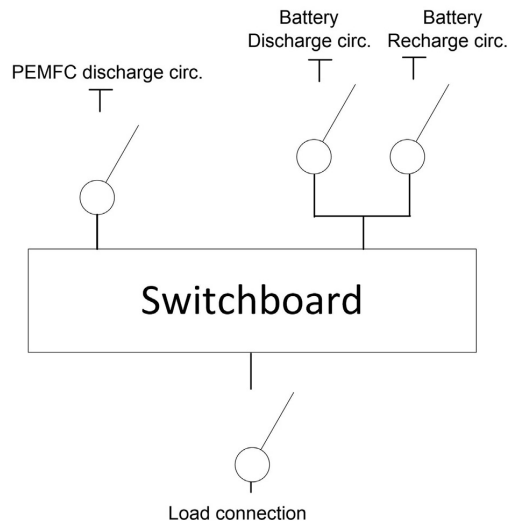

Fig. 17 – Switchboard simplified schematics.

The power demand defined by the operational profile need to be fulfilled by the combination of fuel cell output (P_{fc}) and battery (P_{batt}) output, both multiplied by the relative number of units installed in the system (n_{fc},n_{batt}).

$$P_{tot} = n_{batt} * P_{batt} + n_{fc} * P_{fc} \quad (2)$$

A complex representation for the load, including induction motors for the propulsion system, is considered out of the scope of the paper. The load is therefore modelled as a variable resistive load connected to the DC-Bus (Switchboard). This approach does not allow the observation of the effects of current and voltage waves, once the DC current is converted to AC current for the motors, but still allows to control the current flowing from the power source (PEMFC and battery) to the power sink (load sub-model). The load sub-model is based

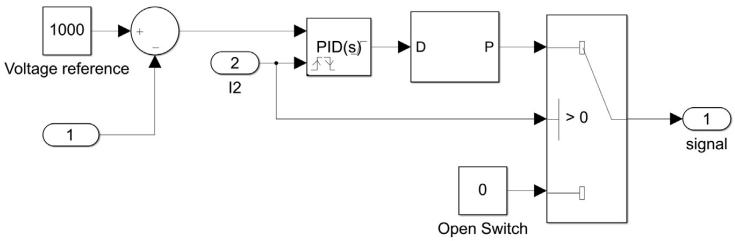

Fig. 16 – Boost mode circuit: battery discharge control.

on Ohm's law and electric power formulation. This is allowed as the components in the software environment do not have any limitations regarding the current that can flow through the controlled resistive load, in addition to no limitation on the power rating and operational temperature.

$$R_{fc} = \frac{V_{bus}^2}{P_{fc}} \quad (3)$$

$$R_{batt} = \frac{V_{bus}^2}{P_{batt}} \quad (4)$$

The resistive value used as input by the load sub-model is calculated, for the fuel cell stacks and batteries, using the formulation of Eqs. (3) and (4). V_{bus} is the same for both battery and fuel cells, equal to the value set by the DC-Grid guidelines for the proposed power-plant, 690 V. The voltage level is kept constant around the defined level by the feedback loop presented in Fig. 16. The value for the power output of the fuel cell (P_{fc}) and the power output of the battery (P_{batt}) is defined by the load sharing strategy coded in the energy management system.

The modelling of the load as a simple resistive electrical load allows also for lower computational complexity in the simulation reducing considerably the computational time compared to the solution including library models of induction motors and variable speed drives.

Energy management system

Targets and strategies

The energy management strategy defines how the load sharing between fuel cells and battery is carried out. A series of inputs, such as total power demand, fuel cell utilization level and battery state of charge is fed to the EMS that evaluates what actions to take according to a series of coded instructions if the system is rule based, or through some optimization algorithm, like for the equivalent fuel consumption minimization strategy.

Once the strategy for the specific operational point is defined, the control on the power delivered is carried out by giving an input to the switches included in the switchboard, connecting the necessary power sources to the load, and setting a target value for the power delivery of each component (P_{batt}, P_{fc}).

The sum of the fuel cell and battery power output should be equal to the value of the operational profile for each considered instant (Eq. (2)). Slight oscillations in the power output value may be present due to the PID way of operating, but the stability of the system is measured on the fact that only minor oscillation can be accepted. The presence of major differences between the power output and the requested power exposes errors in the power rating calculation or in the way the load in delivered.

The energy management system enables the optimization of one or more parameters. Some of these factors are, for example, the minimization of hydrogen consumption or degradation of the PEMFC membrane. For the battery, the main factor is the reduction of high depth of discharge cycles leading to premature degradation [12].

Different control strategies can be implemented to define the load sharing solutions. Some examples include [18]:

1. State based (or rule based)
2. Charge-depleting charge-sustaining (CDCS)
3. Classical PI
4. Equivalent fuel consumption minimization strategy

Rule based EMS

For the model presented in this study, a rule-based strategy has been developed. A rule based strategy consists in a series of coded instructions defining what actions to take and what target values for power delivery are for each possible operational mode (Table 4). The rule-based strategy created for this case study aims at the minimization of fuel cell degradation through load leveling. Load leveling can be implemented taking full advantage of the battery system by storing excess power when possible and deliver it once it is needed. In this case, the time where the fuel cell has to provide power at a high degradation rate is greatly reduced.

In this case, the main variables taken into consideration when coding the rule based strategy are the battery state of charge and the power output level of the fuel cell.

The fuel cell output is limited at 80% of the rated load for the considered 100 kW PEMFC unit for degradation reasons (Table 3). When considering the first attempt solution configuration presented in the hybrid power plant description, this is equal to 1200 kW of available fuel cell power during normal operation. Loads above this value are supplied using the battery pack, that is recharged once the power is available. The power dedicated to the recharge of the battery is indicated as P_{rec}.

$$P_{rec} = V_{batt-rec} * I_{nom} * C_{rate} * \eta_{conv} \quad (5)$$

When controlling the recharge of the 1000 kWh 400 V battery, at 1C, the battery can accept roughly 1086 Ah at 437 V during constant recharge mode. These two factors in addition to the efficiency rating for the bi-directional converter defines the value of P_{rec}. The power to recharge the battery is a quantity that has to be compensated by and increase in fuel cell power delivery. The battery optimal recharge point is when $P_{vessel} + P_{recharge}$ is equal to the maximum efficiency operational point of the PEMFC. This condition can be achieved during Ro-Ro operations. The maximum SoC value for the battery is set to 80%. This means that the battery is never charged using the constant voltage loop during navigation with the current EMS, but the system maintains the possibility to fully charge the battery to 100% from shore power (simulated in an independent voltage source) and by alternative future EMS strategies. The minimum value for the SOC of the battery is limited to 20%. This reduces the degradation of the battery limiting the number of cycles with high discharge rate.

Table 4 – Rule based energy management system instructions.

Power Available	SOC Level	Action Battery	Action FC
$P_{vessel} + P_{rec} \leq P_{fc\text{-}lim}$	SOC ≤ 80%	Battery Recharge	$FC_{target} = \frac{P_{vessel}}{n_{fc}} + \frac{P_{rec}}{n_{fc}}$
$P_{vessel} + P_{rec} \leq P_{fc\text{-}lim}$	SOC > 80%	No Battery Recharge/Discharge	$FC_{target} = \frac{P_{vessel}}{n_{fc}}$
$P_{vessel} + P_{rec} > P_{fc\text{-}lim}$; $P_{vessel} \leq P_{fc\text{-}lim}$	20 ≤ SOC < 100%	No Battery Recharge/Discharge	$FC_{target} = \frac{P_{vessel}}{n_{fc}}$
$P_{vessel} > P_{fc\text{-}lim}$	20 ≤ SOC < 100%	Battery Discharge	$FC_{target} = P_{fc\text{-}lim}$
$P_{vessel} > P_{fc\text{-}lim}$	SOC < 20%	No Battery Recharge/Discharge	$FC_{target} = P_{fc\text{-}lim}$

Simulation results and discussion

Simulation setup

The simulation with the proposed zero-emission hybrid power-plant for the ferry is carried out using the parameters listed in Table 5 and the power data relative to a single ferry crossing from Spodsbjerg to Tårs. A discrete time domain with fixed timestep in the order of the microsecond has been used. The selection of a discrete time domain allows for faster computation and the fixed timestep for the production of data with a consistent timestamp for the final comparison. The timestep selected is 1 μs, to minimize numerical errors and allow good precision in the feedback loops controlling the bus voltage and the battery recharge. A timestep of 1 μs also allows the observation of switching effects in the modelled converters. The solver used is ode3.

Simulation results

One crossing of the duration of 45 min, including an additional 15 min for the Ro-Ro operations, is taken into consideration for the simulation in the case-study. This crossing is one of eighteen carried out during a full day of operation. Once the simulation is completed it is possible to analyze the behavior of the digital system and compare it to the real-world power demand.

In Fig. 18 is represented the power demand of the vessel (blue line), and the power delivered by the hybrid power-plant (orange line). An analysis of the power values highlights how, the mean square error between the demand and the power delivered in kW is equal to 5.7601e+03. This means that for 72% of the analyzed operations, the difference between power requested and power delivered is below 100 kW.

Table 5 – Power-plant configuration for the first simulation.

Total power installed	3500 kW
Bus voltage	690 V
Battery units	2
Battery nom. voltage	400 V
Battery rated capacity	2500 Ah
Initial SOC	50%
Number of fuel cells	15
Rated power PEMFC	100 kW
Response time PEMFC	15s
Response time Battery	2s

The power provided by the powerplant is also lower than the power demand for just 1.47% of the power values, meaning that the power delivery is ensured for 98.5% of the considered time. In this first configuration, the focus of the EMS was to avoid a lack of available power and consequent blackout rather than optimize the power delivery to match the operational profile 100% of the time. The components selected in Table 5 can take care of the power requirements of the vessel for this specific crossing.

Spikes in the power output are visible around 600 s and 3200 s when the battery recharge loop is disconnected and reconnected to the system in rapid succession due to the power demand value oscillating between the two EMS conditions $P_{vessel} + P_{rec} > P_{fc\text{-}lim}$ and $P_{vessel} + P_{rec} < P_{fc\text{-}lim}$. This behavior shows one of the limitations of a simple rule based EMS, that applies coded instructions without knowing the conditions of the system in present or past states. It shows also that the power electronics components such as the converters and the DC-Bus capacitor should be rated to withstand this condition or re-tuned to reduce the intensity of this phenomenon.

It is possible to observe how, during the crossing phase, the system is outputting an excess of power between around 80 kW even if the EMS is providing the correct target value. This shows how the battery, during high load sequences, has a slightly different behavior than expected, and the set point for the battery current during discharge needs to be adjusted to account for this behavior. Alternatively it is possible to modify the load sharing strategy to reduce the stress on the battery or improve the efficiency of the bi-directional converter.

During the time interval analyzed, it is possible to observe how the feedback loop controlling the voltage output of the fuel cell is keeping the voltage level at the defined level for the DC Bus, with small spikes due to the aforementioned oscillations of power between two PEMFC target values (Fig. 19). The battery is influenced too by this power demand oscillation and it is possible to notice around 500 s, how the rapid connection and disconnection of the battery to the system does not allow the correct control of the output voltage on the battery side and creates a spike to 1255 V. These spikes show that both battery and fuel cells need to be able to quickly disconnect from the DC Bus if over-voltage or over-current conditions are present. The battery discharge controller operates well during the crossing phase (designed conditions), where the connection of the discharge circuit to the bus is stable and the output is kept around the 690 V value.

Fig. 20 shows the variation in the state of charge of the two installed batteries during the interval analyzed. The two Li-Ion

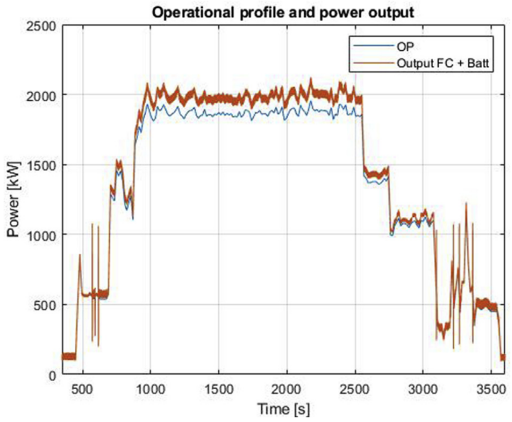

Fig. 18 – Total power output and operational profile comparison.

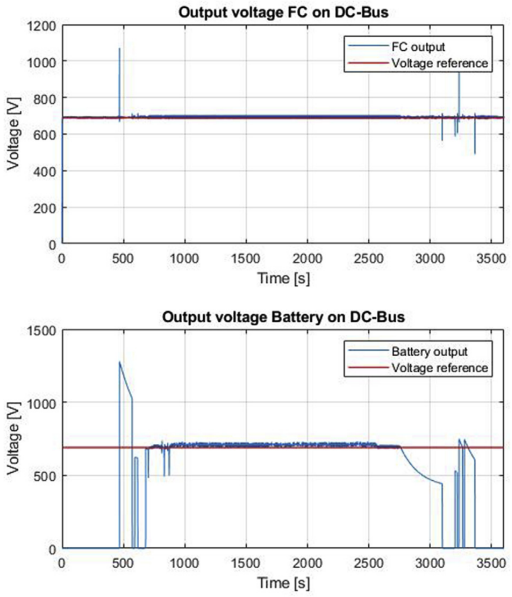

Fig. 19 – Output of battery and fuel cell to the DC-Bus.

packs are assumed identical and with the same dynamic behavior. It is possible to notice that around the last part of the crossing the SOC reaches the lower limit of 20%, but the impact of this condition causes no power deficit as once the battery reaches its lower limit, the ferry enters the maneuvering phase at the dock of destination, using mainly PEMFC power. This indicates that the battery size calculated for the plant is the smallest size that can be installed without experiencing power shortages in these specific conditions, with the given components and EMS.

The adoption of a battery pack of the size indicated in Table 5, operating with the presented components and EMS, allows to occupy a relatively small amount of space on the vessel while providing enough power for the crossing. The flexibility though is heavily impacted. Increasing the overall efficiency of the system reducing the wasted energy in the converters and improving the power delivery of the fuel cells to stabilize the baseline power supply would benefit the battery usage and allow to carry out the complete crossing retaining a power reserve.

Fig. 21 represents the consumption in liters per minute of air and hydrogen for the single fuel cell. The total hydrogen consumption for the crossing with the considered configuration and EMS strategy is equal to 1.4164e+04 standard liters per minute (SLPM), equivalent to around 1.26 kg for the single PEMFC (considering hydrogen density at STP equal to 0.089). By multiplying for the number of fuel cells we find that around 19 kg of hydrogen are required for the single crossing. The possibility to calculate the consumption in SLPM allows the ship operator to quantify the volume required for hydrogen storage on-board according to the storage technique (GH2 or LH2), and the costs of fuel per day.

The degradation of the single fuel cell, with the current setup and EMS strategy, is equivalent to 3.1050e+04 μV for the considered crossing. This value can help quantify the number of cycles that can be carried out by the fuel cell before maintanence is required.

With the system being powered entirely by PEMFC and batteries, the produced greenhouse gasses emission are equal to zero.

The obtained results seem to satisfy the power demand and validate the initial sizing in relation to the selected energy management strategy. These results can be taken as reference to improve the system efficiency, reduce the mean square error between the operational profile and the power produced and reduce the fuel consumption.

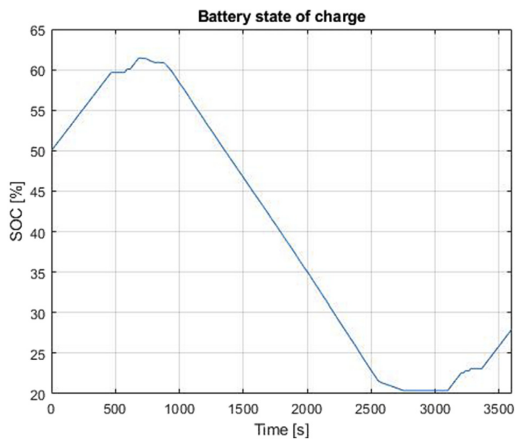

Fig. 20 – State of Charge of the battery.

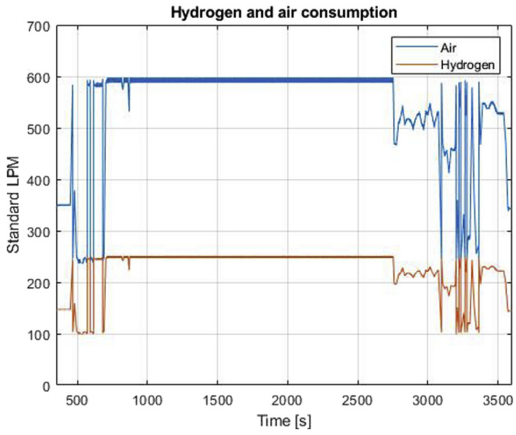

Fig. 21 – Hydrogen and Air consumption for a single PEMFC.

Some improvements that need to be addressed in a future version of the model can be listed below.

First, the oscillation of the power demand around the limit value: $P_{vessel} + P_{rec} < or > P_{fc\text{-}lim}$, used as a condition in Table 4, produces instability due to the rapid connection and disconnection of the recharge circuit multiple times. This leads to unstable voltage regulation, for a limited amount of time, on the battery side, and spikes in the value FC_{target}, that the system tries to follow, producing excess degradation on the PEMFC. This issue can be addressed by improving the rule based EMS including specific boundary conditions on the connection and disconnection of the recharge and discharge system or providing the system with a EMS using a different strategy based on feedback values (classical PI) or a different approach (charge depleting-charge sustaining). The condition can be further improved by improving the tuning of the power electronics components to fit this specific marine application.

Second, the state of charge of the battery reaching the lower limit of 20% is an indicator that the capacity of the battery should be increased or the battery power used in a more efficient way. Increasing the number of fuel cells or allow them to work in high degradation area, is also possible to ensure a certain amount of extra power in case there is a variation in the meteorological conditions or a change in route due to maritime traffic on the crossing route. The increase of the initial battery state of charge is also a possibility that can be considered if it is possible to recharge the ferry at the departure dock. Effects on the initial SOC on the entire day of operation can be carried out using the model and extending the time interval analyzed.

It is also possible to continue the fine-tuning process of the control system and the EMS to reduce the mean square error and eliminate the delivery of excess battery power, during the crossing phase.

All these improvements are a base for further development of the model, towards the optimal power-plant configuration that ensures flexibility and stable power output.

Discussion

The model

The development of a mathematical model, in digital form, representing a hybrid power-plant operating using PEMFC and batteries, serves multiple purposes during both research activity and during the design of new zero-emission maritime vessels.

To research the effects of component sizing in relation to the energy management system and vice versa, for a fuel cell driven ship, it is required to have a fuel cell model, a battery model, a DC grid, and an EMS block all in the same digital environment. This allows the components to interact with each other, simulating the behavior or the powerplant when real-world data is given as input.

Using the model presented in this paper, it is possible to study the behavior of different power-plant configurations and control strategies in relation to factors such as power demand, route length, and hydrogen consumption. The goal of such a model is to further develop the system optimization process through computational resources.

The results produced by the model are not only useful to evaluate to the power system performances, but also enable the calculation of key indicators not directly related to power generation. By calculating the number of components required and their rating, it is possible for maritime design researchers to estimate the size of the engine room, housing the hybrid system, and the relative weight of this configuration. The hydrogen consumption value can be used to calculate the size of the hydrogen tanks and the space required for storage in relation to the route length.

In the industry, a tool to quickly evaluate the behavior of a certain size fuel cell or battery when introduced into the system can allow for a faster design phase. Engineers tasked with the dimensioning problem can test different configuration and their response to energy management strategies to better satisfy their clients.

The model is built to be flexible, adapting to different marine power-plant configurations between 1 and 10 MW. Flexibility is a key attribute for such a model, as fuel cell propulsion in the maritime industry is not a mature technology therefore a tool to quickly evaluate the technical feasibility of the solution is most effective if it can be adapted to multiple vessel classes and sizes.

The presented case study can be considered a demonstration of the capabilities of such a model with future developments being considered in the areas of the energy management and control. Optimization of the computational resources is also a priority, as a faster simulation allows for more configuration and strategies to be tested, or longer operational intervals to be considered.

Last, it is also possible to use this model as a basis to include more specific fuel cell or battery models, which contain aging or temperature effects, in order to get a complete picture over the operational life of the fuel cell, battery or power electronics components.

The zero-emission solution for the ferry

The transition to hybrid systems allows companies and ship operators to meet the goals set by the UN and IMO for emissions and greenhouse gas control.

The configurations presented for the ferry, while merely being a first attempt solution which can be further optimized both from a sizing perspective and an energy management perspective, would allow for a significant reduction of NO_x, HC and CO emitted in the proximity of the two ports of departure and arrival. There are also benefits on the global scale, give a reduction of CO_2 levels introduced into the atmosphere. The elimination of diesel gen-sets operating at low thermal efficiency during Roll-on/Roll-off operations introduces an area where fuel savings become relevant if considering that the operation is carried out 18 times a day, every day of the year. With the technical feasibility of the solution evaluated via the case study, it is possible to assess the economical feasibility with the ship operator, taking into consideration the average cost of ownership and the possible return on investment for the new hybrid solution.

Conclusion

The creation of a digital representation of a maritime hybrid power-plant equipped with PEM fuel cells and battery can aid in the design process of new, zero-emission hydrogen vessels or the retrofitting operation for diesel electric ships.

In this paper, a diesel-electric ferry was used for reference. The power output of the diesel-electric plant becomes, in this model, the power demand for the hybrid system. Using a series of real-time data, in conjunction with a set of dynamic models representing the physical components of the hybrid system in the software environment, it is possible to output a series of data that can help analyze the behavior of the hybrid system. The comparison between the operational profile and the power demand helps validate the size and power rating of the components chosen for the power-plant. The behavior is to be considered satisfactory if the mean square error between the power provided and the power demand is below a certain threshold set by the user. The mean square error also provides a reference for future improvements of the hybrid system or the energy management strategy.

The model also produces a graph representing the state of charge of the battery over time. This graph can aid in the evaluation of the battery capacity and let the user observe the behavior of the energy storage.

An estimated hydrogen consumption value is produced according to the model by Njoya et al. [34]. This enables the evaluation of important factors such as running costs for the ferry. Maintenance can also be planned according to the degradation value calculated taking into consideration the operation of the PEM fuel cell.

The model has been created as a design tool, but also as a platform for future development. Testing of different energy management strategies for the optimization of factors such as hydrogen consumption, fuel cell or battery degradation can be carried out on this digital model with just a few changes. The ultimate goal is to promote the development of zero emission energy solution for the maritime environment. Such solution aids in the reduction of greenhouse gas emissions and pollutants to help mitigate the impact of maritime traffic and coastal communities.

Declaration of competing interest

The authors declare that they have no known competing financial interests or personal relationships that could have appeared to influence the work reported in this paper.

Acknowledgment

This work is supported by The Research Council of Norway trough project number 90436501. The project is headed by Institute for Energy Technology (IFE) in Kjeller, Norway, and this work package is developed at the Department of Marine Technology of the Norwegian University of Science and Technology (NTNU) in Trondheim, Norway.

REFERENCES

[1] Conte FV. Battery and battery management for hybrid electric vehicles: a review. E I Elektrotechnik Inf October 2006;123(10):424–31.
[2] Yuan Yupeng, Wang Jixiang, Yan Xinping, Shen Boyang, Long Teng. A review of multi-energy hybrid power system for ships. Renew Sustain Energy Rev 2020;132:110081.
[3] Hirose H, Yoshida K, Shibanuma K. Development of catenary and storage battery hybrid train system. In: 2012 electrical systems for aircraft, railway and ship propulsion; 2012. p. 1–4.
[4] Zhu J, Li C, Bin W, Lijuan X. Optimal design of a hybrid electric propulsive system for an anchor handling tug supply vessel. Appl Energy 2018;226:423–36.
[5] Kifune H, Nishio T. Fuel savings effect of hybrid propulsion system – case: tugboat is not in service. J JIME 2005;52(6):7.
[6] Kifune H, Asada Y, Nishio T. Fuel sauvings effect of hybrid propulsion system – case: tugboat is on service. J JIME 2005;53(2):7.
[7] Geertsma RD, Negenborn RR, Visser K, Hopman JJ. Design and control of hybrid power and propulsion systems for smart ships: a review of developments. Appl Energy 2017;194:30–54.
[8] Oudalov A, Cherkaoui R, Beguin A. Sizing and optimal operation of battery energy storage system for peak shaving application. In: 2007 IEEE lausanne power tech; 2007. p. 621–5.
[9] The United Nations. Unsustainable Development Goals. Goal 14: conserve and sustainably use the oceans, seas and marine resources. 2020. 04 2020, https://www.un.org/sustainabledevelopment/oceans/.
[10] The International Maritime Organization. Initial imo strategy on reduction of ghg emission from ships. Annex 11. Resol MEPC 04 2018;304(72).
[11] Lu Languang, Han Xuebing, Li Jianqiu, Hua Jianfeng, Ouyang Minggao. A review on the key issues for lithium-ion

battery management in electric vehicles. J Power Sources 2013;226:272–88.
[12] Xu B, Oudalov A, Ulbig A, Andersson G, s Kirschen D. Modeling of lithium-ion battery degradation for cell life assessment. IEEE Tras Smart Grid 06 2016;99(1–1).
[13] Karimi S, Zadeh M, Suul JA. Evaluation of energy transfer efficiency for shore-to-ship fast charging systems. In: 2020 IEEE 29th international symposium on industrial electronics. ISIE); 2020. p. 1271–7.
[14] NCE Maritime Cleantech. Norwegian parliament adopts zero-emission regulations in the fjords. Marie Launes; 05 2018.
[15] Emission reduction in shipping using hydrogen and fuel cells. In: Ocean renewable energy of international conference on offshore mechanics and arctic engineering, vol. 10; 06 2017. V010T09A011.
[16] Product datasheet ballard fcwave. https://www.ballard.com/docs/default-source/default-document-library/fcwavetm-specification-sheet.pdf?sfvrsn=6e44dd80_2. [Accessed 30 September 2020].
[17] Gerstl P, Østvik I, Skår F. Building the first hydrogen-electric ferry. Maritime hydrogen and marine energy, 2019. 09 2019. Florø, https://static1.squarespace.com/static/5d1c6c223c9d400001e2f407/t/5d84d4a8f6cdad589e229490/1568986292274/Norled.pdf.
[18] Bassam AM, Phillips AB, Turnock SR, Wilson PA. Development of a multi-scheme energy management strategy for a hybrid fuel cell driven passenger ship. Int J Hydrogen Energy 2017;42(1):623–35.
[19] Feroldi D, Serra M, Riera J. Energy management strategies based on efficiency map for fuel cell hybrid vehicles. J Power Sources 2009;190(2):387–401.
[20] Cai Q, Brett DJL, Browning D, Brandon NP. A sizing-design methodology for hybrid fuel cell power systems and its application to an unmanned underwater vehicle. J Power Sources 2010;195(19):6559–69.
[21] Jens KN, Asbjørn K, Claus HC, Tejs V. Ammonia for hydrogen storage: challenges and opportunities. J Mater Chem 2008;1(18):2304–10. https://doi.org/10.1039/B720020J.
[22] Makepeace Joshua W, Teng He, Weidenthaler Claudia, Jensen Torben R, Chang Fei, Vegge Tejs, et al. Reversible ammonia-based and liquid organic hydrogen carriers for high-density hydrogen storage: recent progress. Int J Hydrogen Energy 2019;44(15):7746–67 [A special issue on hydrogen-based Energy storage].
[23] Preuster P, Papp C, Wasserscheid P. Liquid organic hydrogen carriers (LOHCs): toward a hydrogen-free hydrogen economy. Acc Chem Res January 2017;50(1):74–85.
[24] von Colbe Jose Bellosta, Ares Jose-Ramón, Barale Jussara, Baricco Marcello, Buckley Craig, Capurso Giovanni, et al. Application of hydrides in hydrogen storage and compression: achievements, outlook and perspectives. Int J Hydrogen Energy 2019;44(15):7780–808 [A special issue on hydrogen-based Energy storage].
[25] Dynamically generated map from google maps; directions from spodsbjerg færgehavn to tars. https://bit.ly/3ginHjM. [Accessed 12 July 2020].
[26] Stig E, Marie L, Jensen JB, Sørensen J. Improving the energy efficiency of ferries by optimizing the operational practices. In: Proceedings of the full scale ship performance conference 2018. The Royal Institution of Naval Architects; October 2018. p. 101–11. null ; Conference date: 24-10-2018 Through 25-10-2018.
[27] Ashrafur Rahman SM, Masjuki HH, Kalam MA, Abedin MJ, Sanjid A, Sajjad H. Impact of idling on fuel consumption and exhaust emissions and available idle-reduction technologies for diesel vehicles – a review. Energy Convers Manag 2013;74:171–82.
[28] Paster MD, Ahluwalia RK, Berry G, Elgowainy A, Lasher S, McKenney K, Gardiner M. Hydrogen storage technology options for fuel cell vehicles: well-to-wheel costs, energy efficiencies, and greenhouse gas emissions. Int J Hydrogen Energy 2011;36(22):14534–51. Fuel Cell Technologies: FUCETECH 2009.
[29] van Biert L, Godjevac M, Visser K, Aravind PV. A review of fuel cell systems for maritime applications. J Power Sources 2016;327:345–64.
[30] Veziroglu A, Macario R. Fuel cell vehicles: state of the art with economic and environmental concerns. Int J Hydrogen Energy 2011;36(1):25–43.
[31] Hu Z, Li J, Xu L, Song Z, Fang C, Ouyang M, Dou G, Kou G. Multi-objective energy management optimization and parameter sizing for proton exchange membrane hybrid fuel cell vehicles. Energy Convers Manag 2016;129:108–21.
[32] Kim M-J, Peng H. Power management and design optimization of fuel cell/battery hybrid vehicles. J Power Sources 2007;165(2):819–32. IBA – HBC 2006.
[33] Schølberg I, Balestra L. Study on the architecture of a zero emission hydrogen fuel cell vessel power generating unit. ASME 2020 39th international conference on ocean. Offshore and Arctic Engineering; 08 2020.
[34] M SN, Tremblay O, Dessaint L. A generic fuel cell model for the simulation of fuel cell vehicles. In: 2009 IEEE vehicle power and propulsion conference; 2009. p. 1722–9.
[35] Fletcher T, Thring R, Watkinson M. An energy management strategy to concurrently optimise fuel consumption & pem fuel cell lifetime in a hybrid vehicle. Int J Hydrogen Energy 2016;41(46):21503–15.
[36] Tremblay O, Dessaint Louis-A. Experimental validation of a battery dynamic model for EV applications. World Elec Vehicle J June 2009;3(2):289–98.
[37] Zhu C, Li X, Song L, Xiang L. Development of a theoretically based thermal model for lithium ion battery pack. J Power Sources February 2013;223:155–64.
[38] Basic calculation of a boost converter's power stage. https://www.ti.com/lit/an/slva372c/slva372c.pdf. [Accessed 7 December 2020].

PAPER III

Proceedings of the ASME 2021 40th International Conference on Ocean, Offshore and Arctic Engineering
OMAE2021
June 21-30, 2021, Virtual, Online

OMAE2021-60451

TOWARDS SAFETY BARRIER ANALYSIS OF HYDROGEN POWERED MARITIME VESSELS

Lorenzo Balestra,* Ruochen Yang, Ingrid Schjølberg, Ingrid B. Utne
Department of Marine Technology
Norwegian University of Science and Technology, NO-7491, Trondheim, Norway

Øystein Ulleberg
Institute for Energy Technology, 2007 Kjeller, Norway

ABSTRACT

This paper focuses on the use of safety barrier analysis, during the design phase of a vessel powered by cryogenic hydrogen, to identify possible weaknesses in the architecture. Barrier analysis can be used to evaluate a series of scenarios that have been identified in the industry as critical. The performance evaluation of such barriers in a specific scenario can lead to either the approval of the design, if a safety threshold is met, or the inclusion of additional barriers to mitigate risk even further. By conducting a structured analysis, it is possible to identify key barriers that need to be included in the system, intended both as physical barriers (sensors, cold box) and as administrative barriers (checklist, operator training). The method chosen for this study is the Barrier and Operational Risk Analysis (BORA) method. This method, developed for the analysis of hydrocarbon releases, is described in the paper and adapted for the analysis of cryogenic hydrogen releases. A case study is presented using the BORA method, developing the qualitative barrier analysis. The qualitative section of the method can be easily adapted to vessels of different class and size adopting the same storage solution. The barrier analysis provides a general framework to analyze the system and check that the safety requirements defined by the ship operator and maritime certification societies are met.

*Address all correspondence to this author.

NOMENCLATURE

BBD	Barrier block diagram
BORA	Barrier and operational risk analysis
CNG	Compressed natural gas
FTA	Fault Tree Analysis
GHG	Greenhouse gas
LNG	Liquified natural gas
O&G	Oil and Gas
RID	Risk influencing diagram
RIF	Risk influencing factors
TCS	Tank connection space

INTRODUCTION

In recent years, a strong environmental consciousness has developed in industry, government and society. New plans have been put into action to reduce emissions along shipping routes and in smog choked coastal cities. The UN Sustainability Development Goal number 14 calls for reduced emissions in the oceans, and new commitments by the International Maritime Organization aim to reduce of 50% Greenhouse Gas emissions by 2050 with respect to 2008 levels [1]. Emissions control can also be used to preserve natural sites. In Norway, the aspiration of the government is to have an emission-free zone in its world heritage Fjords no later than 2026 [2]. This means that finding a carbon-free energy carrier that can deliver similar

performances to fossil fuels is now a priority for the maritime industry.

The use of hydrogen could provide a carbon-free alternative to ship operators without sacrificing range and flexibility. Fuel cell systems can provide a long range zero-emission solution for vessels that cannot be operated on just batteries due to range limitations. The use of hydrogen as an energy carrier not only would diminish harmful emissions, but would also reduce the risk of spillage of harmful hydrocarbons in the sea in case of vessel damage. Hydrogen reserves can be replenished using off-peak power produced by renewable energy, but there are a series of challenges to be overcome regarding safety. Designing hydrogen systems is non-trivial when factoring in the low density, wide flammability range and low ignition energy. The physical and chemical behaviour of gaseous hydrogen and cryogenic hydrogen has always proven to be a critical factor for manufacturers willing to develop transport systems using this energy carrier.

Defining a framework that engineers can use during the design of a hybrid hydrogen vessel to systematically identify critical safety issues is of the utmost importance. For this task, this paper considers on an established methodology from the Oil & Gas (O&G) industry, the Barrier and Operational Risk Analysis (BORA-Release method) method. This method is applied for identification, investigation and performance evaluation of safety barriers. In this paper, the method is used to identify and investigate barriers related to the storage of cryogenic hydrogen on-board a vessel and how these may fail. The method's structure includes a qualitative part, used to identify weaknesses in the vessel's architecture, and a quantitative part, used to quantify the performance of the barriers by calculating the new frequency of the initiating event and the probability of barriers failure using collected data. In presented work the focus is on the qualitative part that can be used as the basis for further developments including the formulation of Bayesian networks, and the organization of workshops for the classification of critical scenarios and the evaluation of scores assigned to dangerous system or organizational failures.

Following the definition of the BORA method, a case study is developed considering the release of cryogenic hydrogen below deck. The case study investigates which safety barriers could be put in place for this specific scenario and their effectiveness. The safety barriers are defined according to the numerous studies developed on the topic [3–5]. The main goal is to contribute to the development of hydrogen systems in the maritime industry and provide a valid tool for ship designers and engineers in the design phase of fuel cell hybrid vessels.

HYDROGEN MARITIME SAFETY

Technical business services organisations and maritime classification societies are formulating a series of standards and regulation for hydrogen powered vessels. These standards are created from the ground up as there is no real precedent for applications, in the megawatt range, of hydrogen in the maritime industry. It is also not possible to use the same standards used for LNG or CNG due to the different physical and chemical differences with hydrogen. The standards to ensure the safe transportation of passengers and goods are being developed in cooperation with the companies that aim to sail hydrogen vessels as soon as 2023. An example would be the project for the Norled ferry [6] in Norway and the Flagship Project [7] in France.

Among the published studies on concept risk assessments related to fuel cell vessels, it is possible to find the studies of Aarskog et al. [8] and Klebanoff et al. [9]. These studies offer an insight into the applications of fuel cells for maritime transport, focusing on fast passenger vessels equipped with power-plants in the range of 500 kW and high pressure gas hydrogen storage above deck. Placing the hydrogen pressure vessels above deck is the safest solution, using natural ventilation to disperse the gas, as demonstrated by Aarskog, complying with the general regulations from the International Code of Safety for Ships Using Gases or Other Low Flash-point Fuels [10].

Comprehensive studies on larger vessels, like double ended ferries or coastal cargo ships in the 5 to 10 MW power range, still need to be fully developed. In these cases, a below-deck storage solution might be dictated by weight distribution and footprint usage constrains. Below deck storage introduces a series of specific scenarios, with more complex dynamics than the on-deck storage solutions, that it is possible to analyze systematically with the method presented in this paper. When considering below deck storage, a series of studies has been reviewed to account for the differences between cryogenic hydrogen and LNG. For scenarios of vented and dispersed hydrogen due to tank overpressure, the studies of S.B. Dorofeev [11] and Gavelli et al. [12] enable the definition of how the dispersion of the gas should be carried out to avoid creating dangerous conditions. The dispersion technique and conditions heavily influences the design of the vessel as dedicated ventilation passages, like a mast riser, needs to be integrated in the vessel's structure. The release of cryogenic hydrogen, generated from tank rupture or valve leakage, has been analyzed by O. Hansen [13] in his studies focusing on hydrogen dense gas behaviour. In Hansen's study, multiple computational fluid dynamics models show the influence of wind and humidity when hydrogen is released and vented through the mast riser of a large vessel. The paper also confirms how safety barriers put into place by the industry for LNG are not sufficient for hydrogen-based solutions. The studies from Giannissi [14] and Hall et al. [15] also provide a valuable insight in the risk assessment of vessels operating with liquid hydrogen as they model dispersion conditions and ignition in various scenarios, in closed and semi enclosed spaces.

SAFETY BARRIER DEFINITION

Haddon [3] defines safety barriers as the measures taken to separate, in space or time, a possible victim from the sudden release of energy originating from a uncontrolled source. These measures can be considered as tangible asset of the system or can include operational and administrative measures. For Johnson [4], a barrier consists of the physical methods to direct energy in wanted channels and control unwanted releases, while Larsson [5] states that the definition of barrier can be expanded to include not only physical measures but also administrative measures, such as procedures and work permit systems. According to Sklet [16], including both physical and/or non-physical means planned to prevent, control or mitigate undesired events or accidents, gives us an improved likelihood of identifying the most weaknesses in a system. Following Sklet's guidelines and Larsson's definition, in this paper, the process of barrier identification is carried out considering both physical and administrative measure. This allows a more comprehensive analysis of the system.

A classification has to be made between proactive barriers and reactive barriers [17]. Reactive barriers are included in the system to respond to already occurred critical events. Proactive barriers act to prevent the dangerous circumstance by triggering appropriate countermeasures. Proactive and reactive barriers are both implemented in complex systems, as the prevention of the critical event is not always possible, and reactive barriers need to step in and control the consequences of previous barriers failure. A key factor to consider in safety barrier analysis is not just the identification of the barriers but also the definition of their interaction. The idea is that barriers are arranged in a multi-layer configuration to ensure avoidance, prevention, control and protection against unexpected dangerous scenarios [18]. Even if one, or more barriers, fail due to latent conditions or active failure measures, the energy release encounters immediately another barrier to control the situation.

Many sectors dealing with complex systems, from a technical and organizational point of view, have examined critical scenarios and accidents with methods based on safety barrier analysis, creating numerous effective applications of this theory [19–21].

BORA METHOD APPLICATIONS FOR HYDROGEN SAFETY

The choice of the method to conduct the barrier analysis for hydrogen release scenarios was carried out in light of the inherent dangerous nature of the fuel and the system's complexity. The Barrier and Operational Risk Analysis (BORA) Release method [22], proves to be fitting our requirements, as it provides to be a solid framework divided in 8 steps to calculate the risk of specific energy release scenarios and identify possible "weak links" in the organization from a safety point of view.

1. **Method fundamentals**: Definition of the boundary condition for the study with respect to a specific scenario. In this case, the section will include physical and chemical properties of the hydrogen, a literature review on the system's components, information on the vessel taken into consideration, etc.
2. **Barrier Block Diagram (BBD)**: This step consists of three actions: (1) Identification of the initiating event for the considered scenario, (2) definition of the barriers implemented to deal with the given initiating event, (3) definition of the outcome in case of barrier success or failure in containing the release of energy. Once identified all the elements it is possible to plot the BBD following the guidelines from the original BORA method.
3. **Risk Influencing Diagram (RID)**: In the risk influencing diagrams are collected the possible factors that lead to the initiating event. These factors can be technical or operational.
4. **Barrier performance evaluation**: In this steps, a fault tree analysis (FTA) is created for each one of the barriers identified in Step 2.
5. **Frequency of initiating event**: Assigning a industry average probability/frequency to the initiating event for the final calculation of the scenario specific risk.
6. **Scoring and Weighting of risk influencing factors (RIFs)**: for the final calculation of the scenario specific risk.
7. **Adjustment of industry average probabilities / frequencies**: By creating a table with the industry average probabilities/frequencies, scores and weights of RIF, it is possible to revise the probabilities/frequencies before starting with the calculation
8. **Calculation of the risk** in order to determine the scenario specific risk.

The steps indicated above can be developed for each single scenario that is deemed critical or a source of possible risk. In this paper, the aim is to focus on the qualitative section of the method (step 1 to 4), laying down the basis for the adaptation of the BORA method to hydrogen. Further steps (from 5 to 8) are developed at a later stage as they are tied to the specific vessel design and require the formulation of extensive Bayesian network and expert validation through workshops.

To limit the study in this paper, the case presented analyzes one scenario in relation to the on-board storage of cryogenic hydrogen and its release below deck. The release event conditions and safety barriers choice derives from both literature review on the state-of-the-art of hydrogen behaviour, and from experts interviews. The experts opinions was provided by maritime certification experts with over 20 years of experience and have been collected during the Florø 2019 Conference on Maritime Hydrogen & Marine Energy and at the

Annual H2 Team Workshop of NTNU.
The barrier analysis is developed, and the performances are evaluated according to factors such as:

1 - Functionality or effectiveness
2 - Reliability and availability
3 - Response time
4 - Robustness

FTA is included in the paper qualitatively to provide information about how the barriers may fail and what events or components are most critical in terms of causing barrier failure. The last considered step relevant to barrier analysis is the identification of the most important risk factors and the creation of Risk Influence Diagrams. These help to identify technical challenges in case the initiating event is created by a physical component or bad practices in the industry if the event is triggered by human/procedure error.
The following steps, requiring industry data regarding frequency of events and risk calculation, are left out of the paper's scope and can be implemented at a later time in a more comprehensive approach calculating the effective risk of multiple scenarios.

STUDY CASE: BARRIER ANALYSIS FOR ABOVE DECK STORAGE RELEASE SCENARIO

System description

The case study focuses on the scenario considering the release cryogenic hydrogen from a tank placed below deck, in an enclosed space. The use of hydrogen in cryogenic form is justified on vessels equipped with multi-megawatt power-plants where the higher energy density, compared to the compressed form, allows for more operational range.
Cryogenic tanks can be placed below deck when the system is well integrated in the vessel design, combining technical aspects with a safety barrier analysis.
A series of components and structures need to be installed to allow for the safe use of hydrogen in an enclosed space such as a below deck watertight compartment. First, the design needs to include a tank connection space (TCS), which encloses the valving coming from a LH2 tank in a ventilated box. The TCS ventilation is independent from the ventilation of the Fuel Room containing the tanks. The TCS allows for the controlled venting of hydrogen in a controlled space able to withstand cryogenic temperatures. A mast riser, connecting the TCS to the outside environment needs to be installed, allowing for the safe dispersion of hydrogen in atmosphere.
The cryogenic hydrogen experiences boil-off over time as heat exchange with the outside environment happens. The hydrogen turned into gas can be fed to the fuel cell when its pressure is brought to a value compatible with the fuel cell inlet. The excess gas needs to be vented through the mast and dispersed in atmosphere to avoid ignition. The cryogenic hydrogen is turned into gas at a controlled rate and supplied the fuel cell to generate electricity. It is possible to observe the schematics of the system in Figure 1.

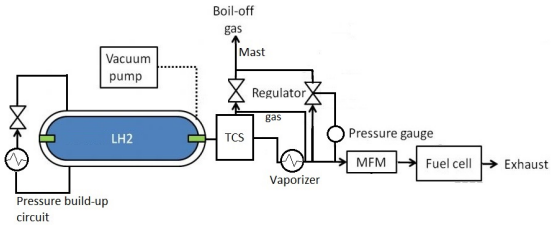

FIGURE 1. System block diagram

The qualitative barrier analysis carried out in this paper is independent on the amount of hydrogen stored on-board. This is due to the fact that hydrogen expands to about 850 times from liquid to gas phase and flammability or explosion limits are reached rapidly even if the quantity leaked is minimal. The interaction between the leaked mass of hydrogen that could reach ignition or explosion limits, and the mass still contained in the tank is not analyzed in this paper.
The case study focuses on the leak of one of the tank valves inside the TCS. While the TCS is a certified component from maritime classification societies, cases where hydrogen is able to escape are a low probability high consequences event that needs to be considered. The escape of hydrogen from the TCS can happen due to improperly sealed connections, or a more catastrophic rupture due to the explosion of the hydrogen inside the TCS.

Qualitative safety barrier analysis

The qualitative safety barrier analysis described in steps one to four of the BORA release method is developed in this section. The goal is to discuss the key elements of the method, the barriers, and their implementation. The focus is on how barriers are determined, how they are included in the barrier block diagram and, finally, how it is possible to investigate their effectiveness. The qualitative analysis from the BORA method provides a generalized analysis for vessels belonging to different sizes, as long as they are equipped with a cryogenic storage method similar to the one described in this paper.
In the considered case, the storage of the cryogenic hydrogen is placed below deck. This case is relevant as many shipyard are considering various locations for the hydrogen tanks to

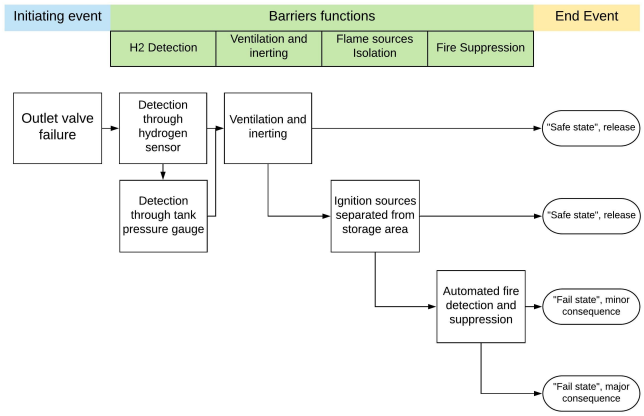

FIGURE 2. Barrier block diagram; scenario "Valve failure due to tank overpressure"

minimize the footprint dedicated to cryogenic storage. The storage of the cryogenic hydrogen is complex and includes multiple valves, piping, heat exchangers and pumps. There is a high number of scenarios that can be analyzed in relation to the system, as the point of possible failure are many. The initiating event considered for this case study is the failure of a valve connected on one side to the TCS and on the other to the vaporizer. This scenario is a high consequences scenario, interesting as in a one-tank configuration all the cryogenic fuel supply passes through the valves contained into the TCS. If hydrogen manages to escape the TCS there is a high likelihood that the limits for an explosive atmosphere are reached in a very short time-span.

With the basic risk model formulated, it is possible to identify the main barriers involved in the considered scenario and build the first BBD. In the BBD the initial event is represented on the left, the barrier functions are represented in the center of the diagram, and in the last column is represented the end event. An horizontal arrow line leading directly to the end event means that the barrier put in place was effective in stopping the threat, leading to an end event, while an arrow line leading to a second barrier function block means that the barrier has failed.

The diagram for the considered scenario can be visualized in Figure 2. The barriers identified as relevant for this scenario fall into the categories of detection, ventilation, isolation and suppression. Two of the indicated barriers are proactive (H2 detection and Flame source Isolation) while the other two are reactive (Fire suppression, ventilation).These four barriers are common to other systems storing cryogenic fuels such as LNG. The difference between the LNG system and the cryogenic hydrogen system lies in how the barriers are implemented. The response time for the hydrogen leak needs to be faster and therefore a sensor able to quickly detect harmful concentration is required. Furthermore the flame source isolation barrier needs to deal with a much wider flammable/explosive concentration range.

Once the barriers have been identified and their order established through the BBD, their performances can be qualitatively investigated. This task can be carried out following the BORA-Release methodology using FTA. The FTA can help analyze the probability that a barrier failure event will occur, identifying a series of factors that have to be taken into consideration when implementing the barrier, such as active or passive redundancy. Figure 3 represents the performances evaluation for the H2 detection barrier, Figure 4 represents the performances of the flame source isolation barrier, Figure 5 is relative to the fire suppression barrier, Figure 6 is relative to the ventilation and inerting barrier. It is possible to observe from the FTA that the barriers can combine both technical and non-technical factors, leading to the barrier failure. This is why a functional approach, as described in the safety barrier definition section, is preferred in this case.

The performances of the hydrogen sensors is dependent on having a constant voltage supplied to the sensor, a good calibration to ensure accuracy and limited noise on the line transmitting the signal. All these factors have to be taken into consideration when implementing this barrier. Hydrogen sensors can today be realized with materials ranging from optical fibers [23] to nano-composite [24], providing a wide range of accuracy, but also different reliability and effectiveness. The detection of hydrogen escaped from the TCS inside the ship's compartment is a critical safety barrier as it has

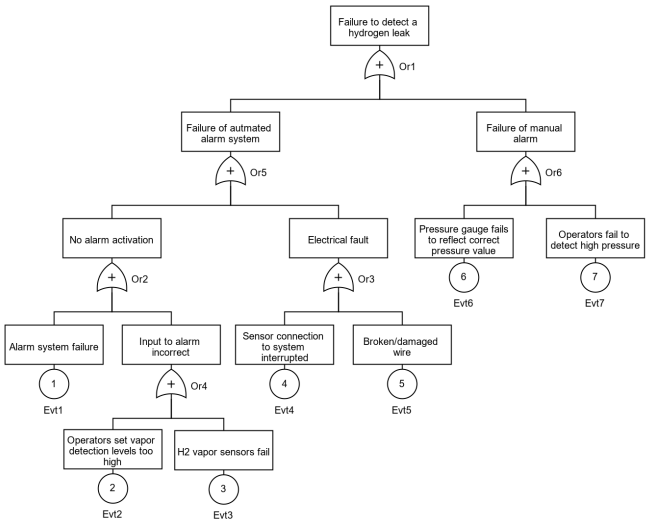

FIGURE 3. Fault tree diagram for H2 Sensor

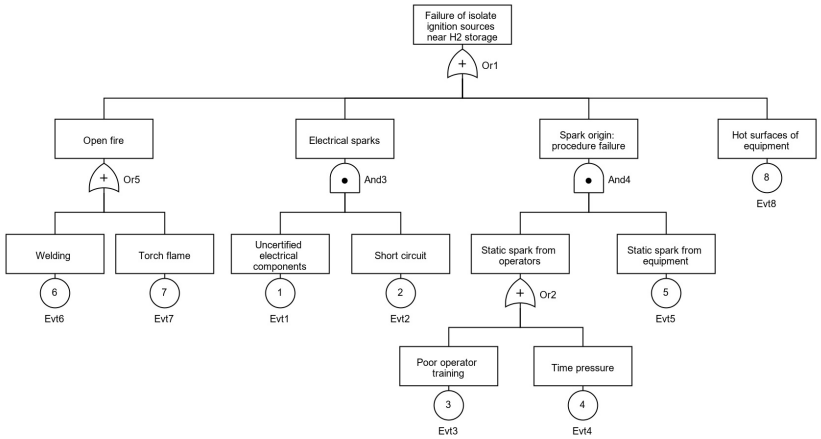

FIGURE 4. Fault tree diagram for flame source isolation

devastating effects if the explosive concentration in air is reached. With optical fibers sensors, depending on both concentration and temperature, detection of concentrations between 1% and 17% with response times shorter than 5 s have been demonstrated [25]. Fast and accurate detection of hydrogen concentrations inferior to the explosive limit is vital to activate the ventilation system and vent the hydrogen to the outside. The release of hydrogen in an enclosed compartment can be also fatal to the crew if undetected, as it may cause asphyxiation. High concentrations of H2 reducing the oxygen level below 19.5% poses a physiological threat to operators that need to evacuate the area.

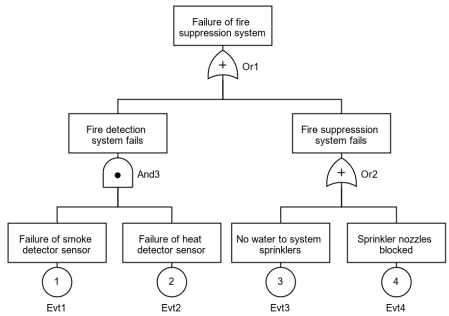

FIGURE 5. Fault tree diagram for fire suppression system

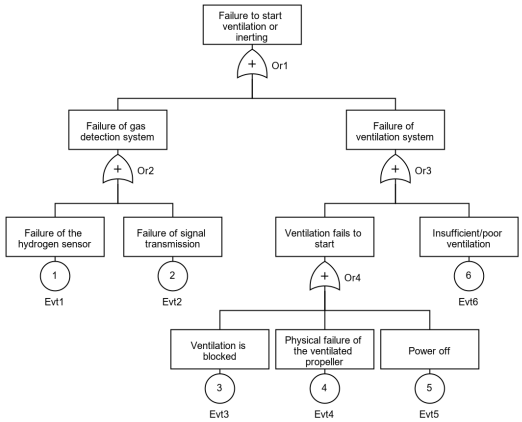

FIGURE 6. Fault tree diagram for ventilation barrier

The second barrier involves ventilation of the compartment in addition to the dedicated ventilation of the TCS. This barrier needs to be implemented taking into consideration the volume of air that needs to be moved considering the effect of buoyancy of the leaked hydrogen in the compartment. The idea is to achieve ventilation producing the 30 room air exchanges required by the U.S. Coast Guard Regulations as safety reference, avoiding strong turbulent flow. References on the interaction of hydrogen releases and ventilation can be found in the work of Cashdollar et al. [26].

The third barrier consists in the isolation of ignition sources (thermal and electrical). This barrier is implemented by avoiding the presence, where the cryogenic storage is located, of equipment that can generate heat or open flames in the compartment or procedures that can generate ignition sources such as sparks. The first solution is defining in the design a safe perimeter or area in which possible electrical sources that could cause sparks or mechanical sources that could cause heat are excluded. This may also include design changes to the routes of pipes carrying steam, hot water or electric cables. Static electricity created by moving objects, water mist, improper storage of polypropylene ropes or operators action could lead also to ignition. Operators should also exercise caution as static discharges from human beings are in the range of 10mJ while the minimum ignition energy for hydrogen is 0.02mJ [9].

The fire suppression barrier is the last resort if the hydrogen is ignited. Hydrogen burns with a colorless flame detectable only from distance with a thermal camera. Hydrogen mixtures ignited at 4% produce very little heat, and flame propagation is almost exclusively upward [9], while at 8% there is a self sustaining fire with propagation in all three directions. Special consideration has to be put into the interaction with the

ventilation system and the fire, as has been done in the work of Peatross et al. [27] for more conventional fuels.
Another problem is the choice of the fire extinguishing agent as spraying simple water onto the fire could cause unwanted reactions with the non-ignited spray or splashing in case of the formation of a pool. A method for extinguishing hydrogen fires comprises introducing to the hydrogen fire a fire extinguishing concentration of heptafluoropropane and maintaining the concentration until the fire is extinguished. The method includes heptafluoropropane at a range of 13-30 % volume/volume in the air. The fire extinguishing methods also include the use of heptafluoropropane in blend with other fire extinguishing compounds [28].
Guidelines on how to implement an efficient fire system can be found more in detail can be found in the studies of Bubbico et al. [29].
The risk influencing diagrams are used to model and enhance the frequency/probability estimations of the top events in the fault trees but can also be used to adjust the initiating event (IE) frequency. In this case the RID is used in a qualitative way and laid out for further quantification of the FTA when the quantitative section is developed. This allows for the assignment in further studies of a score from A to F of the individual factors, influencing the final risk evaluation.
For our initiating scenario are listed:

1 - Technical conditions: H2 Boil-off
2 - Material properties: Seals corrosion or deterioration
3 - Equipment design: Insulation defects
4 - Process complexity: Excessive storage time
5 - Maintainability: System maintanence

The listed factors are represented in Figure 7 in the RID for our specific scenario. It is possible to affirm, even before the assignment of the scores to each factor in the quantitative analysis, that the factor that most heavily influences the probability of the initiating event is H2 Boil-off. This condition is unavoidable with cryogenically stored fuels and is experienced even with the most efficient types of insulation. The Boil-Off problem is a well known challenge in maritime industry and has been extensively explored with LNG [30, 31] even if only part of the knowledge can be transferred due to different physical properties. Other factors have generally an average influence on the initiating event. Excessive storage time, for example, is dictated by time pressure on the operators that can lead to bunker more fuel than needed to save up time during day operations and avoid a second refueling.
With the identification of the risk influencing factors the components of the barrier block diagram presented in Figure 3 have been defined. This, combined with industry realistic scoring/weighting of the factors based on studied release scenarios and an expert assessment on the probability/frequency of the initiating event, should form the core of a the barrier analysis in BORA-Method application for hydrogen releases.

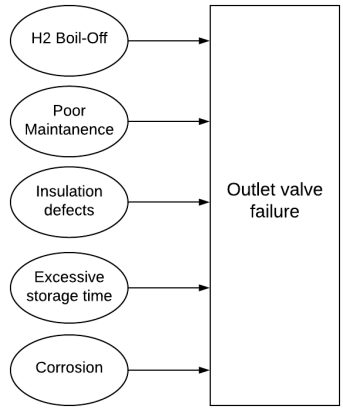

FIGURE 7. Risk influence diagram; scenario "Valve failure due to tank overpressure"

RESULTS AND DISCUSSION

The study case shows that the qualitative section of the BORA-Release method for safety barrier analysis can be used as a valid tool, not only for the release of hydrocarbons, but also for the release of cryogenic hydrogen below deck on a maritime vessel.
This method provides a validated framework to identify and evaluate the safety barriers necessary for the considered scenario. The results of the quantitative safety barrier analysis can aid the design of a vessel powered by cryogenic hydrogen, highlighting measures necessary to reduce the risk of fatal accidents in case of a leak. These measures are identified through fault tree analysis and enclose both technical and administrative aspects. Sensors and physical barriers play a role as important as safety checklists and operators training.
For this specific scenario, the barriers are listed from left to right in the BBD, using the criteria that the more the barrier is placed on the left the less critical are the consequences of its failure. The first barrier, consisting of hydrogen detection, plays a key role in ensuring the safety of the vessel and crew. The second barrier defines the need for a dedicated ventilation system capable of evacuating the flammable gas if detected and avoid reaching explosive concentrations in the storage compartment. The flame source isolation barrier stresses how design choice should meet with the safety concerns for the routing of pipes carrying hot fluid or air and electrical equipment. The fire

suppression system is the last barrier and a key system in the containment of the damage if the worst case scenario is considered, ensuring safe return to port if a fire erupts.
From the RID are observed the main factors influencing the frequency of the initiating event, with this being heavily influenced by the physical nature of the fuel. According to many articles like the studies of Zhang et.al [32] H2 Boil-off is definitively the most influencing factor as the pressure build up creates stress on components like valves. Cryogenic storage not only produces stress due possible overpressure but also weakening of the seals due to extreme temperature [33] and therefore creating a maintanence problem. This should be a focus point for designers of the system.
Overall it is possible to say that the qualitative barrier analysis through the BORA-Release method presents itself as a promising approach for the further study of scenarios related to vessels powered by hydrogen or including a hydrogen storage. The quantitative study can be developed following the considerations made in this paper, assigning numerical scores in relation to the probability of certain events and calculating the improvements that the identified barriers bring.

CONCLUSION

The adapted qualitative barrier analysis framework is an effective way to visualize possible technical or procedural weaknesses in the design of a vessel powered by cryogenically stored hydrogen. Once identified, through consolidated tools like barrier block diagrams and fault tree analysis, it is possible to correct them and obtain a robust design. The case study presented is relative to a key topic in the maritime industry: below-deck storage of cryogenic hydrogen.
A simplified analysis related to hydrogen detection, ventilation, flame source isolation and fire suppression system has been carried out. The qualitative analysis of the method provides a base case study, which it possible to further develop with a quantitative analysis using industry data and assigning numerical scores to barrier performance in workshops with system experts.
In general, the development of protocols and method to evaluate the safety of hydrogen solutions in the maritime industry can help make this zero-emission energy carrier more widespread and ensure that passengers and crew members can travel safely both in domestic water and on oceanic routes.

References

[1] The International Maritime Organization. Initial imo strategy on reduction of ghg emission from ships. Annex 11, Resolution MEPC,304(72), 04 2018.

[2] NCE Maritime Cleantech. Norwegian parliament adopts zero-emission regulations in the fjords. https://whc.unesco.org/en/news/1824#:~:text=The%20Norwegian%20Parliament%20has%20adopted,zero%20emission%20zones%20at%20sea., 05 2018.

[3] R. Rosness; G. Guttormsen; T. Steiro; R. K. Tinmannsvik; I. A. Herrera. Organisational accidents and resilient organisations: Five perspectives. SINTEF Industrial Management Safety and Reliability, shorturl.at/wAOP6, 01 2004.

[4] W. G. Johnson. Mort safety assurance systems. National Safety Council, EditorNew York, NY, Marcel Dekker, Incorporated, ISBN 0598026924, 9780598026927, 04 1980.

[5] Tore J. Larsson. Investigating accidents and reducing risks—a dynamic approach (kjellén and larsson, 1981); its relevance for injury prevention. *Safety Science*, 16(3):439 – 443, 1993.

[6] P. Gerstl I. Østvik, F. Skår. Building the first hydrogen-electric ferry. Maritime hydrogen and marine energy, 2019, Florø, https://static1.squarespace.com/static/5d1c6c223c9d400001e2f407/t/5d84d4a8f6cdad589e229490/1568986292274/Norled.pdf, 09 2019.

[7] L. Grand-Clement. Flagships - eu hydrogen vessel project. Maritime hydrogen and marine energy, 2019, Florø, https://static1.squarespace.com/static/5d1c6c223c9d400001e2f407/t/5d84d4cffe1b1832273f0525/1568986325254/Flagships+-+EU+Hydrogen+Vessel+Project%2C+Laurence.pdf, 09 2019.

[8] Fredrik G. Aarskog, Olav R. Hansen, Trond Strømgren, and Øystein Ulleberg. Concept risk assessment of a hydrogen driven high speed passenger ferry. *International Journal of Hydrogen Energy*, 45(2):1359–1372, January 2020.

[9] L.E. Klebanoff, J.W. Pratt, and C.B. LaFleur. Comparison of the safety-related physical and combustion properties of liquid hydrogen and liquid natural gas in the context of the SF-BREEZE high-speed fuel-cell ferry. *International Journal of Hydrogen Energy*, 42(1):757–774, January 2017.

[10] International Maritime Organization (IMO). The international code of safety for ships using gases or other low-flashpoint fuels. https://www.register-iri.com/wp-content/uploads/MSC_Resolution_39195.pdf, 06 2015.

[11] S.B. Dorofeev. Evaluation of safety distances related to unconfined hydrogen explosions. *International Journal of Hydrogen Energy*, 32(13):2118 – 2124, 2007. ICHS-2005.

[12] F. Gavelli; O.R. Hansenl; S. G. Davis; P. Middha. Equivalent cloud methods used for explosion risk and consequence studies. *Journal of Loss Prevention in the Process Industries*, 26(3):511 – 527, 2013. Papers presented at the 2011 Mary Kay O'Connor Process Safety Center International Symposium.

[13] O.R. Hansen. Liquid hydrogen releases show dense gas behavior. *International Journal of Hydrogen Energy*, 2019.

[14] S.G. Giannissi and A.G. Venetsanos. Study of key parameters in modeling liquid hydrogen release and dispersion in open environment. *International Journal of Hydrogen Energy*, 43(1):455 – 467, 2018.

[15] J.E. Hall, P. Hooker, and D. Willoughby. Ignited releases of liquid hydrogen: Safety considerations of thermal and overpressure effects. *International Journal of Hydrogen Energy*, 39(35):20547 – 20553, 2014.

[16] Snorre Sklet. Safety barriers: Definition, classification, and performance. *Journal of Loss Prevention in the Process Industries*, 19(5):494 – 506, 2006.

[17] G.E. Scarponi, N. Paltrinieri, F. Khan, and V. Cozzani. Chapter 7 - reactive and proactive approaches: Tutorials and example. In Nicola Paltrinieri and Faisal Khan, editors, *Dynamic Risk Analysis in the Chemical and Petroleum Industry*, pages 75 – 92. Butterworth-Heinemann, 2016.

[18] C. Delvosalle, C. Fievez, A. Pipart, and B. Debray. Aramis project: A comprehensive methodology for the identification of reference accident scenarios in process industries. *Journal of Hazardous Materials*, 130(3):200 – 219, 2006. Outcome of the ARAMIS Project: Accidental Risk Assessment Methodology for Industries in the Framework of the SEVESO II Directive.

[19] Luning Xue, Jianchun Fan, Marvin Rausand, and Laibin Zhang. A safety barrier-based accident model for offshore drilling blowouts. *Journal of Loss Prevention in the Process Industries*, 26(1):164 – 171, 2013.

[20] L. J. Kecklund, A. Edland, P. Wedin, and O. Svenson. Safety barrier function analysis in a process industry: A nuclear power application. *International Journal of Industrial Ergonomics*, 17(3):275 – 284, 1996.

[21] J.E. Vinnem, T. Aven, S. Hauge, J. Seljelid, and G. Veire. Integrated barrier analysis in operational risk assessment in offshore petroleum operations. In Cornelia Spitzer, Ulrich Schmocker, and Vinh N. Dang, editors, *Probabilistic Safety Assessment and Management*, pages 620–625, London, 2004. Springer London.

[22] T. Aven S. Sklet and J. E. Vinnem. Barrier and operational risk analysis of hydrocarbon releases (bora-release): Part i. method description. *Journal of Hazardous Materials*, 137(2):681 – 691, 2006.

[23] M. A. Butler. Micromirror optical-fiber hydrogen sensor. *Sensors and Actuators B: Chemical*, 22(2):155 – 163, 1994.

[24] K. Anand, O. Singh, M. Pal Singh, J. Kaur, and R. Chand Singh. Hydrogen sensor based on graphene/zno nanocomposite. *Sensors and Actuators B: Chemical*, 195:409 – 415, 2014.

[25] X Bévenot, A Trouillet, C Veillas, H Gagnaire, and M Clément. Hydrogen leak detection using an optical fibre sensor for aerospace applications. *Sensors and Actuators B: Chemical*, 67(1):57 – 67, 2000.

[26] K.L. Cashdollar, I.A. Zlochower, G.M. Green, R.A. Thomas, and M. Hertzberg. Flammability of methane, propane, and hydrogen gases. *Journal of Loss Prevention in the Process Industries*, 13(3):327 – 340, 2000.

[27] C. Beyler M.J. Peatross. Ventilation effects on compartment fire characterization. *Fire Safety Science*, 5:403–414, 01 1997.

[28] J.S. Rubacha M.L. Robin, C.J. Mazac. Method for the suppression of hydrogen fires. WO1996034661A1 Patent, 09 1996.

[29] R. Bubbico, S. Lee, D. Moscati, and N. Paltrinieri. Dynamic assessment of safety barriers preventing escalation in offshore oil&gas. *Safety Science*, 121:319 – 330, 2020.

[30] I. A. Karimi M.M. Faruque Hasan, Alfred Minghan Zheng. Minimizing boil-off losses in liquefied natural gas transportation. *Industrial & Engineering Chemistry Research*, 48(21):9571–9580, 2009.

[31] I. Komar Đ. Dobrota, B. Lalić. Problem of boil - off in lng supply chain. *Transactions on Maritime Science*, 02:91–100, 10 2013.

[32] J. Zhang, T.S. Fisher, P. Ramachandran, J.P. Gore, and I. Mudawar. A Review of Heat Transfer Issues in Hydrogen Storage Technologies. *Journal of Heat Transfer*, 127(12):1391–1399, 08 2005.

[33] H-P Weise, H Kowalewsky, and R Wenz. Behaviour of elastomeric seals at low temperature. *Vacuum*, 43(5):555 – 557, 1992.

PAPER IV

INTERNATIONAL JOURNAL OF HYDROGEN ENERGY 46 (2021) 38490–38503

Available online at www.sciencedirect.com

ScienceDirect

journal homepage: www.elsevier.com/locate/he

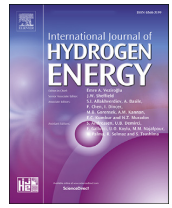

Energy management strategies for a zero-emission hybrid domestic ferry

Lorenzo Balestra[*], *Ingrid Schjølberg*

Department of Marine Technology, Norwegian University of Science and Technology, NO-7491, Trondheim, Norway

ARTICLE INFO

Article history:
Received 21 May 2021
Received in revised form
8 September 2021
Accepted 9 September 2021
Available online 8 October 2021

Keywords:
Hydrogen
Fuel cell
Hybrid propulsion
Digital model

ABSTRACT

The paper presents three approaches for the sizing and control of a maritime hybrid power-plant equipped with proton exchange membrane fuel cells and batteries. The study focuses on three different power-plant configurations, including the energy management strategy and the power-plant component sizing. The components sizing is performed following the definition of the energy management strategy using the sequential optimization approach. These configurations are tested using a dynamic model developed in Simulink. The simulations are carried out to validate the technical feasibility of each configuration for maritime use. Each energy management strategy is developed to allow for the optimization of a chosen set of parameters, such as hydrogen consumption and fuel cell degradation. It is observed that in the hybrid power-plant optimization there are always trade-offs, and the optimization should be carried out by prioritizing primary factors the ship owner considers most important for day-to-day operations.

Introduction

Modern maritime transport is still heavily reliant on fossil fuels, including diesel and heavy oils, containing high levels of asphalt, carbon residues, sulfur (which may amount to as high as 5 wt%) and metallic compounds [1]. The absence of strict regulations combined with the low cost of fossil fuels makes shipping one of the main contributors to global emissions of greenhouse gases (GHG), accounting for 2.5% of global GHG emissions according to the third International Maritime Organization (IMO) GHG study. Maritime vessels are also a source for volatile organic compounds, particulate matter, and hazardous air pollutants (NO_x and SO_x) [2]. The United Nations, with UN Sustainability Development Goal n.14 and the IMO, want to change the current situation, introducing national and international regulations for vessels' emissions aimed at reducing the negative environmental impact of fossil fuels [3,4].

Zero-emission power systems have been in the last decade included in the design of new vessels or retrofitted to older vessels in order to comply with the new regulations [5,6]. These new hybrid or fully-electric systems aim at replacing old architectures based on the internal combustion engine (ICE) without having to compromise on operational flexibility, performance or safety. It is nontrivial to replace the ICE based architecture which has been developed for decades and has reached high peak efficiency values. Furthermore zero-emission systems have generally a lower technology readiness level, lower market adoption, and cannot yet rely on a fully developed supply chain. From a logistical perspective, marine vessels need to rely on the infrastructure of the departure ports and arrival ports for refueling and therefore

* *Corresponding author.*
E-mail address: lorenzo.balestra@ntnu.no (L. Balestra).

https://doi.org/10.1016/j.ijhydene.2021.09.091

need either large energy storage solutions or high density energy carriers to ensure that the range requirements are satisfied. With all these factors considered, no single zero-emission technology is suited for all applications, thus the power-plant configuration is decided as a function of the vessel operations (operational profile). In the 1–10 MW power range, battery propulsion is possible but best suited to short routes where frequent recharging is possible. Hydrogen fuel cells aim at bridging the gap between battery electric configuration with limited range, and the versatile, but polluting, diesel-electric configuration, by maintaining zero-emission output with no need for land-based charging. Proton exchange membrane fuel cells (PEMFC) have received certifications allowing them to be integrated into vessel power-grids [7,8], and can be used to provide baseline energy as prime movers' or backup power as range extenders' in hybrid configurations including energy storage solutions. To provide the same level of performance as ICEs' with respect to range and power production, PEMFC and battery hybrid systems need to be carefully optimized from a component sizing (CS) and energy management strategy (EMS) perspective.

In this paper, the optimization problem is studied considering the operations of a double-ended ferry with a length of 100 m and a beam of 18.2 m, with the capacity for 122 cars and 600 passengers [9]. Data relative to the operations of this ferry have been collected in a database over a period of six months for research and optimization purposes. This ferry is currently equipped with a 4 MW diesel electric power-plant. A previous publication from Balestra et al. proposes an alternative zero-emission hybrid power-plant along with its corresponding digital model representation. The digital model developed in Ref. [10] can be reconfigured and adapted to multiple CS and EMS solutions, and is used in this work to simulate the operations of three different power-plant configurations combined with three different EMSs. The EMSs selected for the study are inspired both by land-based grid applications and road transport applications. These EMSs are:

- Load leveling strategy
- Peak shaving strategy
- Charge depleting/charge replenishing strategy

Once the EMSs are selected, a sequential optimization to determine the number and rating of the PEMFCs and batteries is carried out for each EMS, taking into consideration power and performance requirements. The route considered in the simulations is the same in all of the three cases to facilitate the final comparison between the strategies and the simulation results.

The first objective of the paper is to show how sequential optimization can be used as one possible approach to component sizing, in a hybrid power-plant with PEMFC and batteries. The dependency between CS and EMS must be taken into consideration to achieve the best possible performances when using the system. The second objective of the paper is to demonstrate the dynamic behavior of the hybrid power-plant when operating with the three EMSs and verify that the performance level is satisfactory with respect to the diesel power-plant currently equipped, and does not sacrifice operational flexibility.

Using a dynamic model makes it possible to analyze the behavior of the PEMFCs, batteries and power electronics components. Particular focus is placed on hydrogen consumption, fuel cell degradation and other key operational factors. The final objective of the paper is to collect the data from the three configurations and compare the results and relative performances in order to evaluate which strategy would be best for the presented case study.

Brief system description

The vessel taken into consideration in this study is a double ended ferry with a length of 100 m and a beam of 18.2 m. The ferry can transport 600 passengers and 122 cars and operates a 45 min crossing in Danish national waters. The crossing is 7.7 nautical miles and is operated 18 times in a normal day. The vessel is equipped with 5 diesel generators powering 4 Azimuth thrusters and auxiliary loads [9].

A study previously carried out on this ferry in Ref. [10] was focused on a zero-emission alternative for the ferry's power-plant (Fig. 1). The alternative hybrid-electric power-plant was based on a combination of PEMFCs and Li-Ion batteries delivering the power defined by the operational profile through a DC-grid.

This paper expands upon how different EMSs require different power-plant configurations to operate at the best possible efficiency. Three EMSs are taken into consideration and the component sizing is performed using a sequential optimization approach.

The Matlab-Simulink model developed by the authors is used to simulate the three different hybrid power-plant configurations. This model includes a parametric model for the PEMFC, for the Lithium Ion battery, power electronics components and direct current (DC) load. The flexibility of the

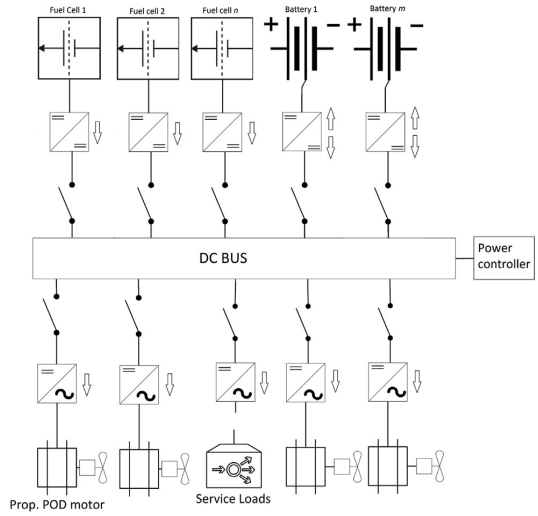

Fig. 1 – Simplified single line diagram of the proposed hybrid configuration.

model allows for a quick re-configuration of the power-plant, assigning *n* number of PEM fuel cells and *m* number of batteries, to test different components sizing approaches. The PEMFC model is based on [11] and configured using the datasheet of a commercial fuel cell rated for 100 kW of power. The characteristics of this unit are listed in Table 1.

The Lithium Ion battery used in the simulation and connected to the system is not modelled upon any commercial model specifically, but is based on the 18,650 Li-Ion cell. The rated voltage for each battery is either 400 or 800 V depending on the power-plant configuration. The capacity of each battery module is considered as a variable and calculated for each EMS. This choice provides flexibility when it comes to selecting the appropriate battery capacity for the specific EMS. Flexibility in selecting the battery capacity allows to define a specific C-Rate at which a battery needs to operate. Choosing the appropriate C-Rate for the battery pack indirectly defines how much degradation the battery is going to experience during operations and also define how much footprint is required for battery storage in relation to the power demand allocated to the battery [12].

The vessel's grid is set to operate using DC current as both batteries and PEMFC output is DC. The voltage level selected for the DC-Bus is equal to 1000 V in all cases.

Methodology

State of the art for power management strategies and component sizing in hybrid vehicles

The power-plant optimization problem for all kinds hybrid energy systems is nontrivial. The optimization process does not have a unique solution as components sizing of the energy system heavily relies on how the components interact, which is defined by the EMS. At the same time, some types of EMS cannot efficiently operate without components in the correct number or rating. This problem is experienced in battery vehicles [13], but mainly in complex power-plant with both energy conversion (fuel cells) and energy storage (batteries) [14,15].

The majority of scientific studies and reviews focus on road transport and specifically on the design of energy management strategies [16–19]. Even if not directly aimed at maritime vessels, these studies provide important knowledge on existing strategies and define a framework that can be used when scaling up the total power installed in a marine multi-megawatt power-plant. Some studies have been recently carried out on a few vessels of small size (<1 MW) where there are multiple similarities with cars and road transport vehicles when considering the power requirements [20–22]. Components sizing methods are a key factor, but are only briefly mentioned in previously listed references. A review considering the dependencies between components sizing and EMS is carried out in Ref. [23], providing a base structure for the development of this paper. This structure is used, in this study, to identify and develop the three case studies presented. The goal is to apply the knowledge developed for road transport vehicles and apply it to large-marine power-plants, verifying the optimization process performances through simulations in the Matlab environment using a dynamic model.

Table 1 – Fuel cell data used for the model configuration.

Rated power (net)	100 kW
Gross output at rated power	320 V/350 A
Peak power EOL … OCV BOL	250 … 500 V
System efficiency (Peak, BOL)	62%
System efficiency (BOL)	50%
Max waste heat	120 kW
Coolant outlet temperature	80C
Fuel inlet pressure	8–12 bar(g)
System pressure	1.6 bar(g)
Ambient temperature	−20 to +50C
Ambient relative humidity	5–95%, non-condensing
Weight	120–150 kg
Volume	300 l

Case study description

The study carried out in this paper focuses on the development of three different hybrid power-plant configurations including energy management strategy (EMS) and components sizing (CS). Each configuration is tested using the model from Ref. [10], with real world data to simulate realistic conditions. The results obtained from these simulations are analyzed and compared to identify advantages and disadvantages of each configuration and possible further improvements.

The power-plant configuration can be obtained using different approaches including sequential optimization, bi-level optimization or simultaneous optimization [23]. In this particular case the sequential optimization approach is selected, with the definition of the EMS in the first step, and the subsequent definition of the power demand for each component leading to the calculation of component number and rating.

An EMS can be defined as a series of rules and controls that allow to regulate the energy production, consumption, distribution and storage in a grid system. Each configuration uses a different EMS and therefore a different load sharing strategy, splitting the power between fuel cells and batteries. The EMS needs to ensure a satisfactory performance level in addition to ensuring a reliable power delivery. The selected EMSs are rule based, with deterministic or fuzzy-logic approaches. All the EMS considered in this study are online EMSs, defining the power distribution at each instant during the stationary, maneuvering and navigation phase of the ferry. Online EMSs can be used in real-time applications as they do not require knowledge of global informations, such as the complete operational profile, and can make dynamic decisions.

Equation (2) defines the ideal condition for every single operational point considered during the simulations. Ideally, the power generated by the PEMFCs and the power generated by the batteries is equal to the power demand (P_{op}) sampled from the diesel electric ferry. In reality, this condition is made more flexible to account for the dynamic behavior of the components during the simulation. The term δ is introduced to define the range of values that are considered acceptable for the power-output of the power-plant. A lower δ determines

lower response time and higher performance, while a higher δ allows for smoother transitions with lower PEMFC and battery degradation. The value of δ is determined for each simulation to define the range of acceptable values.

$$P_{op} - \delta \leq P_{op} \leq P_{op} + \delta \quad (1)$$

$$P_{op} = (P_{fc}\ n / \eta_{bc} + P_b\ m / \eta_{bi-dir}) / \eta_{sys} \quad (2)$$

- P_{op}: power demand (operational profile)
- n: number of PEMFC
- m: number of batteries
- P_{fc}: power output single PEMFC
- P_b: power output single battery
- η_{sys}: On-board electric grid components efficiency.
- η_{bc}: Efficiency boost converter
- η_{bi-dir}: Efficiency bi-directional converter

In this particular case study, by considering a ferry with a scheduled route, it is possible to take advantage of the similarities in power demand between crossings. By analyzing multiple crossings sampled over a period of six months, only small variations in power demand, due to weather conditions and maritime traffic, were observed. For this reason it is possible to evaluate the model and obtain meaningful results on the performances of the power-plant configuration by considering just one typical crossing operational profile (OP). In this case a 1 h crossing carried out in mid November was selected (blue curve in Fig. 2 and Fig. 3). If computational resources are not limited or variability is observed between daily or weekly operations, it is suggested to extend the time interval considered.

System configuration

The Simulink model is configured for each one of the three power-plant configurations, including the code relative to the type of EMS selected and the correct number for PEMFCs and batteries defined in the component sizing calculations. The power-plant layout is based on the single line diagram presented in Fig. 1, with the EMS defining how the energy flows from energy storage/energy conversion to electrical load.

To define the number of PEMFCs required to satisfy the power demand for each case, it is necessary to analyze the load sharing strategy that the EMS implements during operations. For the PEMFC number there are limitations given by the fact that producers create modularized stacks with defined power levels. In this case the rated power of the considered unit is equal to 100 kW (Table 1). Each fuel cell installed in the system is identical and it is assumed that all have the same dynamic behavior when delivering the same electrical load. In each considered EMS the load share assigned to the fuel cells is equally distributed between all units. No unit, in this study, is controlled individually or switched on/off during operations.

The power output of the PEMFC can be expressed in equation (3). The voltage and efficiency curves of the fuel cell are obtained introducing the parameters found in Table 1 into the parametric model. The obtained curves match the ones reported in the PEMFC datasheet. These curves are obtained experimentally and take into account the real voltage (V_{fc}) and current (I_{fc}) output. If the voltage and current output is considered ideal, or the fuel cell consumption needs to be calculated, it is necessary to introduce the value η_{fc} representing the fuel cell efficiency.

$$P_{fc} = V_{fc}\ I_{fc} = V_{fc-ideal}\ I_{fc-ideal}\ \eta_{fc} \quad (3)$$

Unlike PEMFCs, Li-Ion batteries can be built to fit a specific use case, by combining multiple individual cells in series or parallel. The power delivery, determined by the load share of the battery, can be satisfied using a combination of factors such as number of units (m), battery capacity (Q_b) and C-Rating. The only factor that is fixed, in this case, is the rated voltage (V_b) set at either 400 or 800 V to reduce the number of variables. This flexibility allows to compensate for the fixed rated load of the fuel cell, and calculate the optimal battery size for each considered EMS.

As for the fuel cells case, if multiple batteries are installed in the system, each battery installed is identical and it is assumed that all have the same dynamic behavior when delivering the same electrical load. In every EMS the load share assigned to the batteries is equally distributed between all units. No battery, in this study, is controlled individually or switched on/off during operations.

In general, the term representing the power drawn from one battery can be expressed as Equation (4) where the term Q_{batt} is limited by the C-rate (factor of the cell internal resistance).

$$P_b\ t = E_b = V\ Q_b = V_b\ I_b\ t \quad (4)$$

Once the value of n,m, Q_b are defined for each EMS, it is possible to launch the model to simulate the amount of time selected by the user. Once the simulation is finished the results can be compared and analyzed.

In this paper, when calculating a power-plant configuration, specific safety class regulations regarding active and passive redundancy of components are not considered. The total power calculated in the configuration provides a conservative estimate but does not comply with any specific regulation from maritime certification societies.

Load leveling EMS

Load leveling strategies are a common approach in large land-based electrical grids but can also be used in marine power-plants if the ICE generators are coupled with batteries for energy storage. In a diesel-electric configuration, this strategy is used to keep the diesel engine at the operational point where the break specific fuel consumption is minimum, compensating load transients with batteries. Maintaining the diesel engine at the point of peak efficiency reduces considerably the fuel consumption and the level of emissions.

A load leveling strategy can also be adopted for the control of a hybrid power-plant with PEMFC and batteries. In this case the power demand is split almost equally between the fuel cells and large battery packs, with the goal of maintaining the

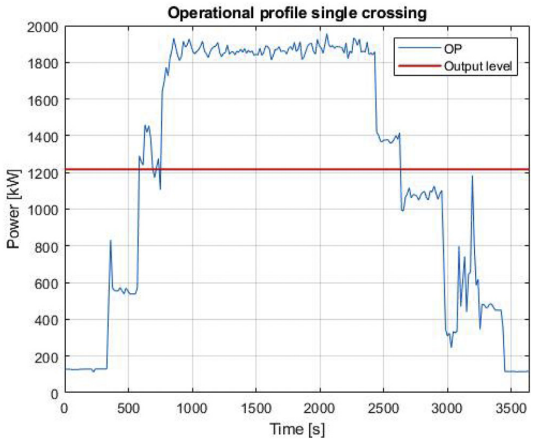

Fig. 2 – Operational profile and set output level with load leveling EMS.

fuel cell profile as flat as possible to limit the degradation given by load transients. The load leveling strategy is developed using an online deterministic rule-based approach.

The first step in the definition of the load leveling strategy is the definition of the rules that the EMS follows. In this case, the rules contained in Table 2 are formulated and implemented into the EMS code. These rules are formulated taking into consideration two variables: available power and the state of charge (SOC) of the battery. Based on these rules, both PEMFC and switchboard are controlled.

The second step in the definition of this strategy is the calculation of an output level (P_{OL}) defining the maximum power output for the PEMFC units during navigation. This P_{OL} value is key in defining the rules of the EMS. In this case the output value is calculated using Equation (5), integrating the operational profile over the amount of time considered for the study. The result is P_{OL} equal to 1217 kW.

$$\int_0^t OP\ dt = P_{OL}\ t \tag{5}$$

Considering the value obtained for P_{OL} it is possible to calculate the number of PEMFCs n. The choice is to install in the system enough PEMFCs to operate at P_{OL} with 80% of PEMFCs rated load. This choice was done based on the study of Fletcher et al. [14] and the values are listed in Table 3, keeping the PEMFC in low power operation and limiting degradation.

In addition, the calculation of n takes into account a value for the efficiency of the boost converter (η_{bc}) equal to 0.97%.

$$n = (P_{OL}\ 0.8\ \eta_{bc}\eta_{sys})/P_{fc-rated} \tag{6}$$

The result of equation (6) can be rounded to 18 PEMFCs. Setting the operational level to 80% of the rated load allows for a conservative estimate on the power installed.

The third step in the definition of the configuration for the load leveling strategy is the sizing of the battery. Because the load leveling strategy is applied not only during navigation, but also during the entire time interval considered, there are limitations with respect to maintaining the PEMFC at P_{OL} at all times. The main limitation is the amount of power that can be stored by the battery when the difference between P_{OL} and P_{op} is higher than the maximum value of P_b. A choice is made to limit the size of the battery to the capacity calculated during the discharge phase, represented by the area above the red line of Fig. 2. This ensures a trade-off between performances and battery size.

A first attempt at battery dimensioning is done by measuring the difference between P_{OL} and the peak power demand sampled during the entire period of ferry data collection (P_{max}, 2425 kW). Considering this peak value and the voltage level set to be constant at 400 V, it is possible to calculate I_b using Equation (7), derived from Equation (2).

$$P_{fc-max}\ n = \frac{P_{max}}{\eta_{sys}} - P_b\ m = \frac{P_{max}}{\eta_{sys}} - V - b\ I_b\ m \tag{7}$$

The value obtained for I_b represents the battery capacity for 1 battery considering a C-Rating of 1-C. With a battery rated for 400 V, the calculated capacity is equal to approximately 3020 Ah at 1C. In this scenario, in the effort to maintain the PEMFC output as close as possible to P_{OL} and to contain the C-rate at which the battery operates, the choice is to install 2 batteries rated at 400 V and 1750 Ah. Installing two batteries allows for a basic level of active redundancy and also for a small power reserve. The C-rate is limited at 2-C.

To check that the calculated capacity is adequate to the crossing it is possible to integrate the section of the

Table 3 – Degradation values from Fletcher et al. [14].

Operating Conditions	Degradation Rate
Low power operation (<80%)	10.17 μV/h
High power operation	11.74 μV/h
Transient loading	0.0441 μV/Δkw
Start/stop	23.91 μV/cycle

Table 2 – Rule based energy management system instructions.

Power Available	SOC Level	Action Battery	Action FC
$P_{vessel} + P_{rec} \leq P_{fc-lim}$	SOC ≤ 80%	Recharge connected; P_{rec} = defined rec. I	$FC_{target} = P_{vessel} + P_{rec}$
$P_{vessel} + P_{rec} \leq P_{fc-lim}$	SOC > 80%	No circuit connected; $P_{rec} = 0$	$FC_{target} = P_{vessel}$
$P_{vessel} + P_{rec} > P_{fc-lim}$; $P_{vessel} \leq P_{fc-lim}$	SOC ≤ 80%	Recharge connected; $P_{rec} = P_{OL}$ - OP	$FC_{target} = P_{OL}$
$P_{vessel} + P_{rec} > P_{fc-lim}$; $P_{vessel} \leq P_{fc-lim}$	SOC > 80%	No circuit connected; $P_{rec} = 0$	$FC_{target} = P_{vessel}$
$P_{vessel} > P_{fc-lim}$	SOC > 20%	Discharge connected; P_{dis} = OP - OOL	$FC_{target} = P_{OL}$
$P_{vessel} > P_{fc-lim}$	SOC ≤ 20%	No circuit connected; $P_{dis} = 0$	$FC_{target} = P_{vessel}$

operational profile above the value of P_{OL}. In this case the value calculated is lower than 3020 Ah and therefore the battery size is defined by Equation (7).

Once the load leveling EMS is defined through the equations in Table 2 and the component sizing is carried out it is possible to proceed with the simulation. With this particular configuration the focus is on maintaining the PEMFC output for as long as possible at the output level defined, producing an almost flat PEMFC output if the conditions allow it. Keeping the PEMFC flat is achieved by recharging the battery at constant current when the surplus of power allows it, and then switch to variable current until the output level is met. Values above the operational level are compensated by releasing the energy stored in the battery packs.

Peak shaving EMS

Peak shaving is the second EMS in this study and aims to eliminate the high frequency load variations experienced by the prime mover of the power-plant during operations. This type of EMS is effective in reducing emissions of diesel-electric power-plants as the high frequency transients are filtered out using a low pass filter, reducing the load variation on the diesel generators and therefore improving efficiency and reducing emissions [24].

The peak shaving EMS can be applied to power-plants with no energy storage solutions, but to achieve better response time and overall performances it is usually applied to hybrid power-plants where energy storage solutions can provide extra power while the prime mover output is capped.

In this study, the hybrid power-plant configuration does not have large individual prime movers, unlike a traditional configuration with an ICEs, but the baseline electric power is generated by the multiple PEMFCs that are connected in parallel. The PEMFCs all share the same load and provide power along the entire operational profile. The power requested during the ferry's operations is filtered through a low pass filter in real-time, smoothing the power demand allocated to the PEMFCs.

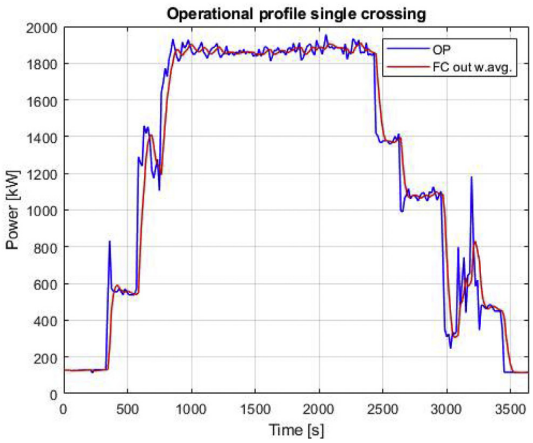

Fig. 3 – Operational profile and fuel cell expected output with peak shaving EMS.

The first step in the sequential optimization approach selected for this paper is the definition of the EMS. In the peak shaving strategy the power demand needs to be filtered in real time using the data collected in the present (t) and in the past (t-n) to define the power that is going to be delivered in the operational point at t + 1. In this case the PEMFCs operational points are defined through a 5 point weighted average calculated using the 5 points sampled in the 5 time steps leading up to the present instant (Equation (8)) with each timestep being equal to 15 s. The first 75 s of operations are unfiltered as the buffer containing the power demand data fills up. This unfiltered interval does not impact the performances of the system as this time interval is taken during Ro-Ro operations where the power demand is low and practically constant.

This filtering approach is one of the simplest that can be adopted, limiting the computational complexity but still providing a smooth and relatively precise profile. It is possible to limit the response delay introduced by the use of an average modifying the weights in Equation (8). If the weights are modified it is important to consider that there is an inverse relation between suppressing high frequency transients and reducing the delay for the specific application.

$$FC_{out} = \frac{P_{t-5}w_1 + P_{t-4}w_2 + P_{t-3}w_3 + P_{t-2}w_4 + P_{t-1}w_5}{w_5 + w_4 + w_3 + w_2 + w_1} \quad (8)$$

Once the EMS approach is defined, it is possible to proceed with the component sizing. In this strategy, the share of power provided by the PEMFCs is always higher than the one provided by the batteries.

The PEMFC number is calculated using P_{max}, limiting the rated load to 80% according to Table 3, and considering η_{sys} e η_{bc}. With the peak shaving strategy the PEMFC output provides the baseline power to the ferry and the battery provides only temporary compensation during transients. The PEMFC number needs to be calculated taking into consideration that it should be possible to operate the ferry on PEMFCs alone without the battery pack. Similarly to the load leveling strategy, the PEMFC output is limited to 80% of the rated load to reduce degradation.

$$n = \frac{P_{max}}{0.8\ \eta_{sys}\ \eta_{bc}\ P_{fc-rated}} \quad (9)$$

The number of PEMFCs n can be rounded to 35 units. Setting the power limit to 80% of the rated load provides a large power reserve.

With the high frequency transients filtered out of the PEMFC output, the battery packs are tasked with compensating the high frequency oscillations to avoid power deficits. Similarly to the load leveling case, the first attempt at dimensioning the battery can be carried out by observing the maximum difference between P_{op} and FC_{out}. In this case there is no pre-set limitation to the maximum PEMFC output, so the difference between P_{op} and FC_{out} needs to be calculated by calculating FC_{out} for a series of profile, measuring the maximum value found. The maximum difference is equal to 740 kW. This value of 740 kW, considering a set voltage of

400 V, translates to a capacity of 1850 Ah if the C-Rate is limited to 1C. In this case, a large storage capacity is not required as the battery mostly provide short bursts of power before the fuel cell output catches up with the demand. For this reason, the battery C-rating in this case can be as high as 2C with a capacity set to 950 Ah. The excess capacity allows for the compensation of losses in the converters and grid.

This power-plant configuration maximizes the share of power allocated to the PEMFCs and reduces to a minimum the power allocated to the battery. The smoother profile also reduces overall degradation as the battery can compensate the fluctuation in load even below a defined output level.

Charge depleting/charge replenishing EMS

The charge depleting/charge replenishing (CDCR) strategy is an approach derived from the charge depleting/charge sustaining (CDCS) EMS used in road transport. CDCS is normally used in hybrid or plug-in hybrid vehicles as the trip length (driving cycle) is not know at the time of starting the car.

In CDCS one or more batteries are discharged during the charge depleting phase, where the vehicles uses only fully electric propulsion. Once the lower limit for the SOC is reached, a range extender turns on and supplies the power demand while the SOC of the battery is kept at a constant value in charge sustaining mode. The adoption of a charge sustaining mode in cars is to ensure the completion of longer trips, while keeping the possibility of running for shorter periods of time using batteries to save fuel or access city areas where ICEs are not allowed. The battery is recharged, once the trip is completed, at a charging station and the cycle can be repeated again.

In this case, this type of EMS is selected to evaluate a power-plant configuration relying primarily on battery power for propulsion and auxiliary loads, with PEMFCs acting as range extenders to include the capability for on-board power generation. The implementation of a CDCS EMS similar to the one applied for road transport would not be optimal for the ferry as, once the battery is depleted, the fuel cells would have to absorb all the high frequency transients defined by the power demand, increasing degradation. The use of CDCS would also mean that, once the battery is depleted, there is the need to recharge using land based infrastructure. For these reasons the CDCS strategy is modified to include a charge replenishing mode, becoming CDCR (charge depleting/charge replenishing). CDCR differs from CDCS as, with the ferry, the length of the crossing is known and the average power demand over time can be calculated. This allows to schedule a battery recharge phase (charge replenishing) onboard, without relying on expensive land based infrastructure that needs to be connected to the electrical grid. The recharging is carried out by the PEMFCs installed on-board.

CDCR uses a deterministic rule-based approach like the load leveling EMS, controlling the power delivery by operating the switchboard connections. The variables used for the control of the system are the power demand and the SOC of each individual battery.

The first step in the definition of the configuration is to specify how the EMS manages the power flow. In this case the choice is made to include 4 batteries in the system. Splitting the power draw between multiple batteries allows to limit the current flowing through the bi-directional converters to obtain better efficiencies. These batteries work alternatively to supply power, and a series of PEMFCs operating as a range extender and recharge energy source (Fig. 4). During normal operations only two batteries from a specific group (1 & 3 or 2 & 4) are in charge depleting mode ($m = 2$), delivering the power defined by the operational profile to the DC load. The other batteries are disconnected from the DC load using the switchboard and are connected to the PEMFCs for recharge (Fig. 4). Disconnecting the battery from the DC load allows a constant-current/constant-voltage (CC-CV) recharge of the battery, replicating the recharging conditions that would be encountered on land. This CC-CV recharging of the battery allows for an easier balancing of the battery pack individual cells therefore limiting degradation and maximizing capacity retention.

Sizing the power-plant for operations with the CDCR EMS starts from the battery packs. Batteries belonging to the same branch of the diagram of Fig. 4 are set to have same dynamic behavior during the simulations as they share the same power demand when in charge depleting mode and are recharged with the same amount of current when in charge replenishing mode. To improve the efficiency of the bi-directional converters that, in this case, need to stabilize the voltage on a much wider range of current outputs, the voltage of the battery is increase from 400 V to 800 V ($V_b = 800$). The capacity of the battery can be calculated using equation (10) and obtaining the capacity from I_b.

$$I_b = \frac{P_{max}}{\eta_{sys}\ \eta_{bi-dir}\ V_b\ m} \tag{10}$$

It is common to increase the capacity calculated in application where the battery is considered the primary source of power for the vessel. The increase in capacity needs to be measured as a trade of between footprint usage and battery depth of discharge (leading to degradation). In this case, a limit is imposed on the lower and upper level of the SOC, with 80% being the upper limit and 20% being the lower limit.

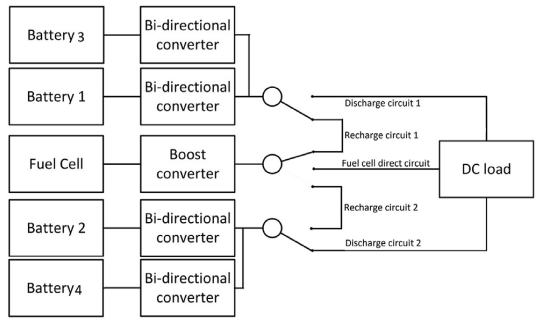

Fig. 4 – Layout configuration with CDCR EMS.

Considering a DC-bus voltage of 1000 V, C-rate of 2-C, a power electronic efficiency of 90% and the limit for the SOC, it is possible to provide a first attempt solution for the battery configuration. Each battery pack is configured for a capacity of 1500 Ah and a nominal voltage level of 800 V.

While the batteries in charge depleting mode are discharged at various rates according to the power demand of the vessel (blue line with different angular coefficients in Fig. 5), the batteries in charge replenishing mode are charged in constant current mode up until the maximum cell voltage is reached (orange line with constant angular coefficient in Fig. 5). It is necessary to specify that, in this case, due to the limitations on the SOC with an upper limit at 80%, the recharge of the battery is carried out only in constant current as the recharge is cut out at 80% SOC before reaching the maximum cell voltage.

The number of PEMFC n selected for this EMS is 18, the same amount defined in the load leveling strategy using equation (5). The calculation of the recharge current value, a function of P_{fc}, is nontrivial as each crossing depletes the SOC of the battery in a different way, not always consuming the whole SOC in one crossing. The recharge current value is therefore not unique and has to be recalculated by the EMS each time a group of battery changes its status from charge depleting to charge replenishing. The recharge current is increased or decreased considering the SOC value of the battery group that switches to discharge mode. If this SOC is lower than the maximum 80% it means that the recharge was not fast enough and the recharge current needs to be increased. This increase is calculated by the EMS using the percentage difference between the initial SOC and the upper limit. This approach is a simplified solution and can be expanded in the future using predictive algorithms to optimize the recharge current. The installation of 18 fuel cells allows to have a wide range of possible recharging currents considering the peak power of the fuel cell installation can reach 1800 kWh. The goal is to obtain a SOC curve as similar as possible to Fig. 5.

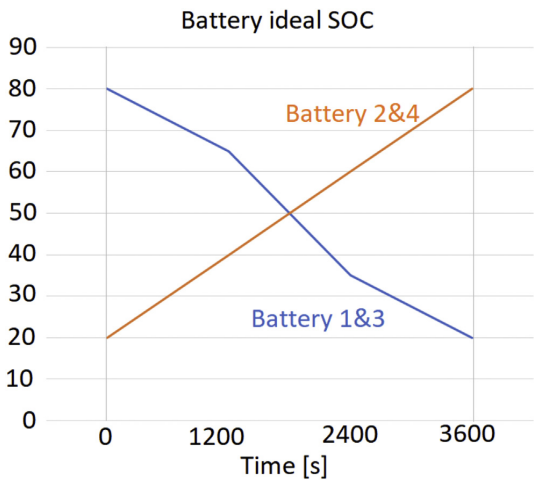

Fig. 5 – Ideal SOC curves with the CDCR EMS.

For this simulation the first attempt solution is to impose a recharge current of 550 A on each battery, that translates to a total of 1100 A that needs to be produced by the fuel cells, using 61% of the total PEMFC power installed.

Results

Results: load leveling strategy

The simulations for the load leveling EMS is carried out using the configuration presented in Table 4.

The first necessary step is to verify that the selected power-plant is capable of carrying out the crossing with no power shortages. This is done comparing the power produced by the modelled power-plant and the initial value of power demand specified (OP). For this comparison the power produced and the OP are considered overlapping if the two values are within ±1% in kW. To take into account transient loading and response time, the aim is to have more than 90% of points within ±20% of the value defined by OP.

The power demand (OP) represented in Fig. 6 is overlapping with the power delivered by the system to the DC bus (output FC + Batt Bus) for 65% of the operational points. The number of samples within the ±20% range is 98%, well within the threshold defined by the author to evaluate the performances of the power-plant configuration. The DC-Bus voltage is stable at the specified level of 1000 V and has slight variations only during the connection and disconnection of the recharge circuit. These variations are quickly compensated by the feedback loop in control of the bi-directional converter, with a fast response.

The difference between the power measured at the source (orange line Fig. 6) and at the bus (yellow line Fig. 6) is equal to the power lost in the converters simulated in the model. This value is influenced by the number of fuel cells and batteries, and therefore converters included in the system, and also by the range of operational values that the converter has to stabilize to 1000 V. In this case the efficiency of the boost converter is equal to 92%. The efficiency of the bi-directional converter is equal to 84%. The bi-directional converter has a lower efficiency compared to the boost converter as it has to stabilize a large battery pack with a wide range of current levels passing through it.

It is assumed that all 18 PEMFC have the same dynamic behavior as load is shared equally between all the units. The

Table 4 – Power-plant configuration for the load leveling simulation.

Total power installed	3200 kW
Bus voltage	1000 V
Battery units	2
Battery nom. voltage	400 V
Battery rated capacity	1750 Ah
Initial SOC	50%
Number of fuel cells	18
Rated power PEMFC	100 kW
Response time PEMFC	15s
Response time Battery	2s

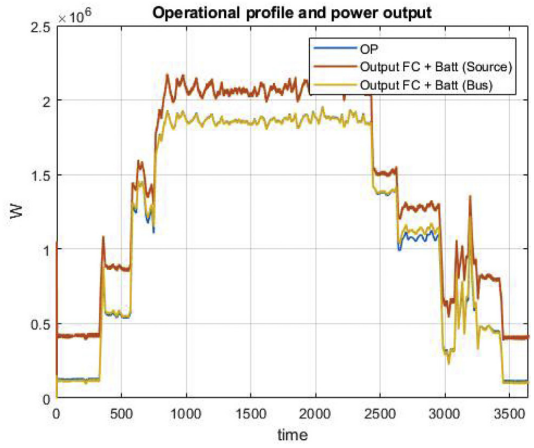

Fig. 6 – Operational profile and power-plant output with load leveling EMS.

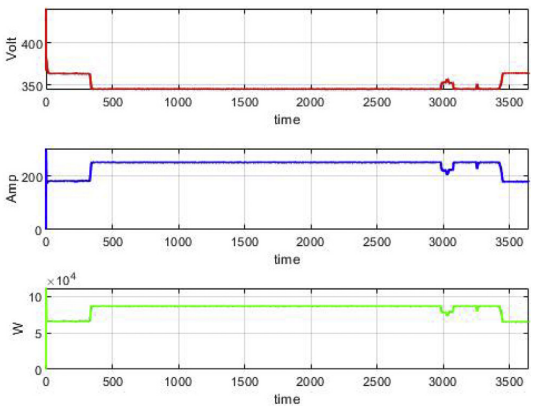

Fig. 7 – Single PEMFC output with load leveling EMS.

load of the single PEMFC can be observed in Fig. 7. In this case, it is possible to observe that for large part of the operational interval the fuel cell is operating at a constant value, defined by the value calculated in Equation (5) divided by the number of fuel cells. This value is on the limit of the low power operation threshold defined in the EMS description. While during this interval at constant power output the degradation of the PEMFC is low, the maneuvering phase has high frequency transients that are filtered out by the battery pack, that is charged with a variable current level.

Observing the state of charge (SOC) curve (see Fig. 8) it is possible to conclude that the batteries included in the system are capable or delivering the requested amount of power during the crossing. In this simulation the recharge of the battery was limited to a maximum value of 0.5C during recharge and 1C during discharge. The final SOC level is also slightly higher than the initial SOC level meaning that there is no need for on-shore recharging during Ro-Ro operations and this particular configuration can operate completely off-grid.

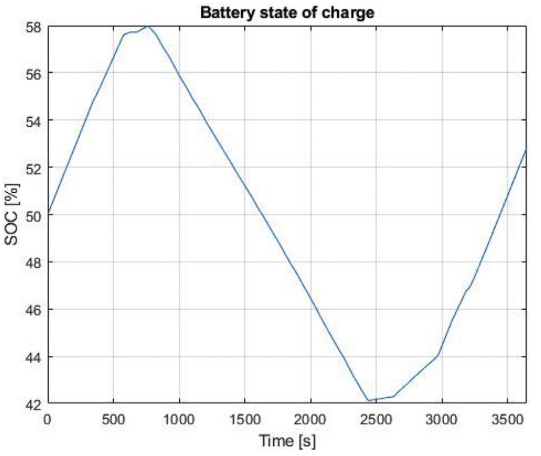

Fig. 8 – SOC of the battery with load leveling EMS.

The degradation for the single PEMFC is equal to 327 μV. The consumption per single FC is equal to 4.03 kg, meaning that the total consumption for the entire crossing is equal to 72.5 kg of hydrogen. By considering the 18 daily crossings that the ferry operates on a regular schedule and the hydrogen quantity that can be stored in fiberglass pressure vessels of commercial size, the ferry would need the equivalent volume of 3.5 20' containers to carry out daily operations. This calculation considers a storage pressure of 350 Bar, and the storage volume can be reduced even further by considering a storage pressure of 700 Bar or cryogenic storage.

Results: peak shaving strategy

The simulations for this EMS is carried out using the configuration presented in Table 5.

As for the load leveling strategy, the first necessary step is to verify that the selected power-plant is capable of carrying out the crossing with no power shortages. This is done comparing the power produced by the modelled power-plant and the initial value of power demand specified (OP). For this comparison the power produced and the OP are considered overlapping if the two values are within ±1% in kW. To take into account transient loading and response time, the aim is to have more than 90% of points within ±20% of the value defined by OP.

Table 5 – Power-plant configuration for the peak shaving simulation.

Total power installed	3502 kW
Bus voltage	1000 V
Battery units	1
Battery nom. voltage	400 V
Battery rated capacity	400 Ah
Initial SOC	50%
Number of fuel cells	35
Rated power PEMFC	100 kW
Response time PEMFC	15s
Response time Battery	2s

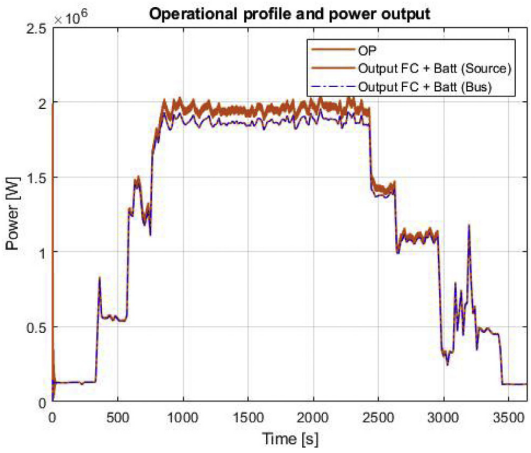

Fig. 9 – Operational profile and power-plant output with peak shaving EMS.

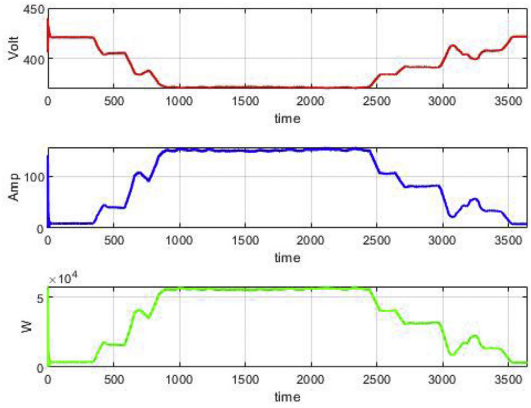

Fig. 10 – Single PEMFC output with peak shaving EMS.

The power demand (OP) represented in Fig. 9 is overlapping with the power delivered by the system to the DC bus (output FC + Batt (Bus)) for 74% of the operational points, and 90.5% of the points are within ±20%. This means that the power-plant is appropriately dimensioned in this case according to the defined criteria. Thanks to the smooth output of the fuel cell and the controlled battery output when charging or discharging, the DC-bus voltage is maintained constant throughout the entire operational interval, with no spikes.

With this EMS the measured efficiency for simulated single boost converters is equal to 95% and the efficiency of the bi-directional converter is close to 98%. These high values for the efficiency are obtained by re-tuning the bi-directional converter to operate in conjunction with the smaller battery capacity.

All 35 PEMFC included in the power-plant have the same dynamic behavior as the load is shared equally between all the units. The load profile of the single PEMFC can be observed in Fig. 10. In this profile it is possible to observe how the high frequency transients have been filtered out, in favor of smoother power output. With a peak power supplied below 60 kW each PEMFC is well within the limit established for low power operation. The degradation measured with this EMS for the single fuel cell is equal to 488.84 μV.

The battery SOC is analyzed to monitor that neither the upper or lower SOC limit, respectively 80% and 20%, are reached. The SOC level for this EMS at the beginning and at the end of the crossing should be equal to 50% as specified in the initial operational profile. This is verified by the results presented in Fig. 11.

Fig. 11 shows how a single battery of just 400 Ah of capacity is able to compensate the small high frequency oscillations during the interval considered.

The hydrogen consumption measured for the single PEMFC during the interval considered is equal to 1.608 kg. This means that, to complete the crossing, 56 kg of hydrogen are required. By considering the 18 daily crossings that the ferry operates on a regular schedule and the capacity of a 20 feet container equipped with fiberglass pressure vessel for storing hydrogen at 350 Bar, the ferry would need the equivalent volume of three containers to carry out operations. This storage volume can be reduced even further by considering a storage pressure of 700 Bar or cryogenic storage.

Results: CDCR strategy

The simulations for the charge depleting charge replenishing EMS is carried out using the configuration presented in Table 6.

Similarly to the two previous EMSs, the first necessary step is to verify that the selected power-plant is capable of carrying out the crossing with no power shortages. This is done comparing the power produced by the modelled power-plant and the initial value of power demand specified (OP). For this comparison the power produced and the OP are considered overlapping if the two values are within ±1% in kW. To take into account transient loading and response time, the aim is to have more than 90% of points within ±20% of the value defined by OP.

The power demand represented in Fig. 12 is overlapping with the power delivered by the system to the DC-bus for 99.6% of the samples obtained in the simulation. This high precision in following the power demand set by the OP is

Table 6 – Power-plant configuration for the CDCR simulation.

Total power installed	6600 kW
Bus voltage	1000 V
Battery units	4
Battery nom. voltage	800 V
Battery rated capacity	1500 Ah
Initial SOC 1	80%
Initial SOC 1	30%
Number of fuel cells	18
Rated power PEMFC	100 kW
Response time PEMFC	15s
Response time Battery	2s

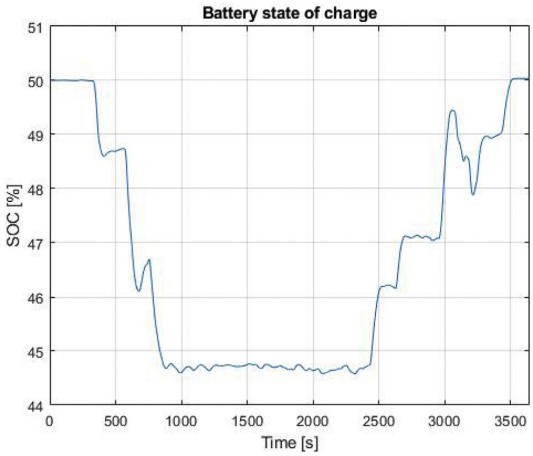

Fig. 11 – Battery SOC with peak shaving EMS.

thanks to the low battery response time, allowing to follow the power demand very accurately, even during load spikes.

The bi-directional converters inductance and capacitance value are recalculated for this specific case to take into consideration the higher current flowing through the sub-model. With the new values for inductance and capacitance it is observed that the feedback loop controlling the bi-directional converters allows an efficient voltage stabilization to the predetermined value of 1000 V during the entire simulation. The efficiency of the boost converter in this case is around 97%, befitting from a constant output on the bus side, while the bi-directional converter efficiency measured during navigation is equal to just 81%, having to stabilize the voltage for a quite wide range of current outputs.

All 18 PEMFC included in the power-plant have the same dynamic behavior as the load is shared equally between all the units. The load profile of the single PEMFC can be observed in

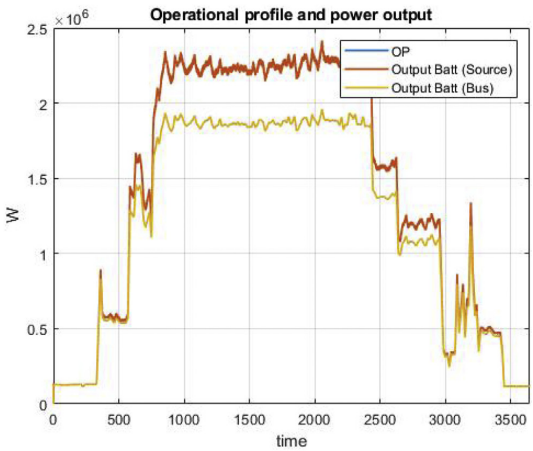

Fig. 12 – Operational profile and power-plant output with CDCR EMS.

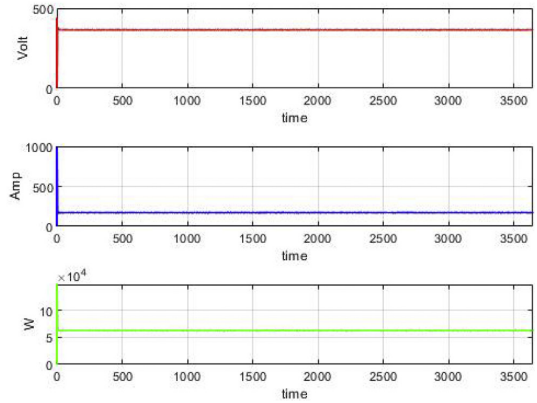

Fig. 13 – Single PEMFC output with CDCR EMS.

Fig. 13. In this profile it is possible to observe that by disconnecting the PEMFC from the DC-bus and operating them only during recharge complitely eliminates transients, with benefits to the fuel cell degradation. The fuel cells supplies, during the simulation, 1100 kW to recharge the battery at the predetermined recharge current of 550 A, using 61% of the total power installed. The degradation measured with this EMS for the single fuel cell, excluding the initial stage at which the fuel cell reaches its operational point, is equal to 45 μV.

The power-plant selected for this EMS is comprised of two groups of batteries: group 1, comprised of battery 1 and 3, and group 2 comprised of battery 2 and 4. All the batteries belonging to a group have the same behavior in the simulation as they are supplying or receiving the same amount of current. This condition is also valid when considering the SOC, with all the batteries in group 1 having the same SOC during the simulation, and same for the batteries of group 2.

In Fig. 14 it is possible to analyze the performances of the two groups of batteries. Group 1, comprised of battery 1 and 3

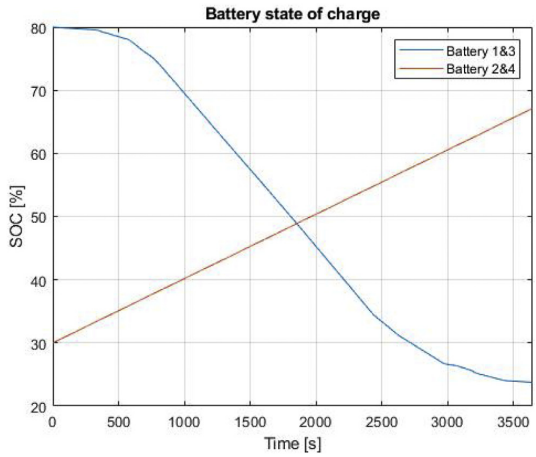

Fig. 14 – Battery SOC with CDCR EMS.

can deliver all the required power for the analyzed crossing. It also shows that at the end of the crossing not all the capacity is used, leaving a residual 5% capacity. Group 2, recharging each battery with a constant 550 A, manages to reach only 67% SOC at the end of the crossing. The fact that group 2 does not reach the upper limit of 80% means that once group 2 is switched to charge depleting mode, it will have a lower SOC than the upper limit. This is taken into consideration by the EMS and the recharge current is increased considering the difference in percentage between the SOC at the time of the connection of group 2 and the upper limit for the SOC.

The hydrogen consumption measured for the single PEMFC during the interval considered is equal to 2.811 kg. This means that, to complete the crossing, 52 kg of hydrogen are required. By considering the 18 daily crossings that the ferry operates on a regular schedule and the capacity of a 20 feet container equipped with fiberglass pressure vessel for storing hydrogen at 350 Bar, the ferry would need the equivalent volume of 3 containers to carry out operations. This storage volume can be reduced even further by considering a storage pressure of 700 Bar or cryogenic storage.

Discussion

The discussion section focuses on the analysis of the results obtained for the three EMS strategies. The pros and cons of each power-plant configuration, including component sizing and energy management strategy are discussed. The results are compared and a score is assigned to different factors to evaluate the overall efficacy of each EMS strategy.

Result analysis

The results obtained with the load leveling EMS show that this strategy is effective in splitting the power demand equally between the PEMFCs and the batteries. The PEMFC output is flat for the majority of the operations, with no high frequency transients (Fig. 7) allowing for a reduction in degradation.

The first limitations with this EMS can be observed in the interval defined by the rule: $P_{vessel}+\searrow P_{rec} > P_{fc\text{-}lim}$; $P_{vessel} \leq P_{fc\text{-}lim}$. In this interval, the PEMFC output is kept constant at the value specified for $P_{fc\text{-}lim}$ by regulating the recharge current of the batteries. This means that the high frequency transients that are observed in Fig. 2, below the red line, are compensated by the batteries during recharge. The analysis of battery degradation phenomena is not considered in this paper, but it is important to specify that this strategy may lead to increased degradation on the battery pack as, by changing the recharge current frequently, it is difficult to perform a balanced recharge of all battery cells. Dead cells in the battery pack result in high maintanence costs that should be avoided if possible.

The results obtained with the peak shaving strategy show how this strategy is effective in delivering the majority of the power demand using the PEMFCs while keeping the degradation value low thanks to the filtering of the power demand. This strategy uses the power-plant with the highest possible power output per unit of volume by reducing to a minimum the size of the battery while still taking advantage of this type of energy storage during high frequency transients.

The power-plant configuration selected for the peak shaving strategy is, in this case, limited by a capped PEMFC output equal to 80% of the rated load to be within the limits of low power operations defined in Table 3. While performance results are satisfactory with the limit on the PEMFCs output, if this condition is eliminated at the expense of an increase in degradation, it is possible to obtain the most energy dense power-plant of all three cases, cutting the number of fuel cells from 35 to 28. This high energy density configuration may be the only viable solution if the footprint allocated for the retrofitting operation of the ferry, or other vessels adopting this EMS, is limited.

One drawback of the peak shaving strategy is that it relies on a high number of low power unit (PEMFC) working in parallel. This increases reliability thanks to active redundancy, but makes necessary to include a high number of boost converters connected to the fuel cells, reducing the overall efficiency of the system. Promising developments in the PEMFC sector, where units of increasing power output are presented regularly, is set to solve this problem when considering that the switch from 100 kWh PEMFC to 200 kWh PEMFC could cut in half the number of converters currently reducing the efficiency of the system.

The results obtained with the charge depleting/charge replenishing strategy highlight that this is the strategy with the lowest possible value for PEMFC degradation while obtaining the best performances when considering transient loading. This configuration still maintains the capability of operating independently from an on-shore recharging station. The low degradation is achieved at the expenses of a large portion of the vessel footprint dedicated to battery storage. This strategy aims at keeping the operating costs for the ship operators low by reducing the maintanence required by the power-plant through low degradation of both batteries and PEMFCs. One drawback of this strategy was evident during the simulations where, with only two large battery packs providing the entire power demand of the vessel, the overall efficiency was impacted, with this strategy having the worst efficiency value when considering the power delivery from power source to DC-Bus. This aspect can be anyway solved with a better re-design of the bi-directional converters or by using multiple smaller batteries.

Comparison between EMSs

To compare the three EMSs is it possible to compile a table that includes scores for each parameter considered. The parameters considered are: PEMFC degradation, single PEMFC consumption, power-plant performance and footprint used. For each parameter, a score ranging between *Low* to *High* is assigned, taking into consideration the values presented in the results section.

The PEMFC degradation parameter depends on the degradation measured during the simulation. The degradation considered is relative to the measurement for the single PEMFC unit. The power-plant performance is a parameter taking into consideration the difference between the power supplied and the power demand. In this case a high number of samples overlapping with the power demand determines the highest score. Footprint usage is a parameter that takes into

Table 7 – Table for the evaluation of key factors with different EMSs.

Parameter	Load Leveling	Peak Shaving	CDCR
PEMFC degradation	Medium	Medium	Low
PEMFC consumption (1 unit)	High	Medium	Medium
Power-plant performance	Low	Medium	High
Footprint usage	Medium	Low	High

consideration the space allocated to the power-plant. In the footprint usage parameter the space required for the storage of hydrogen is not taken into consideration as many different approaches are possible, with very different possible energy density values. The footprint usage is calculated using the approximate dimensions of the PEMFC unit used in this case (volume of 300 l per PEMFC) and the typical energy density of 18,650 battery cells (231.5 Wh/kg [25]). The PEMFC consumption parameter is a function of multiple factors, such as the reliance of the power delivery on the PEMFC output and the loading of the fuel cells in different EMSs. In this case the PEMFC consumption score is not simply a function of the amount of kg of hydrogen calculated in the simulation as this parameter is not directly representative of the efficient or inefficient usage of hydrogen in the power-plant.

The results of this comparison are listed in Table 7.

Conclusions

The simulations and the result analyses carried out in this paper demonstrates that there is no single solution to the optimization problem for a maritime hybrid power-plant equipped with PEMFCs and batteries. The different configurations tested allow for the optimization of primary selected parameters, while assigning a lower priority to other secondary parameters. There is always a trade-off when choosing which factors to optimize, with the resulting configurations always being a compromise due to the limitation of resources (e.g. budget, footprint).

In this paper, the limitations of the optimization process are considered, and three different power-plant configurations, including component sizing and energy management strategies, are presented. These configurations offer different approaches to the optimization of operations when considering the double-ended ferry service. Each configuration considers a different set of primary parameters. In the peak-shaving strategy, for example, the aim is to maximize the energy and power density of the system leading to a minimization of footprint usage, while with the CDCR strategy, the aim is to limit degradation of PEMFCs and batteries to a minimum to reduce the costs of system maintanence. The simulations carried out in these three cases have produced a number of results that can aid the further work on the optimization of the system both on the components sizing perspective and on the EMS perspective.

In this paper the focus is on deterministic or fuzzy-logic online rule-based EMSs, and it was observed that these approaches still have limitations when considering the overall behavior of the system. Online rule-based strategies offer a good trade-off between computational complexity, execution speed and implementation times allowing for real-time application, but still lack the precision of strategies based on dynamic programming. The adoption of online EMSs using optimization based approaches or multi-scheme EMSs turns out to be more complex as the definition of smart cost functions is non-trivial. Optimization based EMSs may increase the computational complexity, but will be the scope of future analysis to further reduce fuel consumption, PEMFC and battery degradation and improvement of performances. The focus of future work is on this type of online EMSs, such as equivalent consumption minimization strategy (ECMS) or model predictive control (MPC). The implementation of these new EMSs can be based on the version of the model that is used in this paper, as it shown that it is possible to be quickly re-configured the layout to follow both different component sizing solutions and energy management strategies.

In this particular case, the ferry company is presented with the required data to make a preliminary decision on which components configuration and EMSs bests fits their use case. This allows them to choose primary factors and secondary factors, defining priorities in the optimization process.

The ultimate goal of this work is to promote the use of clean energy carriers in the maritime industry, providing tools and software that can be used to measure economical and technical feasibility of clean hydrogen solutions to reduce both pollution and greenhouse gas emissions.

Declaration of competing interest

The authors declare that they have no known competing financial interests or personal relationships that could have appeared to influence the work reported in this paper.

Acknowledgment

This work is supported by the Norwegian Research Council trough project number 90436501. The project is headed by IFE in Kjeller, Norway, and this work package is developed at the Department of Marine Technology of the Norwegian University of Science and Technology (NTNU) in Trondheim, Norway.

Appendix A. Supplementary data

Supplementary data related to this article can be found at https://doi.org/10.1016/j.ijhydene.2021.09.091.

REFERENCES

[1] Lin Bin, Lin Cherng-Yuan. Compliance with international emission regulations: reducing the air pollution from merchant vessels. Mar Pol 2006;30(3):220–5.

[2] Miola A, Ciuffo B, Giovine E, Marra M. Regulating air emissions from ships. the state of the art on methodologies, technologies and policy options. Regulating Air Emissions from Ships: the State of the Art on Methodologies. Technologies and Policy Options 2010:978–92. Cited By :37.
[3] The International Maritime Organization. Initial imo strategy on reduction of ghg emission from ships. Annex 11. Resolution MEPC 2018;304(72):4.
[4] NCE Maritime Cleantech. Norwegian parliament adopts zero-emission regulations in the fjords. Marie Launes; 05 2018.
[5] McCoy TJ. Electric ships past, present, and future [technology leaders]. IEEE Electrification Magazine 2015;3(2):4–11.
[6] Reza Alizade Evrin and Ibrahim Dincer. Thermodynamic analysis and assessment of an integrated hydrogen fuel cell system for ships. Int J Hydrogen Energy 2019;44(13):6919–28.
[7] American Bureau of Shipping. Fuel cell power systems for marine and offshore applications, vol. 1862. New York: Incorporated by Act of Legislature of the State of; 04 2019.
[8] Lloyd Aktiengesellschaft Germanischer. Rules for classification and construction additional rules and guidelines vi-3-11. Machinery Installations; 04 2003.
[9] Stig E, Marie L, Jensen JB, Sørensen J. Improving the energy efficiency of ferries by optimizing the operational practices. In: Proceedings of the full scale ship performance conference 2018. The Royal Institution of Naval Architects; October 2018. p. 101–11. null ; Conference date: 24-10-2018 Through 25-10-2018.
[10] Balestra Lorenzo, Schjølberg Ingrid. Modelling and simulation of a zero-emission hybrid power plant for a domestic ferry. Int J Hydrogen Energy 2021;46(18):10924–38.
[11] Souleman Njoya Motapon, Tremblay O, Dessaint L. A generic fuel cell model for the simulation of fuel cell vehicles. In: 2009 IEEE vehicle power and propulsion conference; 2009. p. 1722–9.
[12] Xu B, Oudalov A, Ulbig A, Andersson G, s Kirschen D. Modeling of lithium-ion battery degradation for cell life assessment. IEEE Transactions on Smart Grid 06 2016;99(1–1).
[13] Conte FV. Battery and battery management for hybrid electric vehicles: a review. E I Elektrotechnik Inf October 2006;123(10):424–31.
[14] Fletcher T, Thring R, Watkinson M. An energy management strategy to concurrently optimise fuel consumption & pem fuel cell lifetime in a hybrid vehicle. Int J Hydrogen Energy 2016;41(46):21503–15.
[15] Wilberforce Tabbi, El-Hassan Zaki, Khatib FN, Ahmed Al Makky, Ahmad Baroutaji, Carton James G, Olabi Abdul G. Developments of electric cars and fuel cell hydrogen electric cars. Int J Hydrogen Energy 2017;42(40):25695–734.
[16] Sabri MFM, Danapalasingam KA, Rahmat MF. A review on hybrid electric vehicles architecture and energy management strategies. Renew Sustain Energy Rev 2016;53:1433–42.
[17] Salmasi FR. Control strategies for hybrid electric vehicles: evolution, classification, comparison, and future trends. IEEE Trans Veh Technol 2007;56(5):2393–404.
[18] Çağatay Bayindir Kamil, Ali Gözüküçük Mehmet, Ahmet Teke. A comprehensive overview of hybrid electric vehicle: powertrain configurations, powertrain control techniques and electronic control units. Energy Convers Manag 2011;52(2):1305–13.
[19] Huang Yanjun, Wang Hong, Khajepour Amir, He Hongwen, Ji Jie. Model predictive control power management strategies for hevs: a review. J Power Sources 2017;341:91–106.
[20] Han Jingang, Charpentier Jean-Frederic, Tang Tianhao. An energy management system of a fuel cell/battery hybrid boat. Energies 2014;7(5):2799–820.
[21] Bassam AM, Phillips AB, Turnock SR, Wilson PA. Development of a multi-scheme energy management strategy for a hybrid fuel cell driven passenger ship. Int J Hydrogen Energy 2017;42(1):623–35.
[22] Choi Choeng Hoon, Yu Sungju, Han In-Su, Kho Back-Kyun, Kang Dong-Gug, Young Lee Hyun, Seo Myung-Soo, Kong Jin-Woo, Kim Gwangyun, Ahn Jong-Woo, Park Sang-Kyun, Jang Dong-Won, Lee Jung Ho, Kim Minje. Development and demonstration of PEM fuel-cell-battery hybrid system for propulsion of tourist boat. Int J Hydrogen Energy February 2016;41(5):3591–9.
[23] Huang Yanjun, Wang Hong, Khajepour Amir, Li Bin, Ji Jie, Zhao Kegang, Hu Chuan. A review of power management strategies and component sizing methods for hybrid vehicles. Renew Sustain Energy Rev 2018;96:132–44.
[24] Giakoumis Evangelos G, Rakopoulos CD. Diesel engine transient operation. Berlin: Springer; 08 2009, ISBN 978-1-84882-374-7.
[25] Quinn Jason B, Waldmann Thomas, Richter Karsten, Kasper Michael, Wohlfahrt-Mehrens Margret. Energy density of cylindrical li-ion cells: a comparison of commercial 18650 to the 21700 cells. J Electrochem Soc 2018;165(14):A3284–91.

PAPER V

Hybrid powerplant configuration model for marine vessel equipped with hydrogen fuel-cells

Lorenzo Balestra*[1], Ingrid Schjølberg[1]
[1] Department of Marine Technology, Otto Nielsens Veg 10,
Norwegian University of Science and Technology, NO-7491, Trondheim, Norway
*lorenzo.balestra@ntnu.no, ingrid.schjolberg@ntnu.no

Abstract

The transport sector is investing in new technologies, shifting towards zero-emission propulsion systems. This shift can be observed in the automotive transport sector, but also in maritime transport, where shipowners are evaluating new powertrain configurations and less polluting energy carriers. The innovation in this field is aided by the development of software, based on simulation models representing the powertrain. In this paper, a quasi-static model for a hybrid powerplant is presented. The focus is on hybrid solutions utilizing proton exchange membrane hydrogen fuel cells and batteries. This model can aid the design of powerplants for new hybrid vehicles, or older ones waiting for a retrofit. The model is converted into a Matlab software application for ease of use. Results produced by the model define the powerplant composition and a series of factors, such as fuel cell degradation and hydrogen consumption, that have an influence on running costs. The functionalities of the Matlab software application based on the quasi-static model are demonstrated via one case study considering a harbor tugboat. The results obtained can also be used to measure the technical and economic feasibility of powertrain configurations. The presented model does not include effects related to components aging as all the hardware is considered at beginning of life.

Nomenclature

P_{op}: Vehicle's power demand [kW]

P_{fc}: Power output single fuel cell [kW]

$P_{\text{fc-rated}}$: Rated power fuel cell [kW]

P_{b}: Power output single battery [kW]

P_{f}: Filtered power demand [kW]

P_{L}: Constant power demand [kW]

V_{fc}: Fuel cell voltage [V]

I_{fc}: Fuel cell current [A]

R_{t}: Fuel cell response time [s]

η_{fc}: Fuel cell efficiency

η_{bc}: Efficiency boost converter

$\eta_{\text{bi-dir}}$: Efficiency bi-directional converter

n_{fc}: Number of fuel cells

n_{b}: Number of batteries

t_{tot}: Total simulation time [s]

t_{s}: Sample time operational profile [s]

Hpo: High power deg. rate [μVh^{-1}]

Lpo: Low power deg. rate [μVh^{-1}]

Tl: Trans. loading deg. rate [$\mu\text{V}/\Delta\text{kW}$]

t_{hp}: Time at high-power operation [s]

t_{lp}: Time at low-power operation [s]

1 Introduction

The transport industry has always focused on innovation to improve the design of vehicles, efficiency of the powertrain, and reduce both production and running costs [1, 2]. In this paper the definition of a vehicle is considered to be the most broad interpretation, where a vehicle is any machine able to transport people or cargo, including road, rail and sea transport.

Regulations on pollutants and greenhouse gas emissions [3, 4, 5] have recently influenced different sectors to gradually find alternative solutions to the internal combustion engines (ICE) for power generation, and adopt hybrid or fully electric propulsion to improve the overall system efficiency and reduce the environmental impact [6].

Electric drivetrains prove to be a versatile solution, allowing for the elimination of the mechanical connection between the prime mover and the wheels, or propeller, removing the direct dependency between rotational speed of these elements and the engine crankshaft. This condition permits a more flexible load regulation, with the possibility to be as close as possible to the maximum efficiency operational point, with consequent fuel savings [7].

The transition to electric drivetrains paves the way for the adoption of components such as batteries, fuel cells and supercapacitors. These systems can be integrated into the vehicle's electric grid to replace ICEs for zero-emission operations. However, this transition presents many challenges as these components do not have the same technological maturity as ICEs and are still being developed at a fast pace. State of the art batteries still have relatively low energy density and are limited by the recharge time [8, 9, 10]. Zero-emission vehicles requiring long range capabilities and fast refuelling time need a more energy dense storage solution. For this use-case, hydrogen tanks and a series of proton exchange membrane fuel cells (PEMFC) can be installed on the vehicle to provide baseline energy or function as a complementary source of power when the batteries reach a low state of charge (SOC) [11, 12].

The optimization of a hybrid powerplant with PEMFCs and batteries for different types of vehicles is a non trivial task [13], as the choice of component sizing (CS) and energy management strategy (EMS) heavily influences the performance of the vehicle, its running costs, and maintanence intervals - among many other factors [14]. For this optimization it is important to consider the power demand and the use-case of the vehicle in order to define the operational profile (OP). The optimization also needs to comply with other design requirements such as footprint, weight limitations, or budget limitations.

The quasi-static model presented in this paper was developed as the foundation for an software application developed in Matlab. This software application aims to improve the design process by providing the possibility to study powerplant configurations based on user selected parameters. Different configurations can be saved and compared, verifying that they match with the requirements imposed for the powerplant, with the possibility to validate them in the dynamic model presented in [15, 16].

The developed software application currently includes two Energy Management Systems (EMS) both of the rule-based type, with 3 filters which are suitable for real-time control or hardware in the loop testing. The presented version of the software application is tested via one case study considering the operations of a harbor tugboat. The case study shows the capabilities of the model including validation with real-world data and testing. In the case study, both the peak-shaving strategy and the load-leveling strategy are tested. The model considers mostly ideal components and does not include effects related to components aging. However, this could be included in a later stage.

2 State-of-the-art for hydrogen powertrain models

The creation of models for the validation of a vehicle's powertrain design through simulation of the system is an area of strong interest in recent years. The access to cheap computational power allows both researchers in academia, and engineers in the industry, to create digital models that represent the system into consideration with different degrees of accuracy depending on the scope of the model. Such digital models, when focusing on the powertrain, allow the study of power generation, storage and distribution within the vessel's electrical grid, in addition to the definitions of factors that are impacted by the power flow.

Different types of models have been developed, over the years, to study powertrains including proton exchange membrane fuel cells and batteries. Of particular interest are models developed for the maritime industry with large power requirements, as the model described in this paper has been developed to be used mainly for maritime vessels.

Several approaches consider a system with a predefined component sizing and mainly focus on the study of operation optimization with different energy management strategies [17, 18, 19]. Other approaches focus on the optimal sizing problem of the powertrain [20, 21] while neglecting the EMS optimization or providing basic strategies [22]. There are publications where the component sizing and energy management strategy were considered concurrently for the optimization of the entire system [23, 24].

The large majority of these powertrain models are dynamic models, but quasi-static models have also been developed as they offer faster computational time [25, 26].

The model described in this paper is a quasi-static model providing a platform for the quick-sizing of the power system to be tested using the dynamic model developed in [15]. This model

also tries to fill the gap with respect to quasi-static models used for quick powertrain sizing before validation on a dynamic model that is more resource intensive. The software application of a simple quasi-static model can produce beneficial time saving effects when considering dynamic validation through models or in laboratories for hardware in the loop testing.

3 Framework description

The presented software application was developed using Matlab, and compiled to operate as a standalone software with graphic user interface (GUI). This software application is used to perform the component sizing of a vehicle's hybrid powerplant utilizing PEMFCs and batteries based on the energy management strategy selected. The component sizing is here defined as the number of powerplant components and relative rating or capacity. The focus is on the components that produce, release and store electrical power. The sizing is performed evaluating a series of inputs provided by the user (see Section 4). The sizing is also heavily dependent on the EMS adopted for the considered use-case (see Section 5).

The software application is based on a quasi-static simulation model of the powerplant, ensuring rapid execution time. The drawback of this approach is that the dynamic behavior of the components is not taken into consideration and the results obtained represent a first-attempt solution to the optimization problem that need to be validated in a dynamic simulation, before implementation. Quasi-static simulations adopting the backward method are best suited for a fast analysis and evaluation of the energy and power flow of the vehicle powerplant when computational resources are limited (see Fig. 1).

This model was created to dimension hybrid powerplants, utilizing PEMFCs and batteries, for different type of vehicles including cars, ships, transport trucks and locomotives. The possibility to dimension powertrains in such different power ranges it is given by the inherent scalability of hybrid systems. It is considered that to achieve the user-defined power level it is possible to connect multiple PEMFCs stacks in parallel to reach the desired output. The same approach with the parallel connection can be considered for commercial battery modules. This condition determines a scalability relation that can be considered linear with respect to the power output.

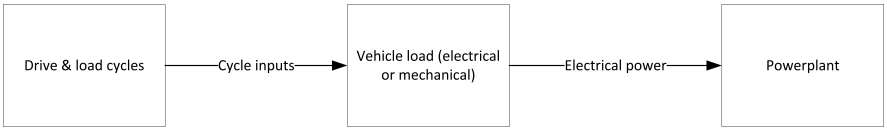

Figure 1: Flowchart representing the quasi-static energy based model (backward method) for vehicle simulation

4 Inputs and configuration

The software application requires a series of user inputs that are typed or uploaded using the GUI (see Fig. 5). The first input is the operational profile of the vehicle considered. The operational profile is an array of values defining the power demand during a considered time interval. In this paper, it is considered that the operational profile represents the power demand at the DC-Bus level, before the distribution to propulsion motors and auxiliary loads. For this reason the efficiency of the electrical grid is considered only up to the DC-Bus, including boost and bi-directional converters, but no inverters, variable speed drives or induction motors.

If the software application is used to configure a new powerplant for the zero-emission retrofit of a vehicle currently in active service, the operational profile can be sampled during operations by measuring the power output required over a specific transit route. The collection of the power data defining the OP sets a target power output for the hybrid zero-emission plant.

The second input needed is the sample rate of the operational profile. The sample rate influences the accuracy of the calculated results, and should be in the order of seconds to allow a correct calculation of the PEMFC transient response and degradation.

Further input is required to define the model of PEMFC selected for the specific system considered. As fuel cell stacks come in pre-packaged commercial units with pre-defined power outputs, the choice was made to have the user specify the fuel cells parameters for the model taken into consideration. The PEMFC characterization is carried out defining the voltage variation and the

efficiency against the current in the operational range of the unit (see Fig. 2). The resulting power curve of the unit can be calculated from the obtained data. Such curves are available on datasheets or can be obtained experimentally with simple measuring equipment.

The definition of a specific PEMFC type provides some boundary conditions for the optimization of the powerplant, where the developed algorithm is tasked with the calculation of the number of PEMFC stacks needed to perform the imposed power demand.

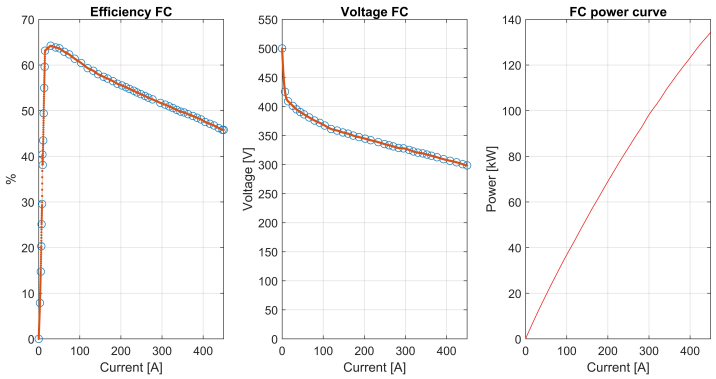

Figure 2: Efficiency (left) and Voltage (center) curve of the selected model of PEMFC. Allows the calculation of the PEMFC power curve (right)

The battery is not defined through user input and its capacity and C-rate is considered as a variable of the optimization problem. The battery characteristics are therefore determined indirectly once the PEMFC stacks output is calculated.

The PEMFC response time, considered as the time the unit needs to go back to stability after a period of transient loading, is an optional user-input that allows to filter out solutions that produce configurations where the required PEMFC response time is shorter than the one indicated by the manufacturer.

The number of PEMFC units or the size of the battery can be limited taking into account possible limitations in the available footprint of the vehicle or the relative cost of the powerplant. The limitation is introduced, for the PEMFCs, by specifying the maximum number of units that can be installed, and for the battery by specifying the maximum capacity.

5 Energy management strategy

The component sizing for the hybrid powerplant is dependent on the type of energy management strategy (EMS) selected. The EMS controls the energy production, distribution, and storage in a vehicle's electrical grid. This control is performed through the definition of a load-sharing strategy. The load-sharing strategy determines how the vehicle's total power demand (P_{op}), defined by the operational profile, is split between the PEMFCs and batteries. In this case the focus is on determining the load-share allocated to the PEMFCs utilized by the system. The battery is used to compensate the power deficit or surplus in the vehicles electrical grid during operations, ensuring that the power demand is always met.

The EMSs considered in this study are categorized as rule-based deterministic strategies, and are characterized through a series of pre-set rules that do not change during the simulation [27]. These rules determine the load-sharing strategy for each operational point.

The first EMS considered in this study is based on a load-leveling strategy. In this strategy the power produced by all the PEMFC stacks in the system ($P_{\mathrm{fc\text{-}tot}}$) is constant throughout the simulation, fixed at a predetermined value (P_{L}). The value of P_{L} can be either calculated, using Equation 1, to determine a balanced solution in terms of powerplant footprint, or defined by the user, for sub-optimal solutions that comply with this condition.

$$P_{\mathrm{fc\text{-}tot}} = P_{\mathrm{fc}}\ n_{\mathrm{fc}} = P_{\mathrm{L}} = \frac{1}{t_{\mathrm{tot}}} \sum_{t=0}^{n} (P_{\mathrm{op}} t_{\mathrm{s}}) \tag{1}$$

The second EMS considered is based on a peak-shaving strategy. In this strategy the power output produced by all the PEMFCs of the system ($P_{\mathrm{fc\text{-}tot}}$) is calculated by applying a low pass

filter onto the operational profile in order to smooth high frequency transients (see Equation 2). The resulting filtered PEMFC power output is defined as P_{f}.

$$P_{\text{fc-tot}} = P_{\text{fc}}\ n_{\text{fc}} = P_{\text{f}} = filter(P_{\text{op}}) \tag{2}$$

In the current version of the software application three filters are included: Butterworth, Gaussian or Chebyshev. Each filter has a different frequency response curve, providing different smoothing options for the OP. For example, the Butterworth filter rolls off more slowly around the cutoff frequency than the Chebyshev filter, but there is no ripple (see Fig. 3).

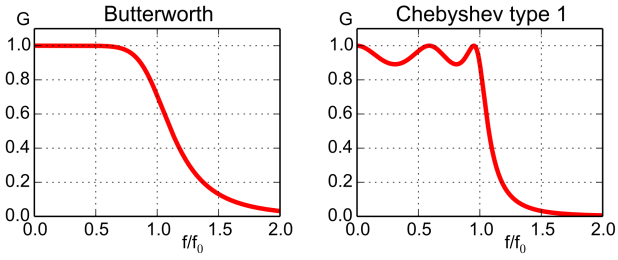

Figure 3: Frequency response curves of Butterworth filter and Chebyshev filter compared, each one as 5th order filter.

Each considered filter is defined by a two parameters that are considered as variables in the model, iterating among possible combinations. For the Butterworth filter the parameters are Order and Cut-Off frequency; for the Gaussian filter are Smoothing kernel and standard deviation (default is 0.5); and for the Chebyshev filter are Normalized pass-band edge frequency and decibels of peak-to-peak pass-band ripple. Each filter performs differently, with distinct responses to high frequency transient loading conditions. The amount of possible solutions obtained using each filter can be expanded or restricted by defining the range of variation for the filters parameters to be considered.

A specific EMSs is chosen considering the primary factors that need to be optimized in the powerplant configuration. A Load-Leveling EMS allows the fuel cell to operate at a constant output producing extremely low values of degradation but requiring more footprint for large batteries to compensate for the wider load range variations. The Peak Shaving EMSs, filtering out high frequency transients allows for a smaller footprint than load-leveling, while keeping the degradation values low.

6 Powerplant simulation model

In this section is described the set of equations upon which the model, and software application, are built. These equations are used to perform a simulation of the system, processing the input data provided by the user.

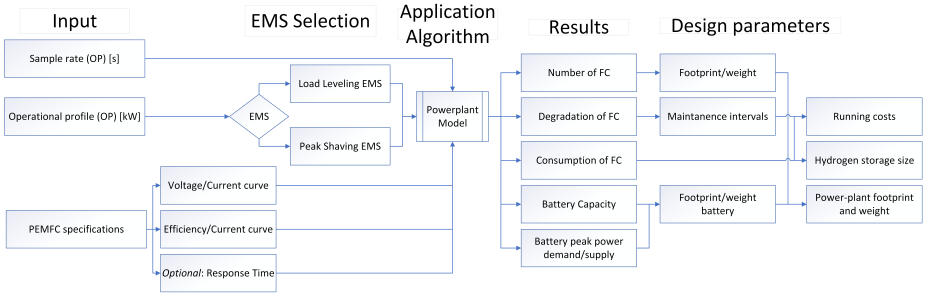

Figure 4: Flowchart describing the simulation process

The PEMFC is modelled as a serial circuit of an ideal voltage source, $V_{\text{fc-ideal}}$ and a total internal resistance R_{fc}. The PEMFC behavior is defined, during the simulation, using the voltage and efficiency data provided as input (see Fig. 2).

$$P_{\text{fc}}(t) = V_{\text{fc}}(t)\ I_{\text{fc}}(t) = V_{\text{fc-ideal}}(t)\ I_{\text{fc-ideal}}(t)\ \eta_{\text{fc}} \tag{3}$$

The model for the battery, similarly to the one of the fuel cells, is a simplified model. The battery is considered as an ideal energy storage, capable of storing and delivering power with an instant response time. No serial resistance is considered in this case determining an Ohmic efficiency of 100%. No thermal effects are considered. The choice of considering the battery as an ideal energy storage was determined by the intention to not tie the calculation to any specific battery technology, as each technology (e.g. Ni-Mh, Li-Ion, AGM) has different internal characteristics and efficiency values.

The model is based on the assumption, represented by the system of Equations 4, that in an isolated vehicle's grid the power demand imposed determined by the OP at each time-step ($P_{\text{op}}(t)$), is equal to the sum of the PEMFCs and batteries output, multiplied for the respective efficiency factors that reduce the power output.

$$\begin{cases} P_{\text{op}}(t) = P_{\text{fc-tot}}(t)\ \eta_{\text{bc}} + P_{\text{b-tot}}(t)\ \eta_{\text{bi-dir}} \\ P_{\text{fc-tot}} = P_{\text{fc}} n_{\text{fc}} = (P_{\text{fc-ideal}}\ \eta_{\text{fc}})\ n_{\text{fc}} \\ P_{\text{b-tot}} = P_{\text{b}} n_{\text{b}} = (P_{\text{b-ideal}}\ \eta_{\text{b}})\ n_{\text{b}} \\ 0 \leq P_{\text{fc}} \leq P_{\text{fc-rated}} \end{cases} \tag{4}$$

The EMS strategy, selected by the user, is used to calculate the value of $P_{\text{fc-tot}}$ at each instant using Equation 1 in the case of the load-leveling strategy, or Equation 2 in the case of the peak shaving strategy, after specifying the type of filter. The definition of $P_{\text{fc-tot}}$ allows the calculation of the number of PEMFCs required to satisfy the load demand. This value is calculated using Equation 5.

$$n_{\text{FC}} = max(P_{\text{fc-tot}})/P_{\text{fc-rated}} \tag{5}$$

The definition of the number of PEMFCs (n_{FC}) can be used to define the power output of the single PEMFC (P_{fc}). This allows the estimation of the degradation for the single PEMFC unit. The accurate calculation of the degradation is challenging as there is only a limited number of articles in the literature presenting degradation studies for PEMFC stacks. The articles utilized here for the estimation of the degradation are Fletcher et al. [28], considering a 4.8 kW PEMFC, and Chen et al. [29], considering a 10 kW PEMFC. Both articles consider stacks with a lower rated output than the one considered in the case studies presented (see Table 2). While the values do not have an influence on the formulation of the equation used to calculate the degradation, it is important to adapt these values to match the power output rating of the fuel cell stack considered in the case-studies to obtain meaningful results.

The values considered for the stack described in Table 2 for low and high power operations are the one obtained by Fletcher et al.; the value for transient loading degradation is recalculated using the article Chen et al. as a baseline. In [29] the transient loading degradation is identified using a value that defines the degradation produced at each cycle when passing from idling (10 < % Load) to high power load conditions ($\sim$ 100 % Load). Considering the nominal power of the stack (10 kW) and the load variation it is possible to obtain a value of 0.045 μV/Δkw in this case.

Table 1: Degradation values used in the developed model for the 100 kW PEM fuel cell

Operating Conditions	Degradation Rate
Low power op. (80 $\leq$ % Load)	10.17 μVh^{-1}
High power op. (> 80 % Load)	11.74 μVh^{-1}
Transient loading	0.0042 μV/ΔkW
Start/stop	23.91 μV/cycle

As it is possible to assume that the 100 kW stack considered in Table 2 is built combining multiple identical cells with the same current density as the one utilized for the stack with a 10 kW output, the value for transient loading degradation is recalculated. The new value has to take into consideration that the nominal power output is 10 times higher, modifying the ΔkW range. With this

considered it is possible to determine a value over the new range that is equal to 0.0042 μV/Δkw (see Table 1).

The calculation of the degradation (d_{fc}) using Equation 6 is done considering the low power degradation interval, the high power degradation interval and transient loading degradation. The total degradation value at the end of the considered time interval is equal to the sum of the three components. No start/stop phase is considered.

$$d_{\mathrm{fc}} = Hpo\ t_{\mathrm{hp}} + Lpo\ t_{\mathrm{lp}} + \sum_{t=0}^{n}(|P_{\mathrm{fc}}(t) - P_{\mathrm{fc}}(t-1)|\ Tl) \tag{6}$$

The hydrogen consumption ($Cons_{\mathrm{H_2}}$) of the single PEMFC can be estimated using Equation 7. The efficiency data provided as input are interpolated and used to calculate the efficiency value at which the PEMFC operates at each time-step (η_{fc}) of the simulation. The value of the hydrogen energy density, equal to 120 MJ/kg or 33.6 kWh/kg, is used to estimate the consumption for each time-step.

$$Cons_{\mathrm{H_2}} = \sum_{t=0}^{n} \frac{P_{\mathrm{fc}}(t)}{H_2\ Energy\ Density}\ \frac{t_{\mathrm{s}}}{\eta_{\mathrm{fc}}(t)} \tag{7}$$

The battery capacity that needs to be installed in the powerplant to satisfy the power demand at each time-step is calculated as a function of $P_{\text{fc-tot}}$. The battery compensates for operational conditions where the PEMFC output determines a power deficit by releasing power, and for conditions where the PEMFC output determines a power surplus by storing power. The value for battery power P_{b} at each time-step, calculated using Equation 8 can be either positive or negative according to conditions of power surplus or deficit, determining a recharge state or a discharge state.

$$P_{\mathrm{b}}(t) = \frac{P_{\mathrm{op}}(t) - P_{\text{fc-tot}}(t)\ \eta_{\mathrm{bc}}}{n_{\mathrm{b}}\ \eta_{\text{bi-dir}}} \tag{8}$$

The value representing the quantity of energy stored inside the battery at each time-stem during operations is calculated using Equation 9.

$$E(t) = \sum_{t=0}^{n}(P_{\mathrm{b}}(t)\ t_{\mathrm{s}}) \tag{9}$$

The minimum battery capacity C_{b} required to satisfy the power demand imposed by the operational profile is calculated using Equation 10.

$$C_{\mathrm{b}} = max(E(t)) + |min(E(t))| \tag{10}$$

Knowing that the energy stored inside the battery cannot be negative, it is possible to calculate the amount of energy that has to be stored in the battery at the beginning of operations (E_{start}). This value determines the minimum initial state of charge (SOC) of the battery.

$$|min(E(t))| = E_{\mathrm{start}} \tag{11}$$

An optional function is included in the model to verify that the load variation happening during a time-window that is equal to the PEMFC response time (R_{t}), is compatible with the technical limits of the unit imposed by the manufacturer, and specified by the user. This option is used with the peak-shaving strategy.

To perform this evaluation the condition represented in Equation 12 needs to be satisfied. This means that 2 or more power-data samples need to be available within the time-window considered to analyze the load variation ($U(n)$).

$$2 \leq \frac{R_{\mathrm{t}}}{t_{\mathrm{s}}} = y; y \in \mathbb{N} \tag{12}$$

If the calculation of y does not return an integer number, the result is rounded to the nearest integer greater than, or equal to that element. This produces a conservative evaluation with respect to the PEMFC response as the length of each time window where U is evaluated is longer than the actual PEMFC response time.

The load variation during the time-window defined by R_{t} is calculated using Equation 13.

$$U(n) = |P_{\mathrm{fc}}(y+n) - P_{\mathrm{fc}}(n)| \tag{13}$$

Every element of the $U(n)$ array has to be lower than the maximum acceptable U value specified by the user for the case study, between 0 and the rated $P_{\text{fc-rated}}$, for the solution to be considered valid.

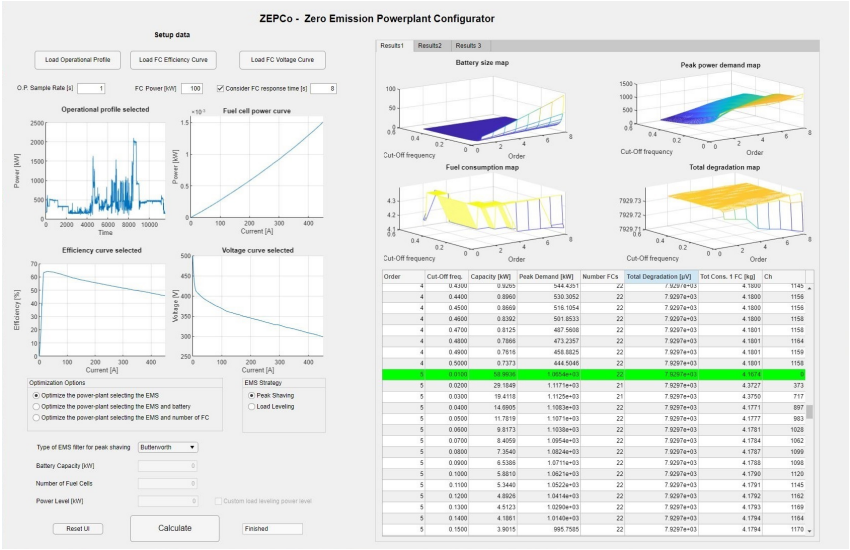

Figure 5: GUI of the model based software application containing the simulation results

7 Case study

In this section is presented a case study where the software application is used to calculate two possible powerplant configuration for the conversion of an harbor tugboat from diesel-electric to a hybrid zero-emission system utilizing PEMFCs and batteries.

The PEMFC stack selected as the main power source for both cases has the characteristics listed in Table 2. The data required for the characterization of stack are obtained from the datasheet of the unit. The efficiency curve and the voltage curve are plotted and can be observed in Figure 2. The PEMFC response time for this type of unit is assumed, with a conservative estimate, to be around 8s.

The values used for the efficiency of the boost converter (η_{bc}), connecting the PEMFC to the grid, and relative to the bi-directional converter ($\eta_{\text{bi-dir}}$), connecting the battery to the grid are respectively 0.98 and 0.95. These values are considered constant during operations and are determined using the efficiency of components in the analyzed power range, as an average between conditions at low load, determining low efficiency, and conditions at high load, determining high efficiency.

Table 2: Parameters from a commercial PEMFC model used to define the operational capabilities of the unit in the quasi-static model

Rated power ($P_{\text{fc-rated}}$)	100kW
Gross output at rated power	320 V / 350 A
Peak power EOL,OCV @BOL	250,500 V
System efficiency (Peak, BOL)	62%
System efficiency (BOL)	50%
Response time (t_{fc})	8s

The considered tugboat is currently propelled by two diesel engines with a combined output of 2648 kW, ensuring a cruising speed of approximately 14 knots and a bollard pull of 48 tons. The operational profile considered in this case study is relative to 3 hours and 15 minutes of operations. In this time interval the tugboat operates inside the harbor taking part in the procedure of pulling a crude oil carrier leaving port.

The first powerplant configuration is calculated using the peak shaving EMS, with the OP filtered using a Butterworth filter (see Fig. 7). The OP has a sample rate of 1 second.
The software application iterates through different combinations of filter's order and cut-off frequencies to find all the possible load-sharing solutions, defining $P_{\text{fc-tot}}(t)$. The values found are utilized in the model described in Section 6 to define the powerplant configuration. The solutions that comply with the conditions imposed in Equation 12, where the maximum value of U is set equal to $P_{\text{fc-rated}}$, are considered suitable for this case.

Figure 6: Tugboat of the same class of the one used in the study.

One solution that complies with the requirements set by the user, is a configuration using the Butterworth filter of order 5 and cut off-frequency of 0.01 Hz. The filtered operational profile can be observed in Figure 7.

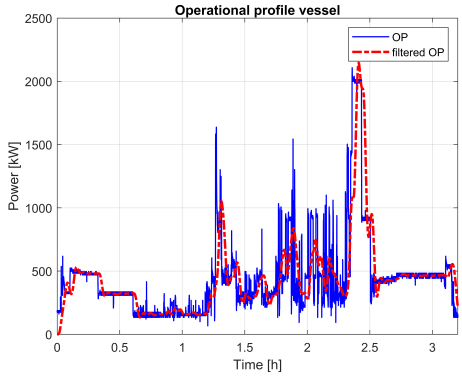

Figure 7: Operational profile of the harbor tugboat before and after filtering

The loading conditions that the single fuel cell stack experiences during the simulation can be observed in Figure 8. The number of fuel cell stacks needed to comply with the power demand calculated is equal to 22 PEMFC stacks, for a total rated power output of 2200 kW.

Based on the operational conditions on the fuel cell stack, the single fuel cell experiences a degradation that is equal to 83.74 μV. The hydrogen consumption of the single PEMFC stack is calculated to be equal to 3.11 kg, for a total hydrogen consumption of approximately 68 kg of hydrogen during the 3.2 hours of heavy operations considered.

With these filter parameters, the resulting minimum battery capacity calculated is equal to 81 kWh, with a peak power demand of 1303 kW. The power supply and demand can be observed in Figure 9. The estimated variation of energy content insider the battery of the tugboat can be observed in Figure 10. Considering the limitations in the depth of discharge it is recommended to increase the battery capacity to 130.5 kWh. This recommended capacity is calculated considering an interval for the state-of-charge between 20% and 80%, operating in the ohmic loss region of the battery's polarization curve, to reduce battery degradation.

Considering the peak power demand and the recommended battery capacity value, it is possible to calculate the C-Rate value that is approximately 10C. The recommended battery capacity

calculated can be further increased by the user analyzing the results, to bring this value down and to match the technical specifications of the battery cells that are considered for this use-case.

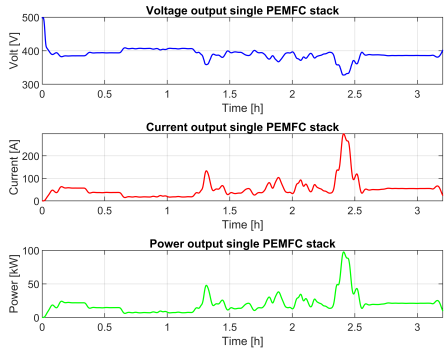

Figure 8: Single PEMFC stack load during the simulation

The presented solution is just one of possible configurations that can be obtained with the filtration of the OP using a Butterworth filter and comply with the user specifications. The execution time for the calculation is approximately 75 seconds, allowing the user to try multiple configurations in a relative short time span.

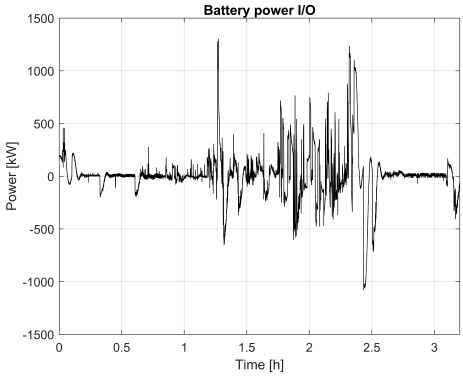

Figure 9: Power I/O for the battery of the tugboat with peak-shaving EMS

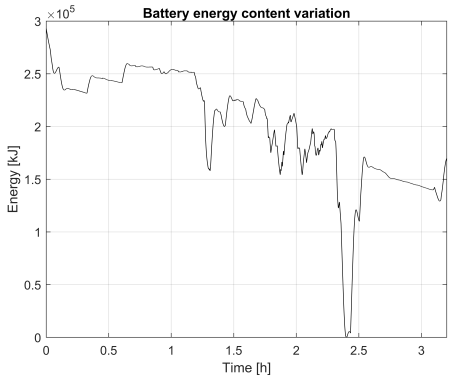

Figure 10: Energy variation in the battery of the tugboat with load-leveling EMS

As a comparison, the configuration of a powerplant utilizing the load-leveling EMS is presented. In this configuration the 5 required PEMFC stacks operate at a constant 88.31kW at an efficiency of approximately 53%. The stack degradation calculated during operations is equal to 35.13 μV. The hydrogen consumption of the single PEMFC stack is calculated to be equal to 15.9 kg, for a total hydrogen consumption of approximately 79 kg of hydrogen during the 3.2 hours of heavy operations considered. The result is, in this case, higher in terms of total hydrogen consumption as the fuel cell operates for a longer period of time at a lower median efficiency rate compared to the one in the peak shaving strategy.

The resulting minimum battery capacity calculated is equal to 246.29 kWh, with a peak power demand of 1762.7 kW. The power supply and demand can be observed in Figure 11. The estimated variation of energy content insider the battery of the tugboat can be observed in Figure 12. Considering the limitations in the depth of discharge it is recommended to increase the battery capacity to 395 kWh. This recommended capacity is calculated considering an interval for the state-of-charge between 20% and 80%. Considering the peak power demand and the recommended battery capacity value, it is possible to calculate the C-Rate value that is approximately 4C.

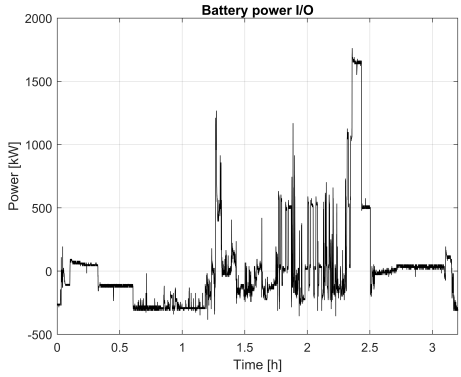

Figure 11: Power I/O for the battery of the tugboat with load-leveling EMS

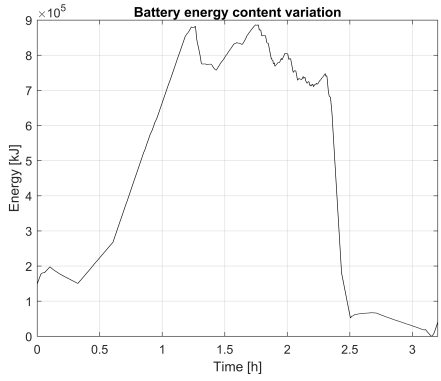

Figure 12: Energy variation in the battery of the tugboat with load-leveling EMS

8 Discussion

The presented case study shows how the developed software application, based on the presented model, allows the user to evaluate different hybrid powerplant solutions starting from the operational profile and the selection of a commercial PEMFC. The obtained results are necessary to make an evaluation on the technical and economic feasibility of a hybrid solution utilizing fuel cells and batteries for a specific use case. Technical feasibility can be evaluated, for example, considering the vehicles available space and weight for the engine compartment, and comparing it to the number of

PEMFCs and the battery size calculated. Another technical factor that can be evaluated using the results include the estimated size of the hydrogen storage based on the calculated consumption. Economic feasibility can be estimated using, for example, the consumption of hydrogen to calculate the cost of daily operations or the degradation values to estimate maintanence costs. The software application is successful in its task in the two analyzed use cases, producing results in line with pre-calculated estimates, and allowing the user to perform the aforementioned evaluations of the powerplant.

Multiple are the developments possible for this type of software application,including the implementation of additional types of EMS, the further development of the battery model to consider the response time, efficiency, and polarization curve for the different battery models. The main goal at the end of the software application development is to provide a tool with a comprehensive set of option for designers and engineers in charge of the design of hydrogen vehicles.

9 Conclusions

The development of a software application which defines powerplant configurations based on the operational profile is an important step towards simplifying the design process of zero-emission vehicles. This current version of the software application is targeted at vehicles equipped with proton exchange membrane fuel cells and batteries across different transport sectors.

Being able to quickly calculate the number of fuel cells and the size of the battery allows the user to assess the footprint needed on the vehicle for the power generation and storage components. This is important in the design of new vehicles, but particularly relevant for zero-emission retrofit projects where the usable footprint may be limited.

Calculating the number and type of components also plays an important role in the quantification of the initial investment needed for the installation of such components. Running costs can be estimated as a function of hydrogen consumption, and maintenance costs can be quantified by taking into consideration the degradation of the PEMFCs.

The developed software application provides results that are useful both in a research environment and in an industrial environment. Values calculated can be used by researchers working on topics influenced by the composition of the powertrain, such as those considering the vehicle weight distribution or aero/fluid dynamic performances. In an industrial environment the results can be used to evaluate the feasibility of an investment and the time needed to realize a return on investment.

Future work can be dedicated to improve the software application, introducing new features and functions to extend it's capabilities. The ultimate goal is to create a comprehensive tool that can aid in the transition to clean energy carriers or energy sources, thus reducing pollution and greenhouse gas emissions in cities and coastal areas and helping to preserve the environment and the health of the human population.

Acknowledgment

This work is supported by the Norwegian Research Council trough project number 90436501. The project is headed by IFE (Institute for Energy Technology) in Kjeller, Norway, and this work package is developed at the Department of Marine Technology of the Norwegian University of Science and Technology (NTNU) in Trondheim, Norway.

Keywords

Hydrogen systems; Hybrid Powertrain; Marine propulsion; Fuel cells; Battery propulsion

References

[1] Tobias Wiesenthal, Ana Condeço-Melhorado, and Guillaume Leduc. Innovation in the european transport sector: A review. *Transport Policy*, 42:86–93, 2015.

[2] Laurent Franckx. Regulatory emission limits for cars and the porter hypothesis: A survey of the literature. *Transport Reviews*, 35(6):749–766, 2015.

[3] Bin Lin and Cherng-Yuan Lin. Compliance with international emission regulations: Reducing the air pollution from merchant vessels. *Marine Policy*, 30(3):220–225, 2006.

[4] A. Miola, B. Ciuffo, E. Giovine, and M. Marra. Regulating air emissions from ships. the state of the art on methodologies, technologies and policy options. *Regulating Air Emissions from Ships: The State of the Art on Methodologies, Technologies and Policy Options*, pages 978–992, 2010. Cited By :37.

[5] E. Martinot. Renewables. global status report. 2009 update, May 2009.

[6] M.A. Hannan, F.A. Azidin, and A. Mohamed. Hybrid electric vehicles and their challenges: A review. *Renewable and Sustainable Energy Reviews*, 29:135–150, 2014.

[7] Alf Kare Adnanes. Maritime electrical installations and diesel electric propulsion. In *ABB*, 2003.

[8] Ghassan Zubi, Rodolfo Dufo-López, Monica Carvalho, and Guzay Pasaoglu. The lithium-ion battery: State of the art and future perspectives. *Renewable and Sustainable Energy Reviews*, 89:292–308, 2018.

[9] Alireza Khaligh and Zhihao Li. Battery, ultracapacitor, fuel cell, and hybrid energy storage systems for electric, hybrid electric, fuel cell, and plug-in hybrid electric vehicles: State of the art. *IEEE Transactions on Vehicular Technology*, 59(6):2806–2814, 2010.

[10] Tabbi Wilberforce, Zaki El-Hassan, F.N. Khatib, Ahmed Al Makky, Ahmad Baroutaji, James G. Carton, and Abdul G. Olabi. Developments of electric cars and fuel cell hydrogen electric cars. *International Journal of Hydrogen Energy*, 42(40):25695–25734, 2017.

[11] Mehmet Gurz, Ertugrul Baltacioglu, Yakup Hames, and Kemal Kaya. The meeting of hydrogen and automotive: A review. *International Journal of Hydrogen Energy*, 42(36):23334–23346, 2017.

[12] D.J. Durbin and C. Malardier-Jugroot. Review of hydrogen storage techniques for on board vehicle applications. *International Journal of Hydrogen Energy*, 38(34):14595–14617, 2013.

[13] L. Valverde, F. Rosa, C. Bordons, and J. Guerra. Energy management strategies in hydrogen smart-grids: A laboratory experience. *International Journal of Hydrogen Energy*, 41(31):13715–13725, 2016.

[14] Mauro G. Carignano, Ramon Costa-Castelló, Vicente Roda, Norberto M. Nigro, Sergio J. Junco, and Diego Feroldi. Energy management strategy for fuel cell-supercapacitor hybrid vehicles based on prediction of energy demand. *Journal of Power Sources*, 360:419–433, 2017.

[15] Lorenzo Balestra and Ingrid Schjølberg. Modelling and simulation of a zero-emission hybrid power plant for a domestic ferry. *International Journal of Hydrogen Energy*, 46(18):10924–10938, 2021.

[16] Lorenzo Balestra and Ingrid Schjølberg. Energy management strategies for a zero-emission hybrid domestic ferry. *International Journal of Hydrogen Energy*, 46(77):38490–38503, 2021.

[17] A. M. Bassam, A. B. Phillips, S. R. Turnock, and P. A. Wilson. Development of a multi-scheme energy management strategy for a hybrid fuel cell driven passenger ship. *International Journal of Hydrogen Energy*, 42(1):623 – 635, 2017.

[18] Ameen M. Bassam, Alexander B. Phillips, Stephen R. Turnock, and Philip A. Wilson. An improved energy management strategy for a hybrid fuel cell/battery passenger vessel. *International Journal of Hydrogen Energy*, 41(47):22453–22464, 2016.

[19] Liangfei Xu, Fuyuan Yang, Jianqiu Li, Minggao Ouyang, and Jianfeng Hua. Real time optimal energy management strategy targeting at minimizing daily operation cost for a plug-in fuel cell city bus. *International Journal of Hydrogen Energy*, 37(20):15380–15392, 2012. The 2011 Asian Bio-Hydrogen and Biorefinery Symposium (2011ABBS).

[20] Diego Feroldi and Mauro Carignano. Sizing for fuel cell/supercapacitor hybrid vehicles based on stochastic driving cycles. *Applied Energy*, 183:645–658, 2016.

[21] Q. Cai, D.J.L. Brett, D. Browning, and N.P. Brandon. A sizing-design methodology for hybrid fuel cell power systems and its application to an unmanned underwater vehicle. *Journal of Power Sources*, 195(19):6559–6569, 2010.

[22] Marco Sorrentino, Cesare Pianese, and Mario Maiorino. An integrated mathematical tool aimed at developing highly performing and cost-effective fuel cell hybrid vehicles. *Journal of Power Sources*, 221:308–317, 2013.

[23] Davide Pivetta, Chiara Dall'Armi, and Rodolfo Taccani. Multi-objective optimization of hybrid pemfc/li-ion battery propulsion systems for small and medium size ferries. *International Journal of Hydrogen Energy*, 46(72):35949–35960, 2021. Special Issue on HYPOTHESIS XV.

[24] Nikolce Murgovski, Lars Johannesson, Jonas Sjöberg, and Bo Egardt. Component sizing of a plug-in hybrid electric powertrain via convex optimization. *Mechatronics*, 22(1):106–120, 2012.

[25] L. Guzzella and A. Amstutz. Cae tools for quasi-static modeling and optimization of hybrid powertrains. *IEEE Transactions on Vehicular Technology*, 48(6):1762–1769, 1999.

[26] Paul Rodatz, Lino Guzzella, and Leonardo Pellizzari. System design and supervisory controller development for a fuel-cell vehicle. *IFAC Proceedings Volumes*, 33(26):173–178, 2000. IFAC Conference on Mechatronic Systems, Darmstadt, Germany, 18-20 September 2000.

[27] Yanjun Huang, Hong Wang, Amir Khajepour, Bin Li, Jie Ji, Kegang Zhao, and Chuan Hu. A review of power management strategies and component sizing methods for hybrid vehicles. *Renewable and Sustainable Energy Reviews*, 96:132–144, 2018-11.

[28] T. Fletcher, R. Thring, and M. Watkinson. An energy management strategy to concurrently optimise fuel consumption & pem fuel cell lifetime in a hybrid vehicle. *International Journal of Hydrogen Energy*, 41(46):21503 – 21515, 2016.

[29] Huicui Chen, Pucheng Pei, and Mancun Song. Lifetime prediction and the economic lifetime of proton exchange membrane fuel cells. *Applied Energy*, 142:154–163, 2015.

PAPER VI

Previous PhD theses published at IMT

Previous PhD theses published at the Department of Marine Technology (earlier: Faculty of Marine Technology) NORWEGIAN UNIVERSITY OF SCIENCE AND TECHNOLOGY

Report No.	Author	Title
	Kavlie, Dag	Optimization of Plane Elastic Grillages, 1967
	Hansen, Hans R.	Man-Machine Communication and Data-Storage Methods in Ship Structural Design, 1971
	Gisvold, Kaare M.	A Method for non-linear mixed -integer programming and its Application to Design Problems, 1971
	Lund, Sverre	Tanker Frame Optimalization by means of SUMT-Transformation and Behaviour Models, 1971
	Vinje, Tor	On Vibration of Spherical Shells Interacting with Fluid, 1972
	Lorentz, Jan D.	Tank Arrangement for Crude Oil Carriers in Accordance with the new Anti-Pollution Regulations, 1975
	Carlsen, Carl A.	Computer-Aided Design of Tanker Structures, 1975
	Larsen, Carl M.	Static and Dynamic Analysis of Offshore Pipelines during Installation, 1976
UR-79-01	Brigt Hatlestad, MK	The finite element method used in a fatigue evaluation of fixed offshore platforms. (Dr.Ing. Thesis)
UR-79-02	Erik Pettersen, MK	Analysis and design of cellular structures. (Dr.Ing. Thesis)
UR-79-03	Sverre Valsgård, MK	Finite difference and finite element methods applied to nonlinear analysis of plated structures. (Dr.Ing. Thesis)
UR-79-04	Nils T. Nordsve, MK	Finite element collapse analysis of structural members considering imperfections and stresses due to fabrication. (Dr.Ing. Thesis)
UR-79-05	Ivar J. Fylling, MK	Analysis of towline forces in ocean towing systems. (Dr.Ing. Thesis)
UR-80-06	Nils Sandsmark, MM	Analysis of Stationary and Transient Heat Conduction by the Use of the Finite Element Method. (Dr.Ing. Thesis)
UR-80-09	Sverre Haver, MK	Analysis of uncertainties related to the stochastic modeling of ocean waves. (Dr.Ing. Thesis)
UR-81-15	Odland, Jonas	On the Strength of welded Ring stiffened cylindrical Shells primarily subjected to axial Compression
UR-82-17	Engesvik, Knut	Analysis of Uncertainties in the fatigue Capacity of

		Welded Joints
UR-82-18	Rye, Henrik	Ocean wave groups
UR-83-30	Eide, Oddvar Inge	On Cumulative Fatigue Damage in Steel Welded Joints
UR-83-33	Mo, Olav	Stochastic Time Domain Analysis of Slender Offshore Structures
UR-83-34	Amdahl, Jørgen	Energy absorption in Ship-platform impacts
UR-84-37	Mørch, Morten	Motions and mooring forces of semi submersibles as determined by full-scale measurements and theoretical analysis
UR-84-38	Soares, C. Guedes	Probabilistic models for load effects in ship structures
UR-84-39	Aarsnes, Jan V.	Current forces on ships
UR-84-40	Czujko, Jerzy	Collapse Analysis of Plates subjected to Biaxial Compression and Lateral Load
UR-85-46	Alf G. Engseth, MK	Finite element collapse analysis of tubular steel offshore structures. (Dr.Ing. Thesis)
UR-86-47	Dengody Sheshappa, MP	A Computer Design Model for Optimizing Fishing Vessel Designs Based on Techno-Economic Analysis. (Dr.Ing. Thesis)
UR-86-48	Vidar Aanesland, MH	A Theoretical and Numerical Study of Ship Wave Resistance. (Dr.Ing. Thesis)
UR-86-49	Heinz-Joachim Wessel, MK	Fracture Mechanics Analysis of Crack Growth in Plate Girders. (Dr.Ing. Thesis)
UR-86-50	Jon Taby, MK	Ultimate and Post-ultimate Strength of Dented Tubular Members. (Dr.Ing. Thesis)
UR-86-51	Walter Lian, MH	A Numerical Study of Two-Dimensional Separated Flow Past Bluff Bodies at Moderate KC-Numbers. (Dr.Ing. Thesis)
UR-86-52	Bjørn Sortland, MH	Force Measurements in Oscillating Flow on Ship Sections and Circular Cylinders in a U-Tube Water Tank. (Dr.Ing. Thesis)
UR-86-53	Kurt Strand, MM	A System Dynamic Approach to One-dimensional Fluid Flow. (Dr.Ing. Thesis)
UR-86-54	Arne Edvin Løken, MH	Three Dimensional Second Order Hydrodynamic Effects on Ocean Structures in Waves. (Dr.Ing. Thesis)
UR-86-55	Sigurd Falch, MH	A Numerical Study of Slamming of Two-Dimensional Bodies. (Dr.Ing. Thesis)
UR-87-56	Arne Braathen, MH	Application of a Vortex Tracking Method to the Prediction of Roll Damping of a Two-Dimension Floating Body. (Dr.Ing. Thesis)

UR-87-57	Bernt Leira, MK	Gaussian Vector Processes for Reliability Analysis involving Wave-Induced Load Effects. (Dr.Ing. Thesis)
UR-87-58	Magnus Småvik, MM	Thermal Load and Process Characteristics in a Two-Stroke Diesel Engine with Thermal Barriers (in Norwegian). (Dr.Ing. Thesis)
MTA-88-59	Bernt Arild Bremdal, MP	An Investigation of Marine Installation Processes – A Knowledge - Based Planning Approach. (Dr.Ing. Thesis)
MTA-88-60	Xu Jun, MK	Non-linear Dynamic Analysis of Space-framed Offshore Structures. (Dr.Ing. Thesis)
MTA-89-61	Gang Miao, MH	Hydrodynamic Forces and Dynamic Responses of Circular Cylinders in Wave Zones. (Dr.Ing. Thesis)
MTA-89-62	Martin Greenhow, MH	Linear and Non-Linear Studies of Waves and Floating Bodies. Part I and Part II. (Dr.Techn. Thesis)
MTA-89-63	Chang Li, MH	Force Coefficients of Spheres and Cubes in Oscillatory Flow with and without Current. (Dr.Ing. Thesis
MTA-89-64	Hu Ying, MP	A Study of Marketing and Design in Development of Marine Transport Systems. (Dr.Ing. Thesis)
MTA-89-65	Arild Jæger, MH	Seakeeping, Dynamic Stability and Performance of a Wedge Shaped Planing Hull. (Dr.Ing. Thesis)
MTA-89-66	Chan Siu Hung, MM	The dynamic characteristics of tilting-pad bearings
MTA-89-67	Kim Wikstrøm, MP	Analysis av projekteringen for ett offshore projekt. (Licenciat-avhandling)
MTA-89-68	Jiao Guoyang, MK	Reliability Analysis of Crack Growth under Random Loading, considering Model Updating. (Dr.Ing. Thesis)
MTA-89-69	Arnt Olufsen, MK	Uncertainty and Reliability Analysis of Fixed Offshore Structures. (Dr.Ing. Thesis)
MTA-89-70	Wu Yu-Lin, MR	System Reliability Analyses of Offshore Structures using improved Truss and Beam Models. (Dr.Ing. Thesis)
MTA-90-71	Jan Roger Hoff, MH	Three-dimensional Green function of a vessel with forward speed in waves. (Dr.Ing. Thesis)
MTA-90-72	Rong Zhao, MH	Slow-Drift Motions of a Moored Two-Dimensional Body in Irregular Waves. (Dr.Ing. Thesis)
MTA-90-73	Atle Minsaas, MP	Economical Risk Analysis. (Dr.Ing. Thesis)
MTA-90-74	Knut-Aril Farnes, MK	Long-term Statistics of Response in Non-linear Marine Structures. (Dr.Ing. Thesis)
MTA-90-75	Torbjørn Sotberg, MK	Application of Reliability Methods for Safety Assessment of Submarine Pipelines. (Dr.Ing.

		Thesis)
MTA-90-76	Zeuthen, Steffen, MP	SEAMAID. A computational model of the design process in a constraint-based logic programming environment. An example from the offshore domain. (Dr.Ing. Thesis)
MTA-91-77	Haagensen, Sven, MM	Fuel Dependant Cyclic Variability in a Spark Ignition Engine - An Optical Approach. (Dr.Ing. Thesis)
MTA-91-78	Løland, Geir, MH	Current forces on and flow through fish farms. (Dr.Ing. Thesis)
MTA-91-79	Hoen, Christopher, MK	System Identification of Structures Excited by Stochastic Load Processes. (Dr.Ing. Thesis)
MTA-91-80	Haugen, Stein, MK	Probabilistic Evaluation of Frequency of Collision between Ships and Offshore Platforms. (Dr.Ing. Thesis)
MTA-91-81	Sødahl, Nils, MK	Methods for Design and Analysis of Flexible Risers. (Dr.Ing. Thesis)
MTA-91-82	Ormberg, Harald, MK	Non-linear Response Analysis of Floating Fish Farm Systems. (Dr.Ing. Thesis)
MTA-91-83	Marley, Mark J., MK	Time Variant Reliability under Fatigue Degradation. (Dr.Ing. Thesis)
MTA-91-84	Krokstad, Jørgen R., MH	Second-order Loads in Multidirectional Seas. (Dr.Ing. Thesis)
MTA-91-85	Molteberg, Gunnar A., MM	The Application of System Identification Techniques to Performance Monitoring of Four Stroke Turbocharged Diesel Engines. (Dr.Ing. Thesis)
MTA-92-86	Mørch, Hans Jørgen Bjelke, MH	Aspects of Hydrofoil Design: with Emphasis on Hydrofoil Interaction in Calm Water. (Dr.Ing. Thesis)
MTA-92-87	Chan Siu Hung, MM	Nonlinear Analysis of Rotordynamic Instabilities in Highspeed Turbomachinery. (Dr.Ing. Thesis)
MTA-92-88	Bessason, Bjarni, MK	Assessment of Earthquake Loading and Response of Seismically Isolated Bridges. (Dr.Ing. Thesis)
MTA-92-89	Langli, Geir, MP	Improving Operational Safety through exploitation of Design Knowledge - an investigation of offshore platform safety. (Dr.Ing. Thesis)
MTA-92-90	Sævik, Svein, MK	On Stresses and Fatigue in Flexible Pipes. (Dr.Ing. Thesis)
MTA-92-91	Ask, Tor Ø., MM	Ignition and Flame Growth in Lean Gas-Air Mixtures. An Experimental Study with a Schlieren System. (Dr.Ing. Thesis)
MTA-86-92	Hessen, Gunnar, MK	Fracture Mechanics Analysis of Stiffened Tubular Members. (Dr.Ing. Thesis)

MTA-93-93	Steinebach, Christian, MM	Knowledge Based Systems for Diagnosis of Rotating Machinery. (Dr.Ing. Thesis)
MTA-93-94	Dalane, Jan Inge, MK	System Reliability in Design and Maintenance of Fixed Offshore Structures. (Dr.Ing. Thesis)
MTA-93-95	Steen, Sverre, MH	Cobblestone Effect on SES. (Dr.Ing. Thesis)
MTA-93-96	Karunakaran, Daniel, MK	Nonlinear Dynamic Response and Reliability Analysis of Drag-dominated Offshore Platforms. (Dr.Ing. Thesis)
MTA-93-97	Hagen, Arnulf, MP	The Framework of a Design Process Language. (Dr.Ing. Thesis)
MTA-93-98	Nordrik, Rune, MM	Investigation of Spark Ignition and Autoignition in Methane and Air Using Computational Fluid Dynamics and Chemical Reaction Kinetics. A Numerical Study of Ignition Processes in Internal Combustion Engines. (Dr.Ing. Thesis)
MTA-94-99	Passano, Elizabeth, MK	Efficient Analysis of Nonlinear Slender Marine Structures. (Dr.Ing. Thesis)
MTA-94-100	Kvålsvold, Jan, MH	Hydroelastic Modelling of Wetdeck Slamming on Multihull Vessels. (Dr.Ing. Thesis)
MTA-94-102	Bech, Sidsel M., MK	Experimental and Numerical Determination of Stiffness and Strength of GRP/PVC Sandwich Structures. (Dr.Ing. Thesis)
MTA-95-103	Paulsen, Hallvard, MM	A Study of Transient Jet and Spray using a Schlieren Method and Digital Image Processing. (Dr.Ing. Thesis)
MTA-95-104	Hovde, Geir Olav, MK	Fatigue and Overload Reliability of Offshore Structural Systems, Considering the Effect of Inspection and Repair. (Dr.Ing. Thesis)
MTA-95-105	Wang, Xiaozhi, MK	Reliability Analysis of Production Ships with Emphasis on Load Combination and Ultimate Strength. (Dr.Ing. Thesis)
MTA-95-106	Ulstein, Tore, MH	Nonlinear Effects of a Flexible Stern Seal Bag on Cobblestone Oscillations of an SES. (Dr.Ing. Thesis)
MTA-95-107	Solaas, Frøydis, MH	Analytical and Numerical Studies of Sloshing in Tanks. (Dr.Ing. Thesis)
MTA-95-108	Hellan, Øyvind, MK	Nonlinear Pushover and Cyclic Analyses in Ultimate Limit State Design and Reassessment of Tubular Steel Offshore Structures. (Dr.Ing. Thesis)
MTA-95-109	Hermundstad, Ole A., MK	Theoretical and Experimental Hydroelastic Analysis of High Speed Vessels. (Dr.Ing. Thesis)
MTA-96-110	Bratland, Anne K., MH	Wave-Current Interaction Effects on Large-Volume Bodies in Water of Finite Depth. (Dr.Ing. Thesis)
MTA-96-111	Herfjord, Kjell, MH	A Study of Two-dimensional Separated Flow by a Combination of the Finite Element Method and

		Navier-Stokes Equations. (Dr.Ing. Thesis)
MTA-96-112	Æsøy, Vilmar, MM	Hot Surface Assisted Compression Ignition in a Direct Injection Natural Gas Engine. (Dr.Ing. Thesis)
MTA-96-113	Eknes, Monika L., MK	Escalation Scenarios Initiated by Gas Explosions on Offshore Installations. (Dr.Ing. Thesis)
MTA-96-114	Erikstad, Stein O., MP	A Decision Support Model for Preliminary Ship Design. (Dr.Ing. Thesis)
MTA-96-115	Pedersen, Egil, MH	A Nautical Study of Towed Marine Seismic Streamer Cable Configurations. (Dr.Ing. Thesis)
MTA-97-116	Moksnes, Paul O., MM	Modelling Two-Phase Thermo-Fluid Systems Using Bond Graphs. (Dr.Ing. Thesis)
MTA-97-117	Halse, Karl H., MK	On Vortex Shedding and Prediction of Vortex-Induced Vibrations of Circular Cylinders. (Dr.Ing. Thesis)
MTA-97-118	Igland, Ragnar T., MK	Reliability Analysis of Pipelines during Laying, considering Ultimate Strength under Combined Loads. (Dr.Ing. Thesis)
MTA-97-119	Pedersen, Hans-P., MP	Levendefiskteknologi for fiskefartøy. (Dr.Ing. Thesis)
MTA-98-120	Vikestad, Kyrre, MK	Multi-Frequency Response of a Cylinder Subjected to Vortex Shedding and Support Motions. (Dr.Ing. Thesis)
MTA-98-121	Azadi, Mohammad R. E., MK	Analysis of Static and Dynamic Pile-Soil-Jacket Behaviour. (Dr.Ing. Thesis)
MTA-98-122	Ulltang, Terje, MP	A Communication Model for Product Information. (Dr.Ing. Thesis)
MTA-98-123	Torbergsen, Erik, MM	Impeller/Diffuser Interaction Forces in Centrifugal Pumps. (Dr.Ing. Thesis)
MTA-98-124	Hansen, Edmond, MH	A Discrete Element Model to Study Marginal Ice Zone Dynamics and the Behaviour of Vessels Moored in Broken Ice. (Dr.Ing. Thesis)
MTA-98-125	Videiro, Paulo M., MK	Reliability Based Design of Marine Structures. (Dr.Ing. Thesis)
MTA-99-126	Mainçon, Philippe, MK	Fatigue Reliability of Long Welds Application to Titanium Risers. (Dr.Ing. Thesis)
MTA-99-127	Haugen, Elin M., MH	Hydroelastic Analysis of Slamming on Stiffened Plates with Application to Catamaran Wetdecks. (Dr.Ing. Thesis)
MTA-99-128	Langhelle, Nina K., MK	Experimental Validation and Calibration of Nonlinear Finite Element Models for Use in Design of Aluminium Structures Exposed to Fire. (Dr.Ing. Thesis)
MTA-99-	Berstad, Are J., MK	Calculation of Fatigue Damage in Ship Structures.

129		(Dr.Ing. Thesis)
MTA-99-130	Andersen, Trond M., MM	Short Term Maintenance Planning. (Dr.Ing. Thesis)
MTA-99-131	Tveiten, Bård Wathne, MK	Fatigue Assessment of Welded Aluminium Ship Details. (Dr.Ing. Thesis)
MTA-99-132	Søreide, Fredrik, MP	Applications of underwater technology in deep water archaeology. Principles and practice. (Dr.Ing. Thesis)
MTA-99-133	Tønnessen, Rune, MH	A Finite Element Method Applied to Unsteady Viscous Flow Around 2D Blunt Bodies With Sharp Corners. (Dr.Ing. Thesis)
MTA-99-134	Elvekrok, Dag R., MP	Engineering Integration in Field Development Projects in the Norwegian Oil and Gas Industry. The Supplier Management of Norne. (Dr.Ing. Thesis)
MTA-99-135	Fagerholt, Kjetil, MP	Optimeringsbaserte Metoder for Ruteplanlegging innen skipsfart. (Dr.Ing. Thesis)
MTA-99-136	Bysveen, Marie, MM	Visualization in Two Directions on a Dynamic Combustion Rig for Studies of Fuel Quality. (Dr.Ing. Thesis)
MTA-2000-137	Storteig, Eskild, MM	Dynamic characteristics and leakage performance of liquid annular seals in centrifugal pumps. (Dr.Ing. Thesis)
MTA-2000-138	Sagli, Gro, MK	Model uncertainty and simplified estimates of long term extremes of hull girder loads in ships. (Dr.Ing. Thesis)
MTA-2000-139	Tronstad, Harald, MK	Nonlinear analysis and design of cable net structures like fishing gear based on the finite element method. (Dr.Ing. Thesis)
MTA-2000-140	Kroneberg, André, MP	Innovation in shipping by using scenarios. (Dr.Ing. Thesis)
MTA-2000-141	Haslum, Herbjørn Alf, MH	Simplified methods applied to nonlinear motion of spar platforms. (Dr.Ing. Thesis)
MTA-2001-142	Samdal, Ole Johan, MM	Modelling of Degradation Mechanisms and Stressor Interaction on Static Mechanical Equipment Residual Lifetime. (Dr.Ing. Thesis)
MTA-2001-143	Baarholm, Rolf Jarle, MH	Theoretical and experimental studies of wave impact underneath decks of offshore platforms. (Dr.Ing. Thesis)
MTA-2001-144	Wang, Lihua, MK	Probabilistic Analysis of Nonlinear Wave-induced Loads on Ships. (Dr.Ing. Thesis)
MTA-2001-145	Kristensen, Odd H. Holt, MK	Ultimate Capacity of Aluminium Plates under Multiple Loads, Considering HAZ Properties. (Dr.Ing. Thesis)
MTA-2001-146	Greco, Marilena, MH	A Two-Dimensional Study of Green-Water

		Loading. (Dr.Ing. Thesis)
MTA-2001-147	Heggelund, Svein E., MK	Calculation of Global Design Loads and Load Effects in Large High Speed Catamarans. (Dr.Ing. Thesis)
MTA-2001-148	Babalola, Olusegun T., MK	Fatigue Strength of Titanium Risers – Defect Sensitivity. (Dr.Ing. Thesis)
MTA-2001-149	Mohammed, Abuu K., MK	Nonlinear Shell Finite Elements for Ultimate Strength and Collapse Analysis of Ship Structures. (Dr.Ing. Thesis)
MTA-2002-150	Holmedal, Lars E., MH	Wave-current interactions in the vicinity of the sea bed. (Dr.Ing. Thesis)
MTA-2002-151	Rognebakke, Olav F., MH	Sloshing in rectangular tanks and interaction with ship motions. (Dr.Ing. Thesis)
MTA-2002-152	Lader, Pål Furset, MH	Geometry and Kinematics of Breaking Waves. (Dr.Ing. Thesis)
MTA-2002-153	Yang, Qinzheng, MH	Wash and wave resistance of ships in finite water depth. (Dr.Ing. Thesis)
MTA-2002-154	Melhus, Øyvin, MM	Utilization of VOC in Diesel Engines. Ignition and combustion of VOC released by crude oil tankers. (Dr.Ing. Thesis)
MTA-2002-155	Ronæss, Marit, MH	Wave Induced Motions of Two Ships Advancing on Parallel Course. (Dr.Ing. Thesis)
MTA-2002-156	Økland, Ole D., MK	Numerical and experimental investigation of whipping in twin hull vessels exposed to severe wet deck slamming. (Dr.Ing. Thesis)
MTA-2002-157	Ge, Chunhua, MK	Global Hydroelastic Response of Catamarans due to Wet Deck Slamming. (Dr.Ing. Thesis)
MTA-2002-158	Byklum, Eirik, MK	Nonlinear Shell Finite Elements for Ultimate Strength and Collapse Analysis of Ship Structures. (Dr.Ing. Thesis)
IMT-2003-1	Chen, Haibo, MK	Probabilistic Evaluation of FPSO-Tanker Collision in Tandem Offloading Operation. (Dr.Ing. Thesis)
IMT-2003-2	Skaugset, Kjetil Bjørn, MK	On the Suppression of Vortex Induced Vibrations of Circular Cylinders by Radial Water Jets. (Dr.Ing. Thesis)
IMT-2003-3	Chezhian, Muthu	Three-Dimensional Analysis of Slamming. (Dr.Ing. Thesis)
IMT-2003-4	Buhaug, Øyvind	Deposit Formation on Cylinder Liner Surfaces in Medium Speed Engines. (Dr.Ing. Thesis)
IMT-2003-5	Tregde, Vidar	Aspects of Ship Design: Optimization of Aft Hull with Inverse Geometry Design. (Dr.Ing. Thesis)
IMT-	Wist, Hanne Therese	Statistical Properties of Successive Ocean Wave

2003-6		Parameters. (Dr.Ing. Thesis)
IMT-2004-7	Ransau, Samuel	Numerical Methods for Flows with Evolving Interfaces. (Dr.Ing. Thesis)
IMT-2004-8	Soma, Torkel	Blue-Chip or Sub-Standard. A data interrogation approach of identity safety characteristics of shipping organization. (Dr.Ing. Thesis)
IMT-2004-9	Ersdal, Svein	An experimental study of hydrodynamic forces on cylinders and cables in near axial flow. (Dr.Ing. Thesis)
IMT-2005-10	Brodtkorb, Per Andreas	The Probability of Occurrence of Dangerous Wave Situations at Sea. (Dr.Ing. Thesis)
IMT-2005-11	Yttervik, Rune	Ocean current variability in relation to offshore engineering. (Dr.Ing. Thesis)
IMT-2005-12	Fredheim, Arne	Current Forces on Net-Structures. (Dr.Ing. Thesis)
IMT-2005-13	Heggernes, Kjetil	Flow around marine structures. (Dr.Ing. Thesis
IMT-2005-14	Fouques, Sebastien	Lagrangian Modelling of Ocean Surface Waves and Synthetic Aperture Radar Wave Measurements. (Dr.Ing. Thesis)
IMT-2006-15	Holm, Håvard	Numerical calculation of viscous free surface flow around marine structures. (Dr.Ing. Thesis)
IMT-2006-16	Bjørheim, Lars G.	Failure Assessment of Long Through Thickness Fatigue Cracks in Ship Hulls. (Dr.Ing. Thesis)
IMT-2006-17	Hansson, Lisbeth	Safety Management for Prevention of Occupational Accidents. (Dr.Ing. Thesis)
IMT-2006-18	Zhu, Xinying	Application of the CIP Method to Strongly Nonlinear Wave-Body Interaction Problems. (Dr.Ing. Thesis)
IMT-2006-19	Reite, Karl Johan	Modelling and Control of Trawl Systems. (Dr.Ing. Thesis)
IMT-2006-20	Smogeli, Øyvind Notland	Control of Marine Propellers. From Normal to Extreme Conditions. (Dr.Ing. Thesis)
IMT-2007-21	Storhaug, Gaute	Experimental Investigation of Wave Induced Vibrations and Their Effect on the Fatigue Loading of Ships. (Dr.Ing. Thesis)
IMT-2007-22	Sun, Hui	A Boundary Element Method Applied to Strongly Nonlinear Wave-Body Interaction Problems. (PhD Thesis, CeSOS)
IMT-2007-23	Rustad, Anne Marthine	Modelling and Control of Top Tensioned Risers. (PhD Thesis, CeSOS)
IMT-2007-24	Johansen, Vegar	Modelling flexible slender system for real-time simulations and control applications
IMT-2007-25	Wroldsen, Anders Sunde	Modelling and control of tensegrity structures.

		(PhD Thesis, CeSOS)
IMT-2007-26	Aronsen, Kristoffer Høye	An experimental investigation of in-line and combined inline and cross flow vortex induced vibrations. (Dr. avhandling, IMT)
IMT-2007-27	Gao, Zhen	Stochastic Response Analysis of Mooring Systems with Emphasis on Frequency-domain Analysis of Fatigue due to Wide-band Response Processes (PhD Thesis, CeSOS)
IMT-2007-28	Thorstensen, Tom Anders	Lifetime Profit Modelling of Ageing Systems Utilizing Information about Technical Condition. (Dr.ing. thesis, IMT)
IMT-2008-29	Refsnes, Jon Erling Gorset	Nonlinear Model-Based Control of Slender Body AUVs (PhD Thesis, IMT)
IMT-2008-30	Berntsen, Per Ivar B.	Structural Reliability Based Position Mooring. (PhD-Thesis, IMT)
IMT-2008-31	Ye, Naiquan	Fatigue Assessment of Aluminium Welded Box-stiffener Joints in Ships (Dr.ing. thesis, IMT)
IMT-2008-32	Radan, Damir	Integrated Control of Marine Electrical Power Systems. (PhD-Thesis, IMT)
IMT-2008-33	Thomassen, Paul	Methods for Dynamic Response Analysis and Fatigue Life Estimation of Floating Fish Cages. (Dr.ing. thesis, IMT)
IMT-2008-34	Pákozdi, Csaba	A Smoothed Particle Hydrodynamics Study of Two-dimensional Nonlinear Sloshing in Rectangular Tanks. (Dr.ing.thesis, IMT/ CeSOS)
IMT-2007-35	Grytøyr, Guttorm	A Higher-Order Boundary Element Method and Applications to Marine Hydrodynamics. (Dr.ing.thesis, IMT)
IMT-2008-36	Drummen, Ingo	Experimental and Numerical Investigation of Nonlinear Wave-Induced Load Effects in Containerships considering Hydroelasticity. (PhD thesis, CeSOS)
IMT-2008-37	Skejic, Renato	Maneuvering and Seakeeping of a Singel Ship and of Two Ships in Interaction. (PhD-Thesis, CeSOS)
IMT-2008-38	Harlem, Alf	An Age-Based Replacement Model for Repairable Systems with Attention to High-Speed Marine Diesel Engines. (PhD-Thesis, IMT)
IMT-2008-39	Alsos, Hagbart S.	Ship Grounding. Analysis of Ductile Fracture, Bottom Damage and Hull Girder Response. (PhD-thesis, IMT)
IMT-2008-40	Graczyk, Mateusz	Experimental Investigation of Sloshing Loading and Load Effects in Membrane LNG Tanks Subjected to Random Excitation. (PhD-thesis, CeSOS)
IMT-2008-41	Taghipour, Reza	Efficient Prediction of Dynamic Response for Flexible amd Multi-body Marine Structures. (PhD-

		thesis, CeSOS)
IMT-2008-42	Ruth, Eivind	Propulsion control and thrust allocation on marine vessels. (PhD thesis, CeSOS)
IMT-2008-43	Nystad, Bent Helge	Technical Condition Indexes and Remaining Useful Life of Aggregated Systems. PhD thesis, IMT
IMT-2008-44	Soni, Prashant Kumar	Hydrodynamic Coefficients for Vortex Induced Vibrations of Flexible Beams, PhD thesis, CeSOS
IMT-2009-45	Amlashi, Hadi K.K.	Ultimate Strength and Reliability-based Design of Ship Hulls with Emphasis on Combined Global and Local Loads. PhD Thesis, IMT
IMT-2009-46	Pedersen, Tom Arne	Bond Graph Modelling of Marine Power Systems. PhD Thesis, IMT
IMT-2009-47	Kristiansen, Trygve	Two-Dimensional Numerical and Experimental Studies of Piston-Mode Resonance. PhD-Thesis, CeSOS
IMT-2009-48	Ong, Muk Chen	Applications of a Standard High Reynolds Number Model and a Stochastic Scour Prediction Model for Marine Structures. PhD-thesis, IMT
IMT-2009-49	Hong, Lin	Simplified Analysis and Design of Ships subjected to Collision and Grounding. PhD-thesis, IMT
IMT-2009-50	Koushan, Kamran	Vortex Induced Vibrations of Free Span Pipelines, PhD thesis, IMT
IMT-2009-51	Korsvik, Jarl Eirik	Heuristic Methods for Ship Routing and Scheduling. PhD-thesis, IMT
IMT-2009-52	Lee, Jihoon	Experimental Investigation and Numerical in Analyzing the Ocean Current Displacement of Longlines. Ph.d.-Thesis, IMT.
IMT-2009-53	Vestbøstad, Tone Gran	A Numerical Study of Wave-in-Deck Impact usin a Two-Dimensional Constrained Interpolation Profile Method, Ph.d.thesis, CeSOS.
IMT-2009-54	Bruun, Kristine	Bond Graph Modelling of Fuel Cells for Marine Power Plants. Ph.d.-thesis, IMT
IMT 2009-55	Holstad, Anders	Numerical Investigation of Turbulence in a Sekwed Three-Dimensional Channel Flow, Ph.d.-thesis, IMT.
IMT 2009-56	Ayala-Uraga, Efren	Reliability-Based Assessment of Deteriorating Ship-shaped Offshore Structures, Ph.d.-thesis, IMT
IMT 2009-57	Kong, Xiangjun	A Numerical Study of a Damaged Ship in Beam Sea Waves. Ph.d.-thesis, IMT/CeSOS.
IMT 2010-58	Kristiansen, David	Wave Induced Effects on Floaters of Aquaculture Plants, Ph.d.-thesis, CeSOS.

IMT 2010-59	Ludvigsen, Martin	An ROV-Toolbox for Optical and Acoustic Scientific Seabed Investigation. Ph.d.-thesis IMT.
IMT 2010-60	Hals, Jørgen	Modelling and Phase Control of Wave-Energy Converters. Ph.d.thesis, CeSOS.
IMT 2010- 61	Shu, Zhi	Uncertainty Assessment of Wave Loads and Ultimate Strength of Tankers and Bulk Carriers in a Reliability Framework. Ph.d. Thesis, IMT/ CeSOS
IMT 2010-62	Shao, Yanlin	Numerical Potential-Flow Studies on Weakly-Nonlinear Wave-Body Interactions with/without Small Forward Speed, Ph.d.thesis,CeSOS.
IMT 2010-63	Califano, Andrea	Dynamic Loads on Marine Propellers due to Intermittent Ventilation. Ph.d.thesis, IMT.
IMT 2010-64	El Khoury, George	Numerical Simulations of Massively Separated Turbulent Flows, Ph.d.-thesis, IMT
IMT 2010-65	Seim, Knut Sponheim	Mixing Process in Dense Overflows with Emphasis on the Faroe Bank Channel Overflow. Ph.d.thesis, IMT
IMT 2010-66	Jia, Huirong	Structural Analysis of Intect and Damaged Ships in a Collission Risk Analysis Perspective. Ph.d.thesis CeSoS.
IMT 2010-67	Jiao, Linlin	Wave-Induced Effects on a Pontoon-type Very Large Floating Structures (VLFS). Ph.D.-thesis, CeSOS.
IMT 2010-68	Abrahamsen, Bjørn Christian	Sloshing Induced Tank Roof with Entrapped Air Pocket. Ph.d.thesis, CeSOS.
IMT 2011-69	Karimirad, Madjid	Stochastic Dynamic Response Analysis of Spar-Type Wind Turbines with Catenary or Taut Mooring Systems. Ph.d.-thesis, CeSOS.
IMT - 2011-70	Erlend Meland	Condition Monitoring of Safety Critical Valves. Ph.d.-thesis, IMT.
IMT – 2011-71	Yang, Limin	Stochastic Dynamic System Analysis of Wave Energy Converter with Hydraulic Power Take-Off, with Particular Reference to Wear Damage Analysis, Ph.d. Thesis, CeSOS.
IMT – 2011-72	Visscher, Jan	Application of Particla Image Velocimetry on Turbulent Marine Flows, Ph.d.Thesis, IMT.
IMT – 2011-73	Su, Biao	Numerical Predictions of Global and Local Ice Loads on Ships. Ph.d.Thesis, CeSOS.
IMT – 2011-74	Liu, Zhenhui	Analytical and Numerical Analysis of Iceberg Collision with Ship Structures. Ph.d.Thesis, IMT.
IMT – 2011-75	Aarsæther, Karl Gunnar	Modeling and Analysis of Ship Traffic by Observation and Numerical Simulation. Ph.d.Thesis, IMT.

Imt – 2011-76	Wu, Jie	Hydrodynamic Force Identification from Stochastic Vortex Induced Vibration Experiments with Slender Beams. Ph.d.Thesis, IMT.
Imt – 2011-77	Amini, Hamid	Azimuth Propulsors in Off-design Conditions. Ph.d.Thesis, IMT.
IMT – 2011-78	Nguyen, Tan-Hoi	Toward a System of Real-Time Prediction and Monitoring of Bottom Damage Conditions During Ship Grounding. Ph.d.thesis, IMT.
IMT- 2011-79	Tavakoli, Mohammad T.	Assessment of Oil Spill in Ship Collision and Grounding, Ph.d.thesis, IMT.
IMT- 2011-80	Guo, Bingjie	Numerical and Experimental Investigation of Added Resistance in Waves. Ph.d.Thesis, IMT.
IMT- 2011-81	Chen, Qiaofeng	Ultimate Strength of Aluminium Panels, considering HAZ Effects, IMT
IMT- 2012-82	Kota, Ravikiran S.	Wave Loads on Decks of Offshore Structures in Random Seas, CeSOS.
IMT- 2012-83	Sten, Ronny	Dynamic Simulation of Deep Water Drilling Risers with Heave Compensating System, IMT.
IMT- 2012-84	Berle, Øyvind	Risk and resilience in global maritime supply chains, IMT.
IMT- 2012-85	Fang, Shaoji	Fault Tolerant Position Mooring Control Based on Structural Reliability, CeSOS.
IMT- 2012-86	You, Jikun	Numerical studies on wave forces and moored ship motions in intermediate and shallow water, CeSOS.
IMT- 2012-87	Xiang ,Xu	Maneuvering of two interacting ships in waves, CeSOS
IMT- 2012-88	Dong, Wenbin	Time-domain fatigue response and reliability analysis of offshore wind turbines with emphasis on welded tubular joints and gear components, CeSOS
IMT- 2012-89	Zhu, Suji	Investigation of Wave-Induced Nonlinear Load Effects in Open Ships considering Hull Girder Vibrations in Bending and Torsion, CeSOS
IMT- 2012-90	Zhou, Li	Numerical and Experimental Investigation of Station-keeping in Level Ice, CeSOS
IMT- 2012-91	Ushakov, Sergey	Particulate matter emission characteristics from diesel enignes operating on conventional and alternative marine fuels, IMT
IMT- 2013-1	Yin, Decao	Experimental and Numerical Analysis of Combined In-line and Cross-flow Vortex Induced Vibrations, CeSOS

IMT-2013-2	Kurniawan, Adi	Modelling and geometry optimisation of wave energy converters, CeSOS
IMT-2013-3	Al Ryati, Nabil	Technical condition indexes doe auxiliary marine diesel engines, IMT
IMT-2013-4	Firoozkoohi, Reza	Experimental, numerical and analytical investigation of the effect of screens on sloshing, CeSOS
IMT-2013-5	Ommani, Babak	Potential-Flow Predictions of a Semi-Displacement Vessel Including Applications to Calm Water Broaching, CeSOS
IMT-2013-6	Xing, Yihan	Modelling and analysis of the gearbox in a floating spar-type wind turbine, CeSOS
IMT-7-2013	Balland, Océane	Optimization models for reducing air emissions from ships, IMT
IMT-8-2013	Yang, Dan	Transitional wake flow behind an inclined flat plate-----Computation and analysis, IMT
IMT-9-2013	Abdillah, Suyuthi	Prediction of Extreme Loads and Fatigue Damage for a Ship Hull due to Ice Action, IMT
IMT-10-2013	Ramìrez, Pedro Agustìn Pèrez	Ageing management and life extension of technical systems- Concepts and methods applied to oil and gas facilities, IMT
IMT-11-2013	Chuang, Zhenju	Experimental and Numerical Investigation of Speed Loss due to Seakeeping and Maneuvering. IMT
IMT-12-2013	Etemaddar, Mahmoud	Load and Response Analysis of Wind Turbines under Atmospheric Icing and Controller System Faults with Emphasis on Spar Type Floating Wind Turbines, IMT
IMT-13-2013	Lindstad, Haakon	Strategies and measures for reducing maritime CO2 emissons, IMT
IMT-14-2013	Haris, Sabril	Damage interaction analysis of ship collisions, IMT
IMT-15-2013	Shainee, Mohamed	Conceptual Design, Numerical and Experimental Investigation of a SPM Cage Concept for Offshore Mariculture, IMT
IMT-16-2013	Gansel, Lars	Flow past porous cylinders and effects of biofouling and fish behavior on the flow in and around Atlantic salmon net cages, IMT
IMT-17-2013	Gaspar, Henrique	Handling Aspects of Complexity in Conceptual Ship Design, IMT
IMT-18-2013	Thys, Maxime	Theoretical and Experimental Investigation of a Free Running Fishing Vessel at Small Frequency of Encounter, CeSOS
IMT-19-2013	Aglen, Ida	VIV in Free Spanning Pipelines, CeSOS

IMT-1-2014	Song, An	Theoretical and experimental studies of wave diffraction and radiation loads on a horizontally submerged perforated plate, CeSOS
IMT-2-2014	Rogne, Øyvind Ygre	Numerical and Experimental Investigation of a Hinged 5-body Wave Energy Converter, CeSOS
IMT-3-2014	Dai, Lijuan	Safe and efficient operation and maintenance of offshore wind farms ,IMT
IMT-4-2014	Bachynski, Erin Elizabeth	Design and Dynamic Analysis of Tension Leg Platform Wind Turbines, CeSOS
IMT-5-2014	Wang, Jingbo	Water Entry of Freefall Wedged – Wedge motions and Cavity Dynamics, CeSOS
IMT-6-2014	Kim, Ekaterina	Experimental and numerical studies related to the coupled behavior of ice mass and steel structures during accidental collisions, IMT
IMT-7-2014	Tan, Xiang	Numerical investigation of ship's continuous- mode icebreaking in leverl ice, CeSOS
IMT-8-2014	Muliawan, Made Jaya	Design and Analysis of Combined Floating Wave and Wind Power Facilities, with Emphasis on Extreme Load Effects of the Mooring System, CeSOS
IMT-9-2014	Jiang, Zhiyu	Long-term response analysis of wind turbines with an emphasis on fault and shutdown conditions, IMT
IMT-10-2014	Dukan, Fredrik	ROV Motion Control Systems, IMT
IMT-11-2014	Grimsmo, Nils I.	Dynamic simulations of hydraulic cylinder for heave compensation of deep water drilling risers, IMT
IMT-12-2014	Kvittem, Marit I.	Modelling and response analysis for fatigue design of a semisubmersible wind turbine, CeSOS
IMT-13-2014	Akhtar, Juned	The Effects of Human Fatigue on Risk at Sea, IMT
IMT-14-2014	Syahroni, Nur	Fatigue Assessment of Welded Joints Taking into Account Effects of Residual Stress, IMT
IMT-1-2015	Bøckmann, Eirik	Wave Propulsion of ships, IMT
IMT-2-2015	Wang, Kai	Modelling and dynamic analysis of a semi-submersible floating vertical axis wind turbine, CeSOS
IMT-3-2015	Fredriksen, Arnt Gunvald	A numerical and experimental study of a two-dimensional body with moonpool in waves and current, CeSOS
IMT-4-2015	Jose Patricio Gallardo Canabes	Numerical studies of viscous flow around bluff bodies, IMT

IMT-5-2015	Vegard Longva	Formulation and application of finite element techniques for slender marine structures subjected to contact interactions, IMT
IMT-6-2015	Jacobus De Vaal	Aerodynamic modelling of floating wind turbines, CeSOS
IMT-7-2015	Fachri Nasution	Fatigue Performance of Copper Power Conductors, IMT
IMT-8-2015	Oleh I Karpa	Development of bivariate extreme value distributions for applications in marine technology,CeSOS
IMT-9-2015	Daniel de Almeida Fernandes	An output feedback motion control system for ROVs, AMOS
IMT-10-2015	Bo Zhao	Particle Filter for Fault Diagnosis: Application to Dynamic Positioning Vessel and Underwater Robotics, CeSOS
IMT-11-2015	Wenting Zhu	Impact of emission allocation in maritime transportation, IMT
IMT-12-2015	Amir Rasekhi Nejad	Dynamic Analysis and Design of Gearboxes in Offshore Wind Turbines in a Structural Reliability Perspective, CeSOS
IMT-13-2015	Arturo Jesùs Ortega Malca	Dynamic Response of Flexibles Risers due to Unsteady Slug Flow, CeSOS
IMT-14-2015	Dagfinn Husjord	Guidance and decision-support system for safe navigation of ships operating in close proximity, IMT
IMT-15-2015	Anirban Bhattacharyya	Ducted Propellers: Behaviour in Waves and Scale Effects, IMT
IMT-16-2015	Qin Zhang	Image Processing for Ice Parameter Identification in Ice Management, IMT
IMT-1-2016	Vincentius Rumawas	Human Factors in Ship Design and Operation: An Experiential Learning, IMT
IMT-2-2016	Martin Storheim	Structural response in ship-platform and ship-ice collisions, IMT
IMT-3-2016	Mia Abrahamsen Prsic	Numerical Simulations of the Flow around single and Tandem Circular Cylinders Close to a Plane Wall, IMT
IMT-4-2016	Tufan Arslan	Large-eddy simulations of cross-flow around ship sections, IMT

IMT-5-2016	Pierre Yves-Henry	Parametrisation of aquatic vegetation in hydraulic and coastal research,IMT
IMT-6-2016	Lin Li	Dynamic Analysis of the Instalation of Monopiles for Offshore Wind Turbines, CeSOS
IMT-7-2016	Øivind Kåre Kjerstad	Dynamic Positioning of Marine Vessels in Ice, IMT
IMT-8-2016	Xiaopeng Wu	Numerical Analysis of Anchor Handling and Fish Trawling Operations in a Safety Perspective, CeSOS
IMT-9-2016	Zhengshun Cheng	Integrated Dynamic Analysis of Floating Vertical Axis Wind Turbines, CeSOS
IMT-10-2016	Ling Wan	Experimental and Numerical Study of a Combined Offshore Wind and Wave Energy Converter Concept
IMT-11-2016	Wei Chai	Stochastic dynamic analysis and reliability evaluation of the roll motion for ships in random seas, CeSOS
IMT-12-2016	Øyvind Selnes Patricksson	Decision support for conceptual ship design with focus on a changing life cycle and future uncertainty, IMT
IMT-13-2016	Mats Jørgen Thorsen	Time domain analysis of vortex-induced vibrations, IMT
IMT-14-2016	Edgar McGuinness	Safety in the Norwegian Fishing Fleet – Analysis and measures for improvement, IMT
IMT-15-2016	Sepideh Jafarzadeh	Energy effiency and emission abatement in the fishing fleet, IMT
IMT-16-2016	Wilson Ivan Guachamin Acero	Assessment of marine operations for offshore wind turbine installation with emphasis on response-based operational limits, IMT
IMT-17-2016	Mauro Candeloro	Tools and Methods for Autonomous Operations on Seabed and Water Coumn using Underwater Vehicles, IMT
IMT-18-2016	Valentin Chabaud	Real-Time Hybrid Model Testing of Floating Wind Tubines, IMT
IMT-1-2017	Mohammad Saud Afzal	Three-dimensional streaming in a sea bed boundary layer
IMT-2-2017	Peng Li	A Theoretical and Experimental Study of Wave-induced Hydroelastic Response of a Circular Floating Collar
IMT-3-2017	Martin Bergström	A simulation-based design method for arctic maritime transport systems

IMT-4-2017	Bhushan Taskar	The effect of waves on marine propellers and propulsion
IMT-5-2017	Mohsen Bardestani	A two-dimensional numerical and experimental study of a floater with net and sinker tube in waves and current
IMT-6-2017	Fatemeh Hoseini Dadmarzi	Direct Numerical Simualtion of turbulent wakes behind different plate configurations
IMT-7-2017	Michel R. Miyazaki	Modeling and control of hybrid marine power plants
IMT-8-2017	Giri Rajasekhar Gunnu	Safety and effiency enhancement of anchor handling operations with particular emphasis on the stability of anchor handling vessels
IMT-9-2017	Kevin Koosup Yum	Transient Performance and Emissions of a Turbocharged Diesel Engine for Marine Power Plants
IMT-10-2017	Zhaolong Yu	Hydrodynamic and structural aspects of ship collisions
IMT-11-2017	Martin Hassel	Risk Analysis and Modelling of Allisions between Passing Vessels and Offshore Installations
IMT-12-2017	Astrid H. Brodtkorb	Hybrid Control of Marine Vessels – Dynamic Positioning in Varying Conditions
IMT-13-2017	Kjersti Bruserud	Simultaneous stochastic model of waves and current for prediction of structural design loads
IMT-14-2017	Finn-Idar Grøtta Giske	Long-Term Extreme Response Analysis of Marine Structures Using Inverse Reliability Methods
IMT-15-2017	Stian Skjong	Modeling and Simulation of Maritime Systems and Operations for Virtual Prototyping using co-Simulations
IMT-1-2018	Yingguang Chu	Virtual Prototyping for Marine Crane Design and Operations
IMT-2-2018	Sergey Gavrilin	Validation of ship manoeuvring simulation models
IMT-3-2018	Jeevith Hegde	Tools and methods to manage risk in autonomous subsea inspection,maintenance and repair operations
IMT-4-2018	Ida M. Strand	Sea Loads on Closed Flexible Fish Cages
IMT-5-2018	Erlend Kvinge Jørgensen	Navigation and Control of Underwater Robotic Vehicles

IMT-6-2018	Bård Stovner	Aided Intertial Navigation of Underwater Vehicles
IMT-7-2018	Erlend Liavåg Grotle	Thermodynamic Response Enhanced by Sloshing in Marine LNG Fuel Tanks
IMT-8-2018	Børge Rokseth	Safety and Verification of Advanced Maritime Vessels
IMT-9-2018	Jan Vidar Ulveseter	Advances in Semi-Empirical Time Domain Modelling of Vortex-Induced Vibrations
IMT-10-2018	Chenyu Luan	Design and analysis for a steel braceless semi-submersible hull for supporting a 5-MW horizontal axis wind turbine
IMT-11-2018	Carl Fredrik Rehn	Ship Design under Uncertainty
IMT-12-2018	Øyvind Ødegård	Towards Autonomous Operations and Systems in Marine Archaeology
IMT-13-2018	Stein Melvær Nornes	Guidance and Control of Marine Robotics for Ocean Mapping and Monitoring
IMT-14-2018	Petter Norgren	Autonomous Underwater Vehicles in Arctic Marine Operations: Arctic marine research and ice monitoring
IMT-15-2018	Minjoo Choi	Modular Adaptable Ship Design for Handling Uncertainty in the Future Operating Context
MT-16-2018	Ole Alexander Eidsvik	Dynamics of Remotely Operated Underwater Vehicle Systems
IMT-17-2018	Mahdi Ghane	Fault Diagnosis of Floating Wind Turbine Drivetrain- Methodologies and Applications
IMT-18-2018	Christoph Alexander Thieme	Risk Analysis and Modelling of Autonomous Marine Systems
IMT-19-2018	Yugao Shen	Operational limits for floating-collar fish farms in waves and current, without and with well-boat presence
IMT-20-2018	Tianjiao Dai	Investigations of Shear Interaction and Stresses in Flexible Pipes and Umbilicals
IMT-21-2018	Sigurd Solheim Pettersen	Resilience by Latent Capabilities in Marine Systems
IMT-22-2018	Thomas Sauder	Fidelity of Cyber-physical Empirical Methods. Application to the Active Truncation of Slender Marine Structures
IMT-23-2018	Jan-Tore Horn	Statistical and Modelling Uncertainties in the Design of Offshore Wind Turbines

IMT-24-2018	Anna Swider	Data Mining Methods for the Analysis of Power Systems of Vessels
IMT-1-2019	Zhao He	Hydrodynamic study of a moored fish farming cage with fish influence
IMT-2-2019	Isar Ghamari	Numerical and Experimental Study on the Ship Parametric Roll Resonance and the Effect of Anti-Roll Tank
IMT-3-2019	Håkon Strandenes	Turbulent Flow Simulations at Higher Reynolds Numbers
IMT-4-2019	Siri Mariane Holen	Safety in Norwegian Fish Farming – Concepts and Methods for Improvement
IMT-5-2019	Ping Fu	Reliability Analysis of Wake-Induced Riser Collision
IMT-6-2019	Vladimir Krivopolianskii	Experimental Investigation of Injection and Combustion Processes in Marine Gas Engines using Constant Volume Rig
IMT-7-2019	Anna Maria Kozlowska	Hydrodynamic Loads on Marine Propellers Subject to Ventilation and out of Water Condition.
IMT-8-2019	Hans-Martin Heyn	Motion Sensing on Vessels Operating in Sea Ice: A Local Ice Monitoring System for Transit and Stationkeeping Operations under the Influence of Sea Ice
IMT-9-2019	Stefan Vilsen	Method for Real-Time Hybrid Model Testing of Ocean Structures – Case on Slender Marine Systems
IMT-10-2019	Finn-Christian W. Hanssen	Non-Linear Wave-Body Interaction in Severe Waves
IMT-11-2019	Trygve Olav Fossum	Adaptive Sampling for Marine Robotics
IMT-12-2019	Jørgen Bremnes Nielsen	Modeling and Simulation for Design Evaluation
IMT-13-2019	Yuna Zhao	Numerical modelling and dyncamic analysis of offshore wind turbine blade installation
IMT-14-2019	Daniela Myland	Experimental and Theoretical Investigations on the Ship Resistance in Level Ice
IMT-15-2019	Zhengru Ren	Advanced control algorithms to support automated offshore wind turbine installation
IMT-16-2019	Drazen Polic	Ice-propeller impact analysis using an inverse propulsion machinery simulation approach
IMT-17-2019	Endre Sandvik	Sea passage scenario simulation for ship system performance evaluation

IMT-18-2019	Loup Suja-Thauvin	Response of Monopile Wind Turbines to Higher Order Wave Loads
IMT-19-2019	Emil Smilden	Structural control of offshore wind turbines – Increasing the role of control design in offshore wind farm development
IMT-20-2019	Aleksandar-Sasa Milakovic	On equivalent ice thickness and machine learning in ship ice transit simulations
IMT-1-2020	Amrit Shankar Verma	Modelling, Analysis and Response-based Operability Assessment of Offshore Wind Turbine Blade Installation with Emphasis on Impact Damages
IMT-2-2020	Bent Oddvar Arnesen Haugaløkken	Autonomous Technology for Inspection, Maintenance and Repair Operations in the Norwegian Aquaculture
IMT-3-2020	Seongpil Cho	Model-based fault detection and diagnosis of a blade pitch system in floating wind turbines
IMT-4-2020	Jose Jorge Garcia Agis	Effectiveness in Decision-Making in Ship Design under Uncertainty
IMT-5-2020	Thomas H. Viuff	Uncertainty Assessment of Wave-and Current-induced Global Response of Floating Bridges
IMT-6-2020	Fredrik Mentzoni	Hydrodynamic Loads on Complex Structures in the Wave Zone
IMT-7-2020	Senthuran Ravinthrakumar	Numerical and Experimental Studies of Resonant Flow in Moonpools in Operational Conditions
IMT-8-2020	Stian Skaalvik Sandøy	Acoustic-based Probabilistic Localization and Mapping using Unmanned Underwater Vehicles for Aquaculture Operations
IMT-9-2020	Kun Xu	Design and Analysis of Mooring System for Semi-submersible Floating Wind Turbine in Shallow Water
IMT-10-2020	Jianxun Zhu	Cavity Flows and Wake Behind an Elliptic Cylinder Translating Above the Wall
IMT-11-2020	Sandra Hogenboom	Decision-making within Dynamic Positioning Operations in the Offshore Industry – A Human Factors based Approach
IMT-12-2020	Woongshik Nam	Structural Resistance of Ship and Offshore Structures Exposed to the Risk of Brittle Failure
IMT-13-2020	Svenn Are Tutturen Værnø	Transient Performance in Dynamic Positioning of Ships: Investigation of Residual Load Models and Control Methods for Effective Compensation
IMT-14-2020	Mohd Atif Siddiqui	Experimental and Numerical Hydrodynamic Analysis of a Damaged Ship in Waves
IMT-15-2020	John Marius Hegseth	Efficient Modelling and Design Optimization of Large Floating Wind Turbines

IMT-16-2020	Asle Natskår	Reliability-based Assessment of Marine Operations with Emphasis on Sea Transport on Barges
IMT-17-2020	Shi Deng	Experimental and Numerical Study of Hydrodynamic Responses of a Twin-Tube Submerged Floating Tunnel Considering Vortex-Induced Vibration
IMT-18-2020	Jone Torsvik	Dynamic Analysis in Design and Operation of Large Floating Offshore Wind Turbine Drivetrains
IMT-1-2021	Ali Ebrahimi	Handling Complexity to Improve Ship Design Competitiveness
IMT-2-2021	Davide Proserpio	Isogeometric Phase-Field Methods for Modeling Fracture in Shell Structures
IMT-3-2021	Cai Tian	Numerical Studies of Viscous Flow Around Step Cylinders
IMT-4-2021	Farid Khazaeli Moghadam	Vibration-based Condition Monitoring of Large Offshore Wind Turbines in a Digital Twin Perspective
IMT-5-2021	Shuaishuai Wang	Design and Dynamic Analysis of a 10-MW Medium-Speed Drivetrain in Offshore Wind Turbines
IMT-6-2021	Sadi Tavakoli	Ship Propulsion Dynamics and Emissions
IMT-7-2021	Haoran Li	Nonlinear wave loads, and resulting global response statistics of a semi-submersible wind turbine platform with heave plates
IMT-8-2021	Einar Skiftestad Ueland	Load Control for Real-Time Hybrid Model Testing using Cable-Driven Parallel Robots
IMT-9-2021	Mengning Wu	Uncertainty of machine learning-based methods for wave forecast and its effect on installation of offshore wind turbines
IMT-10-2021	Xu Han	Onboard Tuning and Uncertainty Estimation of Vessel Seakeeping Model Parameters
IMT-01-2022	Ingunn Marie Holmen	Safety in Exposed Aquacultrue Operations
IMT-02-2022	Prateek Gupta	Ship Performance Monitoring using In-service Measurements and Big Data Analysis Methods
IMT-03-2022	Sangwoo Kim	Non-linear time domain analysis of deepwater riser vortex-induced vibrations
IMT-04-2022	Jarle Vinje Kramer	Hydrodynamic Aspects of Sail-Assisted Merchant Vessels
IMT-05-2022	Tiantian Zhu	Information and Decision-making for Accident Prevention

IMT-06-2022	Øyvind Rabliås	Numerical and Expermental Studies of Maneuvering in Regular and Irregular Waves
IMT-07-2022	Pramod Ghimire	Simulation-Based Ship Hybrid Power System Conspet Studies and Performance Analyses
IMT-08-2022	Carlos Eduardo Silva de Souza	Structural modelling, coupled dynamics, and design of large floating wind turbines
IMT-09-2022	Lorenzo Balestra	Design of hybrid fuel cell & battery systems for maritime vessels